Development and optimization of tools for embryonic electrocardiograph recording for heart dysfunction in zebrafish.

by

Rhiannon Mary Hurst

A thesis submitted to

The University of Birmingham

for the degree of

DOCTOR OF PHILOSOPHY

College of Medical and Dental Sciences

The University of Birmingham

April 2018

Table of Contents

Acknowledgements

I would first like to thank my supervisor Ferenc Mueller for his continued support, advice and encouragement throughout my studies. I would also like to thank my co-supervisor Attila Sik for his support and guidance, particularly with understanding the ECG systems.

I would like to thank all the members past and present of the Muller and Sik labs, for creating a great working environment.

I would also like to thank the British Heart Foundation for funding such an interesting project.

I would like to thank my husband, my parents and family, for all their support and encouragement, without them I would not have reached the end.

Finally, I would like to thank my daughter, Dorothy, my constant inspiration.

Abstract.

In the past decade, the zebrafish, *Danio rerio*, has risen to greater and greater prominence as a vertebrate model system for drug discovery and toxicity testing. Zebrafish larvae represent an *in vivo* vertebrate model, with high throughput potential and proven efficacy as a model of human disease and drug responses. In particular, zebrafish have been used for cardiotoxicity studies and cardiac arrhythmia modelling.

This project aims to develop and optimise tools for electrocardiographic recording in zebrafish larvae for use in cardiotoxicity screening and human arrhythmia modelling. Steps were taken towards a high throughput ECG system for zebrafish larvae through establishing viability of non-contact capillary electrode recording and development of microfabricated electrode arrays capable of replacing glass capillary electrodes. In depth analysis of atrium and ventricle signals using wavelet analysis was performed and the frequency profiles for these chambers examined.

The utility of the larval ECG recording system for characterisation of a cardiac mutant (cacna1c sa6050) was demonstrated through a set of drug treatments and demonstration of drug discovery through ECG analysis of chemical rescue of the mutant phenotype.

Overall, the results presented in this thesis highlight the zebrafish as an effective, robust and reliable model for cardiac arrhythmia and assessing drug responses *in vivo*.

1.1. The human cardiac cycle and drug induced cardiotoxicity

1.1.1 Human cardiac action potential, ion channels and ECG.

The cardiac action potential is responsible for generation and propagation of electrical activity in the heart which drives and coordinates cardiac myocyte contraction for each heartbeat (Seebohm 2005). Electrical activity is initiated by pacemaker cells at the sino-atrial node at the top of the heart and then propagated through the atria causing atrial contraction. The signal is paused at the atrioventricular node to allow for blood from the atria to empty into the ventricles and then the signal is propagated down the bundles of His to the Purkinje fibres where excitation spreads through the Purkinje fibres causing apex to base ventricular contraction (Nerbonne and Kass, 2005). Cardiac action potential activity is caused by carefully organised and coordinated movement of ions, through cardiac ion channels, generating changes in membrane potential which drives signal propagation. The action potential is split into 5 different phases, with different cardiac ion channels involved in each phase (Iaizzo, 2009). The phases are, phase 0 (depolarisation), phase 1 (early repolarisation), phase 2 (plateau), phase 3 (repolarisation) and phase 4 (resting membrane potential restored). These are depicted in **figure 1.1.**

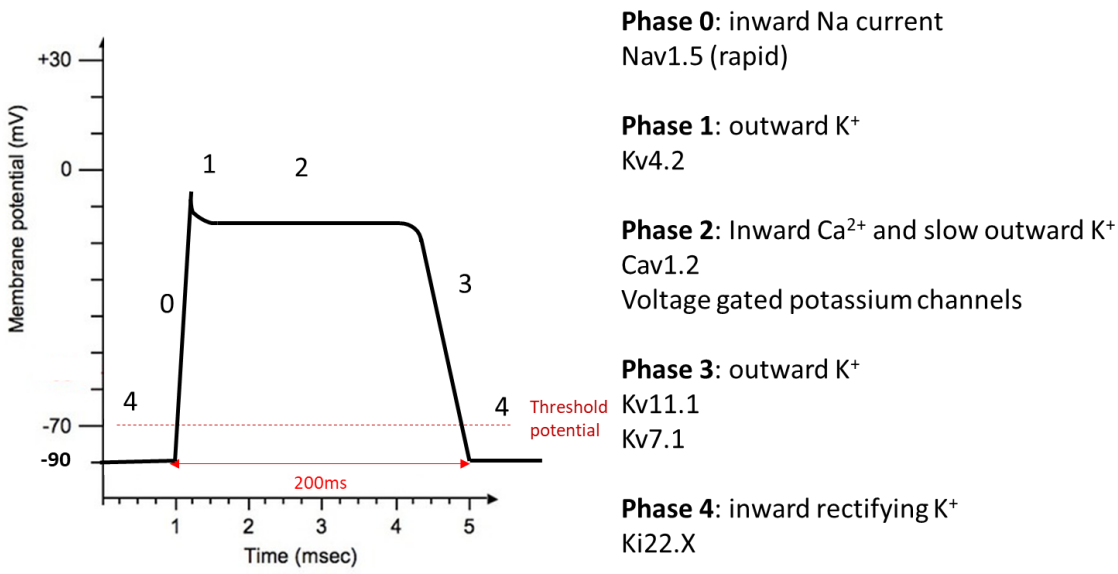

Figure 1.1 The phases of the human cardiac action potential. Phase 4: resting membrane potential of ~-90mV maintained by an inward rectifying potassium current through channel Ki22.X. Phase 0: depolarisation by inward sodium current through Nav1.5 voltage gated sodium channels. Phase 1: Early repolarisation by an outward K^+ ion current through Kv4.2. Phase 2: the plateau phase maintained by balance of inward Ca^{2+} current causing excitation coupled contraction and an outward K^+ ion current. Phase 3: Repolarisation by voltage gated potassium channels kv11.1 and Kv7.1.

During phase 4 the membrane potential is at -70mV which is the resting potential in between heartbeats. The potential is maintained by an inward rectifying potassium current through channel Ki22.X. When a threshold potential of ~ -70mV is reached, phase 0 starts. In phase 0, Sodium ion channels open and a rapid inward Na^+ ion current flows into myocytes causing depolarisation until a membrane potential of ~ +30mV is reached, and the channels shut. Then in phase 1, the sodium channels have closed and an outward current of K^+ ions drives early repolarisation. Phase 2 is the plateau phase, where a massive influx of Ca^{2+} ions into the cell triggers contraction. The plateau is maintained by a concurrent outward potassium current ensuring that ventricular contraction has finished before repolarisation occurs. Phase 3 then follows, where the cell undergoes repolarisation to regain the resting membrane potential. Outward potassium currents facilitated by voltage gated potassium channels are responsible for

repolarisation, namely the Ikr (kv11.1) and Kv7.1. The Ikr is the main channel responsible for repolarisation in phase 3 and is commonly known as the hERG (human ether-a-go-go) channel and deactivates at -40mV. It is also sensitive to blockade by various classes of drugs (Golan *et al,* 2011 and Iaizzo, 2009).

The electrical activity of the action potential can be observed using an electrocardiogram (ECG). The ECG is a recording of all electrical activity that drives each heart beat and is very useful clinically for diagnosis of heart dysfunction. The ECG can be split down into several components, The P wave, QRS complex and T wave. Clinically, the duration of these are measured, namely the PR interval, QRS duration and QT interval. Changes in these measurements can be informative of aberrant electrical activity causing arrhythmia (Hughes, Tarassenko and Roberts, 2004 and Langheinrich, Vacun and Wagner 2008). The ECG can be seen in **figure 1.2.**

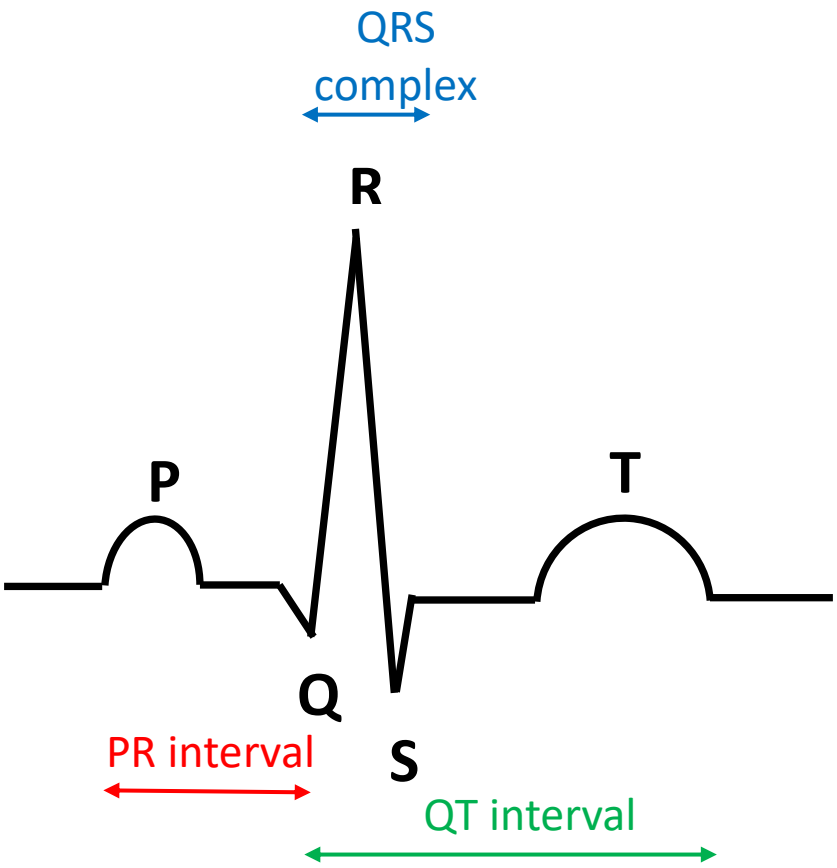

Figure 1.2 The Human ECG components. P: atrial depolarisation, QRS: ventricular depolarisation, T ventricular repolarisation. PR interval: AV conduction time, QT interval: time duration of ventricular depolarisation and repolarisation.

The P wave represents atrial depolarisation and lasts around 80-110ms. The PR measurement is the time between atrial and ventricular depolarisation and is seen as atrioventricular (AV) conduction time and is measured from the start of the P wave to the beginning of the QRS complex. The QRS complex denotes ventricular depolarisation and is the dominant wave in the ECG. Measurement between R waves (RR interval) is used to calculate heart rate. The T wave is ventricular repolarisation, this is where the resting potential is reached ready for the next cycle to start. The QT interval measures ventricular depolarisation and repolarisation and is measured from the start of the QRS complex to the end of the T wave (Wagner and Strauss, 2013). The human ECG can occasionally have a wave following the T wave, called the U

wave, which is also a part of repolarisation in the ventricle, and when present represents the last phase of ventricular repolarisation and is thought to represent Purkinje fibre repolarisation, although this is not conclusive. Prominent U waves are most commonly seen in hypokalemia. They normally have the same polarity of the T wave, but inverted U waves against a positive T wave have been linked to left ventricular hypertrophy and myocardial ischemia (Hughes, Tarassenko and Roberts, 2004 and Iaizzo, 2009 and).

1.1.2 Human cardiac arrhythmia and problems surrounding therapies.

Cardiac arrhythmia refers to a set of conditions where the normal sinus rhythm and electrical activity of the heart is aberrant. Cardiac arrhythmias are highly varied both by mechanism and by patient outlook. Arrhythmia is a comprehensive term for abnormal rhythms both regular and irregular, as well as total loss of rhythm. Different arrhythmia types can be described in various ways such as rate, mechanism, site of origin, and ECG appearance. Some can be harmless, for example, sinus tachycardia after exercise or when anxious. However, some can be very dangerous, for example ventricular fibrillation, which is a life threatening arrhythmia and is often accompanied by cardiac arrest, (Iaizzo, 2009). Congenital malformations and arrhythmias vary widely in mechanism and severity, with over 4300 babies born with a congenital heart defect each year in the UK (Artman *et al,* 2005). They represent a significant challenge in terms of developing novel therapeutic agents (Macrae 2010).

1.1.3 Cardiac toxicity and QT prolongation.

1.1.3.1 The drug development pathway and pre-clinical testing.

The drug development pathway can be broken down roughly into 5 stages. Drug discovery where candidate drugs are identified, pre-clinical testing, and then clinical

trials in phases 1, 2 and 3. Successful candidate drugs after this process gain approval and are made available on the market. Non-clinical studies start during the discovery phase and continue to and sometimes beyond approval. This area of testing covers a very wide range of areas including biological research to understand the mode of action, pharmacokinetics, ADME (absorption, distribution, metabolism and excretion of compounds), and safety pharmacology (Nurnberg & Pierre, 2017). Safety pharmacology covers safety testing in multiple areas including cardiotoxicity, reproductive toxicity, acute and repeat dosing effects, genotoxicity, teratology, and toxicity in all organ systems. After candidate drugs are identified, the first step is to put these compounds through *in silico* predictions and *in vitro* screens. Following these, *in vivo* screens are performed in mammals. The results of these tests in combination dictate which compounds are taken forward for GLP (good laboratory practise) safety assessments described above. If these are successful, then compounds progress into the human clinical trial phases (Nurnberg & Pierre, 2017). The average cost for a drug to successfully progress through the pathway and make it to market is $2.558 billion and takes 10-12 years (Wenchao, 2016). Therefore, it is better to fail early due to the step-wise increases in costs as candidate drugs progress through the drug development pathway. So, to reduce the rising cost of drug development, early and efficient tools to screen out unsuccessful candidate drugs as early as possible in the development process are needed. Priority of which adverse drug reactions to target is based on incidence and impact (Redfern *et al*, 2008).

1.1.3.2 Cardiac toxicity

The biggest cause of drug candidates failing during development is due to toxicity, with cardiotoxicity being the leading causes of drug attrition (Anyuknovsky, 2011). In total

cardiotoxicity accounts for 22-23% of drug failure during development (Wenchao, 2016). Cardiotoxicity is not only the cause of drug failure to be brought to market, but also a main cause of drugs being removed from the market due to subsequently being found to cause cardiac toxicity, with 45% of drugs removed from the market between 1970 and 2005 resulted from cardiovascular related toxicity. These late phase drug failures are costly both in terms of money and time and screening out these compounds as early as possible is crucial to reducing this cost (Wenchao, 2016).

Cardiac toxicity can refer to many different types of adverse action on the heart with varying underlying mechanisms. For instance, QRS prolongation can be caused by blockage of the sodium channels which leads to ventricular depolarisation delay. This blockage can be caused by drugs such as flecainide (Harmer *et al*, 2011). Doxorubicin is an anticancer drug with serious cardiotoxicity. It affects the function of multiple cardiac pumps and channels and causing calcium dysregulation leading to mitochondrial dysfunction and apoptosis. This ultimately leads to impaired ventricular activity and heart failure (Brano, Zamora and Tabernero, 2010). A leading cause of drug failure during development is QT prolongation through blockage of the hERG channel, and there is a lot of focus on utilising and improving screening methods for hERG channel blockers but it is important to remember that there are many other cardiac ion channels which when their function is perturbed causes of cardiac toxicity and hERG centric approaches oversimplify the problem, Safety screens have to balance against multiple adverse drug targets, not just for hERG interaction (Redfern *et al*, 2008).

1.1.3.2 QT prolongation and hERG channel.

One of the main types of cardiac toxicity is an arrhythmia termed QT prolongation, which is a delay in ventricular repolarisation. Long QT is named for the observed ECG deformation where the QT interval is prolonged with respect to normal interval range, **figure 1.3**. A long QT is a clinically significant phenotype as there is the potential for it to progress from long QT to a distinct polymorphic ventricular tachycardia called torsade des pointes (tdp). This tachycardia is dangerous and can result in syncope, ventricular fibrillation and cardiac arrest (Abrams and Macrae, 2014). Congenital long QT syndrome has several identified causal mutations and is a major cause of sudden cardiac death, but toxicologically, the most common cause of a long QT phenotype is blockage of the Kv11.1 (hERG) channel.

As depicted in figure 1.1, the Kv11.1 channel is the main repolarisation channel. It is encoded by the ether-a-go-go gene which is where the human ERG (hERG) channel name is derived. It has a large structure with 4 identical subunits spanning the membrane forming the pore, each with 6 segments in each subunit. It is voltage sensitive, opening and shutting in response to changes in membrane potential due to the cardiac action potential. Blockage of the channel by drugs disturbs the flow of potassium ions out of the cell, slowing ventricular repolarisation. This causes the T wave on the ECG to be larger, hence QT prolongation (Abrams and Macrae, 2014). In humans the QT ranges between 350 and 480ms, with the majority of the population falling within this range with age and gender accounting for some of the variance, (SAD Foundation https://www.sads.org/library/long-qt-syndrome#.Wp59nOjFLIV, accessed March 2018). When the QT interval falls outside of this range, this represents a short QT (< 380 ms) and a long QT phenotype (<450 ms). A short QT is also

clinically significant and patients with inherited short QT syndrome have an increased risk of sudden cardiac death (Antzelevitch, 2001).

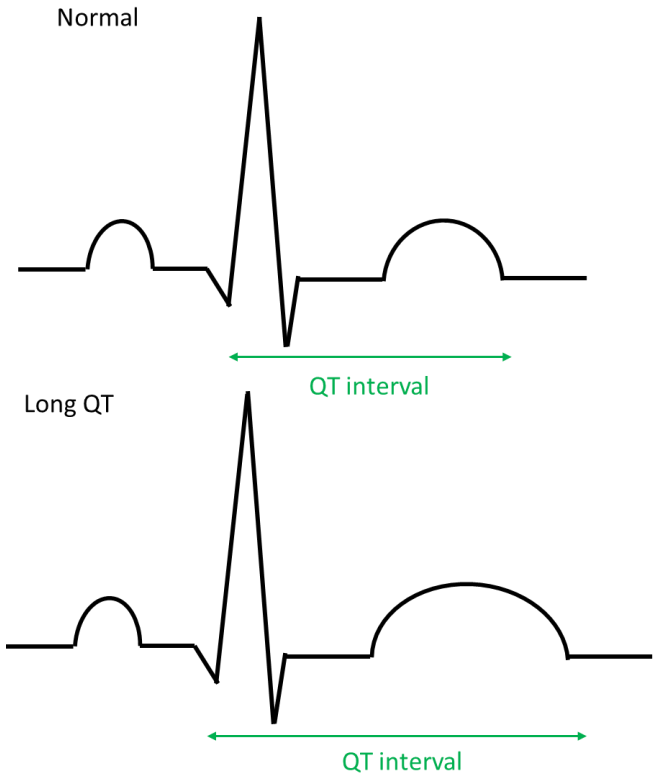

Figure 1.3 ECG waveforms showing normal and prolonged QT interval. Cardiac repolarisation is prolonged when phase 3 potassium ion channels (kv11.1) are blocked by drugs, causing the T wave to increase and the QT interval to be longer.

The hERG channel is very susceptible to blockage by drugs and has been demonstrated to show concentration dependant inhibition by various drugs (Mittelstadt *et al,* 2007). Drugs are now specifically screened for hERG interaction as large numbers of structurally and functionally diverse drugs have been found to be hERG blockers and consequently have been abandoned late into drug development. These drugs include; antihistamines, neuroleptics, and fluoroquinolones have all been shown to interact with the hERG channel (Raschi *et al,* 2008). A most notable example is terfenadine, an antihistamine, which was subsequently removed from the market after people reported

adverse cardiac side effects after using it, and then after testing it was revealed as a hERG channel blocker. Particularly due to the vast diverse drug types, structures and function which have been found to inhibit hERG channel activity, and the fact that the blockage causes long QT which can develop into a potentially fatal tachyarrhythmia, this highlights the need for cardiotoxicity screens for drug safety as early as possible in drug development (Raschi *et al*, 2008).

The zebrafish has emerged as a vertebrate model organism for many human disease states including cardiac disease, and could prove useful as an arrhythmia model for potential cardiac responses to new drugs.

1.2. Zebrafish as a model organism for human disease and drug development screens.

The established method for discovering novel compounds with desired medicinal effects is through systematic screening and isolation of positive compounds. Successful compounds are then put forward for drug safety testing, for toxicity, ADME and efficacy using *in vitro* and *in vivo* tests. *In vivo* models are essential for toxicity, efficacy and metabolism testing. The zebrafish represents an in vivo model which has several advantages over traditional mammalian models and the use of which would be in line with the three R's: refinement, reduction and replacement of animals in research. They have, over recent years grown in prominence as a viable alternative to traditional mammalian or cell line models for drug discovery, safety screening and disease modelling (Johnston *et al*, 2017).

1.2.1 The Zebrafish, *Danio rerio:* Background.

Danio rerio is a fresh water teleost originating from south Asia. Adult fish can grow up to ~6 cm and they reach sexual maturity in 3-5 months of age with a life span of 2 – 3 years. An adult mating pair can produce 200-300 eggs per week and can be maintained in artificial aquaria making them a popular model organism (Santoriello and Zon, 2012). Traditionally, they were used for developmental research due to their high fecundity, transparency and *ex utero* development. It then developed as a genetic model and its genome has been sequenced, and during the last couple of decades it has emerged as a human disease model of choice by many and is widely used for a large variety of different conditions covering all organ systems (Santoriello and Zon 2012). The central database for zebrafish is a resource covering genetic, genomic, phenotypic and developmental data for the zebrafish model organism for human disease modelling (Howe *et al*, 2016).

1.2.2 Zebrafish embryo development

Zebrafish have *ex utero* development. Single cell eggs are hatched by the females and fertilized by the males. The first cell division takes place approximately 20 minutes later. Development then progresses from a 1 cell zygote to 32/64 cell stage within 3 hours at 28^{o}C. Zebrafish development can be split into 8 stages from the single cell zygote to the early larvae at 72 hours post fertilisation (hpf). The first stage, the newly fertilized egg known as the zygote, undergoes the first cell division. Then the cleavage stage covers rapid, synchronous cell divisions 2 through 7 which is where the blastula is formed at stage 3. The blastula is formed by approximately 2.5 hours after fertilisation and this is where epiboly (cell movement) begins. Epiboly movement continues

through the gastrula stage, forming the tail bud. This is followed by segmentation where the somites and pronephros form and primary organogenesis begins, this stage takes development up to 24 hours post fertilisation (Poon and Brand 2013). Cardiac development is rapid, a rudimentary heart tube formed in the first 24 hours providing circulation after initiation of the heart beat at the start of the pharyngula stage (Lu *et al* 2016). From 24-48 hours post fertilisation (hpf), the pharyngula stage, is where pigment starts to develop. Endodermal progenitors fated to become the liver are identifiable from 18-24hrs post fertilisation. By 48 hpf the liver expresses mature liver markers and continues to grow through embryonic and larval stages. Primary liver morphogenesis is complete by 48hpf and the liver is fully formed and functioning by 72 hpf (McGrath and Li, 2008). Embryos hatch from their chorion between 48-72 hpf and have some gross motor movement due to development of pectoral fins and fin blades (Kimmel *et al*, 1995). The zebrafish are now larvae (72 hpf-29 dpf) and continue to grow, completing organ development by 5dpf. At 72 hpf, development is characterised by a protruding jaw, marking the point where embryos can start to ingest nutrients orally as well as dermally, **figure 1.4**. Free swimming develops at 5 days post fertilisation (dpf) when the swim bladder inflates (Lieschke and Currie, 2007). The juvenile period lasts from 30-89 dpf, when the adult fins and full pigmentation has formed. Following this, the fish is considered an adult (Kimmel *et al*, 1995).

Up until the jaw develops at around 72 hpf, embryos absorb oxygen and some nutrients through transdermal diffusion, until the gills form, but nearly all requirements, bar oxygen, are contained in the yolk sac, **figure 1.4** shows the anatomy of a zebrafish larvae 72 hpf. The yolk sac provides all nutrients for the first 5 days of life before free feeding stage is reached at 5dpf. Adults have gills for oxygen uptake like all other fish but the embryo can absorb oxygen by transdermal diffusion (Langheinrich, 2003).

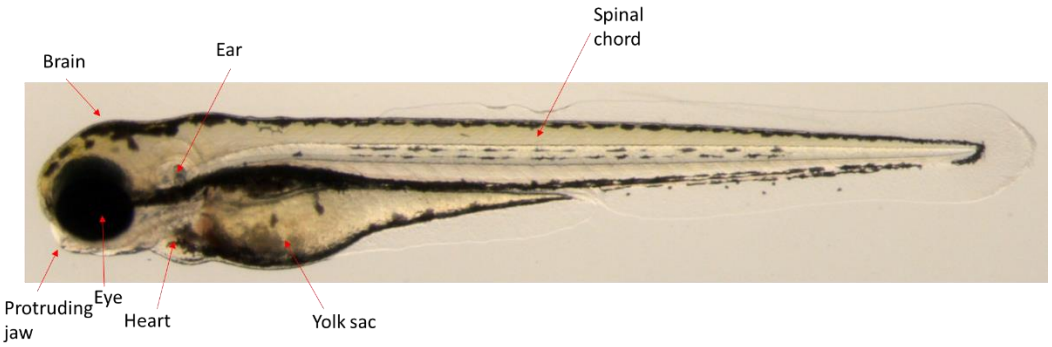

Figure 1.4 Anatomy of a zebrafish larva 72 hours post fertilisation (hpf).

Despite obvious anatomical difference to humans, including a lack of long limbs, lungs, and an intestinal bulb instead of a stomach, zebrafish have many comparative organs and organ systems to human, such as liver, pancreas and heart and cardiovascular system with a conserved function across species (Lieschke and Currie, 2007).

1.2.2.1 Zebrafish cardiac development.

During zebrafish embryogenesis, similar to mammals, the heart is one of the first organs to develop and heart development is rapid, with a beating rudimentary heart tube observed at 24 hours post fertilisation (hpf) (Hu *et al*, 2000). This then loops, known as D-looping, to form a single atrium and a single ventricle (Burggren *et al*, 2017 and Stainier *et al*, 1996). Mesodermal heart precursors specific for atrium and ventricle drive heart assembly and at the 18 somite stage these come together and then fuse, creating a cone structure which then forms the tube by 24hpf. By 48 hpf distinct chambers can be observed, **figure 1.5** (Burggen *et al*, 2017).

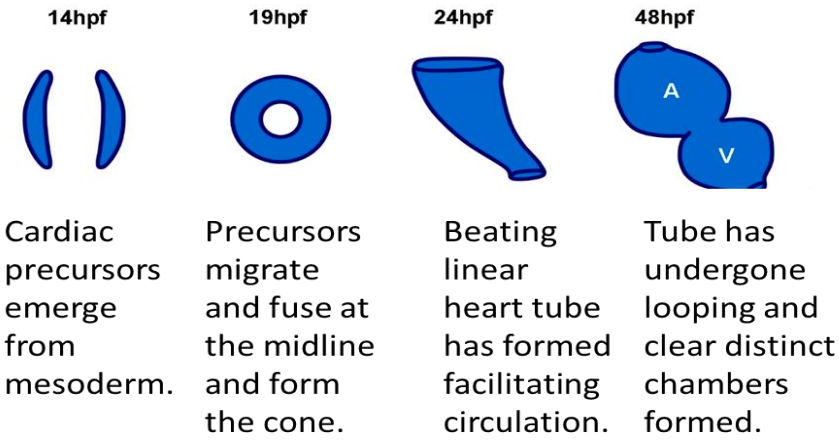

Figure 1.5 Zebrafish early heart development. Structures observed from 14 hpf to 48 hpf. Cardiac progenitor cells from the mesoderm specific for atrium and ventricle emerge. These migrate and fuse to form the cone structure, and then by 24 hpf the beating heart tube has developed. This then undergoes cardiac D-looping to form the atrium and ventricle chambers observed by 48 hpf.

The zebrafish conduction system is a unidirectional with a single atrium and a single ventricle comprising the heart. There are also two extra structures in fish to maintain a low pressure system, bulbus arteriosus and venus sinosus. These chambers aid movement of blood into and through the capillary network in the gills. Once fully developed, in the adult zebrafish heart, the ventricle is more conical in shape and blood is pumped unidirectionally, from the sinus venosus through the atrium, ventricle and out into the bulbus where it is then pumped into the capillary network in the gills and then round the body, **figure 1.6** (Leong *et al*, 2010). The shape of the ventricle helps facilitate the pressure in the blood system. Hu, Yost & Clark, 2001, measured blood pressure gradients in the adult zebrafish. Blood pressure is a major variable in cardiovascular regulation in zebrafish and so pressure for systole and diastole were measured for the atrium and ventricle chambers and the dorsal and aortic blood vessels. Ventricular pressure was measured to be approximately ~2.51/0.42 mmHg (Hu, Yost & Clark, 2001). Larval blood pressure is lower than in adult and pressure increases with

size as they grow. At 5 dpf ventricular pressure was measured to be approximately 0.42/0.003 mmHg (Hu *et al*, 2000).

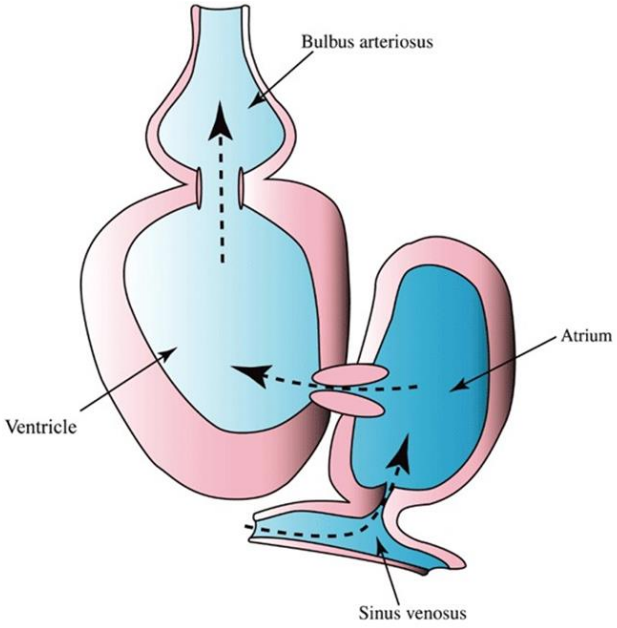

Figure 1.6 The adult zebrafish heart. Dashed arrows show the direction of blood flow. A single atrium and ventricle are joined by the sinus venosus and bulbus arteriosus which are used to maintain a low pressure system. Blood passes from the bulbus into a capillary network around the gills for oxygenation and then is pumped around the body. Figure taken from Leong et al, 2010.

By 3dpf there is a functioning conduction system with a fully formed heart complete with a complex system of cardiac ion channels which display complimentary effects to cardiac acting drugs as some humans (Dhillon *et al*, 2013, Santoriello and Zon, 2012).

1.2.3 Zebrafish model compared to existing *in vivo* models

In vivo models are essential for efficacy, toxicity and metabolism during drug development, and for aiding understanding to discover new drug targets and novel therapies. *In vivo* models are traditionally rodents or dogs. These require large amounts

of compound and long treatment regimens which is expensive. Zebrafish only require small amounts of compound and rapid development would decrease these costs.

1.2.3.1 Advantages of the zebrafish embryo model for drug screening compared to mammalian model systems.

Zebrafish have many advantages over other animal models for use in drug development and in scientific research. In drug safety screening, rodents are widely used and are the *in vivo* model of choice due to their close evolutionary relationship to humans. They have all largely similar anatomy, conserved cellular pathways and drug metabolism, and drugs can be administered the same way as humans with rodents, which is a distinct advantage over zebrafish models. However, they are also much more expensive to use, and development is comparatively slow and occurs *in utero* and have more stringent restrictions and regulations surrounding their use (Lieske and Currie, 2007). Zebrafish advantages over mammalian models are wide-ranging. They have low maintenance costs compared to rodents and due to their small size as up to 30 animals can be housed in a tank roughly the same size as a mouse cage (Gut *et al*, 2017). Their size also means that only small amounts of compound are needed for a study, also reducing cost and because of the yolk sac, embryos do not require feeding until 5 dpf. Zebrafish embryos are transparent, this coupled with their *ex utero* development means ease of visualisation under a microscope. This allows observation of the stages of development and direct observation of drug effects (Langheinrich 2003). Their rapid *ex utero* development and small size also lends them to high throughput screening potential. Embryos are easily housed in 12, 24 or 96 well plates for drug treatment and visual assessment of phenotypes.

It is also important to note that the use of zebrafish in place of rodents and other mammals contributes to the 3 Rs: refinement, reduction and replacement of animals in research, as zebrafish embryos are not protected in law or require a licence until they reach free feeding and swimming stage at ~5 dpf (Langheinrich 2003).

Crucially, as a potential model for drug responses, they have similar toxic responses to humans and other mammals due to evolutionary conserved cellular pathways and systems. Early development is highly conserved in all vertebrates and leads to high similarity in pharmacology, physiology and genetics (Gut *et al,* 2017). They have close conservation with other vertebrate species, with 70% gene homology and 80% homology with disease causing genes in humans (Howe *et al,* 2013).

Zebrafish embryos have features, in addition to those discussed above, that particularly lend themselves to use as an *in vivo* drug screen. They can absorb molecules transdermally which can be utilised as a drug delivery system. However, this route has limitations, for example; size. Compounds also need to be water soluble to be added into the medium surrounding larva for uptake, but zebrafish are reasonably tolerant to DMSO (dimethyl sulfoxide) which can be used to aid solubility of less soluble compounds (Sukardi *et al,* 2011). From 72 hpf drug uptake is also oral as the mouth and jaw are sufficiently developed. The liver is fully formed and functioning by 72 hpf also, with homologous enzymes crucial for comparative drug metabolism (McGrath and Li, 2008). They can survive in small volumes of water in 96 or 384 well plates introducing the possibility for automated drug screens on a large scale with a high throughput. This introduces the potential for zebrafish to be used for big-data approaches (Gut *et al*, 2017). Tissues or organs of interest can be labelled using fluorescent tags to aide screening. From 3 dpf the jaw develops allowing oral ingestion of compounds as well as transdermal absorption (Leong *et al,* 2010). Dimethyl

sulphoxide (DMSO) is used to increase solubility of poorly soluble compounds and zebrafish are tolerant of up to 1.5% DMSO allowing compounds with low water solubility to be tested by zebrafish embryos (Hallare *et al* 2006).

Zebrafish exhibit high similarity to humans in terms of pharmacology, physiology, genetics and toxic effects to drug exposure making them an ideal model organism (Santoriello and Zon, 2012). An important advantage for human disease modelling is that the zebrafish genome has been sequenced which means direct comparison with the human genome can be performed (Howe *et al*, 2013). The zebrafish genome has an additional 2 chromosome pairs and many duplicate genes, but these duplicates often have a different function or expression in different tissues. Often, gene duplicates in zebrafish are species specific with no human orthologue. Duplicate genes can be advantageous in cases where if one gene copy is compromised from mutation, the other copies may compensate and so the overall mutation effect is reduced (Howe *et al*, 2013).

Their high fecundity is an advantage when establishing a new transgenic line as this, coupled with rapid development means it is much quicker and cheaper than in rodents (Santoriello and Zon 2012).

1.2.3.2 Advantages and disadvantages of zebrafish compared to other fish models

Besides zebrafish, other fish have also been used as model organisms. Carp (C*yprinus carpi),* has historical use as a toxicological model, and perhaps is more suitable when greater amounts if tissue are needed or for anatomical assessment, due to its larger size. Puffer fish (*Fugu rubripes)* has been used for genetic studies by virtue of its potential to provide information on gene organisation and regulation and has close homology with

human genes despite having a genome 1/8th the size. A fish very close to zebrafish which has been used is the Japanese medaka (*Oryzias latipes*). The *Tol2* element for the *Tol2* transposon mediated mutagenesis system popular with zebrafish users was discovered in medaka (Leong *et al*, 2010). Medaka are a similar size to zebrafish, mature within 2 months and lay large numbers of eggs. They have provided a breadth of genetic and developmental model information. However, they only have a life span of 1 year in the lab, which is a quick turn over.

While useful, none of these fish models can singularly allow the large variety of technical advantages the zebrafish does, but may, particularly medaka, work complementary to the zebrafish model (Hill *et al*, 2005).

1.2.3.3 Advantages and disadvantages of zebrafish compared to other *in vitro* models for drug screening

Zebrafish, as a vertebrate *in vivo* model, has advantages over *in vitro* screens as *in vitro* cell line testing lacks the complexity of a whole organism and therefore, loss of functionality compared to whole organs and organ systems when testing, for example, cardiotoxicity. Multiple different cell types make up organ systems and cell-cell interactions between cell types will be missed in a simpler test system (Driessen *et al*, 2015). However, as a first response, quick test, *in vitro* screens are very useful and for many represent the current standard for single end point assays . They are cheaper than whole organism models, reduce animal use and do not have the stringent protocols and regulations attached to whole animals (Driessen *et al*, 2015). In addition, toxicogenomic *in vitro* approaches allow gene expression changes upon exposure to compounds to be monitored with a high throughput and low amounts of compound. It is also important to note that the cell culture serum essential for maintaining cell

cultures can act as a barrier to drug uptake by the cells. Serum proteins can bind to drugs, inhibiting them from reaching their cellular targets. In addition, the large data sets generated are time consuming to analyse and are often affected by normal gene expression variation (Pettit *et al,* 2010). Induced pluripotent stem cells offer distinct advantages over other models, both *in vivo* and other *in vitro* systems. These are cells derived straight from patients and therefore are genetically identical. Studies have shown that the use of pluripotent stem cell derived cardiomyocytes show patterns of cardiotoxicity; and have even been shown to be effective in arrhythmia screens (Liang *et al,* 2013 and Navarrete *et al,* 2013). *In vitro* cell based ion channel assays are prevalent in early toxicity screening and are extremely effective for looking at single ion channel interactions, for example those compounds interacting with the hERG channel. These assays are rapid, but only look at single ion channel interaction with a single endpoint. For more complex cardiovascular toxicities with multiple endpoints, a more integrated approach, such as a whole organism are required.

Whilst not comprehensive enough in isolation, *in vitro* testing represents a large component of screening and is best utilised coupled with more complex whole organism *in vivo* models (Pettit *et al,* 2010). These *in vitro* and *in silico* models have the advantage of being quick and comparatively simple to implement compared to *in vivo* models, and do not have the same restrictions, but are not comprehensive enough on their own to identify all cardiotoxic drugs during development.

1.2.3.4 Zebrafish as a complimentary model to existing *in vitro* models

For drug development, the aim would be to introduce zebrafish embryos as a vertebrate *in vivo* high throughput model, which inserts complimentary to existing screens. Currently in drug development, *in vitro* and mammalian *in vivo* models are used in

combination for drug safety screening. As a tiered system, those that pass the *in vitro* tests are put forward for mammalian testing, but there are still many costly late stage drug candidate failures. These could be reduced by introducing high throughput *in vivo* zebrafish screens that sit complimentary to and alongside the other screens prior to GLP safety assessments. This would help ensure that only prime candidates are advanced to the time consuming and costly *in vivo* mammalian screens.

There is evidence that *in vitro* and zebrafish *in vivo* screens would work well together; for example, in nanoparticle safety testing. Some nanoparticles can induce oxidative stress and inflammation, and screening using macrophages and neutrophils (*in vitro*) and zebrafish would be greatly beneficial (Johnston et al 2017). This was taken further and a comparative screen testing for novel cell cycle inhibitors was performed in a mammalian cell line, a zebrafish cell line and zebrafish embryos. The results showed that the zebrafish embryo screen identified 14 compounds, not identified by the cell lines, and 6 of these were subsequently found to have an effect in the mammalian cells. This suggests a conserved effect in vertebrates. There were 3 compounds inactivated by the culture serum, and so no effect seen in the cell line and 1 compound was only effective in the zebrafish cell line and embryos suggesting a species specific effect. These results demonstrate that performing the same screen across multiple platforms; cell lines and zebrafish embryos gives a much greater amount of information than any one screen individually, and can be used to identify compounds that would have been missed without the additional inclusion of a zebrafish embryo screen (Murphy *et al*, 2006). This principal can be applied across drug development and safety screening. Toxicity testing across cell lines and zebrafish embryos yield a greater quality of drug candidates to advance to mammalian *in vivo* tests, reducing the amount of late stage drug failures. This would be especially applicable to cardiotoxicity and hERG channel

interaction, which is the greatest cause of drug candidates being dropped from development.

1.3 Zebrafish as a model of human cardiac conditions and arrhythmia.

1.3.1 Zebrafish as a tool to evaluate cardiotoxicity

Zebrafish have emerged as a model organism for human disease and novel drug development. They have a highly conserved, sequenced genome with around 70% homology to humans and 80% homology of disease causing genes. This makes them a very desirable genetic model (Milan and Macrae, 2008). There are many features of zebrafish which makes them ideal for a phenotype screen, for example, their small size, small amounts of chemical required for dosing and comparatively inexpensive husbandry makes them a cost effective alternative to other vertebrate systems such as murine models. Their *ex utero* development, optical transparency means that close observation of development and phenotype progression is possible. Fluorescent markers can be used to highlight areas of interest and many transgenic lines have been created for a wide range of uses including expressing fluorescent proteins of interest, analysis of enhancers, and modelling genetic abnormalities for modelling human disease (Milan and Macrae, 2008, Roberts *et al,* 2014, Kari, Rodeck and Dicker, 2007). Zebrafish have been used successfully for toxicological studies, as these can be conducted with relative ease using a 24 or 96 well plate, small amounts of compound and effects easily visualised due to optical transparency (Mcgrath and Li, 2008). This approach has led to large-scale chemical screens and mutagenic screens, creating zebrafish mutants modelling human diseases with visible embryonic phenotypes, for

example cardiovascular diseases such as cardiomyopathy and arrhythmias (Lieschke and Currie, 2007 and Rubinstein, 2003). Zebrafish and human cardiac electrophysiology share many similarities.

1.3.2 Zebrafish electrophysiology

1.3.2.1 Comparison of human, mouse and zebrafish action potentials and electrophysiology.

In humans, the pacemaker cells are the source of cardiac electrical activity. Pacemaker cells are also found in the zebrafish which control heart rate and initiation of the zebrafish action potential. There are some differences in physiology; the structure of the vessels is simpler, and the ventricles lack Purkinje fibres and bundles of His, but the zebrafish have ventricular trabeculae which perform a similar function and the ventricles still contract apex to base the same as humans. Most notably, zebrafish only have one atrium and one ventricle, as opposed to the two atrium and two ventricle heart structure in humans (Milan and Macrae, 2008).

Many orthologues of human cardiac ion channels are found in zebrafish, and consequently, a lot of the channels which make up the different phases of the zebrafish action potential are homologous. However, there are some differences. In phase 0, sodium channels are responsible for rapid depolarisation but in zebrafish, calcium channels called t type calcium channels also contribute. This is also present in mammals but only very early in development. Phases 2 and 3 are very much the same as in humans with zebrafish orthologue channels causing the voltage plateau and rapid repolarisation. The major difference between humans and zebrafish embryos is that the

zebrafish embryos lack Kv7.1 and Kv4.3 which generate the early repolarisation in phase 1 (Leong *et al*, 2010).

Adult zebrafish have an average heart rate of 120-150bpm (beats per minute) which is roughly twice the speed of humans, but much closer to the human heart rate than mice, whose hearts beat approximately 10 times that of humans and have evolved to have a rapid repolarisation phase to facilitate this fast heart rate. Zebrafish, like humans have a slow repolarisation phase with very similar ion channels used to generate the action potential, as described above. Mice have a different main repolarisation channel, in order for fast repolarisation to happen. The main repolarisation channel in humans, the kv11.1 (hERG) channel, has a homologue in zebrafish (zERG) which is the main repolarisation channel in zebrafish (Leong *et al*, 2010). However, in mice, while there is a hERG homologue, it is not the main repolarisation channel for the murine action potential. This is because the current flow through this channel is too slow for the fast repolarisation required for the fast heart rate of the mouse. **figure 1.7**.

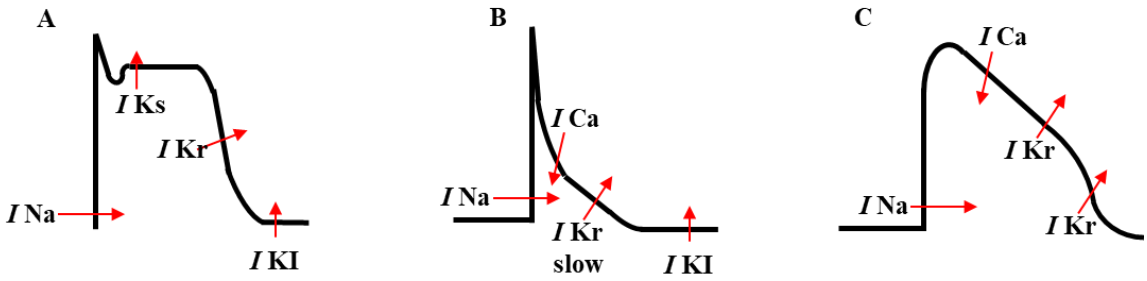

Figure 1.7 Comparison of human, mouse and zebrafish action potentials (AP)
A) Human action potential. Fast depolarisation and slow repolarisation with a plateau phase.
B) Mouse action potential: less plateau and fast repolarisation to facilitate a fast heart beat 10 x that of human. IKr channel is not the dominant channel for repolarisation.
C) Zebrafish action potential, more closely resembles the human AP with a plateau and slower repolarisation. IKr channel is the dominant repolarisation channel which allows modelling of repolarisation abnormalities such as QT prolongation from hERG (zERG) blockade.

The mouse action potential does not have much of a plateau phase and relies on fast a repolarisation current to facilitate the fast heart rate. The zebrafish action potential more closely resembles the human action potential and has a more comparable heart rate. The zebrafish, therefore, is arguably the better model of human cardiac repolarisation abnormalities than mice.

1.3.2.2 The Human ECG compared to the zebrafish ECG.

As expected, due to similar ion channels being responsible for generating the different phases of the human and zebrafish action potentials, the resultant ECG traces for these species, which measures this electrical activity, are also very similar. Like human, there are three main components of the ECG, the P wave, QRS complex and the T wave. These depict atrial and ventricular depolarisation and repolarisation in the same way the human ECG does, and the three main measurements commonly taken from the ECG for analysis; the PR interval, the RR interval and the QT interval, measured the same way as in human. The PR segment shows time taken for the components responsible for carrying the electrical current to be activated. In zebrafish this interval is shorter than in humans, around 30ms, as there is less delay between transference of electrical signal from atrium to ventricle. Also, the P wave is smaller, as there is less muscle in the atrium in zebrafish and the blood pumping is mainly due to the thicker ventricle (Artman *et al*, 2008 and Milan *et al*, 2006). In zebrafish the RR interval is shorter than in human, as they have a faster heart beat (Leong *et al*, 2010). The QT interval in zebrafish is comparable to human, only slightly shorter. The QTc interval is the QT interval corrected for heartrate and can be calculated using the Bazett's formula

QTc=QT/√RR, (Wagner and Strauss, 2013). In mice, the ECG shows differences to human and zebrafish as a result of the differences in the action potential. Most notably, the QRS complex has two peaks, and a negative T wave, in addition, the whole cardiac cycle is around a 10th of humans, **figure, 1.8**.

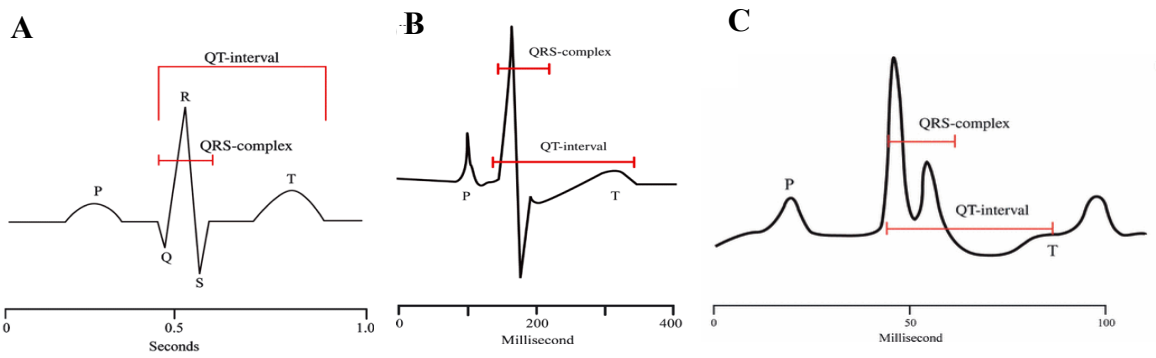

Figure 1.8 Depiction of the human, mouse and zebrafish ECG trace showing the P wave, QRS complex and T wave. Adapted from Leong et al 2010.
A) Human ECG trace.
B) Zebrafish ECG trace, close similarity with the human ECG.
C) Mouse ECG trace, differences seen from the human trace; two peaks for QRS and negative T wave.

Human and zebrafish, have strongly correlating ECG traces, due to similar action potentials (Leong *et al* 2010). Consequently, they respond to different cardiac acting drugs in the same way, and so it is possible to use zebrafish responses to predict human responses to cardiac drugs. This makes them a very attractive model for cardiotoxicity testing (McGrath and Li, 2008).

1.3.3 Zebrafish as a model for Long QT syndrome

As demonstrated, high conservation between human and zebrafish has already been exploited by groups using zebrafish as a model organism for disease states across multiple organ systems which includes cardiovascular. Adult zebrafish arrhythmia

models take advantage of ion channel conservation with humans to closely model arrhythmic responses to drug treatments and genetic arrhythmia models. Particularly repolarisation abnormalities, where the potassium ion channels driving repolarisation in humans (the hERG channel, kv11.1) has a zebrafish orthologue zERG. It is possible to use zebrafish larvae as a screen for cardiac drug safety testing. Larvae at 3dpf have been successfully visually assessed for the presence of bradycardia (slow heart rate) and AV block (conduction between atrium and ventricles impaired, so ventricle contraction is irregular against the atrium), when dosed with known hERG blockers (Bergmans *et al*, 2008).

As previously stated, orthologues of the human cardiac ion channels are found in zebrafish, these include orthologues of hERG and Nav1.5 (Nguyen et al, 2008). The zebrafish zERG channel protein has 1186 amino acids and has 60% sequence homology to human hERG channel with 90% homology at the pore forming region. Both consist of 6 transmembrane domains, S1-S4 voltage sensing and S5-S6 making up the central ion pore (Hassel, *et al,* 2008), **figure 1.9**. A cAMP binding site is located following S6 in the c terminus and this, along with the amino acids in segments 4,5 and 6 are highly conserved with the human othologue, (Langheinrich *et al*, 2003).

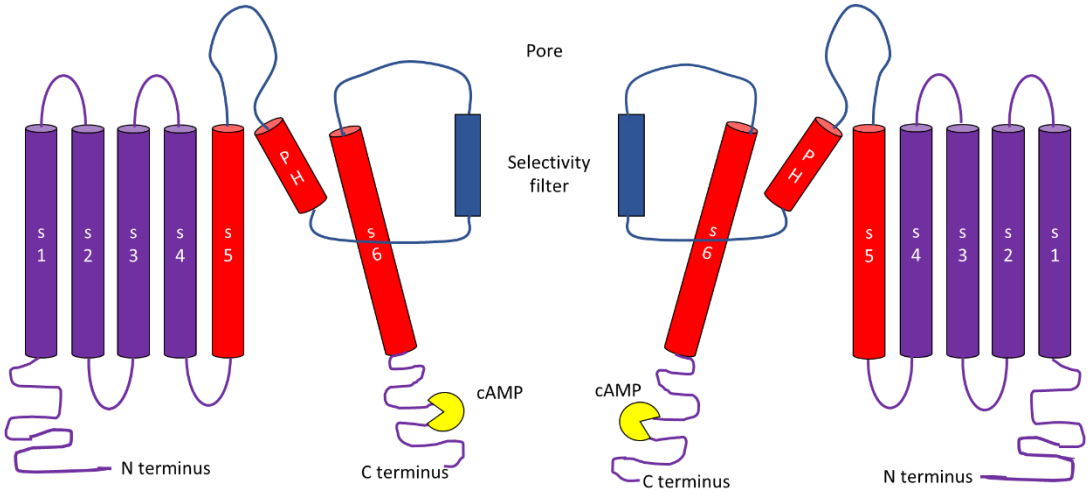

Figure 1.9 The zebrafish zERG channel. A transmembrane voltage gated potassium channel, the main repolarisation channel in the zebrafish heart. It has 6 transmembrane domains S1-S4 forming the voltage sensing components and S5-S6 forming the potassium selective channel. Two domains are shown with S1-S4 in purple form the voltage sensing component and S5-S6 in red form the pore. In S5 and S6 there is a pore helix (PH), a cyclic AMP (adenosine monophosphate) binding domain (cAMP).

The main ventricular repolarisation channel in both human and zebrafish is the hERG channel, known as the zERG in zebrafish and perturbance of channel activity leads to a prolongation of the QT interval on an ECG. This can be genetic or drug induced and is diagnosed in humans as long QT syndrome. The QT interval comprises ventricular depolarisation (QRS) and repolarisation (T wave). When this occurs, there can be a predisposition to arrhythmia, and Torsades de pointes (TdP) which is a life threatening tachycardia characterised by the QRS twisting around the isoelectric baseline, (Chaudhari *et al*, 2013). This can lead to sudden cardiac death. It has been demonstrated that known hERG blockers have the same effect (QT prolongation) in zebrafish, making them an ideal model to screen for adverse cardiotoxicity hERG blockers in an *in vivo* vertebrate large scale chemical screen (Arnaout *et al*,2007).

1.3.4 Current cardiac models

1.3.4.1 *In vitro* and *in silico* cardiac models

Pluri-potent stem cells derived from human cardiac tissues have been implemented as *in vitro* models for testing cardiotoxicity (Navarrete *et al* 2013). They currently constitute an important part of cardiotoxicity testing, alongside *in vivo* models. Human pluripotent stem cell lines derived from the myocytes of healthy and arrhythmic hearts (hiPSC-CMs) have been used to generate single cell level drug response profiles of different arrhythmia types against healthy hiPSC-CMs. Hereditary arrhythmic cell lines included Long QT syndrome, dilated cardiomyopathy and hypertrophic cardiomyopathy. This library exhibited increased susceptibility to cardiac drugs, with differing responses, highlighting that use of such cell lines may be predictive of drug treatment responses (Liang *et al,* 2013). An *in vitro* hERG channel assay has been widely implicated to combat the prevalence of hERG channel blockers discovered late into development and have shown good predictive value at predicting compound interactions. The current gold standard for identifying hERG interaction is by a high throughput *in vitro* whole cell patch clamp assay. This approach is very successful for identifying compounds which interact with the hERG channel accurately and is capable of producing data for hundreds of compounds a week. However, these ion channel assays are single end point and more complex compound interactions and toxicities can not be assessed through these approaches. Zebrafish larvae present a multi-end point model but while there is high throughput potential, manual handling and orientation of embryos needs to be removed in order to compete with the throughput of *in vitro* assays (Redfern, *et al*, 2008). Kramer *et al*, 2013, reported higher predictive value using MICE (multiple ion channel effects) models, with a reduction in false positives and false negatives, so may represent an alternative *in vitro* test (Kramer *et al,* 2013). However,

in vivo testing where all channels of relevance are expressed as are interconnects and external influences provides a more accurate and complete picture of cardiac toxicity than testing for individual channel responses alone. This is where the zebrafish could be used, as a more rapid alternative to mammalian systems.

In silico testing are predictive computational models using collected knowledge of known drug responses to different drugs, their structure and uses this to predict responses to novel compounds. Aronov *et al*, 2005, used this approach to create an *in silico* model to screen for potential hERG blockers. The problem with trying to predict hERG blockers, is that many compounds with diverse drug action and structures have been found to interact with and inhibit hERG channel function, making it a difficult and complex task to predict without further testing. However, homology modelling and QSAR methods, have shown good results.

In silico testing has also been performed for analysis of patients with long QT syndrome. Similar to the study performed by Liang *et al*, 2013, this study evaluated the utility of a computer model to perform a risk assessment of cardiac-acting drugs given to patients with type 1 long QT syndrome. They successfully demonstrated modelling of type 1 LQT repolarisation and drug responses using multivariate analysis (Hoefen *et al*, 2012).

In silico and *in vitro* testing are extremely useful to narrow down drug candidate pools, but cannot be used in isolation with 100% accuracy. These tests must be utilised in combination with *in vivo* models, and zebrafish provide a viable, cheaper alternative to mammalian models.

1.3.4.2 *In vivo* models: mammalian

Traditionally, in drug development, successful candidate drugs that progress past *in silico* and *in vitro* tests are then put forward for mammalian testing in mice and rats. These tests cover toxicity testing (including; cardiac, hepatic, reproductive, respiratory) and long term dose studies. These studies are vital for bridging the gap between bench top research and the clinic. This translational phase relies on validated and predictive mammalian models such as mice and rats (Denayer, Stöhr and Roy, 2014).

In vivo mammalian models can be used to be predictive of novel drug responses, due to the large body of data amassed from decades of standardized protocols, but different model systems are needed to be pieced together to create a full picture, for example; cell-based ion channel assays, *in vivo* assessment of conductivity, physiology and electrophysiology all contribute a different aspect of this multifaceted disease, and no single model encompasses all these aspects (Denayer, Stöhr and Roy, 2014). Mammalian models continue to provide valuable insights into cardiovascular disease and arrhythmia (Smith *et al,* 2016 and Green *et al,* 2016). For example; hypertrophic cardiomyopathy, where the heart muscle becomes enlarged and inefficient at pumping blood through the heart and around the body and lungs, is commonly modelled using mammalian systems. This is a progressive disease, ultimately leading to heart failure and as such is an important area of interest for discovering novel therapeutics (Green *et al,* 2016). Green *et al,* 2016, identified a novel compound which inhibits the hypercontractility associated with the early disease state, by binding to myosin and inhibiting hypercontractility activity when administered to mice (Green *et al,* 2016). Mouse mutant models are also used, for example *SCN5A*-linked Lenègres disease. SCN5A is the main sodium channel in the heart, and mutations in this channel are linked to age related arrhythmias and myocardial fibrosis (Royer *et al*, 2005). Study of

models such as this further understanding of these disease states and help to identify drug targets for intervention.

Study of cardiac arrest has been performed in a number of mammalian model species including; mice, rat, rabbit and canines, where cardiac arrest was induced using electrical pacing to the heart, and different characteristics including toxicology, asphyxia and myocardial infarction were assessed as well as drug intervention, ventilations and compressions noted. Animal models of cardiac arrest test potential new interventions and are widely used for cardiac arrest research (Vognsen *et al,* 2017).

Preclinical testing is a requirement of regulation authorities for a candidate drug to be put forward from bench research into the drug development pathway. Standard preclinical testing covers a wide range of areas including: acute, repeat dosing, genotoxicity, reproductive toxicity, teratology and safety pharmacology. It provides valuable data and insight into its potential performance in clinical trials and is vital to improve chances of the drugs success both in terms of efficacy and safety (Denayer, Stöhr and Roy, 2014). Due to the vast cost involved in detailed animal model studies, the use of a valid, cost-effective alternative, such as zebrafish represents a viable, substitute for some of these pre-clinical testing models.

1.3.5 Current Cardiac zebrafish cardiac models

1.3.5.1 Adult zebrafish cardiac models

1.3.5.1.1 Adult zebrafish cardiac disease modelling.

The zebrafish heart anatomy is different to human, but despite these differences have been used successfully for cardiac modelling (Menke *et al,* 2011, Gut *et al,* 2017). There are many examples of cardiomyopathy in adult zebrafish, including genetic,

chemical and anaemia induced models which also concomitantly uses high resolution imaging and fluorescence (Gut *et al,* 2017, Reischauer *et al* 2014 and Ding *et al,* 2016). Reischauer *et al,* created a transgenic line with actin binding GFP to visualise in 4D and *in vivo,* the myofilament dynamics in early heart development of the zebrafish. They then used this line to identify erbb2 signalling which has a role in myofibril organisation and inhibition of erbb2 causes dysregulation of the myofibrils and cardiomyopathy. Using the dominant-negative *erbb2* transgene, a model of cardiomyopathy in adult zebrafish was created (Reischauer *et al*, 2014). Ding *et al,* 2016 also identified a gene with cardiomyopathy susceptibility using a transposon mutagenesis screen. 44 other transgenic lines indicating a potential role in cardiac regulation were also identified (Ding *et al,* 2016). There are many other examples where zebrafish have been used to identify genes and pathways involved in cardiac failure and developed into useful models yielding important insights into this major cardiac disease problem. There are advantages to using zebrafish to model congenital heart disease (CHD). In humans, severe defects ultimately lead to heart failure. Modelling this progression in zebrafish can be useful as the oxygen requirement for early stage development in zebrafish larvae is fulfilled by dermal absorption. However, due to differences in size and anatomy, zebrafish heart failure can present differently to human analogues, even with the same underlying cause (Brown *et al,* 2016). In zebrafish, heart failure disease progression begins with gradually decreasing contractility causing abnormal changes in heart size, shape and function (Brown *et al,* 2016).

Zebrafish are also a major organism of interest in scientific research due to their ability to regenerate cardiac tissue. In humans if heart muscle dies due to ischemic attack then that becomes scar tissue, reducing the overall efficiency of the heart. Eventually with

repeat attacks, heart goes into heart failure from the lack of working muscle and from compensating for the burden of scar tissue and loss of muscle. If we can learn from the zebrafish and be able to regenerate tissue to functional cardiac muscle it would be a major leap forward in combatting heart disease (Gonzalez-Rosa *et al*, 2017). As well as whole organism studies, *in vitro* studies have also been used to study chronotropic effects of serotonin in zebrafish heart. Extracted zebrafish hearts, were dosed with serotonin and examined using ECG, physiology and pharmacology approaches to investigate 5-HT pathways. ECGs showed that 5-HT pathways act through the heart lowering heart rate, demonstrating the use of zebrafish in autonomic cardiac control (Stoyek *et al*, 2017). Some cardiac techniques developed are adaptable for adult and larval zebrafish. Hoage, Ding and Xu, 2012, developed a red blood flow rate assay using a transparent transgenic line with a red fluorescent heart to study cardiac functions in adult and embryonic zebrafish. The transparency coupled with the fluorescent heart facilitate ease of visualisation of the beating heart in adult fish allowing observation of cardiac function non-invasively. This line can be observed from 24 hours when the heart beat commences throughout development until adulthood and beyond (Hoage, Ding and Xu, 2012).

1.3.5.1.2 Adult zebrafish cardiac arrhythmia models

Milan *et al* 2006, first demonstrated the *in vivo* ECG recording system for adult zebrafish and demonstrated its use for measuring QT prolongation from drug treatment. This opened the door for further development of adult recording systems and these systems have been used to study a variety of arrhythmias in zebrafish. Hassel, 2008, created a mutant line with a short QT phenotype, named *Reggae* (m230), which is a mutation in the zERG channel. Using ECG analysis, the mutation was found to cause

premature channel activation and deficient inactivation resulting in shortened repolarisation phase and the short QT phenotype. Sun *et al* 2009, took a similar recording approach to analyse the ECGs of zebrafish adults pre and post ventricular amputation. The system first described by Milan *et al* 2006 was optimised by Chaudhari *et al* 2013, standardising the immobilisation method, perfusion system and acclimatisation period. More recently, Liu *et al* 2016 published a surface recording protocol for adult zebrafish, using 2 electrode probes. Prior to recording, scale layers were removed from the area covering the heart and pre-opening the pericardial sac. The zebrafish mutant, *breakdance,* was electrocardiographically characterised using this method. *Breakdance,* has a mutation in the zERG channel, and as a result has a QT prolongation. Multi-electrode approaches have also been developed; Yu *et al,* 2012 used microfabricated multi-electrode arrays inserted into the chest so that they were in direct contact with the epicardium. Comparison of these results against intracardial calcium transient signals recorded from excised hearts showed synchrony, demonstrating the utility of the microarrays for real time study of heart activity in small animals. While this is described as a surface recording, there is still considerable preparation, removing outer scale layers and inserting the electrode probes 0.5mm into the muscle layer of the chest (Liu *et al,* 2016). These are invasive and time-consuming procedures, which would not readily adapt to a high throughput screen.

There have been alternative methods developed for adult zebrafish ECG analysis using flexible microelectrode arrays for topical recording (Zhang *et al* 2014 and Zhang *et al,* 2015). Use of microfabrication, allowed development of flexible electronics to cover the atrium and the ventricle from the fish surface (Zhang *et al,* 2014). Zhang *et al,* 2015 developed microsensor jackets for ECG recording. Using these devices, heart rate and QT responses to phenotype response to ventricular resection and amiodarone treatment

(a cardiac drug) were measured. The advantages of this model are that anaesthetic is not required, and the recording process is non-invasive. However, it is not known what the effect of wearing the weight of the jacket will have on the zebrafish and the stress caused to the animal during the application of the electrode jacket, and while wearing it (Zhang *et al,* 2015).

In vitro approaches have also been used for arrhythmia studies, Tsai *et al*, 2011 described a zebrafish adult heart recording protocol as a platform for pharma-testing. Extracted adult zebrafish hearts were examined using micro-electrodes and optical mapping. While ECGs resembled human ECG traces, there was variation introduced by explanting the hearts for recording, where the P and T waves were not always the same polarity as the QRS complex (P, 40% T, 55% of the time not the same polarity as QRS). Inverted T waves and P waves can be an indication of arrhythmia in humans but also of benign conditions from (Tsai *et al*, 2011). Isolated adult hearts have also been used to map electrical activity optically using a voltage sensitive dye (RH-237) to visualise the potentiometric response and blebbistatin to uncouple cardiac contraction from electrical activity to remove motion artefact (Lin *et al,* 2014). Using this approach, heart rate and action potential variation was monitored in response to a temperature range (Lin *et al*, 2014). These approaches, while excellent for small scale experiments, and have some potential for scaling up, lack the complexity of a whole organism response to drug treatment. Also, explanting the hearts can introduce artefacts not seen in typical *in vivo* heart ECGs. As the zebrafish embryo is readily adaptable for high throughput approaches, as a whole vertebrate organism, this is preferable to an isolated heart model for a pharmaceutical setting.

Development of adult ECG recording systems represents a huge step forward for detailed cardiac monitoring of drug responses but is still a largely invasive procedure

with limited capacity for development into a high throughput system which would be a requirement for pharmaceutical screening. A similar platform in zebrafish embryos would capture the advantages of the zebrafish model and high resolution data of ECG monitoring with high throughput capability.

1.3.5.2 The Zebrafish embryo as a cardiac model.

1.3.5.2.1 Zebrafish embryo genetic approachs .

As zebrafish do not have embryonic stem cells, antisense technologies, such as morpholinos have been used to achieve gene knockdown for study and assessment of drug responses. Morpholinos are oligonucleotides that block transcription or splicing resulting in no gene product. They are effective at knocking down gene function but are linked to non-phenotypic general off-target side effects such as oedema in the pericardial sac and necrosis, and so very strict experiment protocols are required when using them (Poon and Brand, 2013). Other methods include ENU mutagenesis, Tol2 transposons and TALENs. ENU mutagenesis, employed by the The Wellcome Sanger Institute for the zebrafish mutation project they undertook, which has yielded hundreds of mutant lines for study of genetic mutation phenotypes applicable to a huge variety of human disease states across all organ systems (Busch-Nentwich, *et al*, 2013). The Tol2 transposon has been highly successful for the creation of transgenic fluorescent marker lines for a multitude of tissues and organs for study. For example; Tol2 transposon technology was used to create cardiac enhancer trap lines in zebrafish as a novel tool for studying cardiac development and disease. The resultant lines could be used for examining cardiac contractility and function in 4D under a confocal microscope, Poon *et al*, 2010. The TALEN (transcriptor activator-like effector nucleases) approach is a popular technique for creating mutants in genes of interest, to generate zebrafish

models of human genetic diseases (Roberts *et al,* 2014). More recently, the CRISPR/cas9 technology has been utilised in zebrafish, rapidly becoming the technique of choice for genome editing as it is more straight forward than Tol2 or TALEN, and has already been used successfully for the creation of mutations and transgenic lines (Hruscha *et al,* 2013).

1.3.5.2.2 Zebrafish embryo cardiac drug screens and arrhythmia models.

Many cardiac mutant lines have been used in drug response studies and have demonstrated that zebrafish can be used for novel drug discovery of cardiac drugs (Kebler, Rottbauer and Just, 2015 and Asnani and Peterson, 2014). The advantages of using zebrafish embryos (as discussed 1.2.3) means that they are readily adaptable for drug screens. Only small volumes of drug solution are required for dosage and embryos can be easily maintained in a 96 well plate. This approach has been utilised for adaptation to a high-throughput model for zebrafish larvae as both a chemical and genetic screen (Pardo-Martin *et al,* 2010). This allows automated transference and orientation of zebrafish larvae for high resolution imaging at a cellular level in three dimensions (Pardo-Martin 2010). However, this loading process is limited to imaging analysis, and still performs imaging on individual larvae consecutively, rather than multiple fish simultaneously, which would be optimal.

Multiple studies have shown that zebrafish show similar cardiac effects seen in zebrafish larvae to known cardiac acting drugs in human (Gut *et al,*2017, Alzuade *et al* 2016, D'Amico *et al,* 2012 and Milan *et al,* 2003). Milan *et al* 2003, demonstrated that drugs which cause repolarisation abnormalities in humans, cause bradycardia in zebrafish larvae. Bradycardia is known to be an effect of Ikr channel (kv11.1 hERG) inhibition. This was a simple, but high throughput assay, highlighting the potential use

of zebrafish embryos in cardiac drug safety testing for repolarisation inhibitors, such as hERG blockers. Cardiotoxicity responses have been tested in zebrafish embryos, using visual assessment for bradycardia and AV block (D'Amico *et al*, 2011). Drug response analysis of known hERG blockers (n=6) and other cardiac acting drugs (n=7) was assessed in zebrafish larvae and found to exhibit a range of phenotypes including; AV block, bradycardia, ventricular fibrillation and death (Alzuade *et al* 2016). While this is strong evidence for a conserved cardiac drug response between zebrafish and human, to fully characterise these responses, assessment by electrocardiographic means would be required to further to validate zebrafish embryos as a model of human arrhythmia.

1.3.5.2.3 Zebrafish embryo ECG development and other technologies for cardiac assessment.

Further to visual observations of arrhythmia and cardiac dysfunction such as those described in Milan *et al* 2003, larval ECG procedures, along with other technologies such as echo scans for larvae have been developed (Milan *et al* 2003, Dhillon *et al* 2013 and Fuad, Kaslin and Wlodkowic 2018).

Recently, a rapid, lab-on-a-chip imaging protocol for micro-echocardiography was developed for assessment of cardiovascular activity (Fuad, Kaslin and Wlodkowic, 2018). They describe a millifluidic system, an imaging platform where embryos are immobilised using suction rather than agarose and prototypes created rapidly using 3D printing of moulds using SLA (stereolithography) and subsequent replica moulding in poly(dimethylsiloxane). This created a platform that removed the need for painstaking orientation and agarose-imbedding of embryos for imaging, increasing throughput and automation. It also improves the capacity for drug testing while on the platform; drug

delivery is not hampered by diffusion through agarose. Imaging was also performed using an automated system, producing programmable time-resolved video data. Larvae were anaesthetised for 5 minutes in MS-222, loaded, and left to acclimatize for 15 minutes prior to data collection, videos were recorded in colour, 60 frames per second and drug treatments lasted 30 minutes. Each chip had the capacity for up to 10 larvae. While representing a major step forward to automated zebrafish cardiac analysis, currently, only heart rate analysis has been reported using this device. More high resolution data, such as that from an ECG recording is needed to analyse phenotypes; for example QT prolongation from hERG channel blockade. However, using a platform such as the millifluidic system alongside integrated electrode arrays may be the solution.

An electrographical method for recording heart activity in zebrafish embryos was first described by Forouhar *et al* 2004. Pre-pulled glass capillaries, commonly used for extracellular recording were utilised, filled with conductive solution and manipulated and positioned onto 5dpf embryos using micromanipulators. Embryos were treated with PTU (phenylthiourea) to prevent pigment formation and were anaesthetised in 0.01% MS-222 (ethyl 3-aminobenzoate methanesulfonate). The resulting ECG traces, identified P and R waves, but the distinct PQRST wave pattern observed in adult traces was missing.

Dhillon *et al* 2013, optimised this single glass capillary electrode recording system for zebrafish embryos. Parameters investigated included; temperature, electrode placement and larval developmental stage. The results displayed clear PQRST wave pattern, and QT prolongation drug responses to known hERG blockers including terfenadine. While requiring further optimisation of parameters, this represented a key step in establishing a larval ECG protocol, but major adaptations would be required for high throughput

use, and single recordings mean collecting a whole data set is time-consuming (Dhillon *et al*, 2013).

1.3.6 Comparison of mammalian and zebrafish drug screens.

Mammalian models such as mouse and rat are widely used and established in the pharmaceutical industry and as a result, there are decades of information and data on these models, which is helpful for predicting responses. Also, this data comes from standardised protocols and husbandry which makes comparison of results across different labs more accurate. The zebrafish model's validity would benefit greatly in similar standardisation; and that would open up pharmaceutical companies to being more receptive to make the necessary adjustments to implement a fish model into their screening procedures. As close evolutionary species to human, they are a natural choice with high gene homology and drug responses to humans (Planchart *et al*, 2016). As well as electrophysiological advantages of using a vertebrate model with a similar heart beat and action potential to human, as opposed to the murine system with a fast heart rate and adapted action potential facilitating this, zebrafish embryos have the advantage of being readily adaptable to high throughput platforms (Leong *et al*, 2010).

Due to the many advantages discussed in this chapter, zebrafish have risen in prominence in recent years with ever increasing numbers of screens and platforms for use of zebrafish in drug discovery and development published. It has been postulated for some time, with a wealth of evidence that zebrafish could be used to predict drug toxicity (McGrath and Li, 2008). The question of the utility of zebrafish embryos as a high throughput toxicity assay for pharmaceutical development was addressed by Redfern *et al*, 2008. It is an established fact that early safety screens are required to try and address the fall in new successful drugs brought to the market. Those that do

succeed have to shoulder the financial responsibility of those that failed before it. This is substantial, as a reported 9 out of 10 candidate drugs fail before they reach market. This number could be reduced if new early screening tools, such as zebrafish embryos were employed (Redfern *et al* 2008). As discussed previously, a leading cause of drug candidate failure is cardiac toxicity through the hERG channel interaction. Zebrafish larvae can be used to detect hERG channel blockers, with high accuracy, causing cardiotoxic hERG blockers to be screened out early, saving funds. In addition, the hERG channel is not the only ion channel adversely affected by drugs, and use of an early *in vivo* screen such as zebrafish would screen for adverse effects across multiple adverse drug targets. Comparison of zebrafish front loading compatible assays with *in vitro* screens, identifies potential screens for cardiac, gut, renal and visual function zebrafish screens which may out perform their *in vitro* counterparts (Redfern *et al*, 2004). The attraction of zebrafish larvae as a model comes down to the ability of having an *in vivo* vertebrate model with high conservation with human on a high throughput platform (Goldsmith *et al* 2004). It is a model that can be utilised using existing toxicological endpoints, across morphology, physiology and behaviour assays (Kari, Rodeck and Dicker, 2007). In addition, advances in technology, for example in embryo manipulation and imaging, mean that robust platforms now exist for hosting high throughput zebrafish assays (Pardo-Martin *et al*, 2010, Yanik *et al*, 2016 and Roper, Simonich and Tanguay, 2018). However, there are obstacles to the implementation of high throughput zebrafish screens; firstly, inconsistency in husbandry practise, including variance in diet and feeding regimes. Diet is the biggest environmental factor and impacts on cellular signalling and has been shown to impact on the offspring's transcriptome. Secondly, toxicity assays require standardisation and validation. Protocol differences across laboratories include chemical purity, exposure

regimen, number of animals per well, all of which influence on chemical uptake (Planchart *et al*, 2016). Thirdly, inadequate description of zebrafish strains. In mammalian research, it has been clearly demonstrated that different strains will have different underlying physiology and therefore different chemical responses. Therefore, choice of strain and clear reporting on which strain has been used for a study is important. And lastly, disease monitoring remains insufficient. Zebrafish, like mammals are susceptible to infections which impacts on health and egg production (Planchart *et al*, 2016).

In addition, for many potential users, there are problems surrounding compound uptake. Zebrafish are dosed by being exposed to drug concentrations in the surrounding medium and responses measured. This assumes efficient drug uptake and metabolism alongside organ system development in the larval zebrafish. With using larvae, compound uptake relies solely on transdermal absorption until 72 hpf where some can be taken orally as the jaw develops (Langheinrich, 2003). This limits compounds pharmacology; for example, size and solubility, to ensure uptake into the larva. This raises questions about how exposure concentration relates to the dose achieved in the animal and how this is compares to dosing in other models. There are also uncertainties over how metabolically active these animals are, particularly given concurrent organ system development taking place, which impacts on (active) drug exposure. These considerations mean it is difficult to accurately determine the final dose achieved. Standardisation and consideration of these elements would go a long way to facilitate direct comparison between laboratory results and gain further support of the zebrafish as a model for use in pharmaceutical drug development. Even so, companies remain sceptical about how translatable certain physiology and biochemistry is and so

extensive validation studies are required to prove the reliability and effectiveness of the zebrafish model (Redfern *et al*, 2008).

As well as drug safety screening, zebrafish have also been used successfully to identify novel therapeutic compounds (Goldsmith *et al*, 2004, Zon and Peterson, 2005 and Kari, Rodeck and Dicker, 2007). Zebrafish are an accepted model for chemical safety assessments by regulatory agents, removing the barrier for their use in chemical screens (Johnston *et al*, 2017). Even with this body of evidence, the pharmaceutical company are still reluctant to invest in new screens, potentially using zebrafish embryos. This may be as although recent data suggests that zebrafish may be able to bridge the gap between *in vitro* models and *in vivo* mammalian models there are still hurdles to overcome before zebrafish can truly be instilled into drug development screening protocols (Sukardi *et al*, 2011 and Planchart *et al*, 2016).

1.3.7. Project Aims

This project proposes a high throughput zebrafish embryo ECG recording system for cardiac toxicity screening and identification of novel therapeutic compounds. This study focused on developing the zebrafish embryo as an arrhythmia model using high resolution ECG recordings *in vivo* of the larval heart. This chapter evaluates current models against zebrafish and concludes that the zebrafish, may be the next logical step for pharmacology screens, particularly for cardiac toxicity. A zebrafish embryo ECG recording system has been successfully demonstrated. Further optimization of this system and making steps towards adapting it for high throughput capability has the potential to change the way cardiac toxicity is detected in candidate drugs (Dhillon *et al*, 2013). Early exclusion of hERG blockers, for example, is crucial to streamline the drug development process and reduce the financial burden on successful drugs brought

to market as well as guaranteeing patient safety. Platforms using analysis tools such as the automated system described in (Hughes, Tarassenko and Roberts, 2004) removes the potential bottleneck of data such approaches would create and produce standardised data readouts of heart rate and ECG parameters, (unpublished data Barrett *et al* 2015). Compared to other arrhythmia analysis approaches, ECG produces high resolution, comprehensive data showing a detailed picture of cardiac function.

The aim of this study is to demonstrate the utility of an ECG recording system for cardiac arrhythmia in zebrafish embryos both by drug induction and from arrhythmic zebrafish lines. This could be a significant, informative tool for both drug discovery and cardiac toxicity testing.

2. ECG PARAMETER OPTIMISATION:

- Investigation into the potential effect of anaesthetic on larval zebrafish heart rate and QTc.
- Investigation into the effect of electrode distance on ECG recording in zebrafish larvae.
- Optimisation of ECG parameters for the development of a high throughput recording system.

All work pertaining to the ECG experiments for non-contact recordings and the effect of anaesthetic in this chapter were performed by me solely. The microfabricated electrodes were designed and manufactured by Richard Barratt. The twisted pair electrodes were made by him and myself. The testing of the microfabricated electrodes were performed by myself (mainly) and in collaboration with Richard Barrett.

2.1. Introduction

2.1.1 Parameter development and optimisation of the single electrode zebrafish ECG recording system.

A protocol for larval zebrafish ECG recording was developed by Dhillon *et al* 2013. This protocol established that recording electrical activity from the developing larval zebrafish heart was not only possible but potentially presented a viable alternative to more invasive and time consuming techniques using mammalian animal systems. Dhillon *et al* 2013 investigated a number of parameters to optimise the recording procedure and to investigate the effect of these parameters on larval heart activity and the recording protocol. These included; temperature, embryo development stage and electrode position across the heart. In this work, parameters were taken and developed further to optimise for more detailed recordings and to make progress towards a high throughput system.

2.1.1.1 The effect of temperature on the ECG parameters recorded.

Temperature is an important parameter to investigate as it is well established that increasing temperature increases heart rate in mammals (Deutschman *et al*,1994). Dhillon *et al* established that this was also true for the larval zebrafish heart and that this also impacted on ECG parameter measurements such as QT. Therefore, it is important to control temperature for the duration of the recording and keep it constant. While the ideal temperature for zebrafish temperature is 28.5^{o}C, practically, this was difficult to control and maintain throughout the recording while keeping the system electrically quiet to reduce interference with the recording signal. Therefore, the majority of recordings for Dhillon et al, 2013 were performed at room temperature.

However, it would be more optimal and more informative of the normal zebrafish ECG signal to record from the heart at the natural environmental zebrafish temperature of 28.5^{o}C. At this temperature, as established by Dhillon et al, 2013, the heart rate is higher and QTc lower that when recorded at room temperature. This means that they will be considered bradycardic at a heart rate much faster than humans when in their normal environment and establishing what is normal for zebrafish is important for then being able to determine and study the larval zebrafish heart when abnormal, either due to external environmental factors such as drug treatments, or due to genetic mutations.

2.1.1.2 Optimal larval zebrafish development stage for ECG recording.

The larval heart develops rapidly so to standardise the recording protocol the larval development stage needed to be kept consistent. Due to licence restrictions it was necessary to keep under 5 dpf. Dhillon *et al* concluded that the optimal development stage was 3 dpf (days post fertilisation). This was the stage ultimately decided upon for the recordings collected for this project. This is because at this stage, the rudimentary heart tube had looped and developed into the two distinct chambers, atrium and ventricle, with co-ordinated contraction due to ion channels established. By 48 hpf the heart and cardiovascular system is fully functional with all ion channels formed and in place (McGrath and Li, 2008). At this stage it is still early enough to maximise facilitation to high throughput development. In addition, performing the experiments at 3 dpf created a better weekly throughput for these experiments, maximising the amount of data collected.

2.1.1.3 Electrode position on the larval zebrafish heart.

Dhillon *et* al investigated the effect of recording at different positions across the heart, and found that there was no significant difference in ECG parameter measurements e.g. QT. Different positions consistently recorded comparable ECG parameter measurements but that it was easier to record different parameters and see a complete PQRST signal waveform with the electrode positioned centrally on the heart at the AV canal (similar to mammalian atrio-ventricular junction). At this position PQRST waveform was easier to detect and clearly recorded with a favourable signal: noise ratio. However, it would be more useful to record electrical activity from the two chambers of the zebrafish heart separately, to improve signal quality and increase the amount of data obtained from these recordings. This is because, while the AV canal is the optimal position to record a full ECG with PQRST waveforms using a single electrode, recording from more positions simultaneously, specifically individual atrium and ventricle recordings would increase the likelihood of detecting the smaller, atrium signals which corresponds to the P wave in a typical ECG. Also, the ability to record with more than one electrode has the advantage of moving the zebrafish recording system to more closely resemble the 12 lead human diagnostic ECG. This allows greater sensitivity and resolution of the ECG data, making it a more useful tool for clinical research. Being able to record and identify separate atrium and ventricle signals will also increase the diagnostic ability of the recording system when applying cardiac drugs that target different parts of the cardiac cycle.

2.1.1.4 Immobilising agents to facilitate ECG recording.

In order to position and record from zebrafish larvae, it is necessary to immobilise them for compliance and to prevent motion artefact in the recording. The established single

electrode recording system used MS-222 at 0.3 mg/ml to sedate the larvae in order to manipulate the larvae, position the electrode and obtain recordings. This is the standard method for immobilising zebrafish for ease of manipulation, (Kimmel et al 1994). Humans under general anaesthesia can experience heart rate variability (HRV) due to increased vagal/autonomic nervous system activity. This results in supressed heart rate, blood pressure, breathing and gastro-intestinal tract movement (Deutschman, *et al* 1994). One of the main considerations in Dhillon *et al* was the immobilising method to facilitate the recordings. It was important to establish an efficient immobilising method and two immobilising agents were compared; ethyl 3-aminobenzoate methanesulfonate (MS-222) and tubocurarine. It was concluded there was no difference in ECG parameters between these two agents. However, to truly test whether the use of immobilising agents has a significant effect on the ECG parameters, recordings from anaesthetised embryos need to be compared to recordings taken from non-anaesthetised embryos. One of the main aims in this study was to establish the effect of commonly used anaesthetic MS-222, on the heart rate and ECG parameter measurements at the concentration that is used on larval zebrafish for ECG recording. To do this, a method of immobilisation without the use of anaesthetic needed to be developed.

2.1.1.5 Parameter development summary

Overall, there are further developments that could be made to optimise the recording system, hence further parameter development and optimisation would improve both the quality of the data recorded and expand on the potential usage of the recording system. Throughout the duration of this project improvements and developments to the recording system in these areas were devised and implemented into the recording set up. These included a temperature controlled recording plate allowing recordings at

28.5^{o}C, a dual electrode recording system to allow signals to be recorded from the atrium and ventricle simultaneously and a method for recording from non-anaesthetised embryos. This chapter will discuss the development of a system to record from non-anaesthetised embryos to investigate the effect of MS-222 on the heart rate and ECG parameters at the concentration used for ECG recording.

2.1.2 Optimisation of parameters with the later goal of high throughput recording

One of the principal aims in this project is to make steps towards a high-throughput recording system for larval zebrafish ECG. The single electrode recording system produces high resolution signals for analysis of heart activity. However, there were two rate-limiting factors that affected the throughput of the recordings. Firstly, the system only has the capacity to record individual zebrafish larvae in turn, whereas the established method for drug treatments on zebrafish larvae used 96 well plates and microscopy to analyse the drug effect (McGrath and Li, 2008), therefore have a much greater capacity. However, ECG data has higher resolution, so greater depth of cardiac data can be obtained, therefore it is preferable. Secondly, it is a laborious and meticulous process to correctly position the electrode on the heart for ECG recording. This means that it is a long, time consuming process to record an entire data set. In order to move towards a higher throughput recording system these issues would need to be addressed first.

2.1.2.1 High throughput parameter testing: non-contact recording

A major factor affecting the throughput is the time-consuming process of positioning the electrode across the heart. The position of the electrode on the heart greatly impacts on the size, shape and quality of the ECG recording signal making it necessary to painstakingly position the electrode to the optimal position across the heart. This is in order to obtain a full, clear, high quality ECG with PQRST waveforms. In particular, the P wave which is the atrial component of the ECG is more difficult to pick up unless correctly positioned. The dominant waveform, the QRS complex is much easier to detect as well as the T wave as these are the ventricle components. The size of the larval zebrafish heart at 3 dpf is approximately 100µm across, so positioning must be accurate to within a few microns in order to detect both atrium and ventricle signal components. This makes positioning the most time-consuming step in the recording process and a potential barrier to high throughput recording. One possible solution to this problem would be to record ECG signal from a position slightly away from the heart, removing the need for painstaking micron-accurate positioning on the surface area over the heart. Dhillon et al, 2013 showed measurements for QTc prolongation, an arrhythmia effecting the ventricle, can accurately be measured consistently across the heart. Therefore, as detecting the P wave is position sensitive, to establish whether recording at a distance from heart was possible, QRS and T wave signals were prioritized so that a measurement of QT could be taken. To investigate the possibility of a system using this technique, the established single electrode recording system was adapted to establish whether it was possible to record quality, QRST, ECG signal from non-contact positions and, if successful, to measure this distance.

2.1.2.2 High throughput parameter testing: development of new reusable, metal electrodes.

The glass capillary electrodes used for the current single electrode recording system are fragile, prone to blockage and damage and as such are replaced frequently. To move to a higher throughput system, these glass electrodes would need to be changed for a more durable, less fragile and more reusable electrode, without compromising the high resolution recordings the glass electrodes yield. This would also introduce the potential for multichannel recording, and the possibility to increase the number of zebrafish recorded simultaneously which in turn would also increase the throughput.

Upgrading the glass capillary electrodes to a metal bespoke electrode design introduced some challenges to overcome with impedance in the electrical circuit. There was a need to think carefully about how the signal is transferred in the capillary and how that changes when a metal electrode is used. The electrical signal in the zebrafish heart is ~5-30µV. This is a very small signal and to detect it the electrode needs to be very sensitive, with a low impedance (>1MOhmat 10Hz), otherwise the signal will not be seen. Glass capillary electrodes have a low impedance as the signal travels from the heart through the capillary tip and to the chloridised silver wire through the potassium chloride solution that fills the capillary. The signal is then transferred to the wire over a very large surface area (the surface area of the wire inside the capillary) and this keeps the impedance low and the signal only has to travel through a resistance circuit due to direct current flow (DC). Metal electrode signal transfer differs significantly. In these electrodes (both microfabricated and twisted pair) this signal transfer happens at the electrode tip, at the surface of the heart. This means that the surface area is much smaller than the surface area available in glass capillary along the silver wire, therefore the impedance is much larger. If the impedance is too high the signal cannot be

recorded. The tip has to be plated to increase the surface area, reducing the impedance to under the threshold impedance of (>1MOhmat 10Hz.

2.1.3 Aims

- To investigate the effect of anaesthetic on the heart rate and ECG signal. To determine this accurately, a comparison needs to be made between an anaesthetic and non-anaesthetic recording. Therefore, a method for ECG recording from non-anaesthetized embryos must be devised. To do this, the embryos must be immobilised for ECG without anaesthetic.

- To establish whether contact is required for successful recording of ECG or whether it is possible to record from a non-contact position, and how far from the embryo this can be done. If recording can be taken from further away from the zebrafish, this will aid development of a high throughput system by removing the need to accurately position electrodes.

- To investigate alternative materials and designs for more durable, reusable and less fragile electrodes capable of recording ECG from larval zebrafish to aide development of a high throughput recording system.

2.2 Methods

2.2.1 Zebrafish Husbandry and embryo collection

For all experiments wild-type AB zebrafish embryos were used. All zebrafish were handled according to the UK animal (Scientific Procedures) Act of 1986 with appropriate home office licensing. Adult zebrafish were maintained using standard conditions in a flow-through system of aerated, charcoal filtered tap water with a 12 hour light/dark cycle (Techniplast; UK).

Breeding pairs were set up in separate breeding tanks, filled with system water and left over night. Embryos were collected the following morning and transferred into petri dishes containing E3 medium (2.2.11) and incubated at 28 ^{o}C until 3 dpf.

If pigment free embryos were required, the E3 medium contained 0.2mM Phenylthiourea which inhibits melanogenesis. This concentration was used as higher concentrations can cause toxicity. Pigment free embryos were used in trials of Microfabricated electrode prototypes to help visualise the heart in the pipette tip set up but were not used for any formal ECG data collection recording.

2.2.2 Single electrode glass capillary recording procedure

For all experiments, unless otherwise stated (non MS-222 experiments) the zebrafish embryos were anaesthetised for immobilisation in MS-222 at 0.3 mg/ml (Sigma).

2.2.2.1 Making glass capillary electrodes

A borosilicate glass micropipette (P84, world Precision Instruments) was pulled on a micropipette capillary puller (Sutter instruments P-80, Brown flaming micropipette puller) to give a 2 μm tip and then filled using MicroFil with 3 M potassium acetate

solution (Sigma) coloured with methylene blue (Sigma) for ease of visualisation under the microscope

2.2.2.2 ECG Recording procedure

To perform an ECG recording, 3 dpf embryos were positioned and orientated on a pre-made, specially designed recording plate. Agarose (molecular grade agarose (Bioline) was set with a hand-made mould to create grooves, in a standard petri dish (100mm x 15mm) (Fisher Scientific) containing 9 ml of E3 with 0.3 mg/ml MS-222. The plate was then positioned under a Nikon SMZ600 microscope and the embryo orientated ventrally in a groove, to give the best view of the heart. Temperature is monitored for the duration of the recording to prevent changes in temperature affecting the heart rate. Temperature was monitored using Cryocon 22C (cryogenic control systems) and recordings performed at room temperature. This whole set up sat inside a Faraday cage to ground and minimise electrical noise.

The electrode tip, was positioned at the AV canal on the skin surface of the zebrafish which is between the atrium and the ventricle using a micromanipulator (Narishige) and a motor arm (Inchworm, Burleigh).

A chloridised silver wire with a complimentary pin soldered to one end was inserted into the capillary and connects, via the pin to the amplifier (NPI electronics, for settings: 2.2.2.3) and the signal is then passed through a filter, Humbug (Quest Scientific) to minimise background noise. The analogue signal was then processed through Powerlab (ADInstruments), an analogue digital converter, and displayed on the computer screen using compatible software Labchart (ADInstruments). A second, reference, electrode was positioned in the recording plate at a distance away from the

fish to complete the circuit. Inchworm (Burleigh), allows incremental adjustments of the position (4 µm steps) until a detailed, stable ECG signal was achieved then the recording was started. Detailed ECG refers to all features (PQRST) visible in the recording. Schematic of recording set up set out in **figure 2.1.**

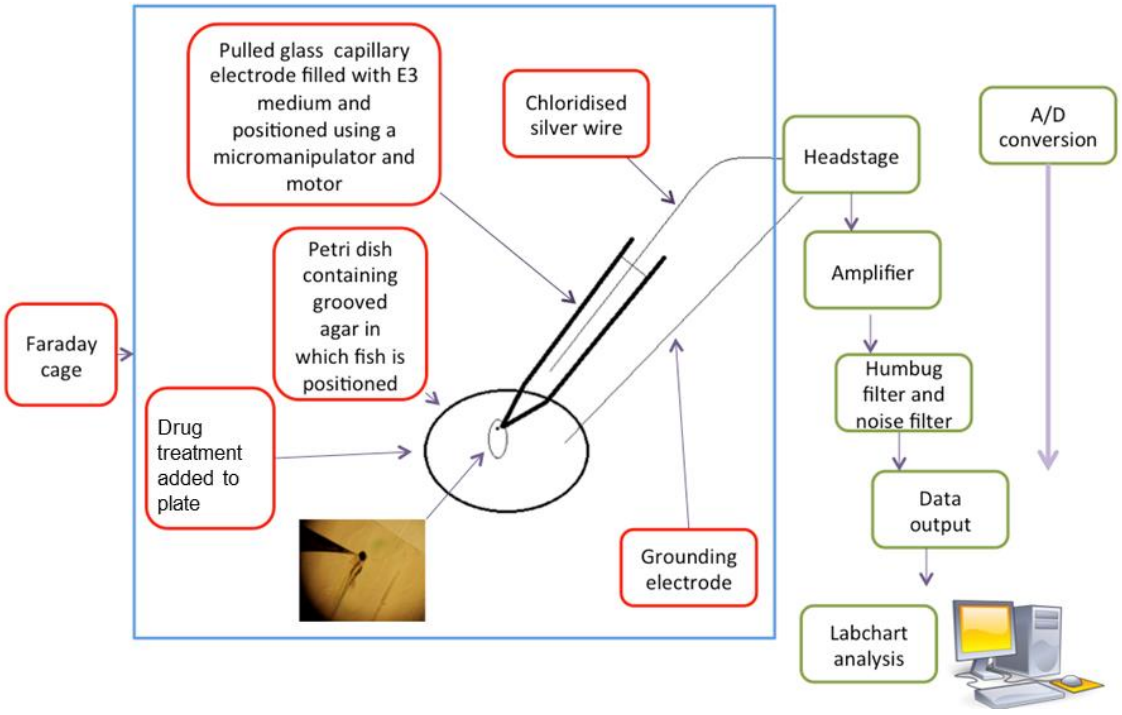

Figure 2.1 Schematic of the recording set up for the single electrode recording system.

2.2.2.3 NPI Amplifier.

A single point amplifier, with applied filter settings to keep the impedance of the system lower. For settings; see table 6.1 (appendices). These filter settings were fixed to allow the maximum amount of data to go through to Powerlab (ADInstruments). Here in Labchart (ADInstruments) more restrictive filter settings were applied, table 6.1 (appendices), to more easily visualise the ECG signal.

2.2.3 Non -contact recording system development: Glass block recording set up and bent electrodes.

2.2.3.1 Glass block set up

To allow an electrode to come in flat perpendicular to the embryo, but still have a groove to stably orientate the embryo, a glass block with a carved cross and a thin coating of agar was used mounted in a 14 cm petri dish (Fisher Scientific). A zebrafish larva (3dpf) is positioned at the intersection of the cross. The rest of the set up follows as the procedure outlined in 3.2b with the reference wire positioned behind the embryo and the bent glass capillary electrode approaches the embryo from the groove in front.

2.2.3.2 Bending glass capillary electrodes.

Bending the electrodes allowed the electrode to approach the embryo perpendicularly and visualise when the point of contact occurs. To create a bent electrode, once the borosilicate glass capillary had been pulled (Sutter instruments P-80, Brown flaming micropipette puller) it was bent to 30 ^{o} using a Microforge (MF 830, Narsighe) according to the scale in the eye piece lens. The electrode was then filled with 3M potassium acetate (Sigma) and used as normal.

2.2.4 Method for ECG recording from non-anaesthetized embryos.

Embryos were immobilised for non-anaesthetized ECG recording using agarose. Embryos were mounted in 1% low melting point agarose (Sigma Aldrich) in a 4 cm petri dish (Fisher Scientific). Zebrafish larvae aged 3dpf were indicidually pipetted into small petri dishes, the excess liquid removed and a drop of molten agarose added. The agarose was allowed to cool to 30^{o}C before a drop was placed over the larva. This was

sufficient to immobilise the embryos effectively. This was then left to set. After being set, 3 ml of E3 embryo medium was added to the plate and the section of agarose around the heart was removed using forceps. This was to stop the glass capillary electrode from clogging up with gel during positioning and recording, which would affect the measurement. Control experiments where embryos were mounted in agarose and anaesthetised, the embryos were pretreated in 0.3mg/ml MS-222 (Ethyl – 3aminobenzoate methanesulfonate, Sigma Aldrich) and then mounted the same way.

2.2.5 Microfabricated electrode manufacture and micropipette tip recording set up to aid zebrafish orientation.

2.2.5.1 Microfabricated Probes

The microfabricated electrodes were designed and produced for this project by Dr Richard Barrett. A layer of gold metal was evaporated onto a layer of plastic and a top coat of plastic overlaid. A 10µm tip was then laser cut out from the plastic to expose the gold. The opposite end would then be wired up with complimentary gold pins to allow the electrode to be attached to the amplifier, Tucker Davis Technologies. The process allows very specific 2D designs to be created.

The electrodes are then plated by being placed in chloroplatanic acid (platinum plating solution) and applying a negative current relative to a silver ground electrode. The plating process was necessary to lower the impedance of the electrode to below 1 M Ohm at 10 Hz, without this low impedance, the ECG recording could not be achieved using these electrodes. The glass capillary electrodes are very low impedance as the potassium solution creates a salt bridge keeping the impedance low, and stable, over a frequency range.

2.2.5.2 Micropipette Tip set up.

Zebrafish larvae are pre-treated in MS-222 (ethyl-3aminobenzoate methanesulfonate) at 0.3 mg/ml) for 10 minutes. The embryo was then collected up using a Pasteur pipette, and inserted, up to the yolksac/pericardial sac boundary into a disposable micropipette tip (50 µm). The pipette tip was then secured to a micromanipulator and lowered into a petri dish containing 0.3 % MS-222 in E3 medium, total volume 9ml using E3 medium. The microfabricated probe was attached to the motor arm and lowered into the petri dish next to the embryo. The embryo position was then adjusted using the micromanipulator until positioned underneath the microfabricated probe in a contact, recording position. Orientating the embryo to the microfabricated device created a more stable contact between the two for a recording to be taken.

2.2.6 Multichannel System

Multichannel recording was performed using the TDT multichannel recording system (Tucker – Davies Technologies). The same grooved agar plate was used for recording as 3.2b. The electrode (glass capillary, twisted pair or microfabricated electrode) is connected to a 16 channel headstage (Tucker Davis Technologies). This headstage had 16 inputs, a reference and a ground electrode. The headstage connected to a pre-amplifier (PZ2-256, S^3 z series, Tucker Davis Technologies) which has a 256 channel capacity. The signal is digitised in the processor (RZ2 BioAmp Processor, S^3 z series, Tucker Davis Technologies). TDT uses Open WorkBench (Open WorkBench 2.12, the user interface of OpenEx Suite, TDT) software to visualise the signal and perform some analysis. This software allows programs to be designed to manipulate the signal as best fits your project. These include filter settings, analogue output to Labchart, recording blocks can be exported to Matlab, and recording channel and reference channel

selection for differential recordings. For continuity, all TDT recordings analysed in this chapter were analysed in Labchart (Powerlab), so direct comparison with glass capillary electrode recordings, also analysed in Labchart, could be done.

2.2.7 Production of twisted pair electrodes.

Twisted pair electrodes are created using long lengths of wire folded in half and twisted together along the entire length. The folded end was cut and soldered complimentary pins to the recording system, for this study, the multichannel Tucker-Davis Technologies system. A wide range of twisted pair electrodes were made, using different wire materials and diameters with different plating material combinations.

2.2.8 Labchart analysis

For all glass capillary recordings, the signal was visualised using Labchart (Powerlab). Labchart is the complimentary software to the Powerlab analogue-digital converter used for these experiments. The TDT recorded signals were output to Powerlab so that these recordings could also be analysed in Labchart. Labchart allows filters to be applied to the raw signal for better visualisation of the signal.

Sections can be highlighted for analysis and then the built in analysis software locates the ‘R’ peaks and marks them along the recording trace. Manual manipulation ensured this was accurate and any outliers where the ’R’ peaks were not correctly identified were excluded from the parameter measurement. These labelled cardiac cycles were then and overlaid to produce average cardiac cycle from the selected section and from this the R-R, QRS, QT and QTc ECG parameters and the heart rate were calculated.

2.2.9 Statistical analysis

The p-values to determine statistical significance of the anaesthetic and non-anaesthetised groups were calculated. Firstly, normality tests, Shapiro-Wilk and Anderson-Darling, were performed which showed normal distribution for all the data groups. Therefore a parametric paired, two-tailed t test was then performed to determine statistical significance between the groups. They were also each tested against the control group in the same way.

2.2.10 Drug stocks

Drug treatments were routinely used to confirm the efficacy of new recording set ups and protocols. For each new recording set up a recording was performed with a glass capillary electrode and a drug treatment (terfenadine or verapamil) applied. This was to ensure that a QT interval change could be recorded and analysed using each set up. This verified the quality of the recording was acceptable for measuring drug induced arrhythmias throughout electrode development. Terfenadine has been demonstrated previously to produce a QT prolongation and this was measured in each electrode development (Dhillon *et al*, 2013). Drug stocks were made up in E3 medium. Terfenadine (Sigma) was prepared in 10 mM stock in E3 and DMSO (10 % Sigma Aldrich), to aide solubility. Stocks were diluted using E3 and the final concentration of DMSO on the recording plate was less than 2 % for both concentrations (0.5μM and 5μM).

2.2.11 E3 Medium protocol

	1 x E3	50 x E3
5.0 mM NaCl (58.44)	0.292g	14.6g
0.17mM KCl (74.55)	0.013g	0.65g
0.33mM CaCl (147.02)	0.044g	2.20g
0.33mM MgSO4 (246.5)	0.081g	4.05g

2.2.12 PTU Phenylthiourea

Standard dilution 0.2mM solution made up using E3 medium.

Table 2.2 NPI amplifier and labchart settings

NPI amplifier	Gain	1000
	Band pass filter	Low:0.3 Hz High 2 K Hz
Labchart	Raw data	No calculation
	Wide band pass filter	Low 0.3 Hz High 20 Hz
	Narrow band pass filter	Low 0.3 Hz High 10 Hz
	Sample rate	4 k/s (1 k/s when used with the multichannel system, TDT: 3.9

Table2.2: NPI Amplifier settings used for glass capillary recordings

2.3. Results

2.3.1 Investigations to determine if anaesthetic affects heart rate and QTc.

It was important to investigate whether there is an anaesthetic effect on the larval zebrafish heart rate and ECG parameters, such as QTc, because it could potentially compromise results. Dhillon et al 2013 compared MS-222 (an anaesthetic) and tubocurarine (a neuromuscular block) as immobilising agents, but did not compare these measurements against ECG's taken from non-anaesthetised embryos. At high concentrations these compounds will affect heart rate, MS-222 decreases heart rate and tubocurarine increases heart rate so it was important to compare against ECG measurements taken from zebrafish larvae without any chemical immobilising agent. Therefore, comparison of anaesthetized embryo recordings and non-anaesthetized embryo recording was necessary to determine the effect of anaesthetic on the heart rate and ECG parameters, recordings using MS-222 as an immobilising agent needed to be compared to recordings taken from non-anaesthetized zebrafish embryos. However, the embryos still had to be effectively immobilised to perform an ECG. This was achieved by mounting embryos in 1 % low melting point agarose This is shown in **figure 2.2**.

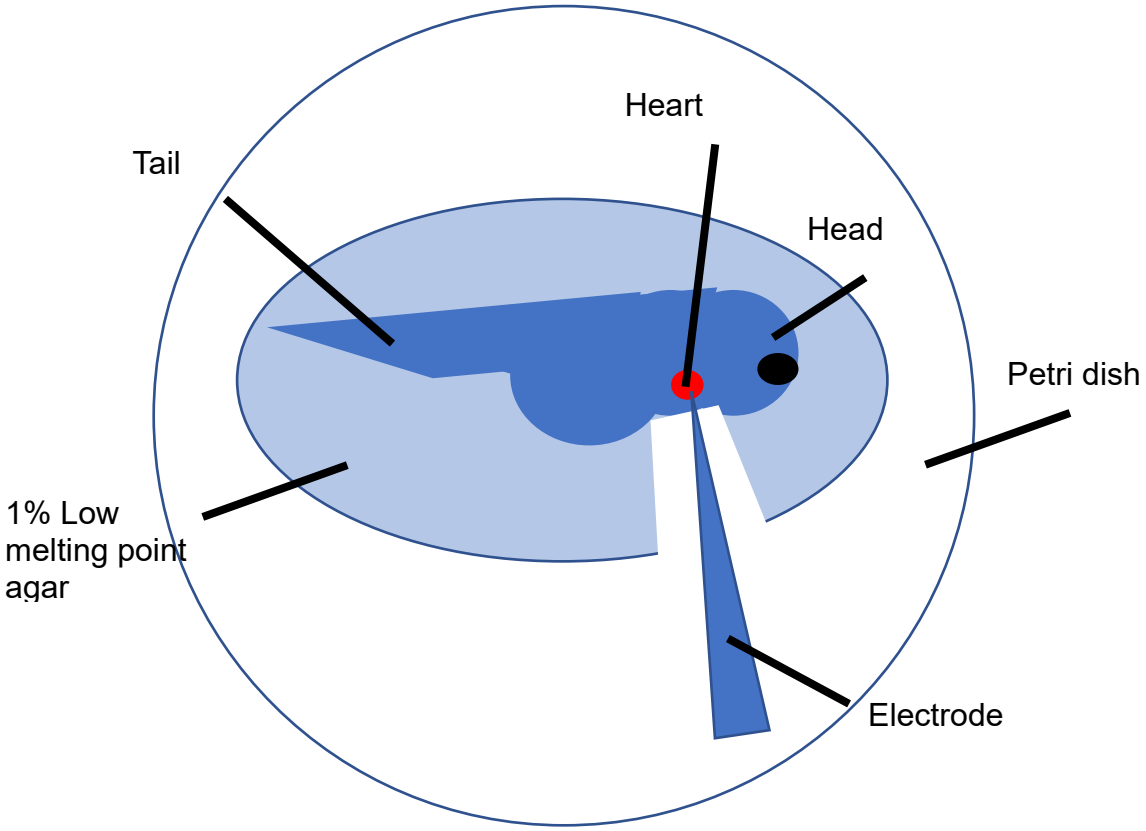

Figure 2.2 Schematic showing the embryo embedded in 1% low melting point agar and the section of agar removed to allow the electrode access to the heart without getting clogged up by the agar.

Following n=5 trial experiments using this technique, an additional step was included. Once the embryos were mounted and the electrode positioned, the trace was started but not recorded for measurement for a further 2 minutes. This is because a fast heart rate is induced through embryo manipulation and electrode positioning, not seen when the zebrafish is sedated using anaesthetic. This delay was to allow the heart rate to stabilise so that a true baseline recorded, at rest, could be taken for comparison against anaesthetised recordings. 5-minute measurements from non-anaesthetised embryos (n=24) were recorded using this method. For comparison, anaesthetised embryos were

also recorded using this method. These were anaesthetised in 0.3 mg/ml MS-222 for 10 minutes prior to mounting in agarose. These 2 data groups were also compared to measurements taken using the standard set up, where the embryos are anaesthetised and not mounted in agarose (n=24).

The results show there is no significant difference in QTc between mounted embryos with and without MS-222 (p value = 0.623) and no difference between mounted and unmounted (p value = 0.710). The heart rate is not significantly lower when under anaesthetic, (p value = 0.508), as shown in **figure 2.3.**

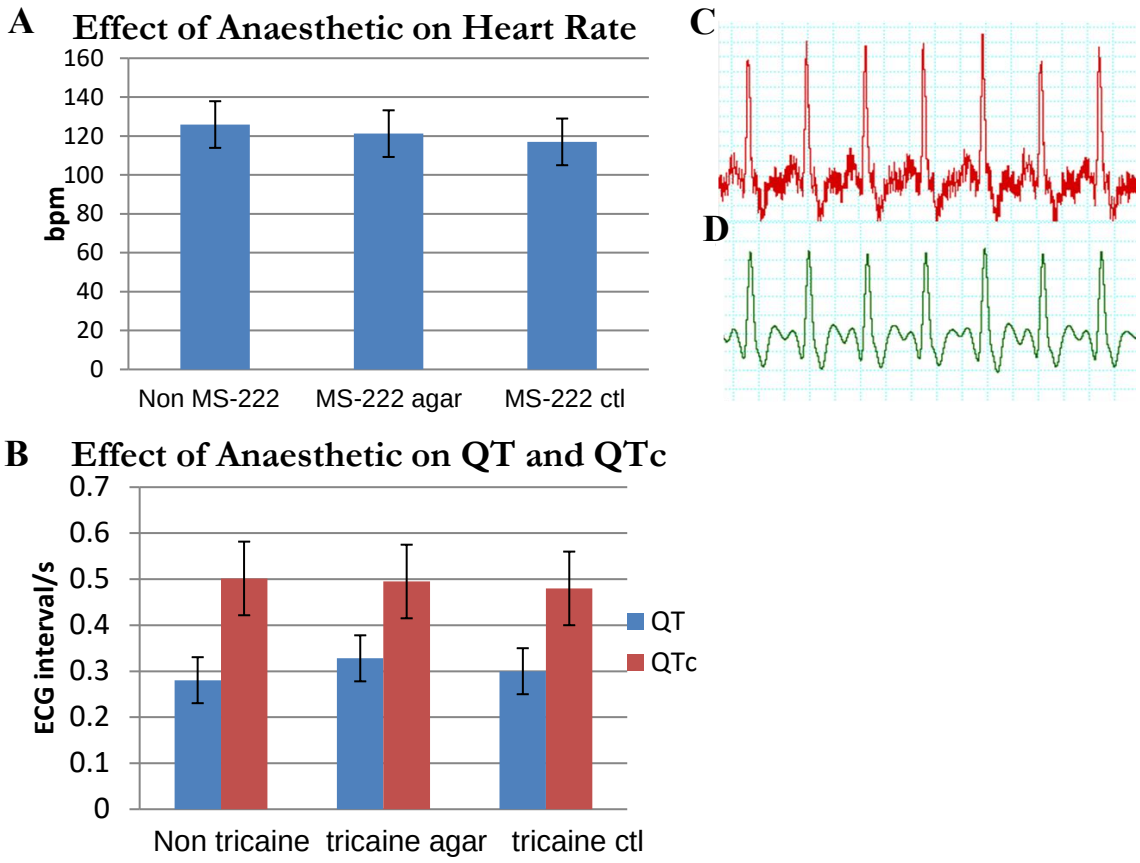

Figure 2.3 Effect of 0.3mg/ml MS-222 on the heart rate and QTc interval of 3dpf zebrafish heart.
A) Average heart rate of a 3 dpf zebrafish embryo mounted in L.M.P. agarose with and without anaesthetic (MS-222). Ctrl is the average heart rate of 3 dpf zebrafish embryo not in mounted agarose and under anaesthetic.
B) For the same groups, average QTc interval. C. Raw ECG recording from a non-anaesthetized 3 dpf zebrafish embryo. D. Filtered ECG using a narrow band pass filter Low: 0.3 Hz, High: 10 Hz.

Therefore, conclude that 0.3mg/ml MS-222 does not significantly affect the heart rate and QTc of 3 dpf zebrafish larvae. In conclusion, while non-anaesthetic recording would be preferable, the set up is time consuming and greatly reduces throughput. The use of MS-222 dosage for immobilisation for ECG recording can continue to be used without affecting ECG recording parameters.

2.3.2 Zebrafish larvae ECG recording from a non-contact position.

The recording procedure for larval zebrafish ECG recording is labour intensive, meticulous and lengthy. In particular, positioning the electrode accurately for detailed PQRST ECG signal is the rate limiting step, and reduces the recording throughput. For high throughput ECG recording it is important to remove the necessity to accurately position the electrode for a signal to be obtained, if the amount of time to position was reduced, this would increase the throughput significantly. Therefore, studies were carried out to determine whether it is possible to record ECG without touching the embryo and the maximum distance away from the heart successful recording could be achieved. This was carried out using a glass capillary electrode and calibrated motor arm to measure the distance. This could then be used as a parameter to build into a high throughput set up.

2.3.2.1 Development of alternative electrode set up for non-contact recording.

2.3.2.1.1: Preliminary experiments highlighting the issues with standard setup.

Initial experiments, to determine whether recording from a non-contact position was possible, were performed using the established single electrode recording procedure. These preliminary experiments to investigate this simply started from the recording position at the AV canal and then took incremental steps back from that position using the inchworm (Berleigh). The steps were calibrated to 4 µm so that a distance from the number of steps could be calculated. There were problems with this approach as although the electrode was moving away from the recording position, it was still moving across the heart due to the angle the electrode approached the heart at, so the

amplitude of signal fluctuated as the electrode moved across the heart in and out of recording positions. This meant that it was not possible to tell clearly when or if the electrode was no longer touching the pericardial sac due to the angle of observation from the microscope in this set up, and therefore any measurement of distance away from the heart could not be reliably measured, see **Figure 2.4**.

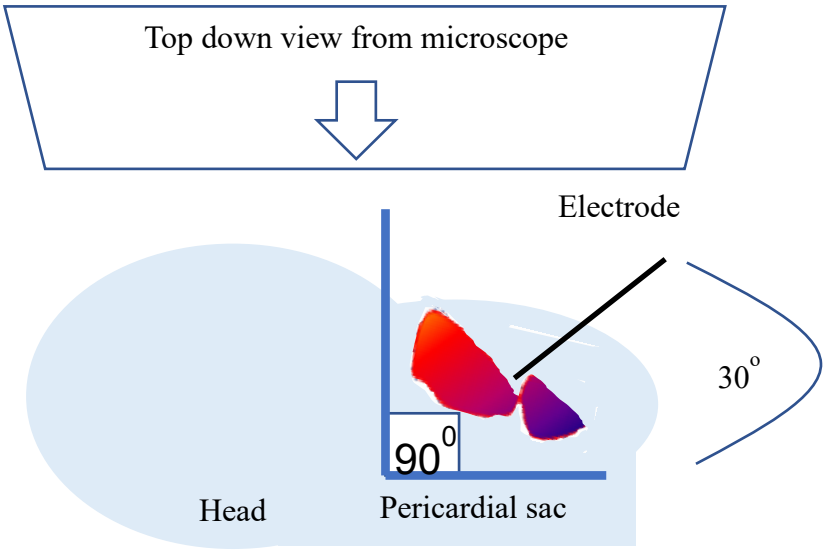

Figure 2.4 Schematic to demonstrate the problem encountered by using the single electrode recording system for non-contact recording. As the electrode moved back on the motor arm it also travelled across the heart causing the signal amplitude to fluctuate making it difficult to determine when it had left the surface of the pericardial sac and to measure the distance. On the standard system the electrode comes in at a 30^{o} angle. In order to see clearly, the set up was changed so that the electrode could come in at a 90^{o} angle to the embryo from a top down perspective through the microscope.

In order to see clearly when the electrode left the surface of the pericardial sac a change to the set up was needed to allow visualisation of this with ease. For this to happen the electrode needed to approach the embryo at a 90^{o} from the top down microscope view.

2.3.2.1.2: Optimisation of visualisation of electrode set up for distance recording.

It was clear from these preliminary experiments that to perform and confirm a non-contact recording, the set up needed to clearly show the edge of the pericardial sac and the electrode tip at a 90^{o} angle to the top down microscope view. As this is a 90^{o} angle from the microscope view, so as to visualise when the electrode is on or off the heart, the electrode needed to come in alongside the embryo rather than from above it. Incremental steps away from this position can then be used to calculate the distance from the embryo that an ECG signal could still be recorded.

To arrange the set up for a position at 90^{o} to the pericardial sac, the glass capillary electrodes needed to be bent. The angle from which the electrode approaches the embryo was calculated to be 30^{o} to the horizontal axis therefore the electrodes needed to be bent to 30o to compensate. Pulled borosilicate capillaries were bent to 30^{o} using the Narsighe microforge. To facilitate using these new electrodes, a new recording plate using a carved glass block was created. The glass block used in the setup has a cross carved into it. This design means that when an embryo is positioned at the intersection of the cross, the recording electrode can approach the heart from one channel and the recording electrode can sit behind the embryo, resulting in the electrode travelling through the embryo, which improves the signal strength. This set up, detailed in **figure 2.5**, allowed the electrode to be positioned at in a recording position just touching the pericardial sac and then move the electrode in 4 µm steps back until the ECG signal is lost.

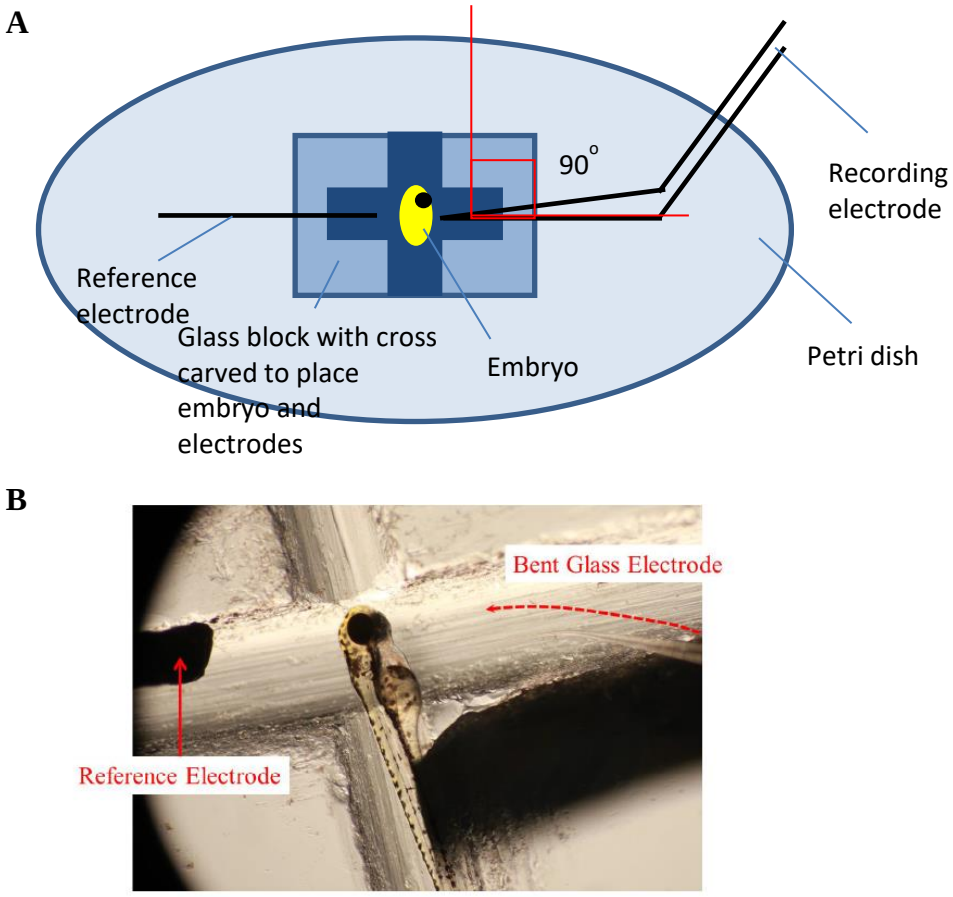

Figure 2.5. Development of set up for non-contact recording.
A) A schematic of the glass block set up showing where the embryo is positioned and the bent electrode and reference electrode as seen from view angle.
B) Image of the embryo and electrodes in the set up. From this orientation it is easily visible when the electrode is on or off the heart.

2.3.2.2 Non-contact recording achieved and visualised using alternative electrode shape and positioning.

2.3.2.2.1 Non-contract recording achieved and confirmed with high resolution imaging.

The set up described above was used and this orientation allowed the recording electrodes to be positioned at a 90° angle to the pericardial sac. Incremental steps at 4µm allowed the distance from the embryo from which an ECG signal was still recorded to be quantified. Using this recording set up, an ECG signal was recorded

from a non-contact position, confirmed by high resolution imaging of the electrode position, see **Figure 2.6**. The larvae in figure 4.5 had a haemorrhage just below the heart, due to prolonged positioning on the glass block. Larval zebrafish ECG recording from a non-contact recording position with glass capillary electrodes has not been previously reported, and represents a significant step towards a high throughput system.

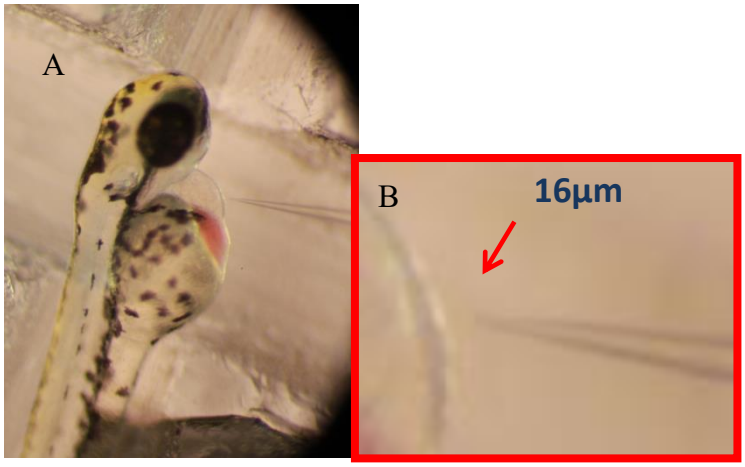

Figure 2.6 Non-contact ECG recording achieved at 16µM from embryo surface.
A) 3 dpf embryo positioned in non-contact set up where the 30º bent electrode approaches the embryo at 90º. This embryo has a haemorrhage below the heart due to prolonged positioning on the glass block. This is observed top down through the microscope. Electrode is positioned ≈16 µm away.
B) close up of the gap between the pericardial sac and the electrode tip shown in 'A'. ECG was recorded from this position n=5.

The ECG recording was considered successful as a clear QRS wave and T wave can be seen which means QT interval can be measured from signal recorded at this distance, **figure 2.7.**

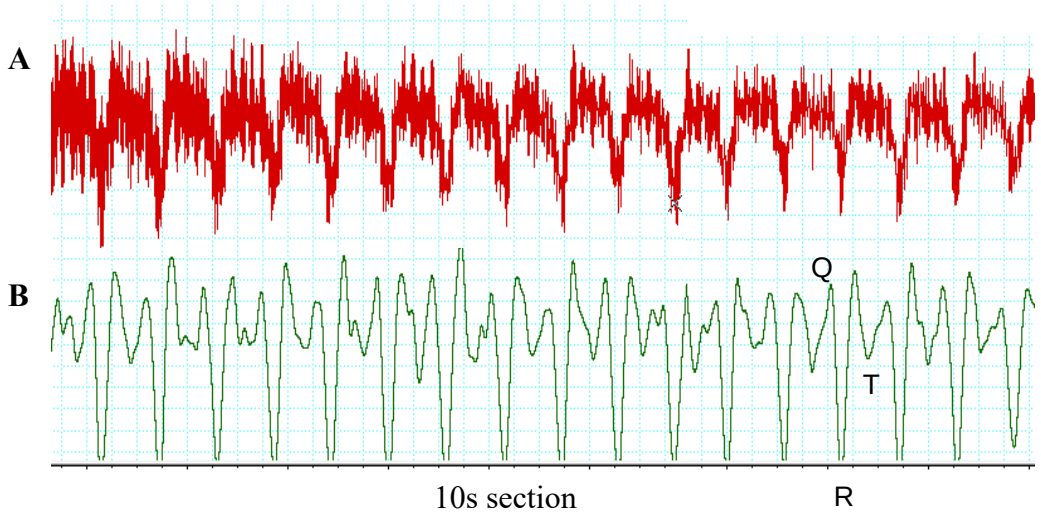

Figure 2.7 10second section of signal recorded at 16µm away from the edge of the pericardial sac.
A) Raw data direct from the analogue-digital converter and amplifier into labchart.
B) Raw signal filtered with band width filter 0.5 -30 Hz.

The distance measured between the electrode tip and the pericardial sac was measured to be 16 µm. This is a significant result, potentially reducing the need for careful electrode positioning. This is important for development of a high throughput method.

2.3.1.2.2 Signal: noise ratio calculated for non-contact positions.

The signal obtained from this position at 16µm away from the heart was smaller and less detailed than signals obtained from a contact position at the AV canal, which was expected. The amplitude of the signal decreased as distance from the heart increased. Signal waveforms were displayed as functions of amplitude and frequency in Amplitude vs Frequency spectra. **figure 2.8.**

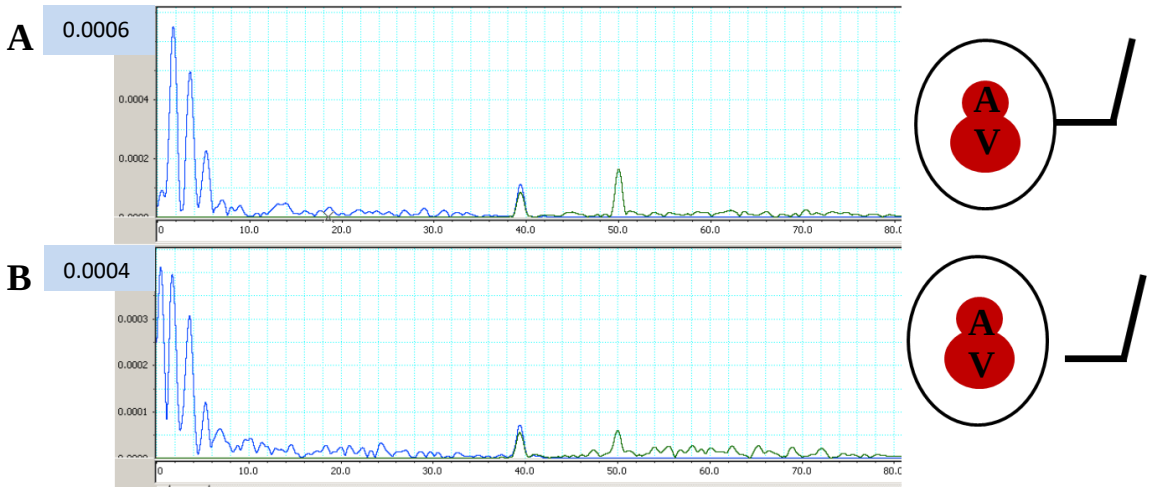

Figure 2.8. Signal amplitudes plotted against frequency to produce Amplitude vs Frequency spectrum. This displays all signal waveforms from a section of recording as the amplitude vs frequency (Hz) for each waveform
A) Amplitude vs frequency spectrum for 'position zero', the position where the electrode is just touching the heart.
B) Spectrum for position measured 16µm away from heart. Amplitude has decreased when further away from the heart. The ECG components of the recording are at lower frequencies, the first few spikes. The top amplitude (R wave) has decreased when recording at 16µm away from the heart.

Background noise at a frequency of 40 and 50 Hz is mostly mains noise. As signal amplitude decreases, it becomes more difficult to identify the ECG signal from the noise signal. Even with a low-pass filter at 30Hz, not all noise was eliminated. A spectrum of signal amplitude against frequency was taken at 5 positions (distances) with respect to the embryo heart. Position 'zero' was the when the electrode was just touching the pericardial sac, the other 4 positions were in 4 µm steps away from that position; 4, 8, 12, 16 and 20 µm. The signal: noise ratio could be calculated from these and the amplitude of signal and noise plotted, **see figure 2.9**.

A

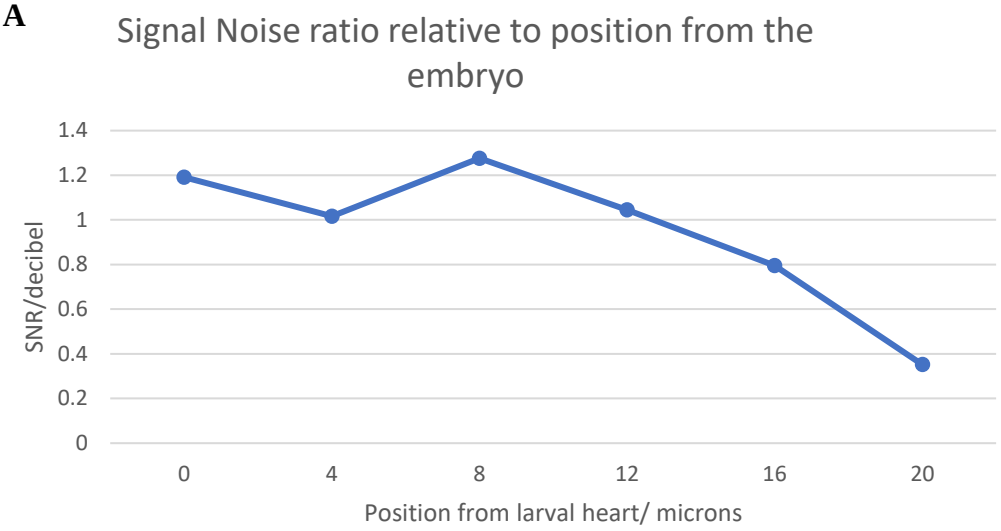

B

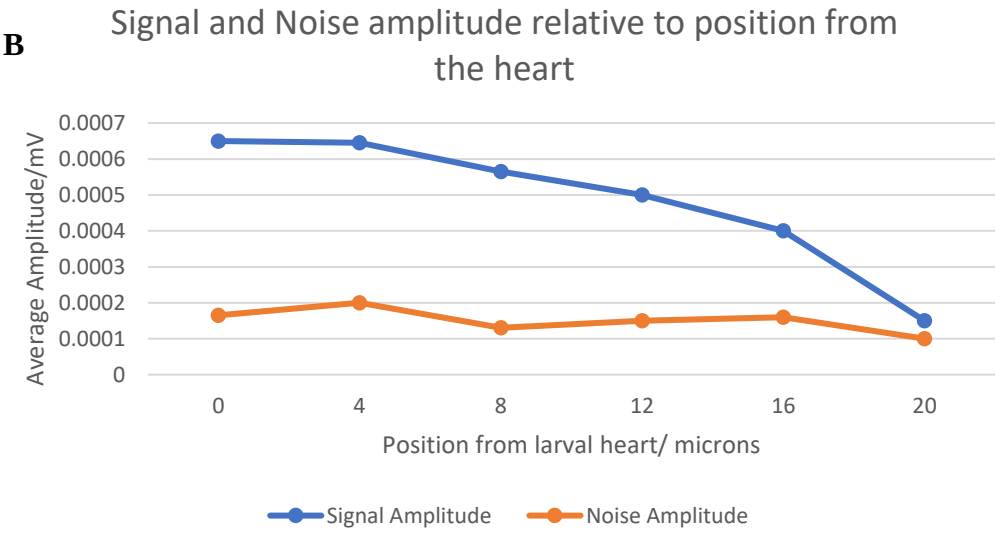

Figure 2.9 Comparison of signal and noise amplitudes at different positions. Signal amplitude decreases as distance from the heart increases. Noise amplitude, compared to signal amplitude, remained fairly constant but noise levels can vary between recordings, independently from electrode position from the heart.
A) Signal Amplitude against position from the heart (blue) Noise signal levels at each distance from the heart (orange) n= 3 for each position, however a reliable signal for position 20 was only achieved 1 out of 5 attempts, due to noise levels.
B) Slight variance in SNR from position 0-8 microns but then the SNR falls consistently with increasing distance from the heart.

A reliable reproducible recording (n=3) was achieved for positions 4 – 16, however a clear, distinct ECG signal could only be achieved from position 20 once in 5 attempts due to high levels of noise and low signal amplitude.

Therefore, it can be concluded that recording from a non-contact position is possible at a distance of up to 16 μm. QT was visible at this distance, **figure 2.9A,** therefore, recording from this distance could be used for analysis of QTc interval. The signal: noise ratios for the recordings were calculated using signal amplitudes from the embryo recordings and from recordings taken without an embryo present. These were plotted, **figure 2.9B**. This highlighted that as signal amplitudes decreased as distance from the heart increased, but noise levels were comparatively constant and the noise range was independent of the positional changes. Noise levels can vary a lot depending on conditions, so repeat recordings were on the same day and time to minimise environmental effects.

2.3.3 Investigations into alternative materials for microelectrode ECG recording of larval zebrafish ECG.

In order to develop the single electrode recording system into a high throughput system, changes to the recording set up were needed. One of the biggest changes to the equipment set up was that the glass capillary electrodes would need to be changed for electrodes which could be reused and were less prone to breakage. They would need to be durable and less fragile so they would not need to be changed each day or in between recordings. In addition to this, they would need to maintain the high resolution signal of the glass capillary electrodes so that the signal quality was not compromised. Two different types of metal-based electrodes were trialled: twisted pair electrodes and microfabricated electrodes. Design and manufacture of twisted pair and microfabricated electrodes were done by Dr Richard Barrett.

2.3.3.1 Metal electrode development: twisted pair electrodes.

The first attempts to move away from the glass electrode system were twisted pair electrodes. These provided a tool to test various metals and plating materials at different diameters. A major advantage of the design of these electrodes is that they create 2 channel electrodes so recordings from 2 positions could be taken, or alternatively a differential recording using these 2 channels could be performed which reduced some of the noise, allowing clearer ECG signals to be recorded. **Table 2.1** shows the combinations of metals, plating material and diameters that were trialled for twisted pair electrodes.

Wire Material	Plating metal	Radius µM	Signal Y/N	Comment
Platinum	platinum	50	N	**Wide diameter** means the heart is entirely covered removing the need for specific positioning but also **averages any signal out**. no usable signal achieved in n=5 attempts
Tungsten	platinum	12	Y but not repeatable due to unstable plating.	**Small diameter** allows for **accurate positioning** across the heart but platinum doesn't plate tungsten very well. So the **impedance is low** enough (<1 M Ohm at 10 Hz) but is **not very stable** and crumbles off when in contact with larvae. n=3 recordings achieved but needed to be replated after each attempt due to unstable plating.

Tungsten	gold	12	N	**Gold plates tungsten better**, however the plating process is slow and the **impedance not low enough** to record a signal.
Stainless steel	platinum	25	Y	**3 repeats taken**. Electrodes record **good clear signal** using a differential style recording. However the diameter is large and **position is still crucial** for an analyzable recording with visible PQRST parameters.

Table 2.1: Overview of different metals, diameters and plating material combinations used to create twisted pair electrodes for dual ECG signal of 3dpf zebrafish larvae. Includes comments on how successful each trial electrode pair was. Successful electrodes, such as stainless steel plated with platinum were taken forward for testing for potential to record drug induced long QT syndrome using terfenadine treatment.

The electrodes were considered successful if a clear PQRST could be seen in the signal recorded, **figure 2.10A,B.** Successful trials were then taken forward to test whether the electrodes were sensitive enough and had high enough resolution to record changes due to drug treatment. This was tested by treating embryos with 5µM terfenadine to induce long QT syndrome whilst recording from the twisted pair electrode. Terfenadine is known to produce an increase in QTc following treatment and this was observable by the 25µm stainless steel wire platinum plated twisted pair, meaning that trial was successful, see **figure 2.10C, D.**

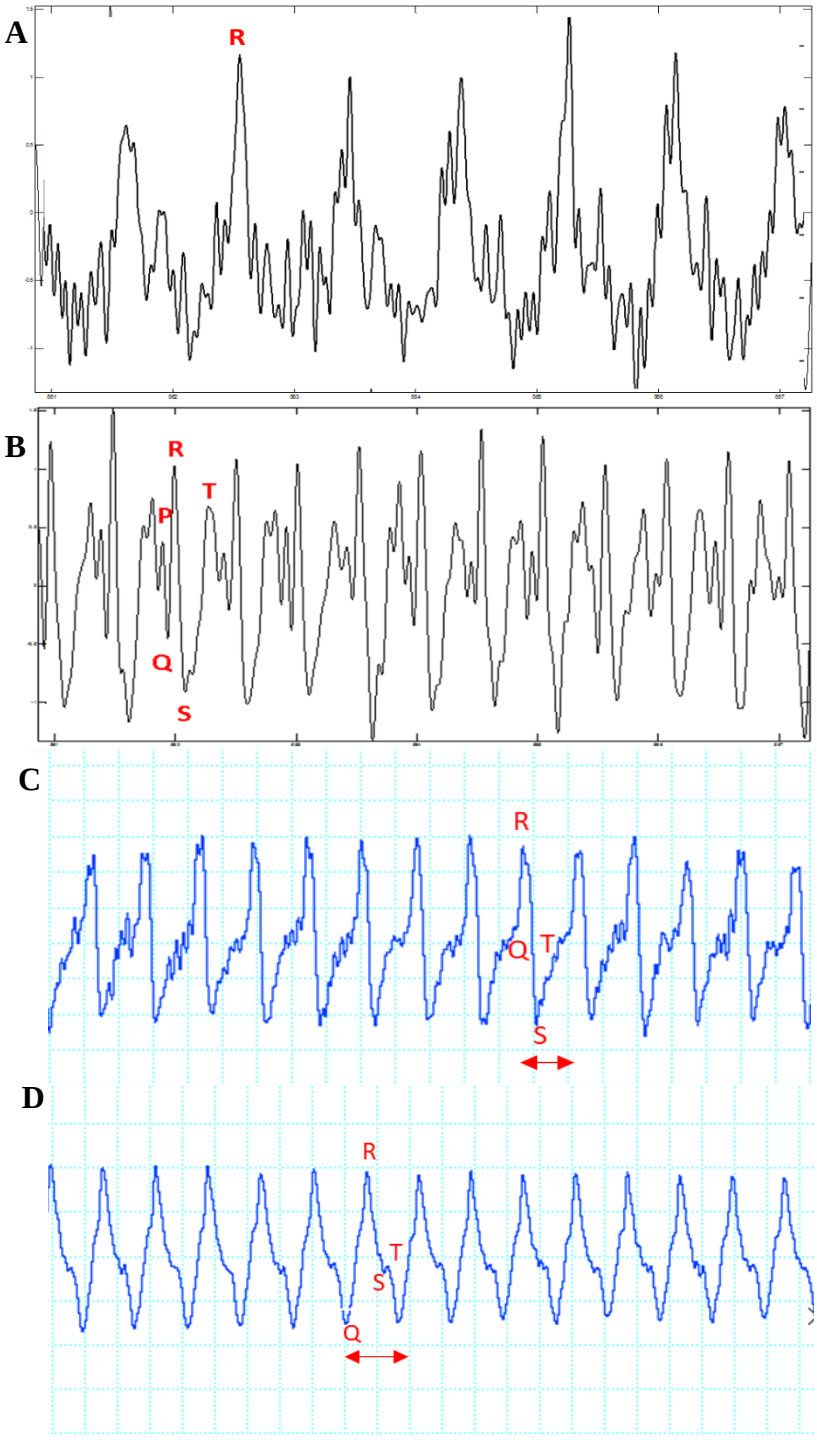

Figure 2.10. Comparison of poor and good signal quality from twisted pair electrodes.
A) Poor quality signal from tungsten platinum plated electrode. PQRST cannot be determined despite a clear R wave.
B) ECG signal from a stainless steel wire electrode plated with platinum. These electrodes produced clear signal, with PQRST easily visualised.
C) ECG trace with labelled PQRST for pre treatment.
D) ECG trace labelled PQRST post 5μM terfenadine treatment, QT interval has lengthened.

This is consistent with glass capillary electrode recording of terfenadine indicating that these electrodes can be used to produce the same result as the glass capillary electrodes. However, these are very time consuming to produce and can only be made one at a time.

2.3.3.2 Metal electrode development: microfabricated electrodes

Following the success of the twisted pair electrode another metal electrode type was trialled. These were microfabricated electrodes. An advantage of these is the production process allows multiple electrodes to be made in one batch, so less time is spent manufacturing the electrodes, and more time available for recording. These were microfabricated SU-8 probes meaning they are gold electrodes coated in an insulating plastic and plated with gold on the exposed electrode recording surface area (10µm diameter). Microfabricated electrode designs were developed and created by Richard Barrett (Post Doc electrical engineer) and then put forward for testing on 3 dpf zebrafish embryos.

These electrodes are much larger and more flexible than the glass capillary electrodes and so they were difficult to position on the embryo in the grooved agar recording plate. Their flexibility meant that the probe bent away from the embryo when it came into contact with the grooved agar plate**, figure 2.11**, or if the electrode was managed to be positioned on the heart, the contact was not stable enough to be maintained throughout a recording. The embryo needed to be secured into position to keep the contact needed for recording.

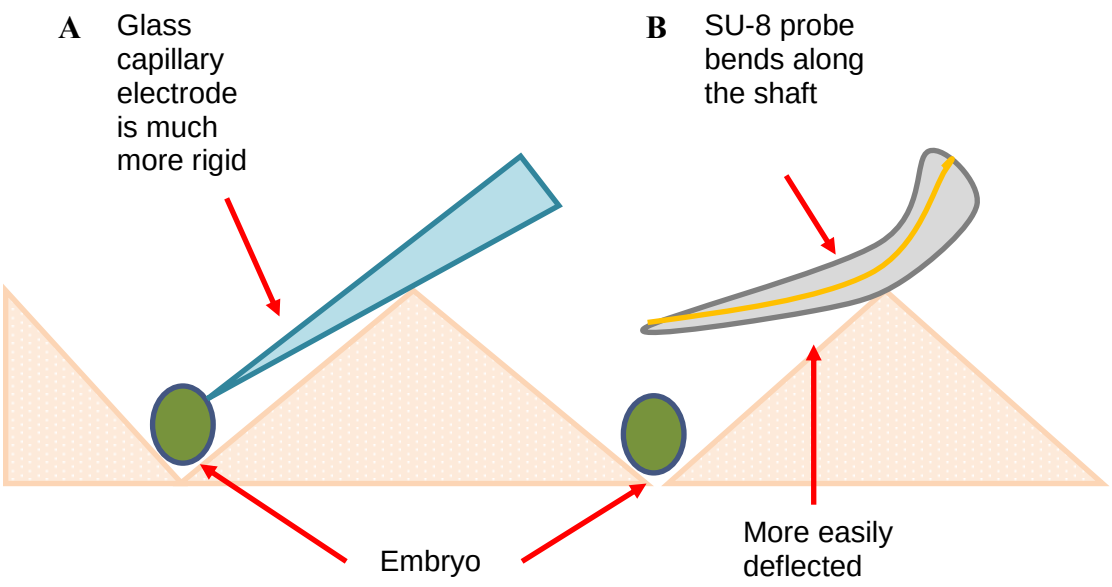

Figure 2.11 Development of the micropipette set up. The grooved agar recording plate is not suitable for recording with the microfabricated SU-8 probes as they are more flexible than the glass capillary electrodes and bend away from the embryo when they touch the agar.
A) Glass capillary electrode is rigid and can easily approach the embryo in the grooved agar plate. It doesn't bend away and contact and positioning on the embryo for ECG recording is possible.
B) Microfabricated SU-8 probes are very flexible and so when they hit the top of the grooves in the agar plate they bend away from the embryo at the bottom of the groove. The set up needs to be adjusted so that the embryo and the microfabricated electrode can be manipulated for correct positioning for an ECG measurement to be recorded.

It was therefore necessary to develop a different way of positioning the electrodes to establish and maintain stable contact between the electrode and the embryo.

The embryo was placed in a disposable micropipette tip and attached to a micromanipulator to allow greater ease of manipulation of the embryos orientation with respect to the probe to aid the positioning of the electrodes. The embryo is held securely, but not too firmly, in the end of a disposable micropipette tip. This is then secured onto a micromanipulator and submerged in a petri dish of E3 solution, allowing

the embryo position to be adjusted. The microfabricated probe is then also lowered into solution within the frame of the microscope and the embryo positioned according to the probe rather than being stationary, **figure, 2.12A.**

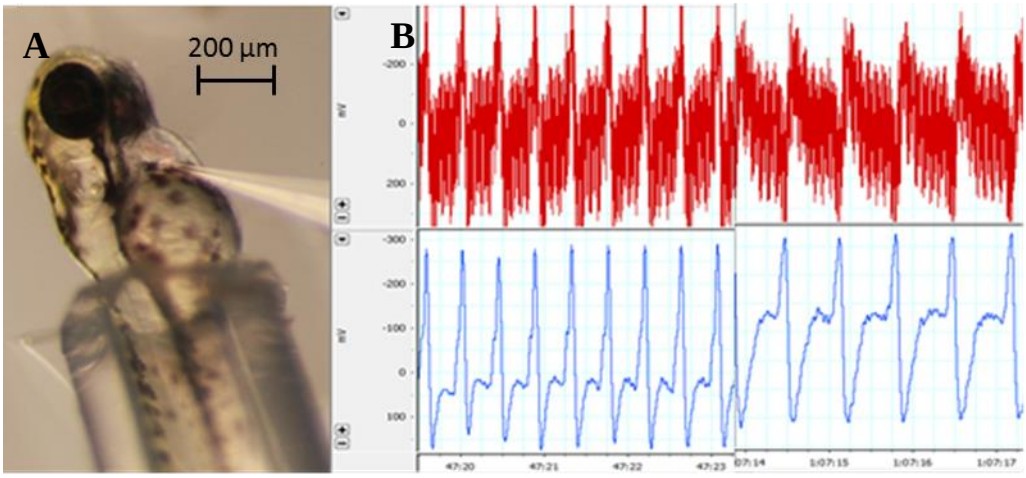

Figure 2.12 Confirmation that the set up using the micropipette to position the embryo does not compromise the recording quality and ECG recording with changes due to drug treatment can be recorded using this set up.
A) Glass electrode test in pipette set up, glass electrode positioned on 3 dpf embryo heart.
B) Recording from glass electrode in pipette set up before and after 5 µM terfenadine, n=3.

This new set up was tested using a glass capillary electrode, and the signal confirmed as ECG using 5µM terfenadine drug treatment, which induces an increase in QT interval of ~30% , n=3 **figure 2.12B**. This step was used as a control for all new set ups to ensure signal quality was maintained. Using this recording set up, it was possible to position embryos and microfabricated electrode in a stable recording position, **figure 2.13B.** From this stable position an ECG signal from a single microfabricated channel was achieved, **figure 2.13E.** This signal had clear QRS complex and T wave so the signal was confirmed as ECG and had sufficient quality for QT analysis. As positioning

was still time-consuming and meticulous, and the microfabricated SU-8 probes were much larger than the glass capillary electrodes, some embryos treated with 0.2mM PTU (phenylthiourea). This inhibits melanogenesis to prevent pigment developing to try and increase visibility of the heart with the larger electrodes, **figure 2.13A.** This was tried in the grooved agar plate and later in the pipette tip set up, but had little effect in reducing the time required to position the electrode, so this step was dropped.

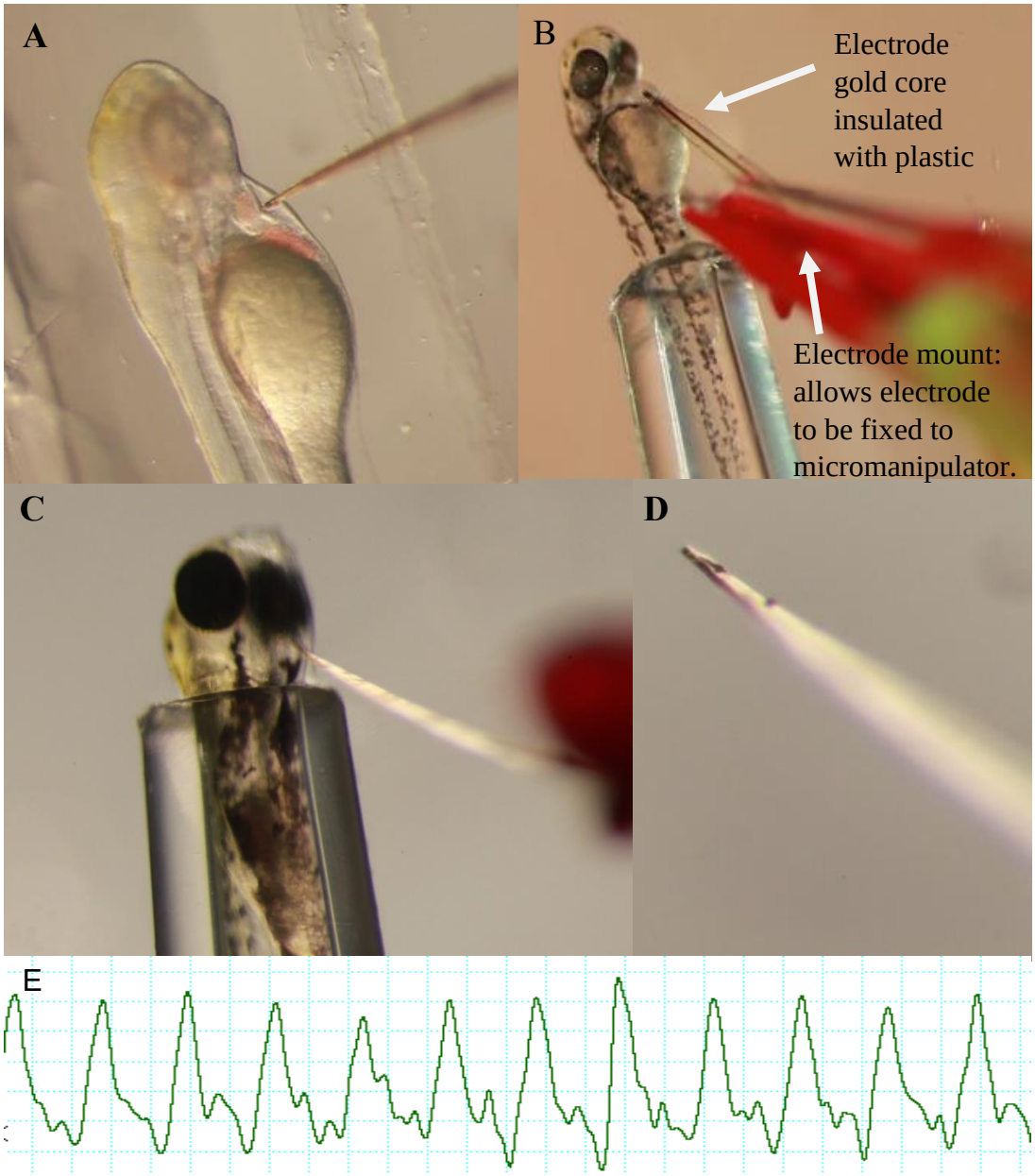

Figure 2.13 Microfabricated SU-8 electrodes successfully recording from 3dpf zebrafish larvae.
A) MF electrode positioned on zebrafish larvae treated with PTU (phenylthiourea)in recording plate N=3 Embryo positioned in grooved agar plate, Video still image which showed how the electrode was not stably positioned and moved over the heart and eventually off the embryo as the recording progressed.
B) Microfabricated electrode positioned in pipette tip to aide electrode positioning and embryo orientation.. The surrounding plastic with the gold core is visible.
C) second embryo inside pipette tip, this time inserted more firmly into the holder. Can see the flexibility of the electrode probe.
D) A close up of the electrode tip. Shows flat design.
E) Successful PQRST recording achieved using the SU-8 probes in this recording setup. This signal has a band pass filter of 0.1-30Hz. P wave is present but not as clear as the other waveforms in this recording.

Not all trials with the SU-8 probes were successful and it was thought that this was down to impedance and maintaining a low impedance. Probes were tested for impedance after plating and before testing, to make sure the impedance was low enough (>1Mohm at 10Hz). Then the impedance was retested after a recording was attempted whether an ECG signal was obtained or not. This showed that unsuccessful probes had impedance values higher than 1 Mohm (mega ohm) at 10Hz after a recording attempt and this is too high to record zebrafish ECG. This instability of plating also impacted on repeat recordings using the same probe. As this was a crucial requirement of high-throughput electrodes this needed to be resolved. The electrodes are plated following fabrication to increase the surface area on the exposed electrode tip without increasing the footprint. This is so that the impedance is lowered, so that recording the small electrical signal from the zebrafish heart is possible, and that the area on the heart the device is recording from is kept to within 10µm, so the signal is not averaged across a large area, loosing detail from the recording. To address the impedance issue; the plating process was analysed. The probes are plated by suspension in an acidic gold solution and a current applied causing dissociated gold ions to be deposited onto the SU-8 probe acting as the cathode.

Alternative plating materials were researched and conductive polymer called PEDOT (poly(3,4-ethylenedioxythiophene)) was chosen. PEDOT is positively charged (PEDOT). This composite has both electrical and ionic conductivity, which has been shown to be effective in biological recordings of the peripheral nervous system in rats (Frost *et al*, 2012). In this study PEDOT plated electrodes had a significantly higher charge capacity and lower impedance than the needle needle electrode allowing signal to be recorded from few simultaneously firing neurons (Frost *et al*, 2012). Therefore, applying this plating strategy to the SU-8 probes, was predicted to yield similarly

positive results. It was also decided that to improve the stability of the plating, a low current was applied so that the plating was built up in layers, which produced more a stable plated layer. The final design of the probes had a layer of gold plating first and then plated with PEDOT over the top. These were more successful and resulted in clear usable signal in repeat recordings from the probe, clearly displaying an advantage to this plating approach over other materials trialled.

Having established that ECG recording was possible in 3dpf zebrafish larvae using metal microfabricated electrodes with high throughput potential, the designs for the probes were changed to increase the channel number. As the design process is so flexible in a 2D space this meant that 4 channel devices with only a small (20µm) distance between them was possible. Therefore, all four channels could be positioned over the heart to record ECG from 4 locations. The 4 channel device was similar in size and shape to the single channel electrode, but flat at the tip to allow 4 exposed electrodes to fit, **figure, 2.14.A.**

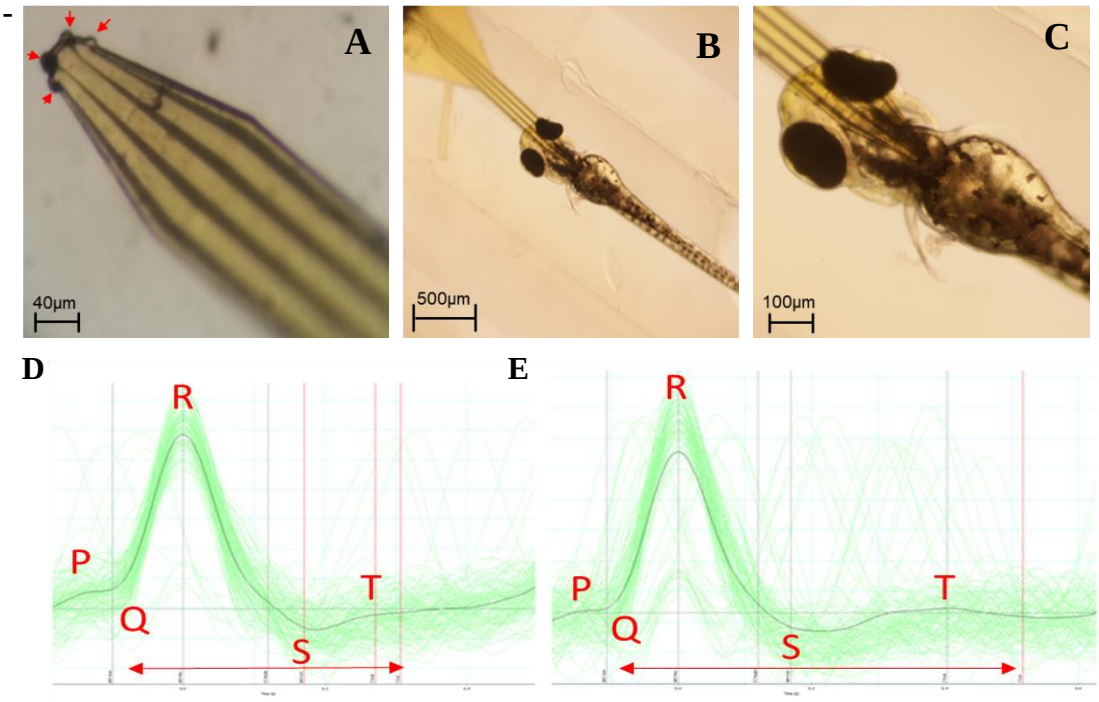

Figure 2.14 The 4 channel microfabricated electrode design and recording signal from one of these channels from a dechorionated 3dpf zebrafish embryo.
A) The tip of the 4 channel device design. Red arrows show location the exposed electrode recording points.
B) 4 channel device positioned on a dechorionated 3 dpf zebrafish heart.
C) Higher magnification of the microfabricated device positioned on the embryos heart Position used for successful ECG recording of 3 dpf zebrafish larvae n=5.
D) Average waveforms before drug treatment.
E) Average waveforms 20mins after 5µM terfenadine treatment.

Successful repeat recordings were achieved with the 4 channel device (n=5) and the ability to place 4 channels on the heart simultaneously meant that positioning was much easier. As the tip of the device was larger, with 4 gold wires connecting running up the shaft to connect the four electrode recording spots, the device was less flexible, allowing positioning in the grooved agar plate. This also meant that positioning was easier and quicker, as the 4 channels covered the heart increasing the through put of the recording, **figure 2.13B,C**. These recording were also of sufficient quality to record and analyse differences due to drug treatment. QT prolongation was induced by 5µM

terfenadine treatment and measured 20mins after dose, **figure 2.14.D,E.**

For n=3 recordings, an ECG recording signal was recorded from all 4 channels, **figure, 2.15.** However, the background noise for these recordings varied. For further development, reducing this noise would be key to ensuring clear ECG recordings from multiple channels.

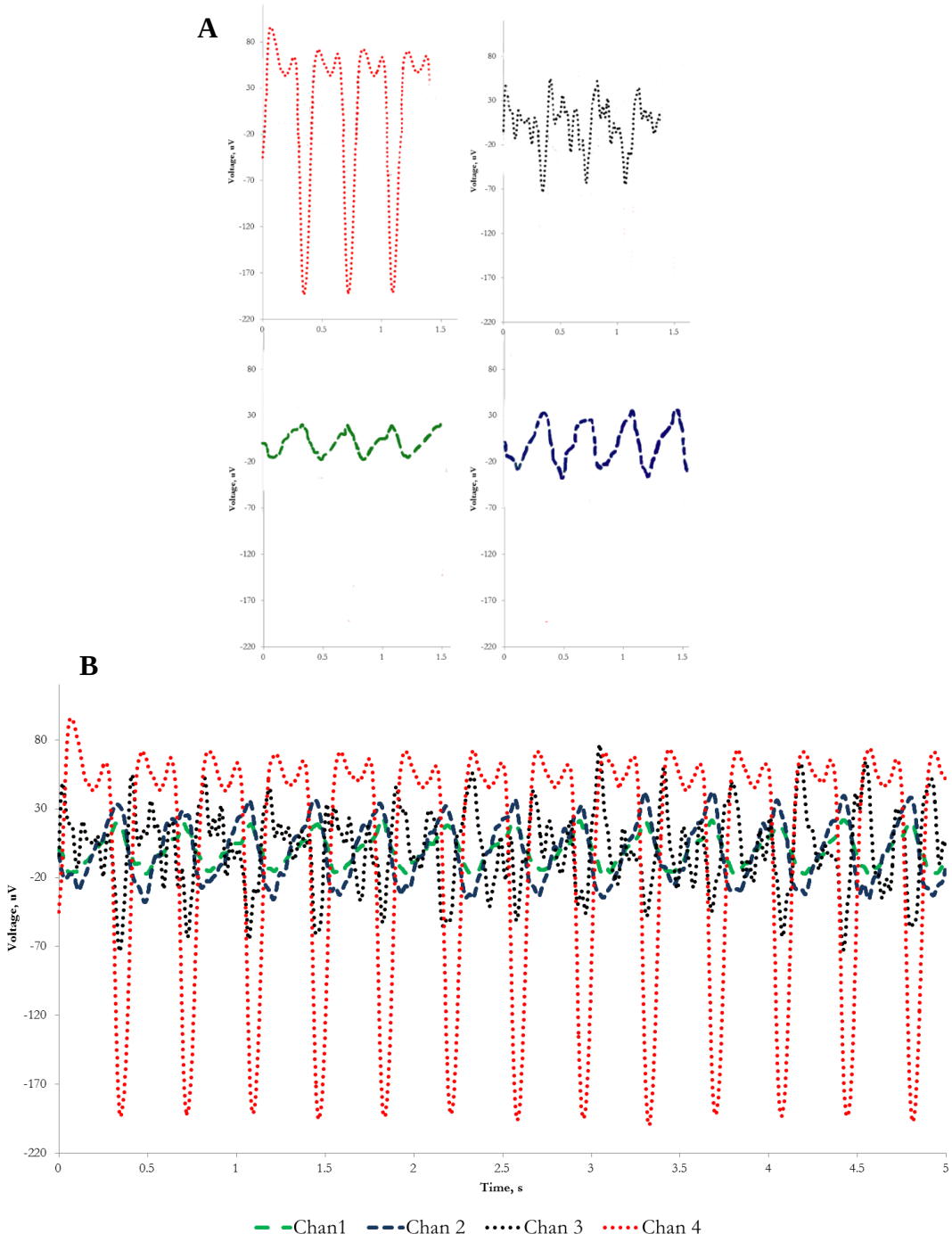

Figure 2.15. Section of recorded ECG signal taken from recording using the 4 channel device. Device was positioned on a dechorionated 3 dpf zebrafish larvae. All 4 channels recorded ECG signal and the traces are overlaid to show amplitude differences from the different locations on the heart. Signals recorded from different locations on the heart will show different amplitudes depending on position relative to the heart electrical signal.

This is a significant result as multichannel microfabricated electrode recordings for

larval zebrafish has not been previously reported and represents a significant

technological step towards a high throughput system. This result shows this possibility of replacing the less durable glass electrodes with reusable microfabricated multichannel electrodes. This opens the door for differential recordings, and also moves towards a model more similar to the 12 lead ECG performed on humans which would be advantageous as more direct comparison could be possible.

2.4 Discussion

2.4.1 0.3mg/ml MS-222 does not significantly affect the heart rate and QTc interval of 3dpf zebrafish larvae.

Effective immobilisation of the zebrafish embryos is imperative for successful ECG recording. To ensure a stable recording, the electrode position needs to be secure, and fixed to prevent movement artefact. Dhillon *et al* 2013, compared two chemical immobilisers, Ethyl 3-aminobenzoate methanesulfonate (MS-222), a commonly used anaesthetic for zebrafish work, and Tubocurarine, a neuromuscular block. It was concluded that there was no significant difference to the QT interval from compared recordings using these two immobilising agents and MS-222 was routinely used for recordings. However, to truly establish whether the use of anaesthetic had an effect on the ECG signal, recordings using MS-222 needed to be compared to recordings obtained without the use of anaesthetic. In particular, it was important to establish that the concentration of MS-222 used to immobilise the embryos for ECG was not affecting the heart rate or QTc interval. It is well documented that anaesthesia, at a high enough concentration, will lower the heart rate in humans, and it was crucial to establish if this was the case at 0.3mg/ml concentration of MS-222 and if so to what degree in the zebrafish. If significant, heart rate and QTc values could be normalised against this change. To compare anaesthetised and non-anaesthetised embryos, the embryos were immobilised in a bed of agarose. Once the fish were mounted and the agar had set, it was important to let the fish settle after handling. Without this step the heart rate at the beginning of the recording was much higher due to the stress of handling. So, it was important to let them acclimatize before positioning the electrode.

N=8 MS-222 treated and non-treated embryos were mounted for comparison and also compared to recordings from MS-222 treated and unmounted embryos.

Analysis of stable ECG recordings revealed no significant difference between anaesthetised and non-anaesthetised embryos, at 0.3 mg/ml. This means that no normalising factor is required for future measurements and the immobilising method using 0.3mg/ml in the grooved agar plates was sufficient for detailed ECG recordings without effecting the heart rate and QTc interval.

2.4.2 Non-contact recording from zebrafish larvae is possible and a maximum distance of 16µM can be reached.

A principal aim of this study was to make steps towards, and to investigate the feasibility of specific parameters required for, a high throughput recording system for larval zebrafish ECG. The most time consuming part of the glass capillary single electrode recording process is the positioning of the electrode on the heart. It is an intricate and highly skilled job and the removal of this step would greatly increase the throughput of these recordings. One way in which this might be achieved is the ability to record at a distance from the heart. So that if the electrode is within a certain distance away from the heart, a reliable ECG signal can be recorded. In addition to this advantage, recording at a distance would also decrease the amount of embryo manipulation required, which would also save time, and increase throughput.

Initial experiments used the existing set up with embryos aligned in the grooved ager plates, but due to the angle at which the electrode met the embryo with respect to the view from the microscope, visibility of the exact point where the electrode left the heart was difficult. In order to test whether non-contact recording was possible with the

borosilicate glass capillaries a different recording stage and electrode shape was required to be able to observe the electrode approaching the heart at a 90^{o} angle from the top view microscope. Usually the electrode approaches the embryo at a 30^{o} angle. Bending the electrode by 30 degrees allowed it to come in at 90 degrees to the top down microscope view, so that the point at which the embryo is just touching (position zero) vs not touching (positions 1-6) were easily visualized. The carved glass stage was also designed for visibility and to orientate the embryo while providing a flat channel for the electrode. Using this alternative electrode set up allowed signal to be recorded from accurately measured distances of up to 20 µm away from the heart. The signal noise ratio at each of these distances was calculated. The SNR is a calculated measurement to compare desired signal against levels of noise in a recording system. It can be calculated using average power of signal and noise, or mean signal amplitudes over time. In this instance average signal amplitudes at each distance relative to the heart were used to calculate SNR. This was possible as the impedance was the same for both signal and noise. The calculation for SNR is the square of the amplitude ratio (Signal/noise), **figure 2.19A.** The SNR is usually represented as a decibel, on a logarithmic scale and was calculated using the formula in **figure 2.19B.**

A

$$SNR = \left(\frac{P\ signal}{P\ noise}\right) = \left(\frac{A\ signal}{A\ noise}\right)^2$$

B

$$SNR\ (dB) = 10\log_{10}\left[\left(\frac{A\ signal}{A\ noise}\right)^2\right]$$

Figure 2.15 Formula used for calculating SNR (signal noise ratio) and signal noise ratio in decibels. P= average power over time. A= mean amplitude over time. SNR calculation for signal recorded at increasing distances from the heart average amplitudes(mV) were used. SNR is usually displayed as a logarithmic decibel, calculated using formula B.

A distance of 16 µm away from the heart reliably produced a measurable ECG signal with a clear QT interval for analysis. Signal was also achieved at a distance of 20µm away from the heart, but this was only possible n=1 out of 5 attempts due to a very low signal noise ratio (SNR). The low signal noise ratio means that the ECG signal is not very visible above the noise, and therefore makes it very difficult to record detailed ECG from which QT analysis could be performed. The SNR varied more between 0 and 8 microns due to varying noise levels, with a comparably lower noise level recorded at 8 microns than at any other distance. This is most likely due to external factors for those particular recordings and not difference in recording technique. To reduce variances in environmental noise factors such as other electrical equipment in adjacent labs, the recordings were taken at the same time and day, when the lab was quiet. Recorded noise amplitudes ranged between 0.0001 and 0.0002 and variance was independent of distance, there was no distance dependent trend observed. Conversely, signal amplitude decreased as distance from the larval heart increased. A reliable ECG

signal was recorded up to 16µm away from the heart with identifiable R and T wave so QT analysis is possible, which is in line with high throughput requirements.

While this is an important result for the development of a high throughput recording system it is likely that such a system would not utilise glass electrodes as they are fragile, prone to breakage and blockage. In order to design a system which uses non-contact ECG recording this would have to be tested in a similar way to test the viability of such a system.

2.4.3 Recording ECG from 3 dpf Zebrafish larvae using twisted pair and microfabricated metal electrodes: a move towards a high throughput system.

The single electrode recording system described in Dhillon *et al* 2013, produces high resolution recordings from 3dpf larval zebrafish. These can be used for analysis of normal heart rate activity at this development stage and also to record heart responses to different drug treatments. While this is a very useful tool, this recording system is limited by the rate at which whole data sets can be produced as these recordings can only be performed singularly. A principle aim of this project was to make steps to move away from a single electrode recording system to a multichannel system in order to increase the throughput.

Designing new electrodes which did not depend on glass capillaries posed a problem due to the scale of the zebrafish larvae at 3dpf (approx. 3mm head to tail). The glass capillary electrodes have an impedance independent from frequency and as such have a low impedance of less than 1Mohm (mega ohm). The zebrafish has cardiac electrical signal in the range of 5-30uV and as such, the new non-glass electrodes also need to be

have an impedance of ~1Mohm a 10Hz in order to record this signal. However, this needed to be achieved without increasing the size of the electrodes (glass capillary tip size 2uM) as this will increase the recording area of the zebrafish heart (which is approx. 100uM in diameter) and the resulting signal will be averaged across a large area and so detail will be lost. An averaged ECG signal would lose detail such as the p wave, which is difficult to capture. To keep the high resolution data obtained from the glass capillary recording the new non-glass electrodes needed to be less than 10microns in diameter.

2.4.3.1 Measurable QTc differences can be recorded using metal twisted pair electrodes.

The twisted pair electrode design has significant advantages on glass capillary electrodes. Firstly, they adhere to the requirements for high-throughput electrodes, they are durable and reusable, and with the right combination of metal, diameter and plating material, they can record detailed ECG signal with PQRST waveforms. Secondly, due to the nature of their design, they are 2 channel electrodes which allows a signal to be recorded from 2 places. This could be a dual recording on the heart, or a differential recording where the signal recorded from the channel positioned away from the heart is subtracted from the channel positioned on the heart. This subtracts addition noise not filtered out, potentially making it easier to 'clean up' the signal and obtain a clear, detailed ECG with PQRST waveforms. This was achieved using stainless steel twisted pair with a 25µm radius and plated with platinum. With a 25µm radius and stable plating, the impedance was low enough (>1Mohm at 10Hz) for a detailed ECG with PQRST waveforms to be recorded. This level of detail matches the glass capillary recordings, and therefore can be used as an alternative.

Using this successful twisted pair electrode, a recording was performed where the zebrafish larvae were dosed with 5µM of terfenadine to induce QT prolongation, to test whether this ECG change due to drug treatment could be measured using this electrode. The result showed the 30% increase in QTc measurement, first established by glass capillary recording, showing that these electrodes yield the same quality of measurement. This result shows that these electrodes could potentially be used as part of a high throughput system for recording ECGs in zebrafish larvae.

A drawback of these electrodes is that they are time consuming to produce and plate. Each has to be made individually, whereas the microfabricated electrodes can be batch made. The design for the single microfabricated electrodes produced 40 electrodes per batch. Each batch took 2 weeks to make, and then were individually plated ready for testing. This was much quicker than creating individual twisted pair electrodes. Also, long term, these would require fairly consistent repeat plating to keep the impedance low enough, and they were maximum 2 channels, as there was no room on the recording plate to add any further electrodes. It was extremely difficult to try and position both channels on the heart for a dual recording and this was only possible with the lower radius metals such as the tungsten with 12µm radius, but this was difficult to plate and keep the impedance low enough for recording. This means that these twisted pair electrodes are predominantly single channel devices, therefore, do not lend themselves for use in high throughput systems with multichannel recording. In conclusion, the microfabricated electrodes were more versatile, as bespoke designs tailored for this specific project were created, and had the potential for more than 2 channels, such as the specially designed 4channel device.

Throughput this chapter different recording approaches have been applied in order to develop further the single electrode recording system described in Dhillon *et al,* 2013.

This is the first time metal electrode devices have been reported for use on zebrafish larvae and the first time reported recording from unanaesthetised embryos and from a non-contact position. All of which represent novel recording approaches developed as part of this work. As described above (2.4.3.1), recording from metal devices represents a significant challenge, but is vital to the development of a high throughput device.

2.4.4 ECG signal can be recorded from microfabricated electrodes; a potential electrode type for high throughput recording.

As previously described, moving from a single electrode recording system to a multichannel recording system will increase the throughput of zebrafish larval ECG recordings. Work with twisted pair electrodes concluded that while initially it was thought that these could serve as 2 channel devices, practically they were too bulky to facilitate this. Following on from the work with twisted pair electrodes, microfabricated electrodes were trialled. These were more expensive initially to produce as the bespoke designed 'masts' required for creating the designs, produced externally were expensive. After this step, the rest of the manufacturing process was performed by Dr Richard Barrett, a post-doc electrical engineer on the project.

The bespoke electrode mast design process opens the door for multichannel devices. The design process is extremely flexible in a 2D space so very individualised electrodes can be created. Multichannel electrodes would aid the development of a high throughput system as you could position the electrode over the heart, very easily and quickly, knowing that with multichannel at least one of the electrodes on the device would be in a position to record ECG. This removes the need for painstaking electrode

positioning, increasing the throughput. Also, if positioned on the device close enough together, there is the potential for ECG recording across multiple channels.

The first microfabricated electrodes were single channel devices to test the feasibility of using these electrodes to record the small electrical signal (5-30μV) of the 3 dpf larval zebrafish heart. The microfabricated electrodes created were SU-8 probes, these are gold electrodes coated in an insulating layer of plastic, top and bottom. A 10μm electrode tip is left exposed as the recording area which is plated with gold to increase surface area to achieve the low impedance required for zebrafish ECG recording (>1Mohm at 10Hz) without increasing the recording area footprint which would average the signal over a larger area of the heart reducing detail in the recording.

These initial devices were difficult to work with due to their flexibility and required a different approach to allow greater embryo manipulation to position the electrodes on the heart, firmly. This was resolved by using a disposable electrode tip attached to a micromanipulator and using this setup, recording from these single channel microfabricated recording devices was achieved. However, there was a problem with replication and not every device created, despite being from the same batch and identical treatment, performed the same. Impedance measurements taken after plating, before and after recordings showed that the impedance values didn't stay low after positioning on the embryo. This led to time being wasted consistently re-plating individual electrodes in order to be able to test them for recording ECG. Also, a major requirement for high throughput electrodes as a departure from the glass capillary electrodes is that they need to be reusable. In order for the microfabricated electrodes to be developed for high throughput recording, this plating unreliability needed to be resolved. Different plating materials were researched and a conductive polymer, PEDOT was chosen. PEDOT has proven success in biological recordings. Frost *et al*,

2012 demonstrated the use of PEDOT in peripheral nervous system recordings in rats with PEDOT plated electrodes performing better than alternatives. This is because PEDOT plated electrodes have a higher charge capacity and a low impedance. The higher charge capacity helps the signal transfer at the electrode tip from the zebrafish pericardial sac surface to the electrode. A low impedance is required to record the small electrical signal of the zebrafish heart, and the lower impedance of the PEDOT plating greatly helps to record. It is also much more stable and so the impedance stays low, allowing repeat recordings with the same electrode without having to re-plate. Reusability is a requirement for high throughput electrodes, so it was important ensure that with the electrode design and plating protocol this was achieved. The final plating protocol used a layer of gold plating and a layer of PEDOT plating on top. However, positioning still took time with extra help for embryo orientation and establishing stable contact needed using the pipette tip set up. Also, despite a vast improvement with the PEDOT plating, the signal quality was still not at the standard as the glass capillary electrode, however, the signal quality was sufficient to be able to detect the QRS, R wave and T wave, so QT analysis is possible from recordings using these electrodes.

Once effective, reliable metal microfabricated electrodes had been established, the next step was to upscale this result from single channel electrodes to multichannel. This was the next important requirement for high throughput recording. With more channels, the laborious, meticulous electrode positioning would not be necessary, as increasing the number of channels on the electrode increases the chance of 1 of those electrodes recording ECG signal without having to take extra time and care to place the electrodes precisely. Using the same design process as the single electrodes, a 4 channel device was designed and created and was plated with gold and PEDOT as per the successful single electrode devices. This device was successfully used to record detailed ECG

signal (n=3). This is a very important and novel result for the development of a high throughput channel, recording signal that is detailed enough for analysis of drug treatments is a big step towards a high throughput system. Although only a very small sample size this is a proof of concept result which demonstrates the potential of a high throughput zebrafish larvae ECG recording device for hERG channel cardiotoxicity and novel drug screen therapies.

3. Characteristic analysis of the electrocardiograph signals from the chambers of a 3dpf zebrafish heart using Fourier transform analyses.

All ECG work and analyses pertaining to this chapter was performed by myself. *In silico* modelling work performed by James Crowcombe.

3.1 Introduction

3.1.1 The Human 12 lead ECG procedure

Diagnosis of a multitude of human cardiac conditions depends, at least in part, on a 12 lead ECG recording as a standard method for determining cardiac dysfunction. This is because it is a robust, high resolution and informative tool for observing the electrical activity in the heart. The 10 electrode, 12 lead standard ECG procedure gives a detailed picture of electrical activity and, therefore, is highly informative in a disease state. Depending on which electrode/lead abnormalities are showing, in conjunction with which section of the ECG is affected can suggest different arrhythmia conditions as well as indicating an atrial or ventricle problem. For example: QT prolongation can be diagnosed by examining Leads II, V5 or V6 and analysing a section of cardiac cycles (Nachimuthu, Assar and Schussler, 2012). Currently, it is not possible to replicate this on the larval zebrafish due to the small scale of the zebrafish larvae. However, it would be useful to determine if there are measurable differences in the atrium and ventricle signals which could then be used, in a cardiac disease state to identify chamber specific arrhythmias in larval zebrafish. This will aid development of the zebrafish as an arrhythmia model for human arrhythmias and further understanding of the larval zebrafish heart.

3.1.2 Atrium and ventricle specific signals

Atria and ventricles have distinct differences in transcription profiles, resulting in chamber-specific differences in structure, ion channel expression and electrophysical properties. This reflects their different functions and can lead to chamber-specific induced or in inherited arrhythmias. As a result of these specialised transcription

profiles, atria and ventricles can show differences in responses to drug treatment (Tabibiazar *et al*, 2003). There are many examples of arrhythmias which are chamber specific to either the atrium or ventricle, for example atrial and ventricle specific fibrillation, chamber specific re-entrant arrhythmias and ventricular tachycardia. Even ion channels can have chamber specific expression patterns and therefore associated arrhythmias can be isolated to specific chambers, for example; T-type calcium channels which in adulthood are predominantly not expressed in ventricles but are present and have a role in sinoatrial node function, facilitating pacemaker cells depolarisation (Betzenhauser, Pit and Antzelevitch, 2015).

Zebrafish also display chamber specific differences in responses to drugs, for example Langheinrich, Vacun and Wagner, 2003 showed chamber-specific bradycardias in response to drug treatment. Known hERG blockers induced 2:1 atrioventricular block where the ventricle beats half as often as the atrium (Langheinrich, Vacun and Wagner, 2003) and also induced QTc prolongation (Dhillon *et al*, 2013). Some zebrafish mutants such as *Reggae* which displays a sinoatrial exit block and a short QT also feature chamber specific phenotypes (Hassel *et al*, 2008) and several mutants have been created which show silent chambers (Rottbauer *et al*,2001, Milan and Macrae, 2008).

To expand the potential use of the zebrafish larvae as an arrhythmia model system, investigations were conducted to examine whether the atrium and ventricle signals could be identified and isolated. This would mean that atrial and ventricle specific arrhythmias could be examined in this model.

3.1.3 Analysis of ECG using wavelet transformations.

An ECG electrocardiographic signal, is a recording of the electrical activity of the heart. This activity is a change in voltage potential where myocyte cells depolarize and repolarize, facilitated by movement of positively charged ions across the cell membrane, causing the voltage potential across the membrane to change from minus 70 to plus 30 and back again. This voltage change is propagated in synchrony across the heart, driving coordinated myocyte contraction and relaxation. The wave of change in voltage potential across the heart can be measured by an electrode, producing an ECG trace which records voltage (V) against time (s). The waveforms this creates, the P wave, QRS complex and the T wave, occur at different frequencies (Hz). Wavelet analysis, where a fast Fourier transform is applied to waveforms and displays them as components of frequency (Hz), power (μV^2) and time (s). A fast Fourier transformation is a calculation to decompose the signal into composite parts. This gives different information than standard trace analysis, where the ECG is analysed in terms of interval duration (Saritha, Sukanya and Murthy, 2008). Further wavelet analysis can also produce 3D spectrograms which show frequency/power relationships across time. These analyses may provide an alternative approach to quantifying responses from drug treatment, as well as also proving useful for analysing signals from noisy recordings, where it is difficult to visually identify clear PQRST waveforms without further analysis (Lilly, 2017).

3.1.4 Aims

This study aimed to investigate whether it was possible to record atrium and ventricle signals separately and distinguish individual features for these chambers, similarly to

human ECG. This was to establish ‘normal’ functionality parameters for the two chambers to then be able to identify when these parameters are abnormal, such as in a disease state. Therefore ECG could be used diagnostically for identifying atrium and ventricle specific arrhythmias in the zebrafish larvae. This could then be extrapolated to human conditions, if relevant, and provide novel zebrafish drug screening tools for chamber specific arrhythmias.

The aims are:

- To establish whether accurate recording from atrium and ventricle chambers could be taken and whether the differences between these signals could be determined.
- To analyse these signals using fast Fourier transform techniques and wavelet analyses.
- To establish a dual electrode recording system for zebrafish larvae with appropriate controls to allow simultaneous recording from 2 electrodes positioned on the heart.
- To establish whether ECG differences due to drug treatment could be detected using these techniques.

3.2 Methods

3.2.1 Zebrafish lines and husbandry

All zebrafish were handled according to the UK animal (Scientific Procedures) Act of 1986. Wild type AB fish were used for preliminary single electrode experiments and thereafter chamber specific fluorescent lines (Tg:VMHC-red and Tg:AMHC_cherry-NTR) were used (Zhang *et al*, 2013, obtained lines from this lab, slightly different to the paper when requested through the author). These lines were also used for imaging the fish. Dual electrode recordings used wild type AB zebrafish.

3.2.2 Single electrode recording method

Same procedure as described in section 2.2.2.

3.2.3 Imaging: ScanR

The Olympus ScanR high content screening microscope (Olympus) was used to image the two transgenic lines (Tg:VMHC-red and Tg:AMHC_cherry-NTR). Low-resolution prescreen data was acquired using a single z-slice per embryo and channel using a 2.5× (N.A. = 0.08) objective. Embryos were imaged with a 4× (N.A. = 0.13) (60 z slices, Δz = 10 µm). This was repeated with the RFP channel to capture fluorescence.
Images were then processed, formatted and overlaid in Image J (Java-based processing program, NIH). Maximum projection images were produced and then overlaid to produce an image of the 2 fluorescent chambers for optimisation of electrode positioning. A grid was placed over the image to guide electrode placement of electrodes.

3.2.4 Standardising atrium and ventricle electrode positions

In silico modelling work performed by James Crowcome was used to predict the optimum positions for recording atrium and ventricle recordings (Crowcombe *et al,* 2016). This work created a 3D rendering of the 3 dpf zebrafish larva and mapped electrical currents across the heart to create a 3D finite electrical model of the ECG signal of a larval zebrafish at 3 dpf (Crowcombe *et al,* 2016). This electrical map predicted where signal amplitudes from the 2 chambers were largest and most distinct.

To facilitate putting these predicted positions into practise, an image using fluorescent lines was created and a grid overlaid. Atrium recordings were taken from G8 and ventricle recordings taken from E7, see **figure 3.1.**

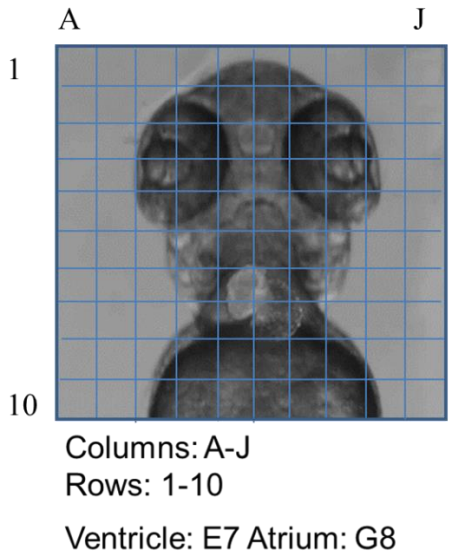

Figure 3.1: Grid overlaying ScanR image with ventral view of 3dpf embryo with a fluorescent heart. Columns run A-J and Rows run 1-10. Atrium recording position, G8, ventricle recording position E7.

3.2.5 Dual electrode recording method

The recording system used for these experiments is the multichannel system by Tucker Davis Technologies (TDT system). The setup is the same as for the single electrode

recording protocol, but there is a micromanipulator, motor arm and electrode capillary set up on both sides of the recording petri dish, the left side measured the ventricle and the right measured the atrium. Each of these recording arms are attached to a 16 channel headstage (TDT). This headstage allows 16 inputs plus 2 reference and ground electrodes. The headstage is connected to a pre amplifier (PZ2-256, S^3 z series, TDT) which can have up to 256 separate channels and the signal is then digitised in the processor (RZ2 BioAmp Processor, S^3 z series, TDT). The signal is then displayed using Open WorkBench (Open WorkBench 2.12, the user interface of OpenEx Suite, TDT). Programs can be designed within this software to allow effective manipulation of the signal. These include filter settings, analogue output to Labchart and recording channel and reference channel selection for differential recordings. The signal is recorded in blocks which can be transferred to MatLab for analysis. Signals are analysed in MatLab using Wave Solution. Analogue signals were also output to Powerlab for Labchart analysis as per 2.2.8.

3.2.6 MATLAB: Wave solution analysis

As well as labchart analysis performed as per 2.2.8, 1 minute segments of raw data were taken from Labchart and converted to MATLAB ((MATLAB R2010a, MathWorks) files for analysis using Wave Solution. Wave Solution is custom written analysis software created by Richard Csercsa and Andor Magony that can be used to evaluate electrophysiological signals. Data were resampled at 500Hz to reduce processing requirements for analysis. A band-pass filter of 1-30Hz was applied before analysis to eliminate large noise artefacts occurring at 50Hz. This is also the same band pass filter applied in Labchart filter settings, for continuity. A fast Fourier transform was applied to each section, allowing calculation of the power of the signal over time at

different frequencies. This enabled analysis of the data through periodograms (graphical representations of the spectral density of the signal across different frequencies, plotting frequency (Hz) against power (uV^2)) and spectrograms (3D graphs representing time, frequency and power on the X, Y and Z axes respectively). This was used to analyse power/frequency differences between atrium and ventricle, and to determine how the power of the signal changes before and after drug treatment. 3D spectrogram graphs were created by sampling 10 second sections from the recording for analysis. The FFT calculation then reproduced this section coloured for highlighting higher and lower power frequency areas in the recording. Periodograms had 100 smoothing points applied and Spectral density colour maps were optimised using standardised index number settings (blue marker: 2, turquoise marker: 18, yellow marker: 37, red marker: 55) for ease of visualisation of the higher and lower power areas.

3.2.7 Temperature control

All recordings were taken at a temperature between 24.5. and 25.5 degrees Celsius. Temperature affects heart rate, and by extension the ECG interval measurements. Steps were taken to try to monitor and control temperature, but finding a solution which did not impact on electrical noise was difficult, any equipment required for heating, controlling and monitoring temperature would need to be inside the Faraday cage, therefore introducing more electrical noise in proximity to the electrodes. For this reason, the recording area inside the Faraday cage was heated using a radiator to 25.5^{o}C and then switched off for the recording. The Faraday cage was insulated against heat loss by covering the cage in tin foil, with a retractable flap at the front to allow access for positioning. The radiator was switched off prior to recording to limit noise. The

temperature during the recording was monitored using a temperature probe (ATC 1000 DC temperature controller, World Precision Instruments). When the temperature dipped below 24.5 ^{o}C, the recording was stopped and the recording area reheated.

3.2.8 Statistical tests.

Data sets were tested for normality using Shapiro-Wilk and Anderson-Darling tests. Normal distribution plots were also used to check and validate these results.

The normalised frequency values for the 3 periodogram peaks taken from the atrium and ventricle fluorescent lines (Tg:VMHC-red and Tg:AMHC_cherry-NTR) were analysed for significance using Mann-Whitney and Wilcoxon tests.

Comparison of atrium and ventricle amplitudes from both single and dual electrode experiments were tested for significance using Wilcoxon paired-signed test.

3.3 Results

Atrium and ventricle recordings were taken to determine firstly, if it was possible to distinctly record signals from these chambers, secondly if there is a difference between atrium and ventricle signals, and thirdly to try and quantify this difference and apply appropriate statistical tests to determine whether the difference was significant.

3.3.1 Atrium and ventricle signals recorded using single electrode recording method.

The first preliminary experiment to observe atrium and ventricle recordings, used the established single glass electrode recording system and took sequential atrium and ventricle recordings from n= 18 wild type embryos (AB strain). This was performed using a single glass electrode positioned first on the atrium for 5 minutes followed by a 5 minute recording from the ventricle. This allowed analysis of the atrium and ventricle signals from the same embryo using the existing single electrode recording method and an instant direct comparison between the two signals could be made.

These recordings were analysed for average cardiac cycle wave morphology to see if there were distinct characteristics between these two groups of recordings**, figure 3.2**.

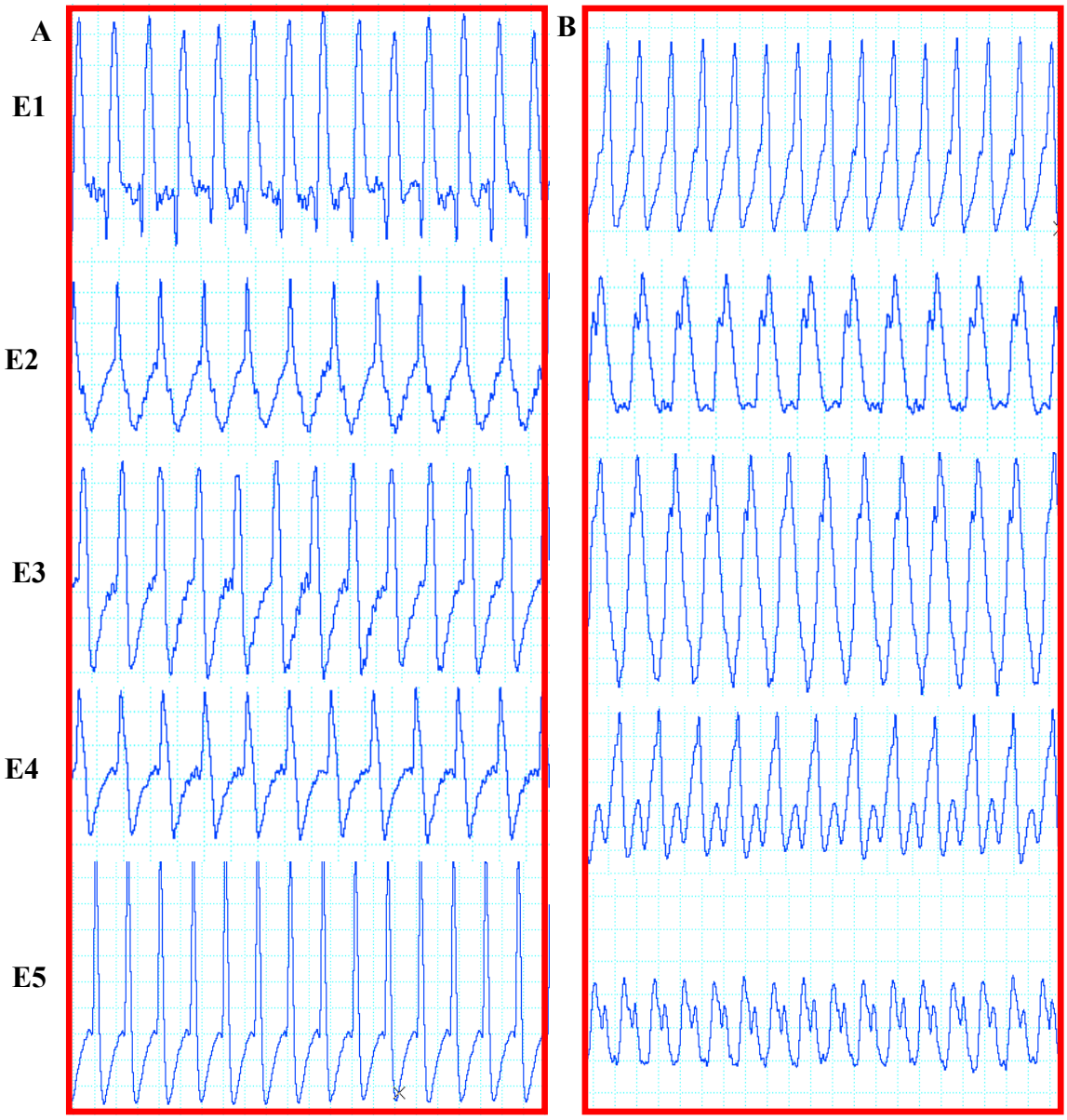

Figure 3.2 Example atrium (A) and ventricles (B) signals for 5 3dpf embryos (E1-E5) recorded using the single electrode recording system. Some overall patterns observed for atrium and ventricle but not conserved for all embryos. Variation in amplitude and morphology. N=18 embryos analysed in total. Figure shows matching chamber signals from 5 embryos as examples from the n=18 performed in total.
A) n= 5Atrium recorded signals
B) n= 5Ventricle recorded signals

There were no consistent morphological distinctions between atrium and ventricle recorded signal across all embryos; there were some overall patterns but none that were shared by all embryos. However, signal shape is in part dependant on electrode position

so it was thought that standardising and controlling electrode placement and position may produce clearer similarities between repeat recordings. Minute long sections of each recording were extracted as MATLAB files and analysed using MATLAB programme Wave Solution developed by Andor Mahony and Richard Csercsa. This programme applies a fast Fourier transform to the signal to produce periodograms and spectrograms, which displays signals as components of frequency, time and power. This displays the ECG signals as components of frequency/Hz, power/μV^2 and time/s. Spectrogram analysis of the atrium and ventricle recordings from the n=18 embryos was carried out to look at power frequency patterns, **figure 3.3**. These analyses give information about the frequencies which make up the components of the ECG and action potentials of the larval zebrafish heart.

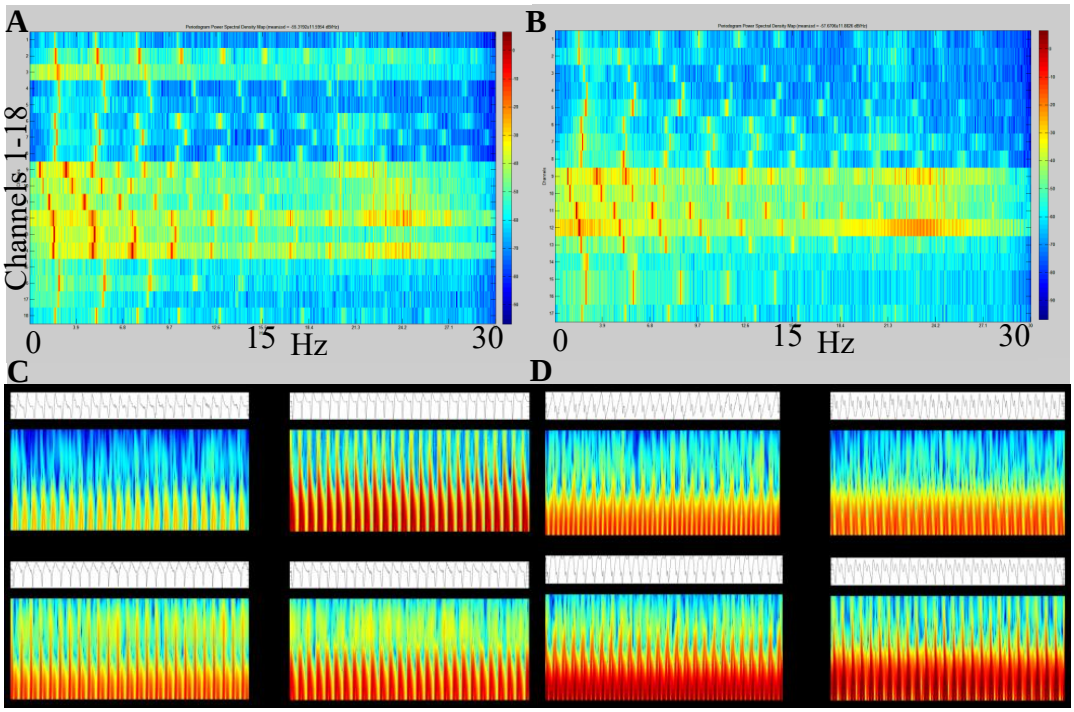

Figure 3.3 ECG signals displayed as components of time, frequency and power, Power frequency spectrums are a different way to look at ECG signals and analyse the frequencies of the PQRST waveforms. Colour on all charts represents Power density/μV^2. Higher power is towards the red end of the spectrum, lower power towards the blue.
A) n=18 Atrium signal Power spectral density maps collated together in rows 1 row = 1 recording signal
B))n=18 ventricle signal power spectral density maps collated together in rows 1 row = 1 recording signal
Rows between A and B correspond to the same embryo.
C) 4 example atrium signals and spectrograms: X axis: time/s Y axis: Frequency/ Hz.
D)4 example ventricle signals and spectrograms: X axis: time/s Y axis: Frequency/ Hz.
Example atrium and ventricle traces taken from same embryos (n=4).

Stacked power density spectrogram analyses showed that there were repeated bands of high power at certain frequencies, throughout all n=18 recordings for atrium and ventricle, **figure 3.3 A,B.** Individual spectrograms for each recording showed these higher power frequency bands corresponded to waveforms of the ECG, **figure 3.3 C,D.** Analysis of these spectra showed potential repeatable differences between the atrium and ventricle signals, indicating a difference could be quantified. To analyse these

potential repeatable differences in more detail further refinement of the experimental procedure is needed to standardise the electrode positions to reduce the variation between repeats.

3.3.2 Atrial and ventricle recordings taken from fluorescent lines using standardised electrode positions.

To develop the protocol further, it was necessary to standardise the positions used for atrium and ventricle recordings. To make sure the atrial and ventricle positions for recordings were consistent, a grid was overlaid on an image of a 3dpf larval heart. Specific atrial and ventricle fluorescent transgenic lines were used to more accurately map the electrode position on the heart. This was used in reference for positioning the electrode on all the embryos. The grid can be seen in **figure 3.4A**. *In silico* modelling predictions, performed by James Crowcombe, were used to determine the optimal positions for recording the atrium and ventricle separately, **figure 3.4 B** (Crowcombe *et al,* 2016)**.** The two positions were chosen as they lie at the extremes of the heart and are therefore the best positions to obtain atrial/ventricle signals in isolation. To analyse the potential difference seen from the preliminary experiments further, atrium and ventricle recordings were taken, n= 20 AMHC atrial and n= 20 VMHC ventricle at specific positions taken from a grid formation over a 3 dpf larval zebrafish heart.

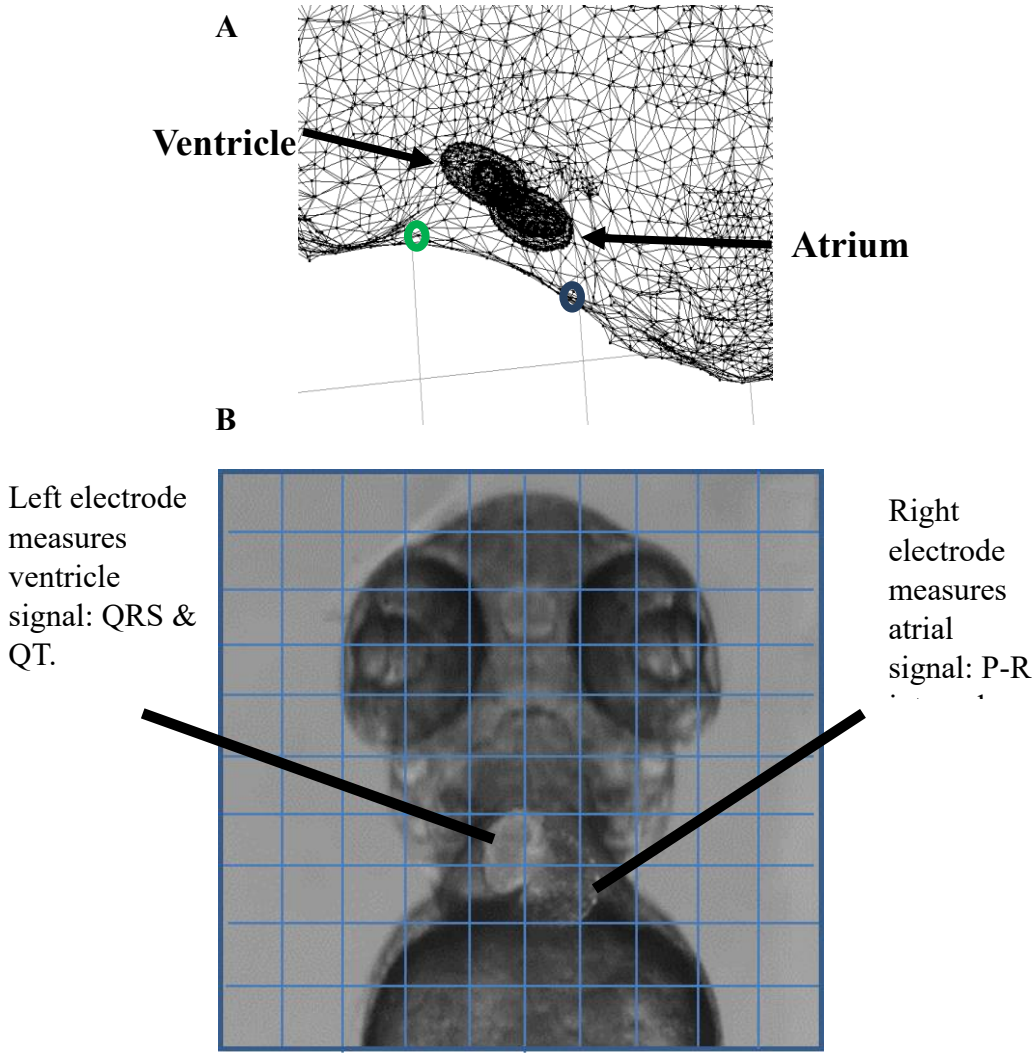

Fig 3.4: Determining atrium and ventricle electrode recording positions using computational modelling of zebrafish heart.
A) Computational modelling (in silico) work mapping electrical activity on the surface of the larval zebrafish heart, produced by James Crowcombe (Crowcombe et al, 2016). This predicted the positions for atrium and ventricle recording electrodes by selecting position where signal amplitude for that chamber was greatest. Blue and green circles mark the predicted positions for atrium (blue) and ventricle (green).
B) Grid reference used for positions of the atrium and ventricle recordings. Image produced by overlaying ScanR images of Tg(AMHC:mcherry-NTR) and Tg(VMHC:red).Black lines represent electrodes.

Atrium and ventricle signals were recorded as single electrode recordings using the Tg(AMHC:mcherry-NTR) for atrium recordings and Tg(VMHC:red) for ventricle recordings. The temperature was monitored throughout all the recordings and

controlled such that the temperature was within a temperature range of 24.5 and 25.5 ºC for all recordings. 2-3 minute recordings were taken and 1 minute sections were then extracted as MATLAB files for analysis. Each recording, n=20 atrium and n=20 ventricle, were analysed by applying a fast Fourier transform and from this a periodogram showing frequency/power peaks, **figure 3.5 A** and spectrograms displaying 10s sections of recording as 3D maps of frequency and power / time, **figure 3.5B**. Spectrographic analyses were also collected and stacked for atrium and ventricle recordings for direct comparison, **figure 3.5 C, D**. These sections were also analysed using Labchart to obtain R-R intervals used for analysis, **figure 3.5E.**

Comparison of each of these analyses showed cross correlation. The bands of high power observed in the stacked spectrograms for all n=20 atrium and n=20 ventricle recordings corresponded with the peaks observed from the periodograms. For example, the first high frequency band (boxed in red, **figure 3.5 C, D**) corresponds with the first peak on the periodogram. Also, in the 3D spectrograms showing 10s sections of recording as frequency and power against time, the high power areas (in red/orange from the colour scale, **figure 3.5B**), correlate with the waveforms of the ECG, most notably, the R peak (QRS complex). A secondary wave of lower frequency is also observable, which could represent the T wave, reading off a frequency value off these graphs is difficult as it is difficult to accurately determine the point of highest power, but the dark red (highest power on colour scale) appears to be under 5Hz, which correlates with the other analyses. Variation of frequency between repeat atrium and ventricle recordings can be seen from the stacked spectrograms, where the first peak for each falls within the red box, but this covers a frequency range of 0-5 Hz.

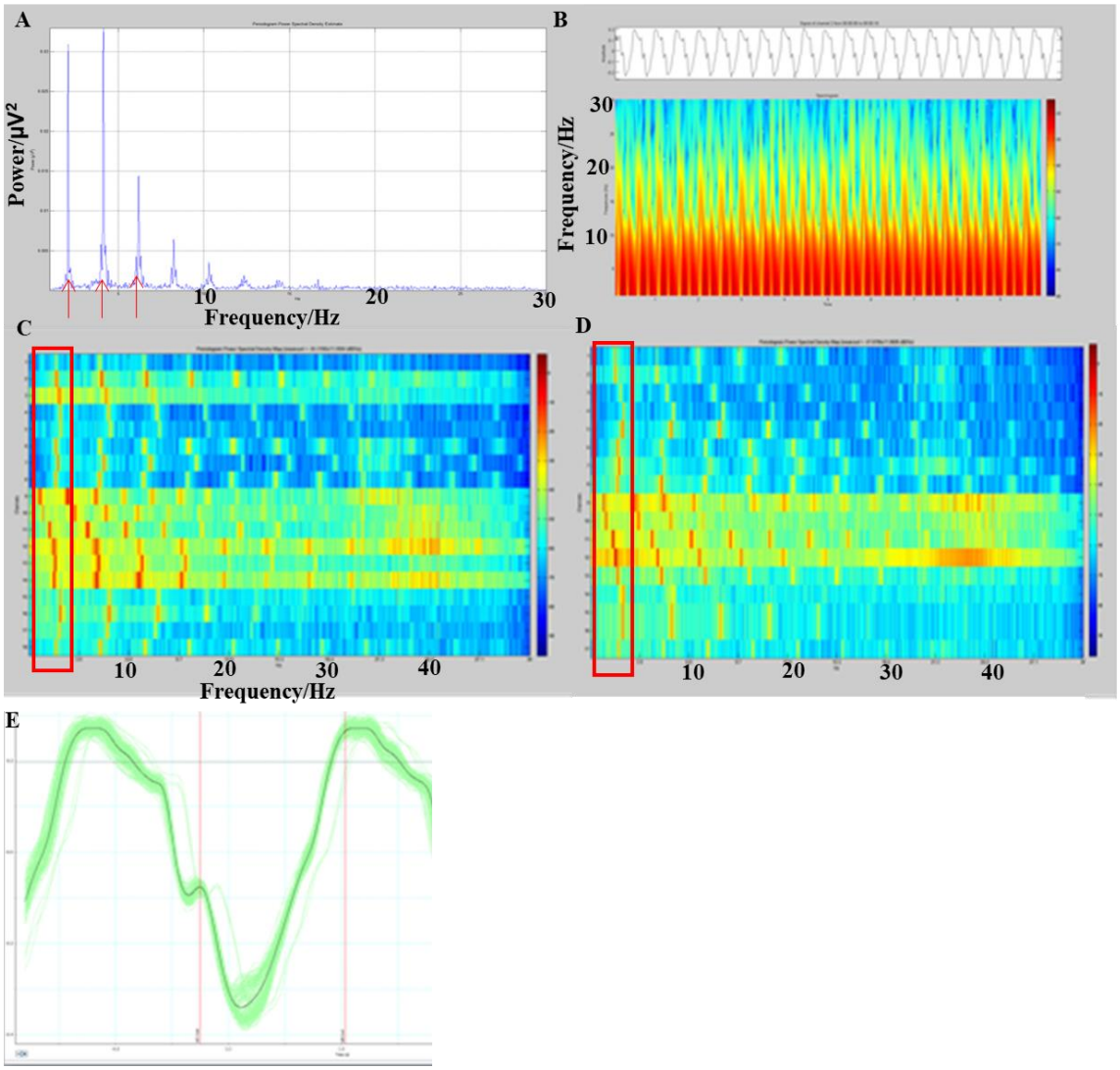

Fig 3.5. Spectrographic and Labchart analyses of atrium and ventricle recorded ECG signals from 3dpf heart using fluorescent transgenic lines Tg(AMHC:mcherry-NTR) for atrium recordings and Tg(VMHC:red) for ventricle recordings (n= 20 AMHC atrial and n= 20 VMHC ventricle) from grid references E7(ventricle) and G8 (atrium.)
A) Example periodogram, frequency values for the first 3 peaks from each recording taken for analysis. The first 3 peaks were the most consistent across recordings. Taken from a ventricle recording.
B) Example Spectrogram for 10s of signal expressed as time, frequency and power. Areas of high power (red/orange) correlate with the R peaks and other ECG features. Taken from a ventricle recording.
C) n=20 stacked spectrograms of frequency/power for atrium recordings.
D) n=20 stacked spectrograms of frequency/power for ventricle recordings.
C&D) The red box highlights the range of frequencies for the first peak observed in the periodograms for each recording.
E) Example Labchart average waveform morphology analysis to look at ECG intervals, such as RR interval.

There were no noticeable differences between the transgenic lines used and the traces recorded from wild type embryos, use of the transgenic line was to aid positioning only and had no effect on the ECG.

Analysis of the spectrograms and signal patterns between atrium and ventricle recordings, **figure 3.5 C**,D showed that there may be repeatable frequency differences, indicating the difference can be quantified through frequency analysis. To quantify this signal difference, the frequency values for the first big three peaks of the periodograms were taken, three were chosen as most of the recordings showed 3 peaks, so this looked to be the most reproducible pattern, **figure 3.5, A**. Frequency values were taken from the periodograms rather than the other analyses as these gave exact frequency readouts, and as such are more accurate and less prone to error than the reading of frequency values off the other spectrographic analyses charts. These frequency values were extracted from the periodograms and normalised against the heart rate, calculated in Labchart, to remove frequency differences due to changes in heart rate. The averaged normalised frequency points for each peak, for atrium and ventricle are seen in **figure 3.6**. The general trend, is as expected: frequency decreases as RR interval increases (heart rate decreases).

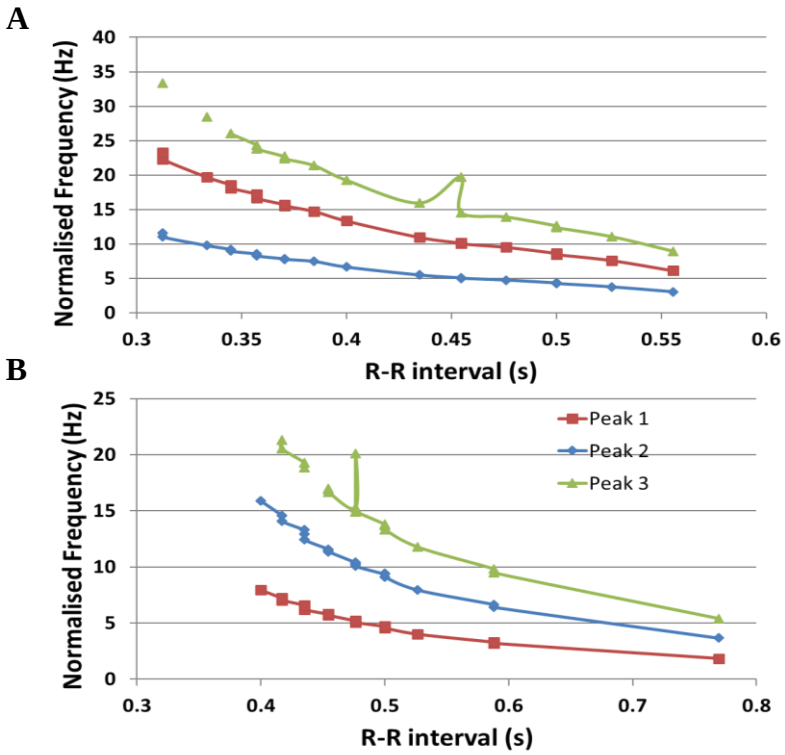

Figure 3.6. Averaged frequency peaks against RR interval normalised with respect to heart rate. Taken from n=20 atrium and n=20 ventricle periodograms.
A) Normalised frequency vs RR interval for the averaged 3 peaks for atrium.
B) Normalised frequency vs RR interval for the averaged 3 peaks for ventricle.
Taken from n=20 Tg(AMHC:mcherry-NTR) for atrium recordings and n=20 Tg(VMHC:red) for ventricle recordings.

One anomaly was observed from the readings from peak 3 where one embryo didn't fit the trend line. In this embryo the frequency was lower than expected with respect to heart rate. This anomaly was still there after normalising against heart rate.

The normalised frequency values were then plotted in a histogram format to determine distribution and it was found that the distribution was not normal, and a Mann-Whitney and Wilcoxon tests applied. The atrium and ventricle frequency differences for all three peaks are significant with ventricle signals consistently producing lower frequency peaks, **figure 3.7**.

A

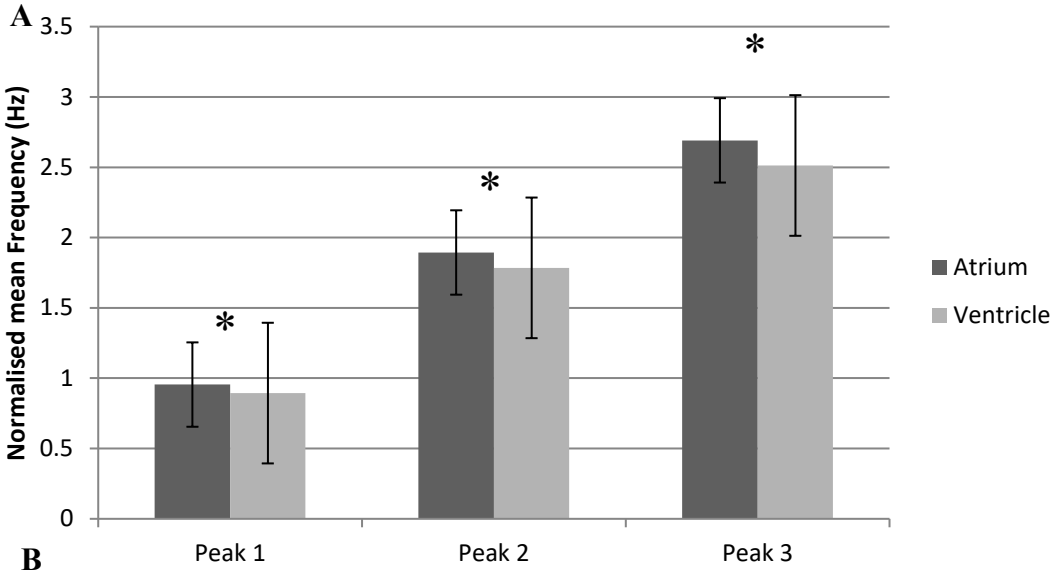

B

	Peak 1	*Peak 2*	*Peak 3*
Atrium	*1.64 – 3.37*	*3.27 – 6.74*	*4.88 – 10.10*
Ventricle	*1.34 – 2.67*	*2.68 – 5.34*	*3.98 – 8.01*

Figure 3.7 Mean Frequency values for Atrium and Ventricle for each Peak, normalised against heart rate.
A) Chart shows atrium vs ventricle periodogram peak frequency values, normalised against heart rate. There is a statistically significant difference between atrium and ventricle for all 3 frequency peaks.
B) Table shows the frequency range for each peak prior to normalising against heart rate: ventricle frequencies are consistently lower than the atrium measured frequencies across all three peaks.
Taken from n=20 Tg(AMHC:mcherry-NTR) for atrium recordings and n=20 Tg(VMHC:red) for ventricle recordings.

This demonstrates that there are separate frequency ranges for atrium and ventricle signals, which are consistent across n=20 repeats.

3.3.3 QRS amplitude recorded in atrium / ventricle.

Further *in silico* work (performed by James Crowcombe) modelling the larval zebrafish heart predicted that we should see a 25% increase (1.3X larger) R wave amplitude height in the ventricle compared to the atrium. It is potentially easier to see this in recordings from the same embryo, which is why the recordings produced in 3.3.1 were used where atrium and ventricle recordings were taken from the same wild type embryo consecutively. The recordings were analysed in Labchart: producing an overlaid average wave form for a selection of data and P,Q,R,S,T intervals assigned. The resulting intervals and amplitude heights were recorded for each embryo for both atrium and ventricle, f**igure 3.8**.

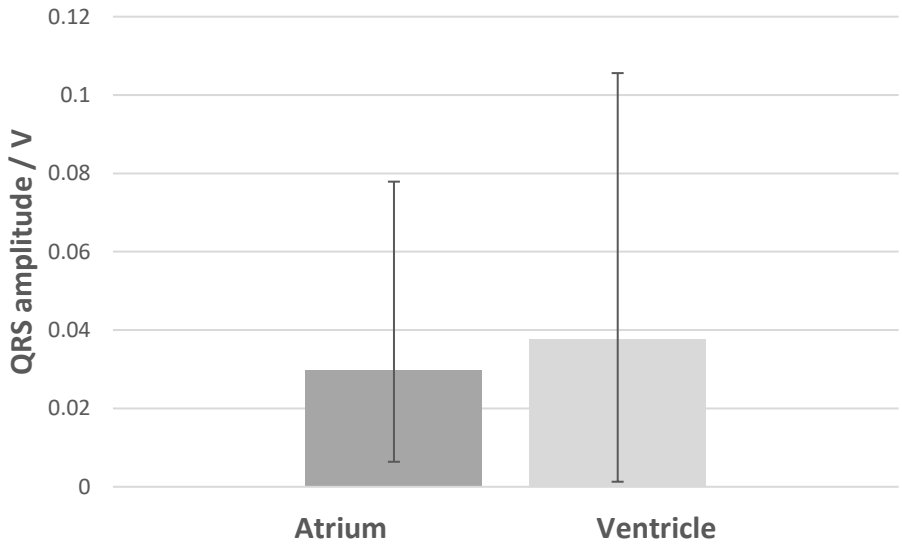

Figure 3.8. Analysis of R peak amplitude recorded from the atrium and ventricle of 3dpf larval zebrafish heart. Amplitude differences between the two chambers were predicted. R peak amplitude was larger in the ventricle than in the atrium across all recordings, however due to the variation in amplitudes recorded, the error bars were large and so the results were not significant. N=18 wild type 3 dpf embryos. Error bars: standard deviation.

As **figure 3.8** shows, the QRS amplitude for the ventricle was consistently larger than in the atrium, but the range of amplitudes across the data set meant that the error bars

(standard deviation) were large, and so the result was not significant. Due to multiple factors affecting amplitude height, this is not a reliable approach for analysing atrium and ventricle signal differences. The first step to reducing variation in recordings for atrium and ventricle analysis would be to record from these chambers simultaneously.

3.3.4 Stimulation signal used to standardise signal differences between the 2 electrode systems

Thus far, the recording method used for ECG recording was the previously established single glass capillary electrode system. The best way to directly compare the ECG signals recorded from atrium and ventricle positioned electrodes is to record them simultaneously. To facilitate this, a second recording station complete with electrode holder and inchworm motor arm was installed into the system with both electrode arms connected to a multichannel channel pre amp (Tucker Davis Technologies). To standardise the electrode settings in both electrode recording arms it is important to control the electrode properties, position and distance. Using identical pulled borosilicate glass capillaries with the same taper, tip diameter and length to control the electrode properties and in addition to the chloridised silver wire used to connect the electrode to the pre amp was kept to 4 cm and 3 minutes chloridisation for consistency. Electrode placement was controlled using an inchworm motor arm attached to each electrode and the positions used were the *in silico* modelling derived atrium and ventricle positions previously described (E7 ventricle, G8 atrium). To confirm that the signal from each electrode arm set ups were consistent, a stimulation signal was sent between the electrodes in both directions and recorded. Two recordings were taken; the first, stimulation signal sent from the left and recorded in the right and then sent from the right and recorded in the left. The signal sent was of a set voltage and amplitude, so

therefore the difference seen in the receiving electrode used to normalise the cardiac signal. The difference in the signal was taken as the difference in R wave amplitude, which is measured in mV, **figure 3.9**.

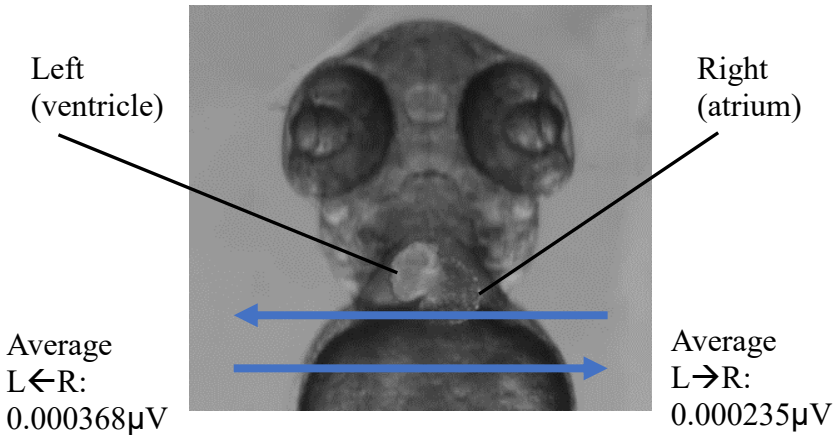

Figure 3.9. Standardisation of 2 electrode arms for dual recording of atrium and ventricle signals. Stimulation signals at set voltage and amplitude were sent from the left electrode and recorded in the right and from the right electrode and recorded in the left. Signal received on the left is 0.000135µV higher than the right, therefore right side (atrium) is 0.0001325 bigger than left (ventricle) electrode so ventricle R amplitude is multiplied by the difference (0.000235/0.000368). This difference was applied to dual electrode embryo recordings to standardise and normalise the two electrode signals. N=8 wild type3 dpf embryos.

This stimulation control of sending artificial signal of known current (1 mV) between two recording electrodes, allowed the difference between the two electrode arms to be used to correct heart recorded ECG signal. For subsequent dual ECG recordings; the electrodes were positioned, then the stimulation control was performed, the dual heart signal was recorded and the stimulation repeated. These were performed in triplicate, and averaged, corrected amplitudes used for results**, figure 3.10 B.**

Having standardised and normalised the dual electrode system, signals from the atrium and ventricle were recorded simultaneously. This allowed direct comparison in real

time of the signals recorded from these two positions. The signals were overlaid to analyse signal morphology differences, and a larger amplitude was measured in the ventricle signal, **figure 3.10A.** Labchart analysis measured R peak amplitude, and these were corrected by electrode stimulation control difference. Recordings of n=8 wild type 3 dpf embryos, each recording with stimulation control done in triplicate were averaged and the results plotted, **figure 3.10B.** This experimental approach showed a significant difference between atrium and ventricle signal R peak amplitudes and variation between recordings reduced. Periodograms and 3D spectrograms of these signals were created from 1 minute extracted sections and compared. Periodograms, **figure 3.10C, E** and 3D spectrograms, **figure 3.10D,F** were created for the dual signal shown in **figure3.10A.** These also showed the frequency differences described in 3.3.2, corroborating that result. Ventricle signals showed lower frequencies, and also lower power than atrium signals.

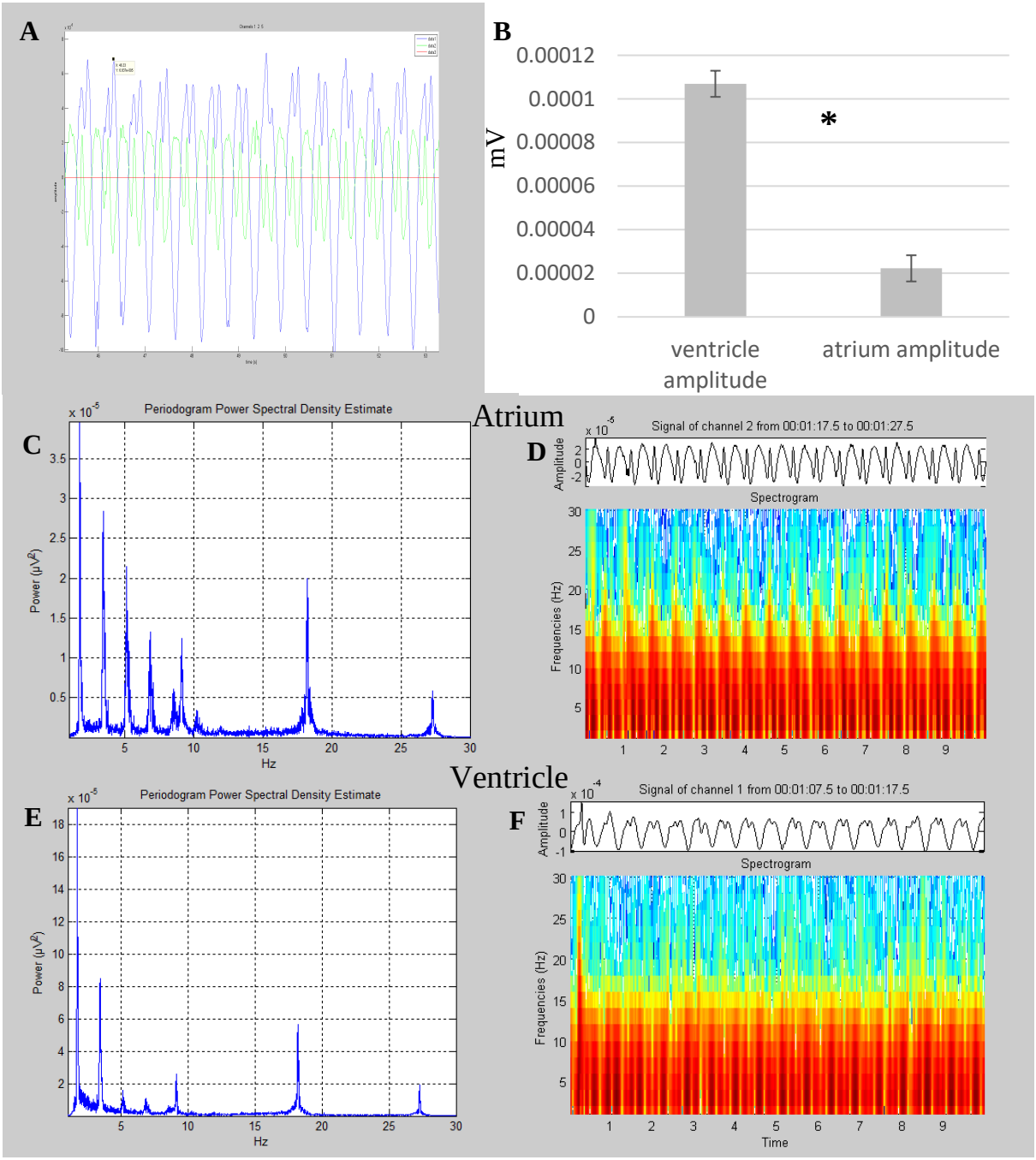

Figure 3.10. Dual recording of atrium and ventricle signals in the wild type 3 dpf larval zebrafish heart, and analyses. N=8
A) Overlaid signals: Blue: channel 1 (left-side, ventricle) Green channel 2 (right-side, atrium) Red Stimulation channel. Amplitude difference between atrium and ventricle R amplitude observed.
B) Amplitude difference between atrium and ventricle signals is significant. Error bars: standard deviation.
C) Periodogram of atrium signal from dual signal shown in A)
D)3D spectrogram analysis of atrium signal from dual signal shown in A).
E) Periodogram of ventricle signal from dual signal shown in A)
F)3D spectrogram ventricle of signal from dual signal shown in A).

3.3.4 Using Fast Fourier transform to analyse ECG changes from drug treatment.

Further to the frequency spectrum analysis shown in 3.3.2, it was investigated as to whether the heart rate and QT differences from drug treatment could be measured using Fourier transform calculations and therefore the changes leading to QT prolongation can be viewed as changes in frequency and power. ECG recordings for before and after 5µM terfenadine were performed in wild type 3 dpf embryos (n=4) and fast Fourier transform applied. Clear shifts in high power bands to lower frequencies were observed after drug treatments, **figure 3.11.**

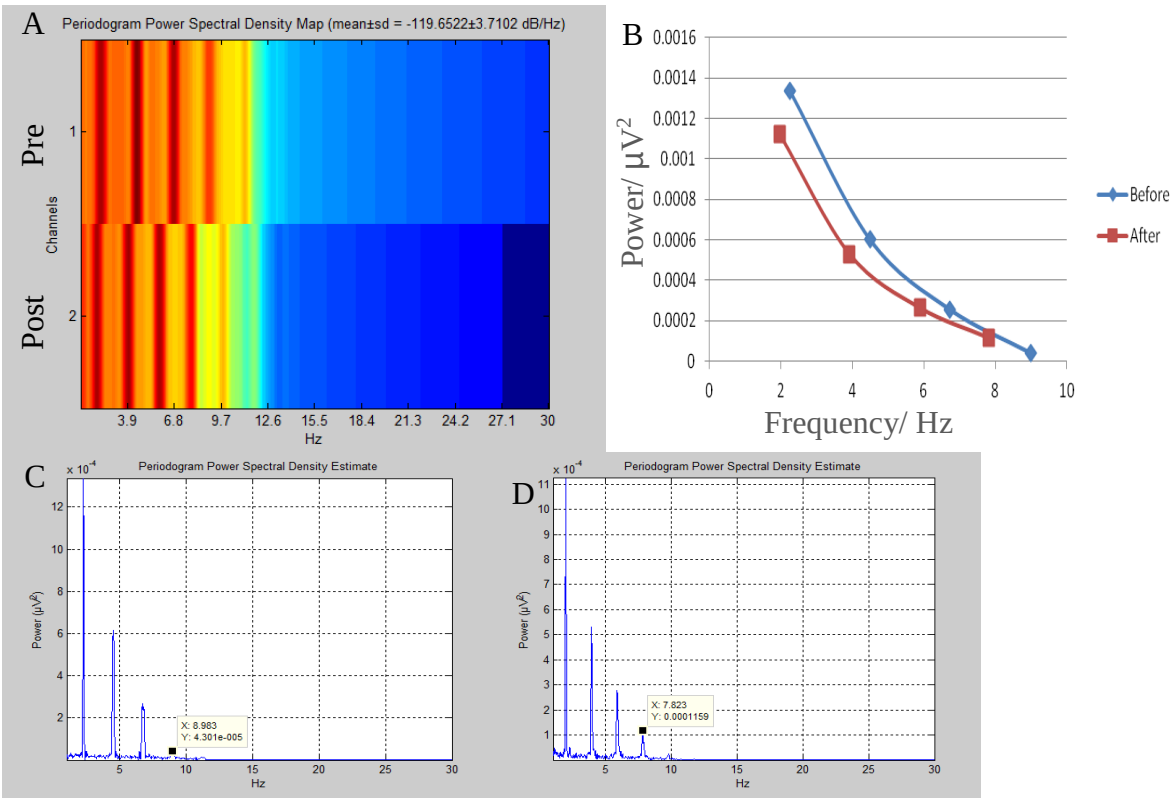

Figure 3.11. Spectrogram and periodogram analyses of before and after 5µM terfenadine treatment. These results were measured from the single electrode system, positioned at the AV junction between the atrium and ventricle. N=4 wild type 3dpf embryos.
A) Spectrogram showing shift in frequency power to lower frequencies after drug treatment. Top row, before 5µm terfenadine and bottom row, 20 mins post treatment.
B) Comparative periodogram mapping frequency and power shows a shift to lower frequency after terfenadine treatment.
C) Periodogram before drug treatment and D) Periodogram after drug treatment C&D used to create the comparative periodogram chart.

To extend this result further, a dual electrode recording with 5µM terfenadine treatment was performed (n=4 wild type 3 dpf embryos). Terfenadine treatment also showed differences in response between atrium and ventricle**, figure 3.12**.

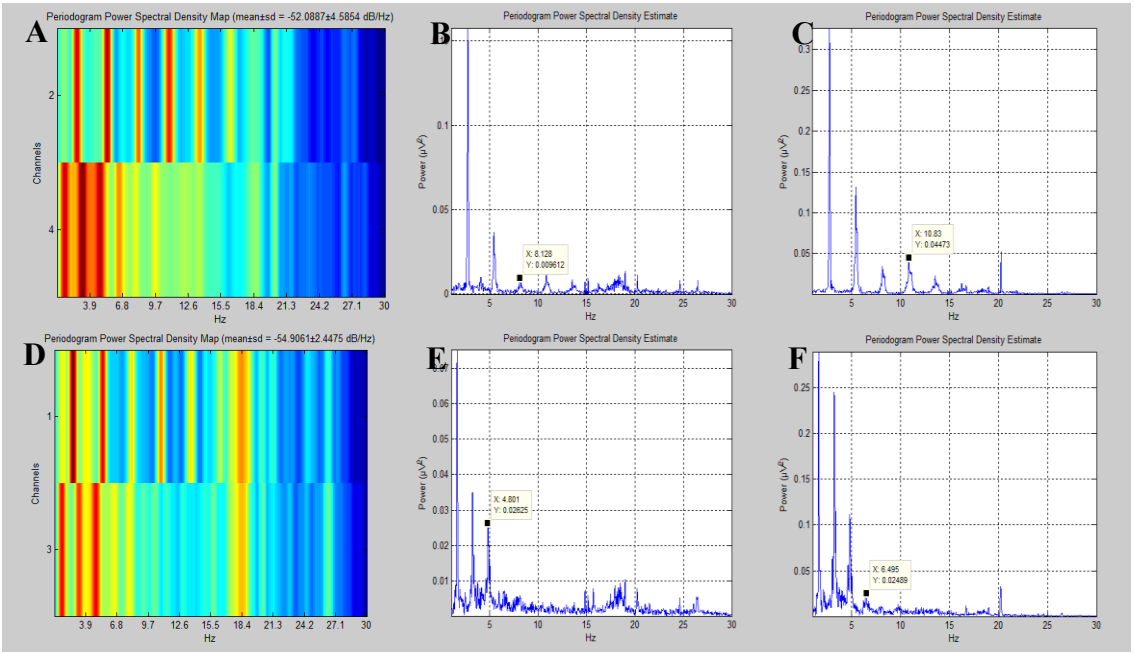

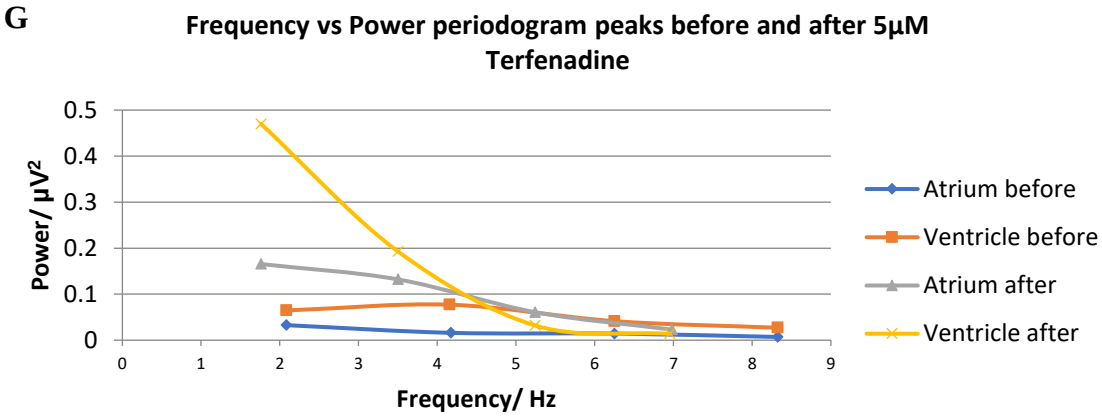

Figure 3.12 Analysis of atrium and ventricle signals recorded simultaneously pre and post 5μM terfenadine treatment in wild type 3 dpf embryos n=4.
A) Spectrogram showing shift in frequency from before drug treatment (top row) to after drug treatment (bottom row) for atrium signal.
Periodogram shows a difference before B) and after C) drug treatment and in atrium signal responses
D) Spectrogram showing shift in frequency from before drug treatment (top row) to after drug treatment (bottom row) for ventricle signal.
Periodogram shows a difference before E) and after F) drug treatment and in atrium signal responses.
G) Signals show shift in frequency patterns post treatment and there is a marked increase in power in the ventricle signal post treatment.

Stacked spectrograms showing pre and post terfenadine treatment were created for atrium **figure 3.12A** and ventricle **figure 3.12D.** Both showed shifts in high power

bands to lower frequency after drug treatment. This was also reflected in the periodograms created for pre and post treatment for atrium **figure 3.12 B, C** and ventricle **figure3.12 E,F.** The chart shown in **figure 3.12 G**, also demonstrates this frequency shift but also shows a marked increase in power in the ventricle recorded electrode, indicating a difference in atrium and ventricle response. A bigger difference in the ventricle electrode for a QT prolongating drug such as terfenadine would make sense, as QT prolongation affects ventricular repolarisation and therefore the ventricle should have a more marked response compared to the atrium. Therefore, this is a demonstration of an ECG recorded chamber specific difference analysed by frequency analysis. This analysis approach is automatable, making it a potential method for analysing ECG drug treatment response and may also indicate chamber-specific responses.

3.4 Discussion

This chapter aimed to analyse atrium and ventricle signals in the larval zebrafish heart and determine if there was any difference between signals recorded at the atrium and ventricle, and to quantify this difference. Several approaches were utilised for analysis, including single and dual recorded signals, ECG morphology, Fourier transform and wavelet analyses, and signal amplitude. Standardisation of electrode position and stimulation controls allowed confirmation of significant differences between atrium and ventricle signals by frequency analysis and by signal amplitude. Wavelet analysis was also applied to signals recorded pre and post drug treatment to determine whether differences caused by drug treatment could be analysed using these approaches. Frequency shifts post drug treatment could possibly be used for quantifying drug treatment effects and this type of analysis would more easily be automated than ECG interval measurements.

3.4.1 Preliminary look at atrium/ ventricle signals

Atrium and ventricle recordings were taken consecutively from n=18 3 dpf embryos to determine firstly, if there is a difference between atrium and ventricle signals and secondly to try and quantify this difference and apply appropriate statistical tests to determine whether the difference was significant. These signals were then analysed for the shape of the ECG cardiac cycle. There was a large amount of variation and 75% of embryos showed similar patterns for atrium and ventricle signals indicating there are possibly specific characteristics for atrium and ventricle recordings. However, there were no consistent patterns present in all embryos. Signal morphology is in part dependant on the position of the electrode on the heart, so it became important to

standardise the electrode positions for the atrium and ventricle electrodes to improve the quality and comparability of repeat recordings between embryos.

To analysis these signals further, 1 minute sections were extracted as MATLAB files and analysed in Wave Solution. Fast Fourier transform analyses were applied to these sections and displayed as frequency power spectrograms and periodograms. This also suggested differences between atrium and ventricle ECG signals, with similar high power frequency bands, indicating that analysis of the ECG waveform frequencies would highlight atrium and ventricle differences. It was predicted that atrium and ventricle frequency profiles would be distinct enough for statistical significance, but further refinement of the recording procedure was required to reduce inconsistency between repeats and reduce the frequency range observed between recordings. It was decided that combining *in silico* modelling work with a grid format would standardise the electrode position for the following experiments.

3.4.2 Significant difference between atrium and ventricle recorded signals detected using fast Fourier transform analyses.

Following on from the preliminary experiment, atrium and ventricle signals were recorded using the transgenic lines fluorescent for atrium Tg(AMHC:mcherry-NTR) and ventricle Tg(VMHC:red), electrode positions standardised for consistency. Wavelet analysis producing periodograms and spectrograms for these recordings were produced and frequency peaks taken for analysis. Statistically significant differences were observed between periodogram peaks suggests distinct frequency ranges for atrium and ventricle recorded signals, with ventricular frequencies consistently lower than atrium across all three peaks. This correlates with the ECG parameter measurements: PR

interval 0.12 – 0.2s, QRS 0.04 – 0.12s and QT <0.42s This suggests that on these spectra analyses, the QT interval which corresponds to ventricular repolarisation, is the largest wave, and as such would have the lowest frequency. The PR interval, which is the atrial component in the ECG atrial depolarisation, has the shortest interval, and so would have the highest frequency. In humans, similar patterns are seen and waveform features of time and frequency components can be used to detect arrhythmic waveforms, for example; the frequency of ventricular fibrillation is between 4-7Hz. Spectra and power spectra vary with arrhythmia, as seen here with analysis of zebrafish ECGs (Lin, 2008).

This type of electrophysiological signal analysis is important as it is possible it can be used as part of an automated signal analysis software for the development of high-throughput system. The end goal of this project is to produce a high throughput ECG recording system for zebrafish embryos, and part of this is to have implemented an online software analysis system to decrease analysis time. However, these analyses should not be in place of more established signal analysis methods, where the ECG cardiac cycle is averaged across the recording and ECG interval times (P-R, QRS, QT) are determined. They can be used in combination to extract more information from the recording.

3.4.3 Standardisation of a dual electrode recording system.

Introducing a second recording arm for simultaneous electrode recording from 2 positions on the 3 dpf larval heart represents a significant step forward and opens up possibilities for more in-depth analysis of the larval zebrafish heart activity. Particularly, using this system, significant differences in amplitude between the atrium

and ventricle R peaks were measured. Standardisation of the electrodes using the stimulation control is necessary as the voltage being measured and compared is so small from the embryonic zebrafish and this maximises the sensitivity to pick up these small changes in voltage/frequency/time when the ECG changes in response to external stimulus such as drug treatment. Using this system may also increase sensitivity for recording accurate PQRST differences, particularly atrial differences, as positioning for a clear P wave is the most time-consuming step in the set up process, as it is the smallest wave and the most difficult to obtain a reliable reading.

3.4.4 Amplitude difference in QRS complex in atrium and ventricle signals.

Amplitude can vary greatly depending on a number of factors including; position across the heart, distance from the heart (how much electrode is pressed onto the heart using the inchworm), stage (older embryos have a larger heart) and therefore a larger, more easily recorded signal. The initial experiment for QRS amplitude analysis re-analysed previous recordings, recorded during 3.3.1 (preliminary experiment). These recordings had a range of amplitudes too great for a significant difference to be calculated for both atrium and ventricle results. So, in order to investigate this parameter further this variation needed to be reduced. In order to do this, the atrium and ventricle signals needed to be recorded simultaneously. Development and standardisation of a dual electrode recording system allowed a significant difference in QRS amplitude height to be recorded and analysed. Dual recorded signals showed a 23% increase in amplitude height in the ventricle compared to the atrium signal. This corresponds with the predicted amplitude variance made from the *in silico* modelling at 25%. In humans, there are distinct differences between atrial and ventricular action potentials and

different amplitude differences from recorded ECG signals in zebrafish may indicate a similar distinctness in zebrafish.

This experiment was less to do with comparison of atrium and ventricle and more to do with differences in recording position. The amplitudes taken from these recordings were the dominant peaks, i.e. the QRS which corresponds to ventricular depolarisation. Being the dominant wave, it covers the smaller amplitude atrial repolarisation wave which occurs at the same time. In human, differences in amplitude height can denote arrhythmia. For example, increased amplitude height in children has been linked as a precursor symptom predictive of sudden cardiac death later on. This amplitude can differ in different leads. Human ECG procedure is a 12 lead process. It is the amplitude in the limb leads which has been identified as a marker for sudden cardiac death with a sensitivity of 94% (Osten-Smith *et al,* 2010). Having demonstrated that the recording procedures developed here are sensitive enough to detect amplitude differences between recording positions, these markers could be studied in this model.

3.4.5 Analysis of drug induced differences in ECG traces using fast Fourier transform analyses.

Investigations into whether ECG changes from drug treatment were detectable using Fourier transform and whether these changes could be attributed to atrium or ventricle differences due to the drug treatment. This was performed to see if an alternative form of analysis was possible, to use as an alternative or alongside ECG parameter measurements. Terfenadine is a drug known to cause QT prolongation and a reduction in heart rate, as such it was predicted that this should reduce the frequency seen in the periodogram ECG frequency peaks post treatment. ECG recordings pre and post treatment were analysed using wavelet analysis and periodogram and spectrogram

analyses were performed. The results showed a shift in frequency to lower frequencies post terfenadine treatment. A prolonged QT interval has a larger T wave than normal and would therefore be a lower frequency than a normal T wave. The lower frequency ECG waves recorded post terfenadine treatment would indicate the waves are wider, hence the lower frequency (Hz). This could be interpreted as a QT prolongation, consistent with the known effect of terfenadine on the QT. In addition, terfenadine treatment showed an overall increase in power after drug treatment and showed clear differences between atrium and ventricle recordings. A more marked difference was measured in the ventricle, which corresponds to QT prolongation (ventricle repolarisation), again consistent with known effect of terfenadine. This result highlights another potential approach for analysing ECG response to drug treatment and measuring chamber-specific responses, but further investigation would be required, with a larger sample size and a range of atrium and ventricle acting drugs to trial. In addition, using this type of analysis for ECG recordings is more easily adaptable for use in a high throughput system.

Use of this approach using wavelet analysis to quantify ECG changes in response to drug treatment could be useful, as it would be easier to automate for a high throughput system than ECG parameter measurement which has a large 'human judgement' component where the averaged and compiled cardiac cycles have the PQRST points placed on the averaged cycle. However, during the course of this project, an automated system for PR and QTc interval analysis was developed. As this is the more comparable and more standardised ECG analysis approach, this was pursued instead of further development of wavelet analysis of ECG drug treatment responses (Barrett *et al,* 2016 - as yet unpublished).

4. Investigations to test the sensitivity of the ECG recording system for the analysis of arrhythmic mutants: Phenotypic characterisation of an L-type calcium channel mutant.

All work pertaining to testing the ECG recording system for dual vs single electrode recording system for mutant analysis, the analysis of ECG phenotype of *cacna1c* mutant compared to wild type, comparison of drug treatment response for the 5 cardiac acting drugs and control drug was performed solely by me. Genetic analysis of selected 2dpf *cacna1c* clutches were performed by Sanger Institute. Chlorzoxazone treatment and video analysis was performed in collaboration with Ben Wilkinson. Salinity and orbital shaker experiments were performed in collaboration with Edina Garai.

4.1 Introduction

So far work in this study has concentrated on measuring the effects of cardiac-acting drugs on the larval zebrafish ECG. This chapter will focus on establishing the use of the larval zebrafish ECG system for measuring the differences caused by mutation.

There are several advantages for using zebrafish as a genetic model of disease, beyond the advantages of its small size, ocular transparency and *ex utero* development. The zebrafish genome is sequenced and transgenic lines can easily be created for extremely diverse uses and mimicking a wide variety of human disease states (Santoriello and Zon, 2012, Vornanen and Hassinen, 2016). In particular, there has been massive advancement in the use of zebrafish as a model of cardiovascular disease and arrhythmia (Brown *et al,* 2016, Asnani and Peterson, 2014). Like other animal models, zebrafish undergo manipulations to develop cardiovascular diseases which are similar to human for study. Models of different components with contrasting mechanisms can be produced to allow study into various types of cardiovascular disease state. This allows insight into the human disease process. These include thrombosis, arteriogenesis, inflammation, cardiomyopathy and cardiac regeneration (Chi *et al,* 2008). The relative ease of creating mutant and transgenic lines in zebrafish through transposon-mediated systems has led to the generation of many cardiovascular lines for study. Injection of constructs into freshly fertilized eggs has created a wide range of transgenic zebrafish lines to facilitate study, including many cardiovascular lines (Santoriello and Zon, 2012). As previously discussed, there is high conservation between human and zebrafish, with zebrafish orthologues of all the main human cardiac ion channels, facilitating genetic models centred on ion channel derived arrhythmia to be created (Alday, *et al,* 2014). The creation of a wide variety of cardiac disease transgenic lines has greatly aided the study of human cardiac disease conditions

including cardiac arrhythmia. Cardiac arrhythmia is defined as the perturbance of normal heart rhythm or rate away from normal sinus rhythm. This can occur in many different forms with many different causes. Therefore, transgenic lines created in zebrafish to model arrhythmia are also very diverse in their underlying genetics (Poon *et al*, 2013).

This chapter looks at modelling repolarisation abnormalities such as long QT syndrome as a result of genetic manipulation as opposed to drug treatment.

4.1.1 Genetic causes of long QT syndrome.

This study has focused on long QT syndrome in zebrafish, both drug induced and as a result of genetic manipulation. This is because it is an easily observed ECG phenotype, arising from aberrant cardiac ion channel function causing perturbance of the cardiac action potential. Long QT syndrome is a heterogeneous group of conditions with multifactorial causes (Abrams and Macrae, 2014). While it can arise from certain cardiac acting drugs, in particular hERG channel blockers (kv11.1), it more commonly arises as a congenital condition, and many causal genetic mutations have been identified. Some of these are listed in **table 4.1**. LQTS is split into difference types depending on the mutation causing the long QT, most commonly, loss of function mutations in potassium channels (Schwartz, Crotti and Insolia, 2012).

LQT TYPE	Gene	Protein
LQT 1	KCNQ1	I_{Ks} K^+ channel α subunit
LQT 2	KCNH2 (herg)	I_{Kr} K^+ channel α subunit (kv11.1)
LQT 3	SCN5A	I_{Na} Na^+ channel α subunit
LQT 4	ANKB	Ankyrin-B
LQT 5	KCNE1	I_{Ks} K^+ channel β subunit
LQT 6	KCNE2	I_{Kr} K^+ channel β subunit
LQT 7	KCNJ2	$I_{Kr2.1}$ K^+ channel α subunit
LQT 8	CACNA1c	Cav1.2 calcium channel α subunit

Table 4.1 Adapted from Hedley et al 2009 and Schwartz, Crotti and Insolia 2012. Table shows the nomenclature, gene name and protein for each genetic mutation reported to cause the main 8 forms of long QT.

While loss of function mutation in potassium channels are the most common mutations linked to LQT, gain of function mutations in sodium channel (Brugada) and calcium channels (Timothy syndrome) are also linked to forms of long QT syndrome (Hedley *et al*, 2009). The zebrafish mutant selected for this study is an L-type calcium channel mutant with a progressive severe cardiac phenotype developed by 5 dpf, ultimately leading to heart failure. This was suspected to display a pronounced arrhythmia, including a long QT by 2-3dpf for ECG analysis. Therefore LQT 8 was the focus as this arises from a calcium channel mutation in the Cav1.2 L-type calcium channel.

4.1.2 The *cacna1c* gene encodes the Cav1.2 protein, an L-type calcium channel essential for normal cardiac function.

4.1.2.1 Structure of the alpha 1c subunit of the L-type calcium protein

The *cacna1c* gene encodes the alpha 1C subunit of an L-type calcium channel. L-type calcium channels are heteromeric proteins consisting of an alpha 1 subunit alongside other alpha, beta and gamma subunits. The alpha unit consists of a voltage sensor, the calcium ion selectivity pore and dihydropyridine drug binding sites (Rottbauer, *et al*, 2001). It has 4 transmembrane domains (I-IV) each made up of 6 transmembrane segments (S1-S6) with cytosolic N and C termini.

It has an important role in the cardiac action potential, the channel opens in phase 3 and the influx of calcium into the cardiac myocyte triggers the cell to contract (Splawski *et al*, 2004).

Overall structure is highly conserved between human and zebrafish with both containing the same 4 transmembrane domains each with 6 segments including the highly conserved positively charged S4 segment (Rottbauer, *et al*, 2001).

4.1.2.2 The Cardiac action potential and excitation-contraction coupling: the role of Calcium.

As previously described in detail, the cardiac action potential, which drives each heart beat has four phases, with different cardiac ion channels involved at each phase. Disturbance of any of these channels can cause arrhythmia, and several are linked to different types of Long QT syndrome (LQTS) (Seebohm, 2005).

The cardiac action potential causes cardiomyocyte contraction through excitation-contraction coupling, a highly synchronised process linking the action potential to ventricular contraction through movement of ions (Reuter, 1984). L-type calcium channels are essential in this process, it is the movement of calcium ions during phase 2 of the action potential (plateau phase) which triggers the myocyte to contract and then relaxes when calcium moves back out of the cell. This pulse of calcium ions into and out of the myocyte cytoplasm is what causes each heartbeat and synchronous propagation of the action potential through the ventricle, thereby resulting in apex to base contraction of the whole ventricle. Therefore, calcium movement, and by extension the calcium channels that facilitate calcium movement during the cardiac action potential are vital to normal sinus rhythm (Rottbauer *et al*, 2001). It important to notes some differences between ECC in human and zebrafish. In mammals, sarcoplasmic reticulum (SR) Ca^{2+} release is the main source of calcium in the cell for transient calcium movement causing contraction/relaxation. In zebrafish, the SR is less complex as in higher animals and has a reduced capacity to store and release Ca^{2+}. This means that the SR calcium release is less important in zebrafish ECC, although still present and functional (Verkerk and Remme, 2012). Zebrafish have both T-type and L-type calcium currents and use of L-type calcium channel blockers have shown the importance of the L-type calcium current for normal action potential duration (Nemtsas, 2010).

4.1.3 LQT 8 and Timothy Syndrome.

Long QT syndrome 8 is caused by a missense gain of function mutation in the *cacna1c* gene, encoding the alpha 1c subunit of L-type calcium channel Cav1.2 (Splawski *et al*, 2004). This is the main calcium channel in the human and zebrafish cardiac action

potential and also has important roles in development (Vornanen and Hassinen, 2016). This LQTS8 mutation is diagnosed clinically as Timothy syndrome (Liao and Soong, 2009). Timothy syndrome is a rare multi-system disorder resulting from a point mutation in the *cacna1c* gene encoding the Cav1.2 protein. This is the alpha 1C subunit of an L-type voltage-dependant calcium channel (Splawski *et al,* 2004). This condition has an autosomal dominant inheritance pattern, but less severe cases can result from somatic mosaicism. Timothy syndrome is caused by recurrent de novo Cav1.2 missense mutation G406R located on exon 8 and alternative splice variant exon 8a, both encoding transmembrane segment S6 of domain 1 at the c terminus end, with the splice variant 8a being the most common form diagnosed clinically (Dufendach, *et al,* 2013). Mutation G402S located on exon 8 has also been described. In humans, the splice form containing exon 8 has higher expression in heart and brain tissues (Splawski *et al,* 2005). The different mutations and locations denote variances in the disease, and can range from autosomal dominant to maternal mosaicism. The mutation causes the inward depolarising Ca^{2+} current to be maintained, with near complete loss of voltage dependence left functioning. L-type calcium channels are involved in a wide range of systems; including major roles in development, maintaining normal cardiac rhythm and neurological function (Splawski *et al,* 2005). As a result of L-type calcium channel diverse function, Timothy syndrome has a widely varied group of symptoms across multiple systems. L-type calcium channels are highly expressed in the brain and therefore, there are neurological symptoms including, cognitive impairment, autism and seizures. Another characteristic symptom which is useful diagnostically is syndactyly, which can be corrected surgically. Overall, Timothy phenotypes span the heart, skin, eyes, teeth, immune system and brain (Splawski, 2004).

4.1.4 Current models of Cav1.2 dysfunction and Timothy Syndrome.

There are two previously reported zebrafish mutants of this channel report mutations in the S5 and S6 segment resulting in a truncated protein at these points, **figure 4.1**.

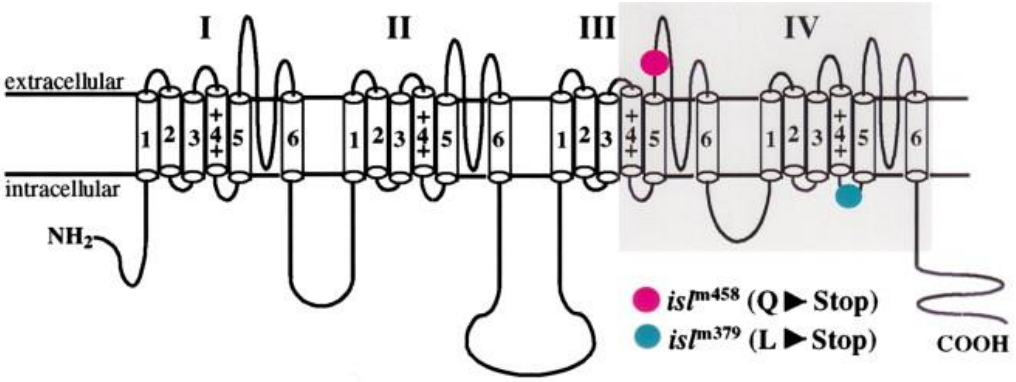

Figure 4.1. Adapted from Rottbaurer et al, 2001. Figure shows the structure of the 4 domains each with 6 transmemebrane spanning segments. Labelled in pink and blue are the locations of the 2 published mutations, each resulting in a truncated protein with loss of function.

This produces a very severe cardiac phenotype with an under developed and silent ventricle by 3 dpf and are therefore expected to be foetal fatal mutations in human (Rottbauer *et al,* 2009). The atrium in this mutant is structurally normal, but the ventricle is smaller in sizes than typical and has fewer myocytes, indicating L-type calcium channel role in normal cardiac development (Verkerk and Remme, 2012). The *cacna1c* mutant chosen (sa6050) has not been used for publication prior to this study. The *cacna1c* sa6050, has a less severe phenotype, with an arrhythmic but beating heart at 3dpf. Therefore, it may be a better model for human calcium channelopathies observed clinically. This mutant, however, does highlight how essential the L-type calcium channel is for normal heart function and development. Total loss of function

has a devastating impact on normal heart rhythm and cardiac development (Rottbauer *et al*, 2009).

Mice have been use to map the Cav1.2 cellular distribution in Timothy syndrome and expression was found throughout the brain. Including the hippocampus, cerebellum and amygdala where abnormalities have been linked to autism. Expression was also found in the heart, digits, eyes and teeth, which match the multisystem phenotypes seen in Timothy syndrome (Splawski *et al*, 2004). More recently, mouse mutant models with the Timothy syndrome mutation, have been shown to have different social responses and demonstrate autistic traits (Bader *et al*, 2011). In this study, the homozygous mutation was fatal, so heterozygous G406R mouse mutants were studied for behavioural phenotypes and displayed altered social behaviour. These included increased contextual fear memory and altered ultrasonic vocalisation, these distinct behaviours differences mirror the key aspects of autism (Bader *et al*, 2011). While this model has allowed insight into the behavioural and neural consequences of Timothy syndrome, the arrhythmogenic components of Timothy syndrome have not been identified in this mouse model. Timothy Syndrome has also been modelled in iPS cells, where human myocyte iPS cells from a Timothy patient were used to study arrhythmia and identify drugs. While a useful model for analysing the mutation effect in one cell type and having the advantage of a higher throughput compared to *in vivo* models, cellular models lack the complexity to model a multisystem disorder such as Timothy syndrome (Yazawa and Dolmetch, 2011). Zebrafish embryos, as a small, vertebrate *in vivo* model with high throughput capability, could be a useful tool for analysing Cav1.2 channel abnormalities such as in Timothy syndrome.

4.1.5 Characterisation of a novel calcium channel mutant *cacna1c* (sa6050).

A principle aim of this study was to establish the use of the zebrafish recording system for analysis of cardiac electrical perturbance observed in the ECG due to genetic mutation. Work so far has focussed on drug induced arrhythmia and it was important to confirm that the recording system was sensitive and robust enough to reliably record changes induced due to genetic variance. Study of mutations associated with human cardiovascular disease (in particular arrhythmia) in an *in vivo* zebrafish mutant model advances understanding of these conditions and allows screens to be developed for potential treatments.

The zebrafish mutant *cacna1c* (allele sa6050) was generated as part of the Wellcome Trust Sanger Institute zebrafish mutation project using ENU protocol (http://www.sanger.ac.uk/sanger/Zebrafish_Zmpgene/ENSDARG00000008398#sa6050).

As in human, the zebrafish *cacna1c* gene codes the $Ca_v1.2$ protein; the alpha 1C subunit of the L-type voltage dependant calcium channel which is essential for normal cardiac function (Alday *et al,* 2014). This gene is a homologue to the human *cacna1c* gene, and as already described, mutations of this gene have been implicated in human cardiac diseases, including arrhythmia and hypertrophy. Human diseases associated with genetic changes in the *cacna1c* gene fall into gain of function or loss of function mutations with different implications. In human disease the most notable examples of these groups are Timothy (gain of function) and Brugada (loss of function) syndromes, (Betzenhauser *et al,* 2015). Timothy syndrome, as described in section 1.4 is a multisystem disorder with an associated cardiac phenotypes of a long QT with and resultant bradycardia (Fukuyama *et al,* 2014). The causal mutations of Timothy

syndrome are gain of function mutations in the *cacna1c* gene produce the characteristic long QT phenotype seen in these patients (Wemhömer *et al,* 2015). Brugada syndrome is characterised by a short QT phenotype and an ST segment elevation caused by a loss of function mutation (Antzelevitch *et al,* 2007). It has also been linked to sodium channel gene SCN5A, the same gene associated with LQT 3. The SCN5A mutations linked to Brugada cause frameshift and deletions leading to failed channel expression and reducing I_{Na} availability, also missense mutations linked to loss of voltage dependant activation/inactivation (Antzelevitch, 2001).

The zebrafish mutant imported for this project has a point mutation at an essential splice site in the *cacna1c* gene, and is expected to have a pronounced arrhythmia phenotype observable on an ECG. Visual observation at 5 dpf of the mutant by the Sanger institute describes a severe bradycardiac and cardiac malformations, so a bradycardic, prolonged action potential is expected. Analysis of this mutant may show that it has parallels with human disease states associated with L-type calcium channel abnormalities such as Timothy or Brugada syndromes.

4.1.6 Utilising the larval recording system for detecting ECG differences due to genetic mutation.

A high resolution ECG recording system to analyse cardiac responses to drug treatment will be advantageous for cardiac drug safety testing. Previous work has shown that the larval zebrafish recording system is robust and sensitive for analysing ECG changes due to drug treatment, and this study has demonstrated the potential and feasibility of a high throughput larval zebrafish ECG recording system for this purpose. ECG analysis of cardiac function will be a useful tool for investigating cardiac mutant phenotypes. To expand further the potential applications of the larval recording system, this study

aimed to demonstrate the utility of this system for recording ECG changes as a result of genetic mutation. To test the sensitivity of the recording system, ECG recordings from an arrhythmic mutant were performed.

A zebrafish mutant with a point mutation in the L-type calcium channel alpha 1C subunit (*cacna1c* gene) was selected. This channel is responsible for movement of calcium during the action potential in the heart and is essential for normal cardiac function. It is a T>G conversion at an essential splice site, and it was expected that this mutation would cause cardiac arrhythmia phenotypes in the ECG.

4.1.7 Aims

- Testing the sensitivity of the ECG recording system for detecting and analysing cardiac mutant phenotype via detecting ECG signal abnormalities
- To use the larval zebrafish recording technique to detect potential presence of an arrhythmia in the *cacna1c* mutant (allele 6050, Sanger institute) compared to wild type embryos.
- To use a profile of cardiac acting drugs to assess their effect on the *cacna1c* mutant and wild type embryos to analyse changes to phenotype in response to these drugs and potential rescue effects.
- To draw comparisons to human calcium channelopathies such as Timothy syndrome and critically assess the potential use of the *cacna1c* mutant (sa6050) as a disease model.

4.2. Methods

4.2.1 Zebrafish husbandry

For all experiments, with the exception of the mutant experiments, wild-type Tubingen long fin zebrafish embryos were used as this is the background of the *cacna1c* mutant. All zebrafish were handled according to the UK animal (Scientific Procedures) Act of 1986. Adult zebrafish were maintained using standard conditions in a flow-through system of aerated, charcoal filtered tap water with a 12 hour light/dark cycle (Techniplast; UK).

Breeding pairs were set up in separate breeding tanks, filled with system water and left over night. Embryos were collected the following morning and transferred into petri dishes containing E3 medium (Sigma Aldrich) and incubated at 28 ^{o}C until 3 dpf. The *cacna1c* embryos were taken out at 2dpf for visual screening into separate petri dishes containing E3 medium and then returned to the incubator.

4.2.2 The cacna1c sa6050 mutant

The zebrafish mutant line used for the mutant data was an L-type calcium channel mutant, *cacna1c*. This mutant was produced at the Wellcome Trust Sanger Institute as part of their zebrafish mutation project. Sanger produced this mutant using ENU mutagenesis followed by screening for embryos displaying atypical phenotypes. Sanger had previously confirmed a mutation in the F2 line with considerable cardiac and systemic effects observable at 5 days post fertilisation (dpf).

4.2.3 Visual screening for *cacna1c* homozygous mutants

The *cacna1c* mutant embryos clutches were visually assessed for a cardiac phenotype at 2 dpf. This was to screen out homozygous mutants away from heterozygous and wild type siblings. At 2dpf (days post fertilisation), the embryos were removed from the incubator and 1ml of 4% MS-222 (ethyl-3-aminobenzoate methanesulfonate , Sigma-Aldrich) was added to the plate. This anaesthetised the embryos for ease of manipulation for visual screening. As it was already established from Sanger that by 5 dpf a pronounced cardiac oedema has developed, it was predicted that there would be some sign of this phenotype developing at 2 dpf. Larvae were orientated ventrally and on their side to assess for cardiac phenotype. Once it was discovered that a subgroup within the clutch had a cardiac oedema, this phenotype was used as the screening criterion for homozygous mutants at 2 dpf. Visual screening took place under a light microscope (Nikon SMZ600). Following visual assessment, embryos were split into those with and those without an oedema. Embryos were rejected if the cardiac oedema was coupled with yolk necrosis, tail bending or other deformations as the oedema can not in those instances be confidently attributed to the mutation. The screened embryos, those with and without oedema were then returned to the incubator in separate petri dishes in fresh E3 medium to recover from the anaesthetic. Embryos with severe oedema were rejected for ECG analysis. This is because distance from the electrode can affect the quality of the signal, particularly with arrhythmic fish. ECG recording of the embryos at 4 or 5 dpf when the severe oedema and very slow heart rate had developed was extremely difficult due to the massive fluid build up. Following initial screening and ECG analysis, a phenotype of bradycardia was identified and also included in the visual screening criteria.

4.2.4 Genotyping analysis performed by Sanger Institute.

Fin clips and embryos were fixed in methanol and genotyped at the Sanger Institute. A selection of screened 2dpf *cacna1c* mutant line were selected and placed into a 96 well plate, the liquid removed, the plate sealed and then put on ice to prevent degradation. 23 positive and 23 negative embryos were selected. Plates were sent to the Wellcome trust Sanger institute for Genotype analysis. The genotyping tool used was KASP (Kollective allele specific PCR). This is a fluroecence based PCR reaction performed using a 96 well plat format allowing multiple samples to be analysed simultaneously. Results are displayed using the 96 well format and assigns a colour to each well representing the genotype.

KASP genetic analysis was performed on the selected groups in duplicate and the results were then sent back. This was done to access accuracy of the screening process at 2 dpf.

4.2.5 Assessment of 2 dpf analysis as a screening tool

To determine the specificity and sensitivity of 2dpf screening, embryos were reassessed at 5dpf when the phenotype had developed further. Screening immediately prior to ECG recording was not possible due to time constraints on recording days (3 dpf). Reassessment of screened homozygous mutants after ECG was necessary as genotyping showed visual screening at 2 dpf was not always accurate. Embryos were kept in 96 well plates after ECG recording and if the more pronounced oedema had not developed by 5 dpf, the result was excluded from the development. This ensured accuracy in the mutant characterisation but unfortunately introduced bias into the experiment.

4.2.6 ECG procedure

For all experiments, unless otherwise stated (non-MS-222 experiments) the zebrafish embryos were immobilised in 0.3 mg/ml MS-222 (Sigma).

4.2.6.1 Recording set up

For all experiments, 3 dpf embryos were orientated on a custom recording plate previously described, (2.2.2a) with 9ml E3 medium with 0.3mg/ml MS-222. The recording plate was then placed onto the heating pad compatible with Cryocon 22C (cryogenic control systems) temperature control (4.2.6). Throughout the recording temperature is monitored as slight changes in temperature can affect heart rate. The ECG recording system used for these experiments was the powerlab system as previous (2.2.2b) with the exception that the NPI single end point amplifier was exchanged for a 2 channel amplifier to facilitate dual electrode recording (EXT-02 B, NPI) This facilitated atrium and ventricle recording.

4.2.7 Temperature control

The temperature was controlled using the, Cryocon 22C (cryogenic control systems) temperature control system that maintained the temperature of the recording plate at 28^{o}C. A custom heating plate was created compatible with this system to heat the recording plate to 28^{o}C. The heating plate used insulated conductive wire folded in half and twisted along the length. This was then glued onto a petri dish lid in a spiral from the centre of the lid. At the edge, a gap was cut out the lip of the lid to allow the wires to exit and the plate to sit flat. The wires were then cut and a connector compatible with the Cryocon system was soldered on. This heated the plate evenly and maintained

temperature throughout the recording. The twisting and spiral pattern cancelled out noise generating from the wires from the recording, this was always the difficulty in creating a temperature controlled recording environment as whatever heating element used would be inside the faraday cage and so had to be electrically quiet. The temperature was monitored throughout the recording by the Cryocon temperature probe.

4.2.8 ECG analysis and Statistics

The digitised ECG signal was displayed using Labchart software and filters were applied to increase clarity of the signal, a bandpass filter (0.1-30Hz).
Analysis of the signal was carried out using Labchart, which calculated the R-R, QRS, QT and QTc ECG parameters and the heart rate as per section 2.2.8.

4.2.9 Drug stocks

All drug stocks were made up in E3 medium. Terfenadine (Sigma) and Verapamil (Sigma) was prepared in 10 mM stock in E3 and DMSO (10 % Sigma Aldrich), to aide solubility. Isoprenaline was made up to 500mM stock, penicillin, 10Mm stock, flecainide, 1mM stock and metoprolol 500μM stock. Stocks were diluted using E3 and the final concentration of DMSO on the recording plate at 1 %. Chlorzoxazone stock was made up with 12% DMSO with E3 to a 6mM solution. This created the whole dosing range.

4.2.10 Literature search to seek candidate drugs to rescue phenotype

A literature search was carried out to identify candidate drugs which may have a rescue effect on the mutant phenotype. Chlorzoxazone was chosen as try as it was an already marketed drug as a muscle relaxant, that it has been shown to have a positive effect in calcium overload in the brain and because it acts on calcium activated potassium channel (Gao *et al* 2012 and Liu, Lo and Wu, 2003).

4.2.11 Chlorzoxazone LC50 bioassay

The concentrations for basing the LC50 assay were calculated using the mouse LD50 numbers as work has shown that there is a close correlation for these calculations between the two species (Ali, Mil & Richardson, 2011). The lowest human/murine LD50 for chlorzoxazone is 50mg/kg and a concentration of 300μM for zebrafish calculated. Estimations of zebrafish weight were used based on Hu *et al*, 2000. From this concentrations were decided on for the LC50 assay. The concentrations selected were: 30μM, 100μM, 300μM, ,(n=18 mutant, n=20 wild type) 600 μM and 1000 μM (n=14mutant, n=16 wild type) plus 2% DMSO and E3 control groups ,(n=18 mutant, n=20 wild type).

Wild type and *cacna1c* mutant embryos were placed singularly in a 96 well plate and incubated at 28^{o}C. Each well contained 200μl of test solution. Acute responses were taken at 15 minutes post treatment. After 24hrs each concentration was assessed for mortality. Observations for acute and 24hours post treatment performed under a light microscope (Nikon SMZ600). Larvae health was checked at 30 minutes, 1 hour and 24 hours post commencement of treatment. Larvae were primarily checked for indications of cardiotoxicity (bradycardia, oedema, arrhythmia) and secondly, overall toxicity (death, necrosis). Data collected was used to create a mortality plot from which the

LC50 estimate was taken.

4.2.12 Screening for asystolic events

From initial visual observations a subpopulation of *cacna1c* mutants were identified, that showed a phenotype where several heart beats were 'missed' before normal sinus rhythm resumed. These were termed asystolic pauses. On closer assessment of these embryos during ECG recording it was observed that there was a loss of ECG signal associated with the cardiac asystole where the heart totally stopped beating for several beats, longer than a traditional sinus pause. This phenotype was added to the visual screening criteria. 2dpf larvae were visually assessed for these pauses as well as oedema. To visually assess for pauses, *cacna1c* larvae were observed in turn for the duration of 1 minute. Any larvae displaying the pauses phenotype were selected out as homozygous mutant and collected for ECG analysis. Larvae were removed one at a time from the incubator to time to reduce cool down period which affected heart rate assessment.

4.2.13 Introducing environmental stress through high salinity and orbital shaking procedure.

The asystolic pauses phenotype was easy to screen for and a more definitive cardiac mutant phenotype, however it occurred at such a low incidence with in the homozygous population. To try to increase the incidence of the pauses phenotype within those screened as having bradycardia and oedema (homozygous mutants), environmental stresses were applied to try and induce this phenotype in other homozygous mutants. Increasing the incidence of this phenotype within the mutant population would greatly aid visual screening and improve accuracy. Embryos were exposed to high salt

concentrations and 5 minutes on an orbital shaker at 100 rotations per minute to stress them to try and induce the pauses phenotype to aide successful visual screening of homozygous mutant. The larvae were visually screened as normal and then split into 7 groups for salinity exposure. E3 medium is a mix of salts and this was used at increasing concentrations 1 x (normal running concentration - control), 12.5x, 25x, 35.5x, 50x, 75x, and 100x. 30 minutes after exposure the embryos were re-screened and number of embryos screened for the pauses phenotype before and after each concentration compared. In total n=50 across 3 biological repeats.

Embryos were also exposed to 30 revolutions on a shaker (Orbital shaker, Stuart SSL1) as an alternative stressor to induce arrhythmia. This method is an adaptation of the method taken from Eto *et al*, 2014. This was to 'shake' up the embryos causing stress. A total of n=50 x3 embryos were assessed. These were also visually screened and counted before and after stress exposure for comparison. Mortality rate were also recorded.

4.2.14 Statistics.

All data groups were tested for normal distribution using Shapiro-Wilk and the Anderson-Darling tests for normality to guide further statistical analysis. The Anderson-Darling test was used as a validation to the results from the Shapiro-Wilk test as though normality tests generally have a low power for small sample sizes, the Shapiro-Wilk test has been shown to be the most powerful test when assessing normality.

Statistical significance of heart rates between wild type, those screened as homozygous mutant and siblings controls was determined using a 3 way Anova test.

Statistical significance of dual electrode recorded drug treatments was performed using a 2 tailed T test. This compared the interval difference recorded in each electrode to compare if the same result was achieved for the 3 ECG parameters in these 2 electrode positions. To compare PR, QRS and QTc intervals recorded from *cacna1c* mutant and sibling controls, the Kruskal-Wallis and Mann-Whitney tests were employed.

For the drug treatments (5 cardiac acting drugs, control drug and chlorzoxazone rescue treatments), the non-parametric Wilcoxon paired-signed test was used to compare pre and post drug treatment to determine significance. To compare *cacna1c* results against wild type shaker and salinity results, again the Kruskal-Wallis and Mann-Whitney tests were employed.

4.3. Results

4.3.1 Phenotype screening of *cacna1c* mutants

This study has displayed the use of the recording system to record ECG changes due to cardiac drug treatment. The next objective was to test the utility of the recording system to detect changes in cardiac electrical activity observed in ECG signal from a typical signal to a diseased state due to a genetic mutation. The ability to record, analyse and identify cardiac effects due to genetic mutation expands on the use of the recording system.

This was a key aim for the study; to establish the use of the recording system for analysing successfully genetic cardiac conditions observable on an ECG.

In order to test for the sensitivity of the larval recording system to detect ECG differences due to genetic mutation, rather than drug treatment, an appropriate mutant with an abnormal cardiac phenotype and therefore possible arrhythmia was chosen.

4.3.1.1The *cacna1c* sa6050 mutant

The zebrafish line chosen was an L-type calcium channel mutant with a point mutation at an essential splice site (allele name sa6050), developed at the Wellcome Trust Sanger Institute. This mutant develops a severe cardiac oedema in the pericardial sac as a result of the calcium channel abnormality by 5 dpf which is very easily observable, **Figure 4.2A, B**. This study was focused on analysing the ECG differences directly as a result of the mutation before the secondary severe oedema and the more systemic effects observed at 5 dpf developed. ECG recording from embryos before the massive oedema at 5 dpf was also more straightforward as the increased fluid around the heart increased the distance between the heart and the electrode making locating the signal more

difficult. This was compounded with the fact that the heart was beating much more weakly and under stress and the pericardiac sac filled with fluid..

4.3.1.2 Visual phenotype screening of the *cacna1c* mutant at 2 dpf.

Genetic screening was not possible to perform per embryo so visual screening for phenotypes relevant to the mutant was performed. Clutches from individual pair-wise crosses were collected and grown up to 2 dpf and visually screened at this stage. Embryos were screened for any perturbance to the normal healthy embryo, in particular cardiac phenotypes. There was an observable cardiac deformation at 2dpf which by 5 dpf had become an established observable cardiac oedema. Positively screened mutants from pair-wise clutches were compared against negatively screened siblings and wild type controls, example embryos for these groups shown in **figure 4.2C, D, E**. Genotypes for these embryos were confirmed by analysis performed by Sanger institute.

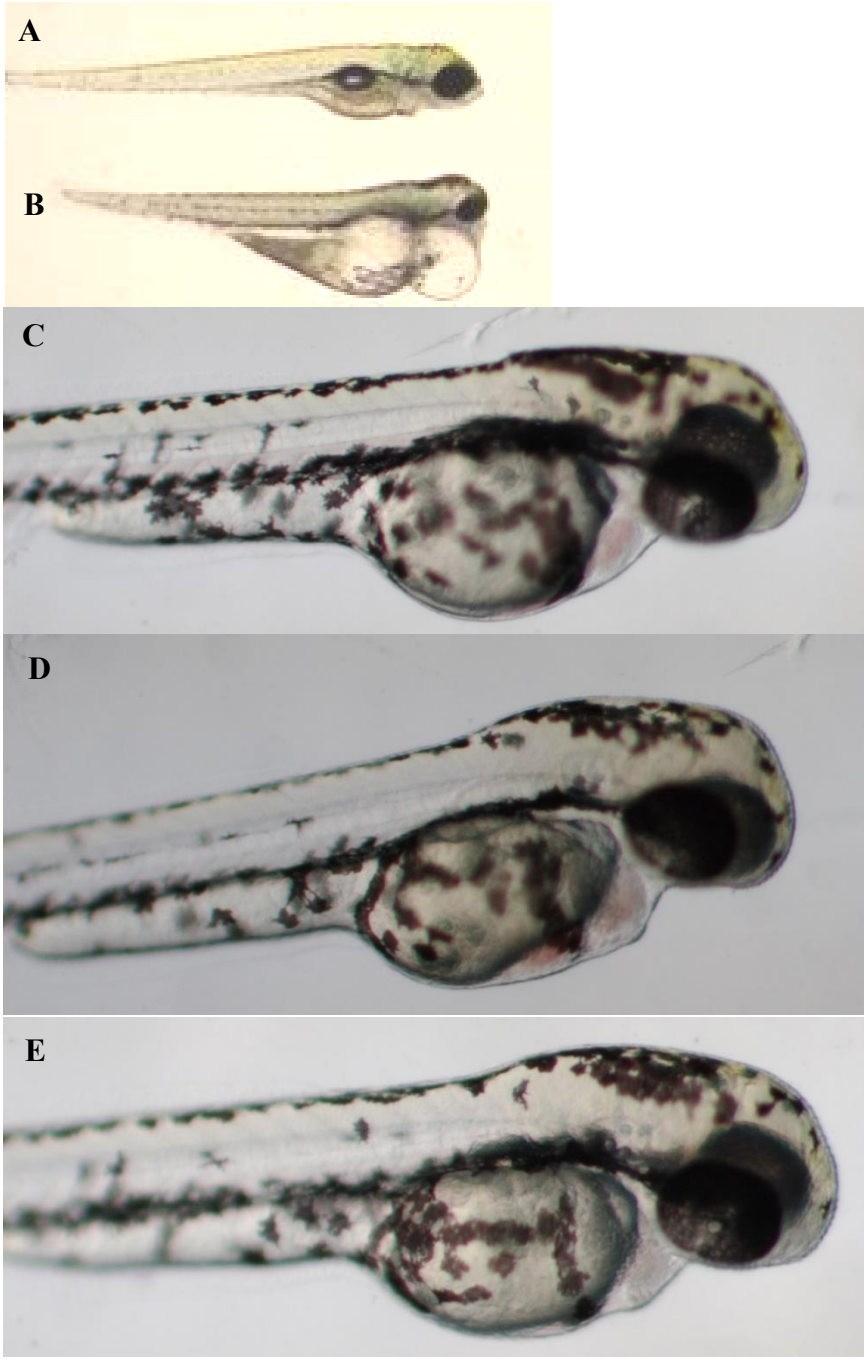

Figure 4.2. Assessment of visual phenotype of the cacna1c mutant.
A) wild type 5dpf zebrafish
B) Ref photo Sanger institute demonstrating the extent of the cardiac oedema which develops by 5 dpf.
http://www.sanger.ac.uk/sanger/Zebrafish_Zmpgene/ENSDARG00000008398#sa6050
C) wild type control 3dpf
D) positively screened mutant 3dpf
E) negative sibling control 3dpf

Once clutches were screened, they were counted to check for Mendelian distribution. This was to establish whether visual screening was sufficient and reliable enough to detect homozygous *cacna1c* mutants at 2 dpf, example clutches shown in Table 3.1. In addition to the structural cardiac deformations observable in figure 3.1, D, there were some embryos amongst the positively screened mutants which had an abnormal heart beat. There were periods, observed under the microscope, where the heart had asystolic events, usually for between 10 and 20 beats before resuming normal sinus rhythm. These periods were termed pauses and the proportion of mutants displaying this phenotype are also displayed in **table 4.2**.

	Total	wild type	Heart defects	%	pauses	%
	66	43	23	34.85	6	26.09
	150	103	47	31.33	8	17.02
	75	46	29	38.67	3	10.34
	95	66	29	30.53	4	13.79
	60	50	10	16.67	5	50.00
	82	58	24	29.27	2	8.33
	123	75	48	39.02	2	4.17
	164	113	51	31.10	9	17.65
	207	143	64	30.92	5	7.81
	190	160	30	15.79	10	33.33
	423	343	80	18.91	3	3.75
TOTAL AVERAGE	**143.66**	**109.09**	**39.55**	**28.82**	**5.18**	**16.69**

Table 4.2 Percentage heart defect and asystolic pauses distribution in cacna1c clutches from pair-wise crosses.

4.3.1.4 Genetic analysis of the *cacna1c* mutant performed at Sanger Institute.

To check whether the phenotype was strong enough at 2 dpf to accurately identify positive mutants against negative siblings, a selection of positive and negatively screened embryos were genotyped. A pair-wise clutch was screened and separated out into positively screened mutants and negative siblings. These were placed into a 96 well plate, the liquid removed, the plate sealed and then put on ice to prevent degradation. 23 positive and 23 negative embryos were selected. Plates were sent to the Wellcome trust Sanger institute for analysis. KASP genetic analysis was performed on the selected embryos. KASP (Kompetitive allele specific PCR) is a fluorescence based genotyping tool which utilises PCR. It accurately identifies wild type, heterozygous and homozygous mutant alleles. Samples are analysed on a 96 well plate so multiple samples are analysed simultaneously. Results are displayed using the 96 well format and assigns a colour to each well representing the genotype.

The results showed that all the negatively selected siblings were either wild type or heterozygous, which was expected. Unfortunately, the positively selected mutants showed heterozygous and wild type embryos as well as homozygous mutants. This genotyping result showed that visually screening the embryos at 2dpf was not robust enough to accurately identify homozygous mutants, **figure 4.3**.

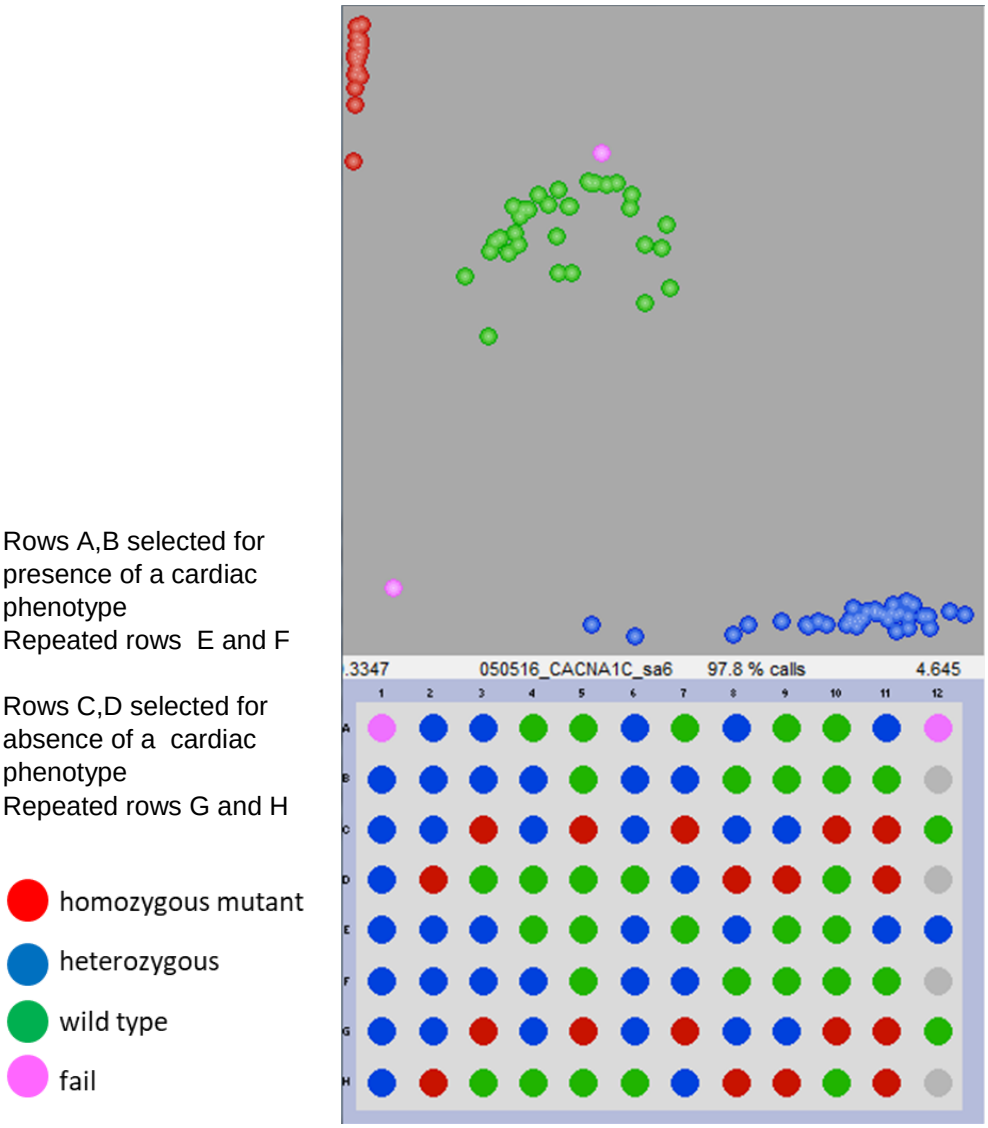

Figure 4.3. Genotyping performed by Sanger Wellcome Trust institute. KASP genetic analysis of embryos screened for presence or absence of cardiac phenotype. Result shows that only wild type and heterozygous embryos were selected as negative siblings but that these were also selected along with homozygous mutants in the positively screened group. This means the screening process at 2dpf is adequate for accurate selection of negative siblings, but not accurate enough to screen out positive homozygous mutants. Red: identified homozygous mutant, blue: identified heterozygous embryo, green, identified wild type embryo, pink: failed well with no result.

This result indicated that additional screening was required after 2dpf to ensure accuracy in screening for homozygous mutants in heterozygous adult clutches. Therefore, homozygous mutants were confirmed after ECG analysis on 5 dpf when the severe oedema had developed, and so the phenotype more pronounced. Once the ECG

had been performed, the traces were labelled with a corresponding 96 well plate reference. This allowed ECG analysis to take place on 3dpf before the secondary systemic effects of the mutation had developed but ensured that true mutants were successfully identified and used for subsequent analysis.

4.3.1.3 The heart rate of the *cacna1c* mutant is significantly slower than wild type embryos.

At 3dpf, the heart rate of each of the screened groups, wild type, siblings and mutants were also recorded and the screened *cacna1c* mutants were found to have a significantly lower heart rate than the control groups, **figure 4.4**.

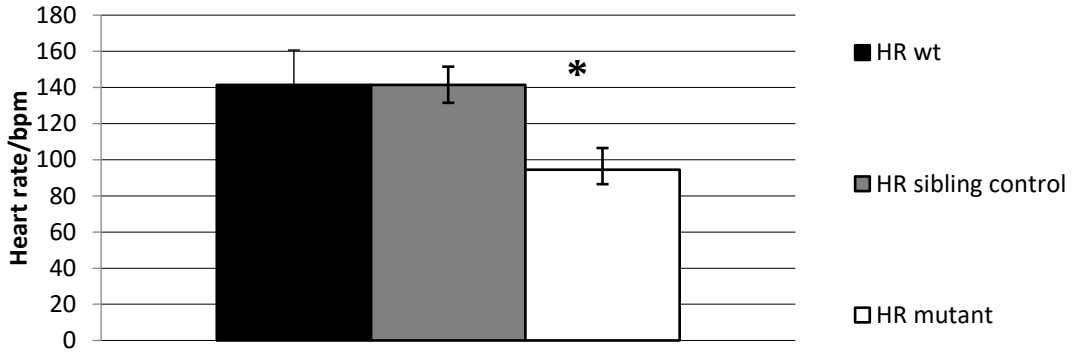

Figure 4.4 Average heart rate for wild type, negative screened cacna1c siblings and screened cacna1c mutants P-value 0.00037. n=20.

This Bradycardia was then used to confirm all positive screens as this phenotype is more closely associated with the calcium channel mutation. The bradycardia was first observed following ECG recording analysis of positively selected mutants. This coupled with the ECG differences helped to confirm the mutant phenotype. To increase the accuracy of the screening process, this bradycardia was included as a criterion to visually screen for in heterozygous pair-wise clutches by counting beats for 15 seconds

then multiplying by 4. The data displayed in figure 3.2 is from ECG measured heart rate averaged across a 2 minute section of recording, rather than the measurement from the 15 second visual assessment used for initial screening. This was due to those measurements being available from the recordings analysed through Labchart and ensured embryo heart rate and ECG interval analysis was from the same embryos.

4.3.2. ECG analysis of the *cacna1c* mutant

Following successful screening at 2 dpf for positive *cacna1c* homozygous mutants, the next step was to record the ECG of the screened groups and then analyse these compared to wild type recordings. For this reason, the ECG signals from the embryos were taken at 3 dpf as all previous in depth analysis of the normal larval zebrafish ECG is recorded from this stage. This allows close careful comparison of this data to the ECG recordings from the *cacna1c* mutants.

4.3.2.1 Optimisation of dual electrode recording system for *cacna1c* mutant ECG analysis.

Having developed positions for atrium and ventricle recording previously, see chapter 2, this was utilised for a two electrode system to record from the atrium and ventricle simultaneously to allow direct comparison between the two chambers. The dual positions were as described in chapter 2, grid format **figure 4.5A.**

To confirm that this dual recording was the most appropriate recording method for this experiment, dual atrium and ventricle signals were recorded pre and post 5µm Terfenadine treatment (3 dpf embryos n=20) and then the ECG intervals PR, QRS and

QTc were plotted for both electrode positions, atrium positioned electrode and the ventricle positioned electrode, **figure 4.5B, C, D.**

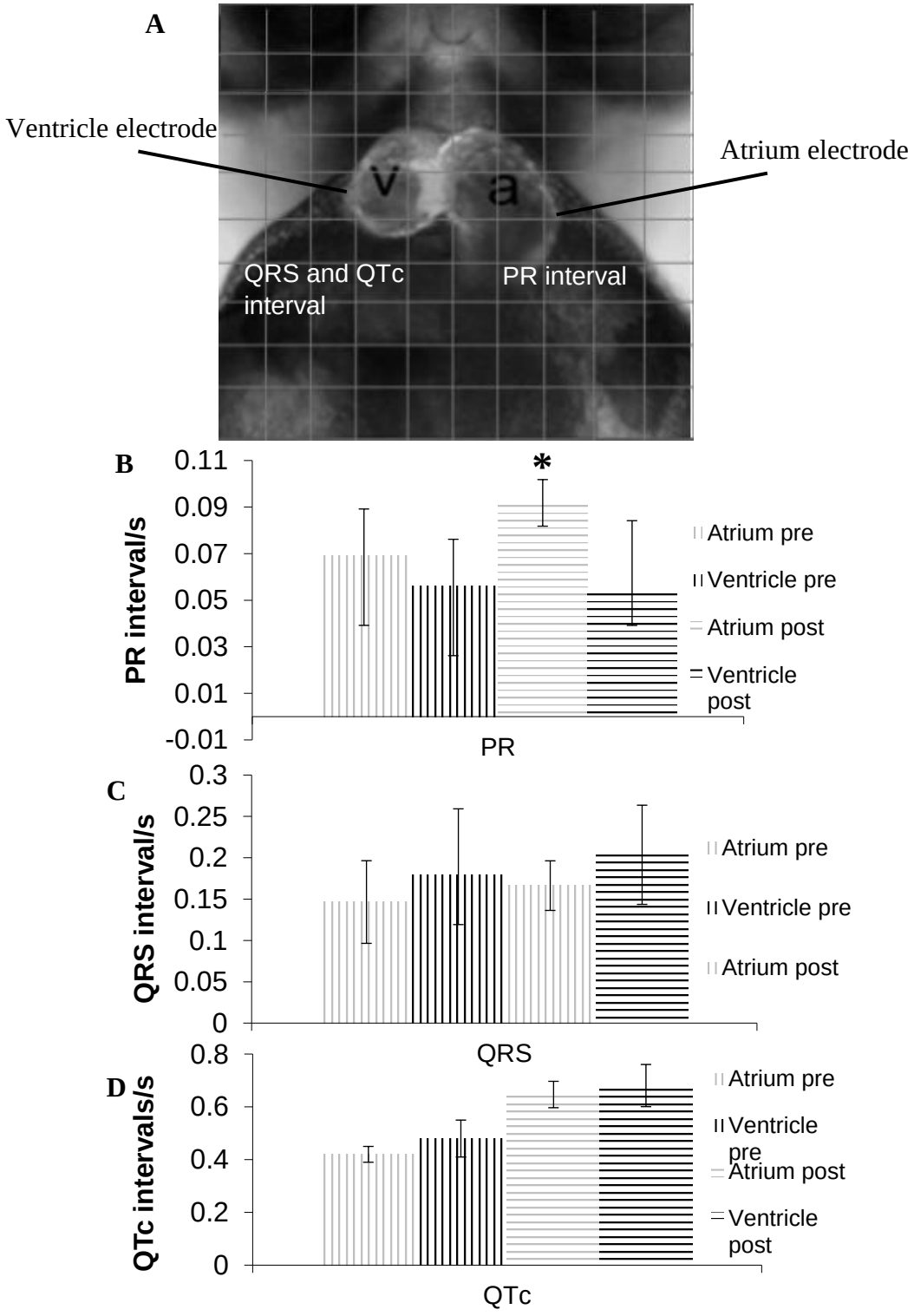

Figure 4.5 electrode position and parameter recording in dual electrode system.
A) Electrode positions for atrium and ventricle electrodes are labelled.
B,C,D) ECG intervals pre and post 5 µM Terfenadine treatment recorded from both electrodes from 3 dpf embryos.
B) PR Intervals: Atrium electrode records PR interval increase more accurately than ventricle electrode and this increase is significant.
C) QRS intervals: consistent in both electrodes.

D) QTc intervals: consistent across both electrodes.
For detecting changes in PR interval, an atrial specific electrode is required. N=20 embryos for these dual drug treatment recordings.

To perform direct comparison between the atrium and ventricle electrode recordings, statistical analysis using a tailed t test was performed. This compared the interval difference recorded in each electrode to compare if the same result was achieved for the 3 ECG parameters in these 2 electrode positions. Only the PR interval result showed a difference between the two electrodes, demonstrating that a more pronounced PR interval drug response was recorded from the atrium positioned electrode, highlighting the need for an atrium positioned electrode to analyse drug and mutant effects on this ECG parameter. The ventricle positioned electrode did not pick up the changes post drug treatment in the PR interval that the atrium positioned electrode picked up, figure 3.3B. The QRS measurements were consistent in both electrodes with both showing the same increase in QRS interval, therefore comparison between the two recording showed no significant difference. Corroborating the result shown in Dhillon *et al* 2013, the QTc measurement was consistent across both recording positions and therefore comparison analysis was not significant. For analysing PR, QRS and QTc intervals in the *cacna1c* mutant, based on these results, the atrium component of the ECG signal, the PR interval, was measured from the atrium electrode and the ventricle ECG components (QRS and QTc) were measured from the ventricle positioned electrode. This was to maximise the accuracy of these measurements and allow analysis into finer differences such as the PR interval, which is more difficult to record due to the smaller size of the p wave.

4.3.2.2 ECG interval analysis of *cacna1c* mutant and sibling controls performed at 28^{o}C.

Dual atrium and ventricle recordings of *cacna1c* mutants (those visually screened as homozygous mutant) and sibling controls (those visually screened as having no cardiac phenotype) were taken at 3 dpf to analyse chamber specific differences between these two groups. These two groups were from embryo clutches visually screened at 3 dpf and recorded the same day. Due to time constraints and the n number needed this was not possible for the rest of the data groups as the whole day at 3 dpf was required for recording. Recording plates compatible with Cryocon 22C (cryogenic control systems) temperature control were developed to allow the ECG signal to be recorded at 28^{o}C with consistent temperature monitoring. This is the optimal temperature for zebrafish embryo development so recording the heart activity via ECG at this temperature gives the most accurate picture of heart function in wild type and *cacna1c* mutant embryos. Previous attempts to record with controlled temperature failed as methods were either too electrically noisy for electrophysiological measurements or did not keep the temperature consistent and allow live monitoring of the temperature throughout the experiment. The *cacna1c* mutant and sibling control repeat recordings (n= 8 x3) were analysed using Labchart pro7 software (ADInstruments). This software produces an average cardiac cycle for highlighted sections of recording and gives the ECG parameter intervals for the averaged waveform allowing for outliers to be excluded, example cardiac cycles for mutant and control signals shown in **figure 4.6A**.

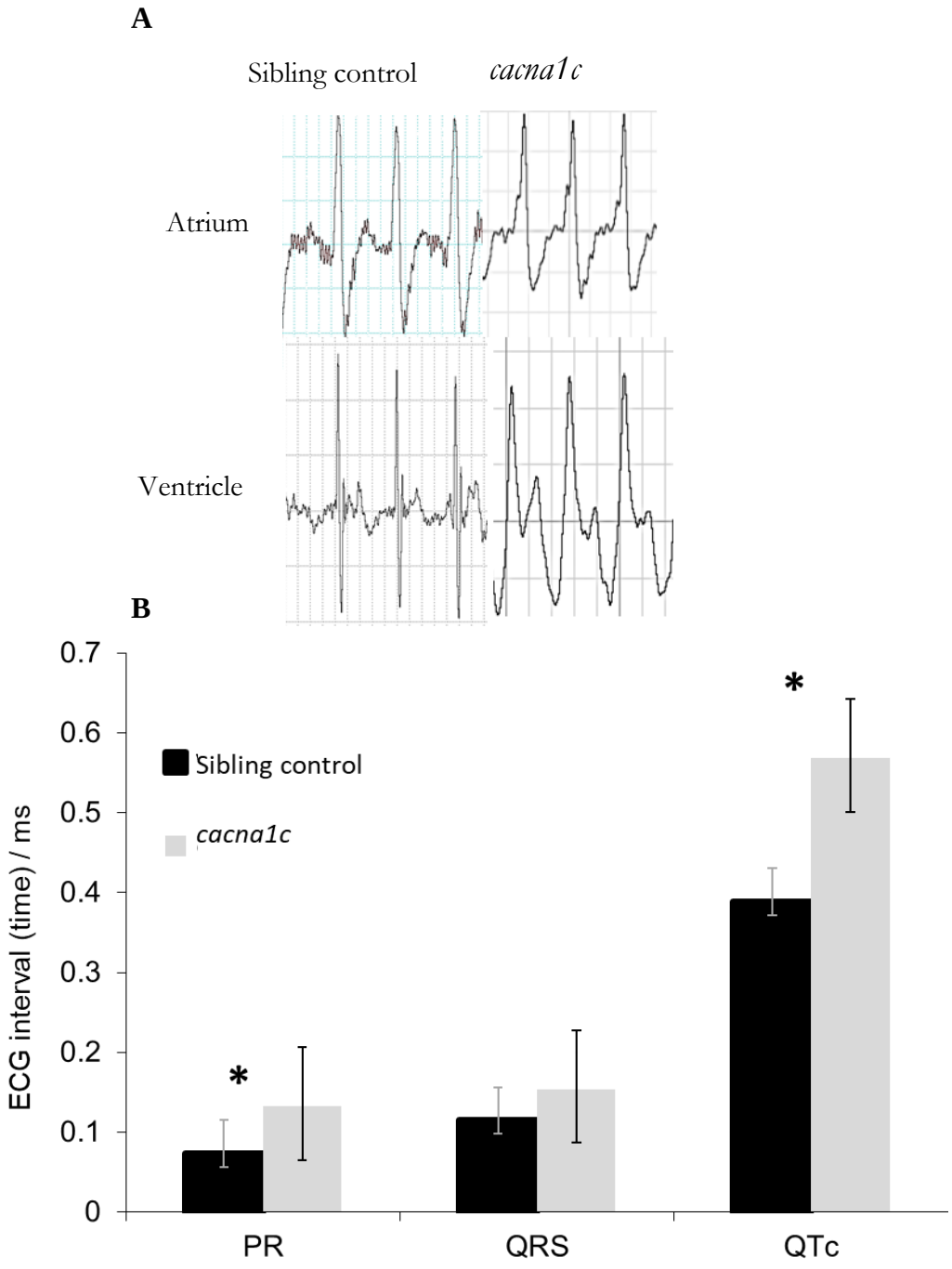

Figure 4.6 Analysis of the ECG phenotype in the cacna1c mutant.
A) Example atrium and ventricle ECG signals from cacna1c mutant larvae and non-phenotypic siblings at 3dpf
B) ECG intervals for wild type and cacna1c.n=20 3dpf embryos.

The P-R, QRS and QTc intervals, taken from the relevant chamber recording, PR from the atrium electrode and QRS and QTc from the ventricle electrode, of the control and

cacna1c mutant were plotted and analysed for statistical significance. The ECG intervals in the *cacna1c* mutant embryos were consistently longer than those recorded in the control and the PR and QTc intervals were found to be significantly larger than the control **figure 3.4B**. This result shows a clear significant difference between screened homozygous mutants and sibling controls.

4.3.2.3 Selection of diverse cardiac drugs for assessment effect on *cacna1c* mutant ECG.

A set of cardiac acting drugs were chosen, each with a different mode of action on the heart, and their effects on the *cacna1c* mutant ECG assessed. Drugs were selected to target the different ion channels of the heart and affect the heart rate. Human cardiac acting drugs previously reported as showing cardiac activity in zebrafish were selected from the literature used for this project, these included some previously tested and some newly selected. Concentrations for these drugs were also taken from the literature (Dhillon *et al,* 2013, D'amico *et al,* 2012, Milan *et al,* 2003, Mittelstadt, *et al,* 2008, Berghmans*et al,* 2008 and Alzualde *et al,* 2016). The *cacna1c* mutation effects the voltage gated L-type calcium channel, so drugs affecting the function of this channel and the other cardiac ion channels were selected. This was to determine how blocking different channels, and therefore different phases of the zebrafish action potential, effect the *cacna1c* mutant ECG. The drugs selected were terfenadine (potassium channel blocker), verapamil (calcium channel blocker), and flecainide (sodium channel blocker). As well as these channel blockers, two further drugs were chosen to increase and decrease the heart rate: isoprenaline (non-selective beta receptor agonist) to increase cardiac output and metoprolol (selective β 1 Beta-blocker) to reduce heart rate. Penicillin was used as a non-cardiac acting control drug. The effect of these drugs on

the mutant phenotype were compared to wild type (tubingen long fin) responses. The sa6050 mutant was created in the long fin strain so this was used for wild type controls.

4.3.3 Potassium channel blocker produces additive effect to the *cacna1c* mutant.

The potassium channel blocker selected was terfenadine. This was because this drug has previously been used as a drug treatment analysis on wild type embryos. Terfenadine released onto the market as an antihistamine and was subsequently found to block the Kv11.1 potassium channel causing QT prolongation arrhythmia and was therefore removed from public use.

ECG recordings were analysed by taking average measurements of the PQRST waves of the cardiac cycle across 2 minute sections (2 minute sections taken pre and 20 minutes post treatment) . Examples of wild type and *cacna1c* mutant cardiac cycles pre and post 5 µM terfenadine treatment are shown in **figure 4.7A,B.** PR, QRS and QTc interval measurements taken from average cardiac cycles pre and 20 minutes post treatment of potassium channel blocker terfenadine. Terfenadine was found to exacerbate the mutant phenotype. There was a significant increase in the QRS and QTc intervals at 0.5µM and PR, QRS and QTc intervals at 5µM, in the *cacna1c* mutant; however this was also seen to a lesser extent, but still significant, in the wild type embryos **figure 4.7C** showing a bigger difference post treatment in the mutant compared to the wild type embryos.

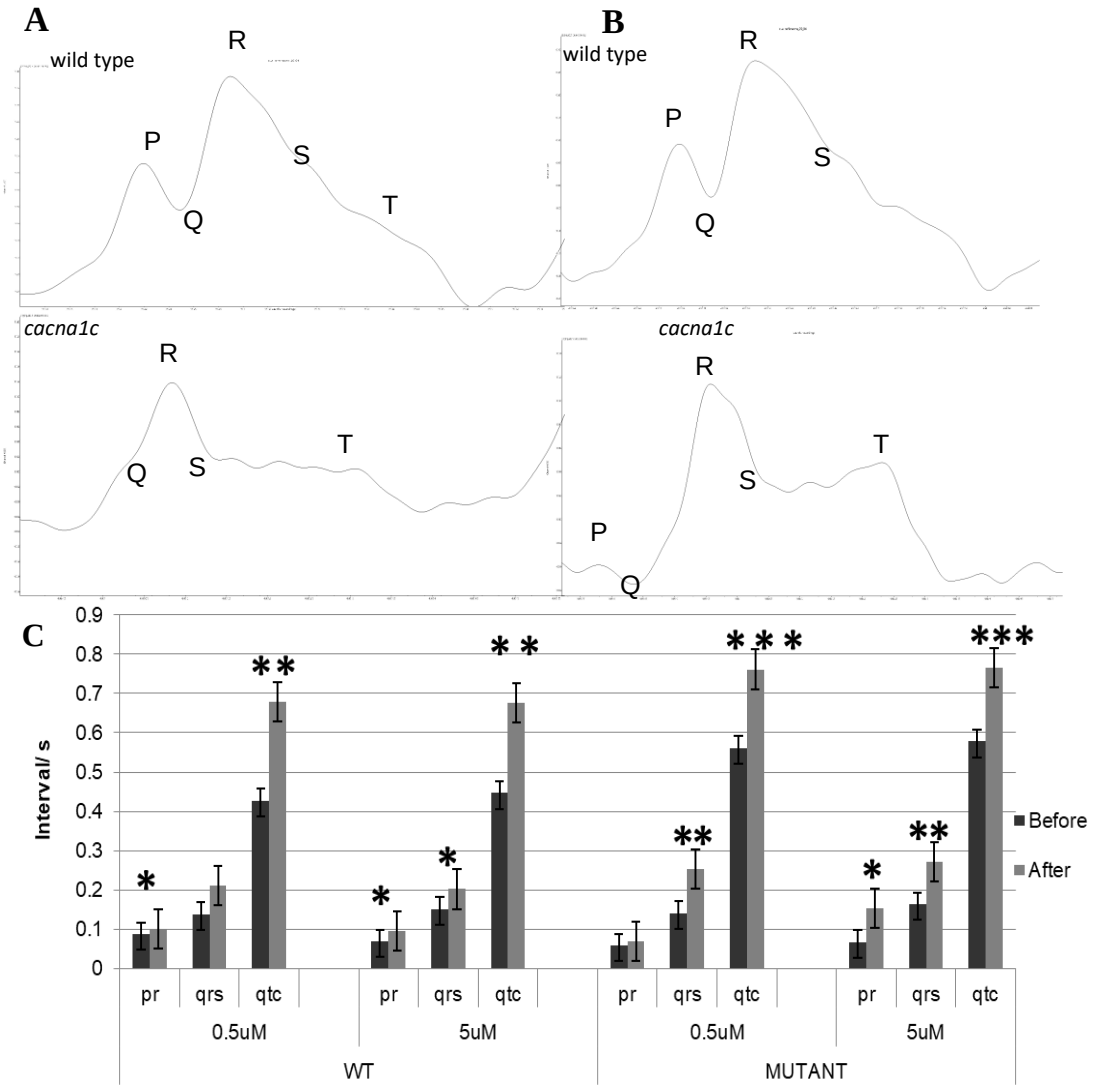

Figure 4.7. The effect of a potassium channel blocker terfenadine in the cacna1c mutant at 0.5 μM and 5μM.
A) ventricle signal from 3dpf wild type and cacna1c larvae.
B). Ventricle signal from 3dpf wild type and cacna1c larvae 1min post 5uM Terfenadine treatment.
*C) ECG intervals for before and after Terfenadine treatment in wild type and cacna1c mutant 3dpf embryos. * indicate statistical significance between pre and post treatment measurements. *=<0.5 **=<0.05 ***=<0.005 p value.*

The final ECG interval measurements after 20 minutes treatment was not significantly different to the effect on wild type embryos, however this effect was reached in the mutant much quicker than in the wild type. When looking at the effect on the QTc interval overtime, post treatment, the QT prolongation effect seen in both the wild type

and *cacna1c* mutant post 5µM terfenadine treatment happens within the first 2 minutes in the mutant and only after 10 minutes in the wild type and at 0.5µM takes the 20 minutes to reach the same final QT interval, **figure 4.8**.

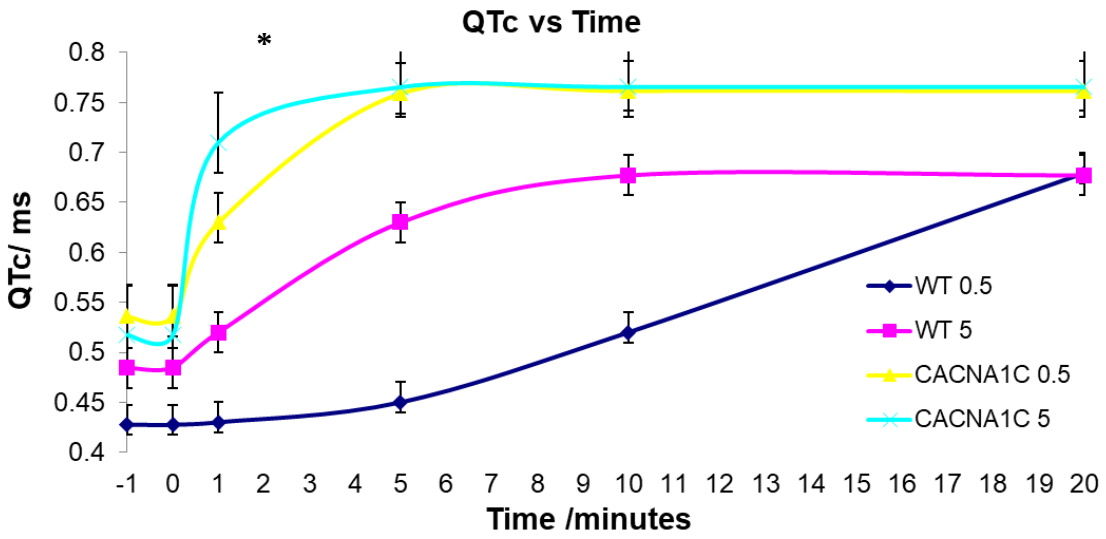

Figure 4.8. Plot of QTc interval across time from 2 mins before drug treatment and up to 20mins post drug treatment. 5 µM *Terfenadine added at time=0.5 wild type and cacna1c mutant ECG responses to Terfenadine treatment at two concentrations.*

The difference between wild type and mutant at only 2 minute post drug treatment is significant for both concentrations. This demonstrates a more acute response to the drug treatment in the *cacna1c* mutant compared to the wild type. The QTc interval in the mutant measured at 2 minutes post Terfenadine treatment is significantly larger compared to the interval measured at 2 mins post treatment. This indicates the mutant is more sensitive to the drug effect than wild type embryos.

4.3.4 Wild type zebrafish more profoundly affected by calcium channel blocker than the *cacna1c* mutant.

The calcium channel blocker chosen was verapamil. This was because verapamil had previously been used for drug treatment analysis on wild type embryos. Verapamil is marketed as a treatment for hypertension, angina and some arrhythmia disorders and it works by relaxing the muscles of the heart and blood vessels.

Average cardiac cycles from before and after both concentrations (0.5μM and 5μM) of Verapamil were used for analysis, example cardiac cycles from the ventricular electrode shown in **figure 4.9A,B**. For both the wild type and *cacna1c* mutant embryos the QTc was significantly affected with much bigger QT prolongation seen in the wild type compared to the mutant, for both verapamil concentrations **figure 4.9C**.

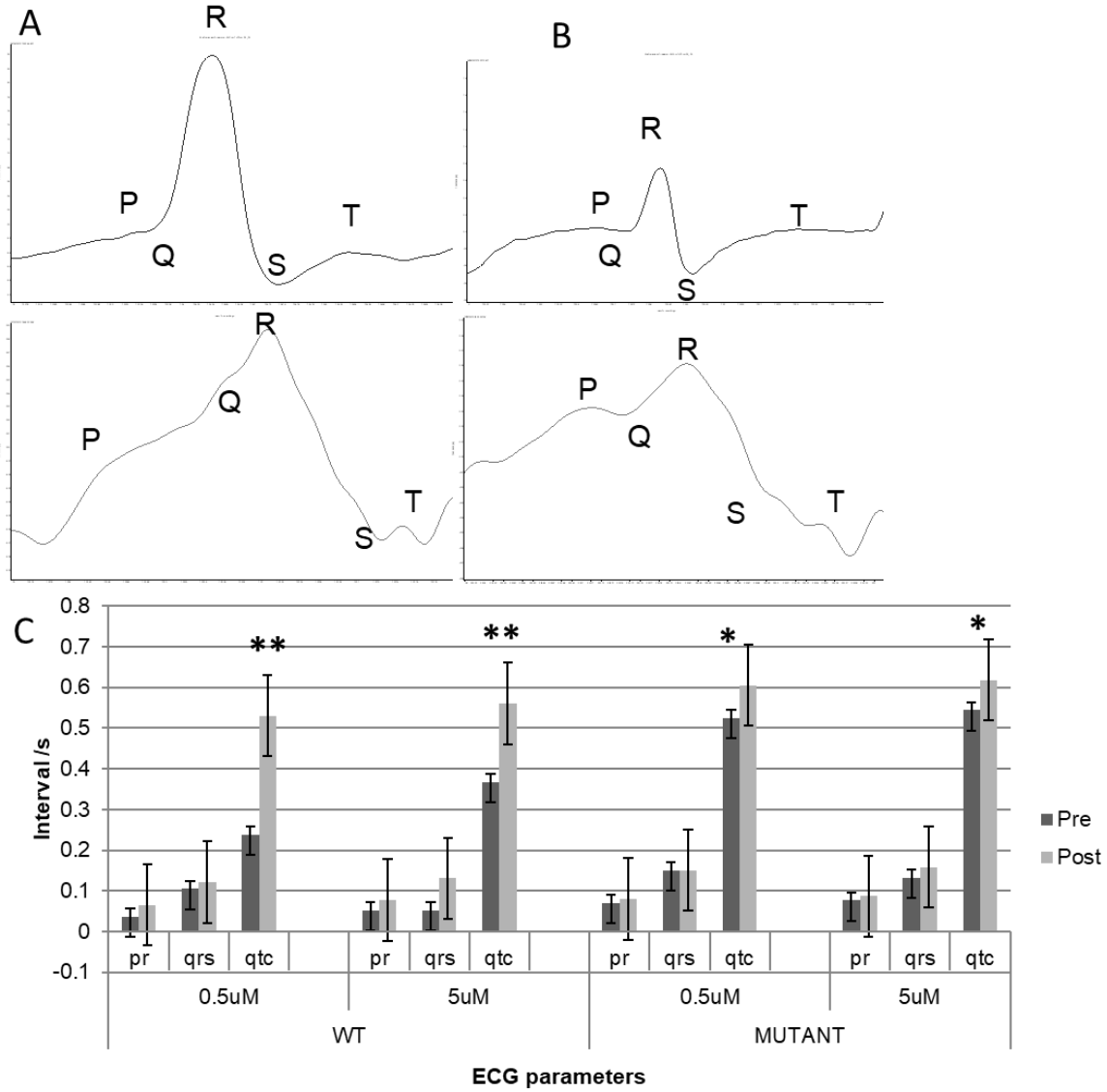

Figure 4.9. Analysis of calcium channel blocker verapamil on the cacna1c mutant at 0.5µM and 5µM.
A) ventricle signal from 3dpf wild type and cacna1c larvae.
B) Ventricle signal from 3dpf wild type and cacna1c larvae 1min post 5uM Verapamil treatment.
*C) ECG intervals for before and after Verapamil treatment in wild type and cacna1c mutant 3dpf. . * indicate statistical significance between pre and post treatment measurements. *=<0.5 **=<0.05 p value.*

Verapamil treatment at 0.5µM and 5µM and produced a significantly prolonged QTc interval compared to pre-treatment measurements and at the 5µM dose there was a significantly increased QRS interval in the wild type embryos.

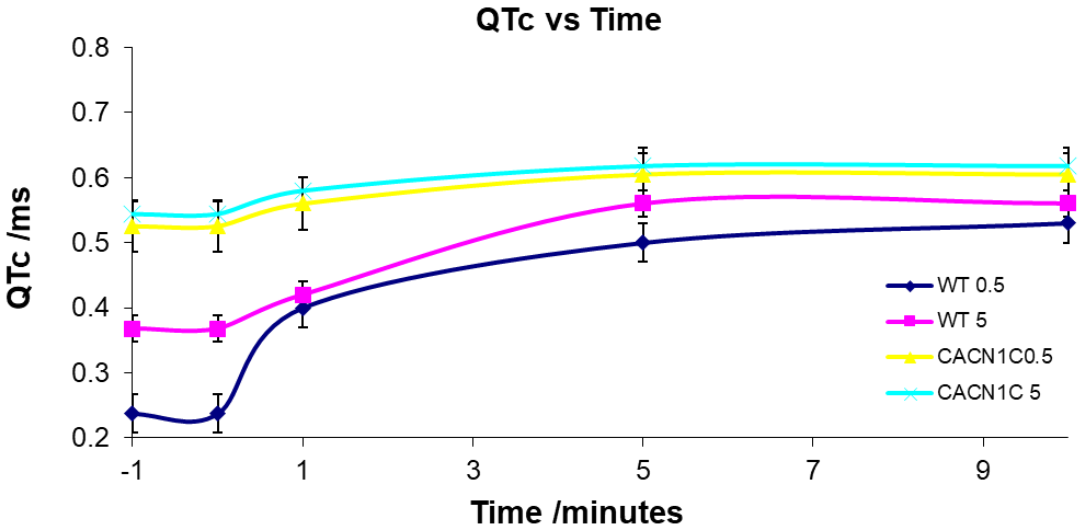

Figure 4.10: Plot of QTc interval across time. Drug added at time=0.5 wild type and cacna1c mutant ECG responses to Verapamil treatment at two concentrations.

When looking at the QTc interval over time post Verapamil treatment, the wild type has a more marked, but not statistically significant, response in the first two minutes compared to the *cacna1c* mutant, **figure 4.10**. Therefore, treatment of a calcium channel blocker on the *cacna1c* mutant does not have an effect on the ECG phenotype compared to wild type controls.

4.3.5 Non-selective Beta-agonist partially compensates the mutant phenotype

Isoprenaline was selected to assess the effect of increasing cardiac output and heart rate on the *cacna1c* mutant. It is a non-selective beta-adrenergic agonist and is used for the treatment of Bradycardia and heart block. Isoprenaline was predicted to increase heart rate which may improve cardiac output and decrease the ECG intervals.

Isoprenaline consistently decreased ECG parameter inte-rvals across wild type and *cacna1c*. However, the more profound effect was seen in the *cacna1c* mutant with significant decreases in interval time for PR, QRS and QT, therefore tending towards normal range, **figure 4.11A**. The wild type interval difference was only significant in the QRS. There was also a significant increase in the heart rate in both the wild type and the mutant **figure 4.11B.**

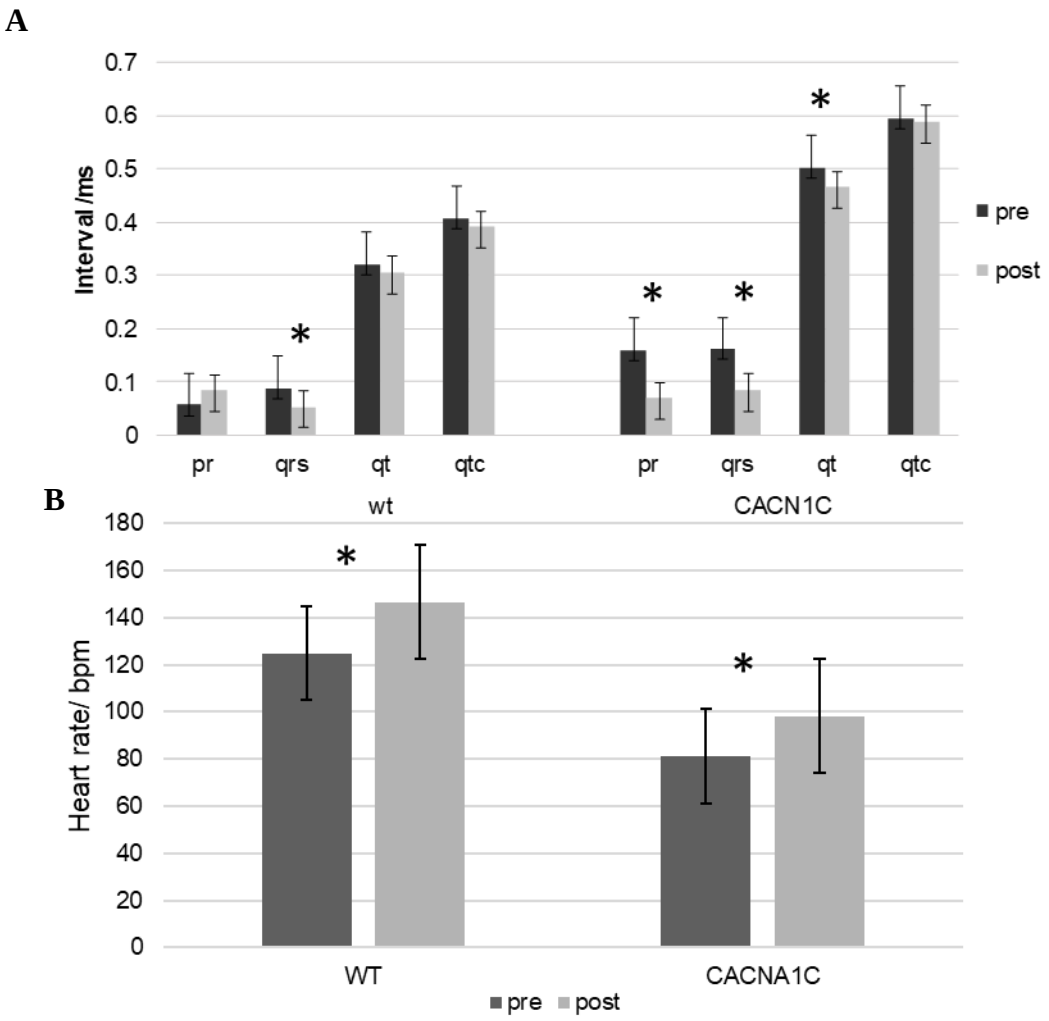

Figure 4.11: Analysis of non-selective beta agonist on the cacnalc mutant.
A) ECG intervals of 3dpf wild type and cacna1c mutant larvae post Isoprenaline treatment. ECG parameters tend towards normal in the mutant post treatment.
B). Heart rate increase in wild type and cacna1c mutant post 10uM Isoprenaline treatment.

As previously described, some positively screened mutants displayed the heart beat pauses phenotype where the heart ceased cardiac output for between 10-20 seconds before resuming normal rhythm. When these embryos were treated with isoprenaline, the pauses phenotype was resolved and normal rhythm maintained, **figure 4.12**.

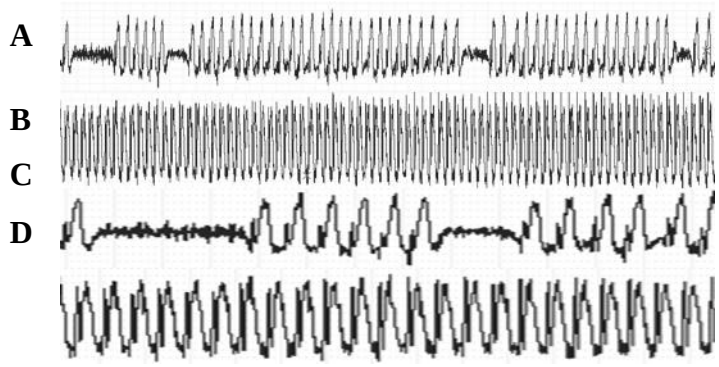

Figure 4.12 Pauses seen in 15% on mutants is corrected with 10uM Isoprenaline.
A) 1 min section before treatment
B) 1 min section post treatment
C) 20 second section before Isoprenaline treatment
D) 20s section post treatment.

While this is an interesting result, it is not a true rescue of the mutant phenotype as increasing cardiac output does not address the underlying calcium charge imbalance due to channel dysfunction. Also interesting to note that when QT is corrected for heart rate (QTc) the difference between treated and untreated was not significant, suggesting that the changes are only due to pacing the heart to increase heart rate and not changing cardiac ion channel function. However clinically, TdP is treated by pacing the heart so this result may be clinically significant.

4.3.6 Non-cardiac acting control drug has no effect on the *cacna1c* mutant.

The non-cardiac drug selected was Penicillin. This has been used as a control drug previously and therefore was known not to affect cardiac function (Dhillon *et al*, 2013). Penicillin is used as a beta-lactam antibiotic has not been reported to cause any cardiotoxicity in humans or zebrafish. Control drug penicillin induced no effect on the ECG intervals PR, QRS and QTc in either the wild type or *cacna1c* mutant embryos, **figure 4.13**.

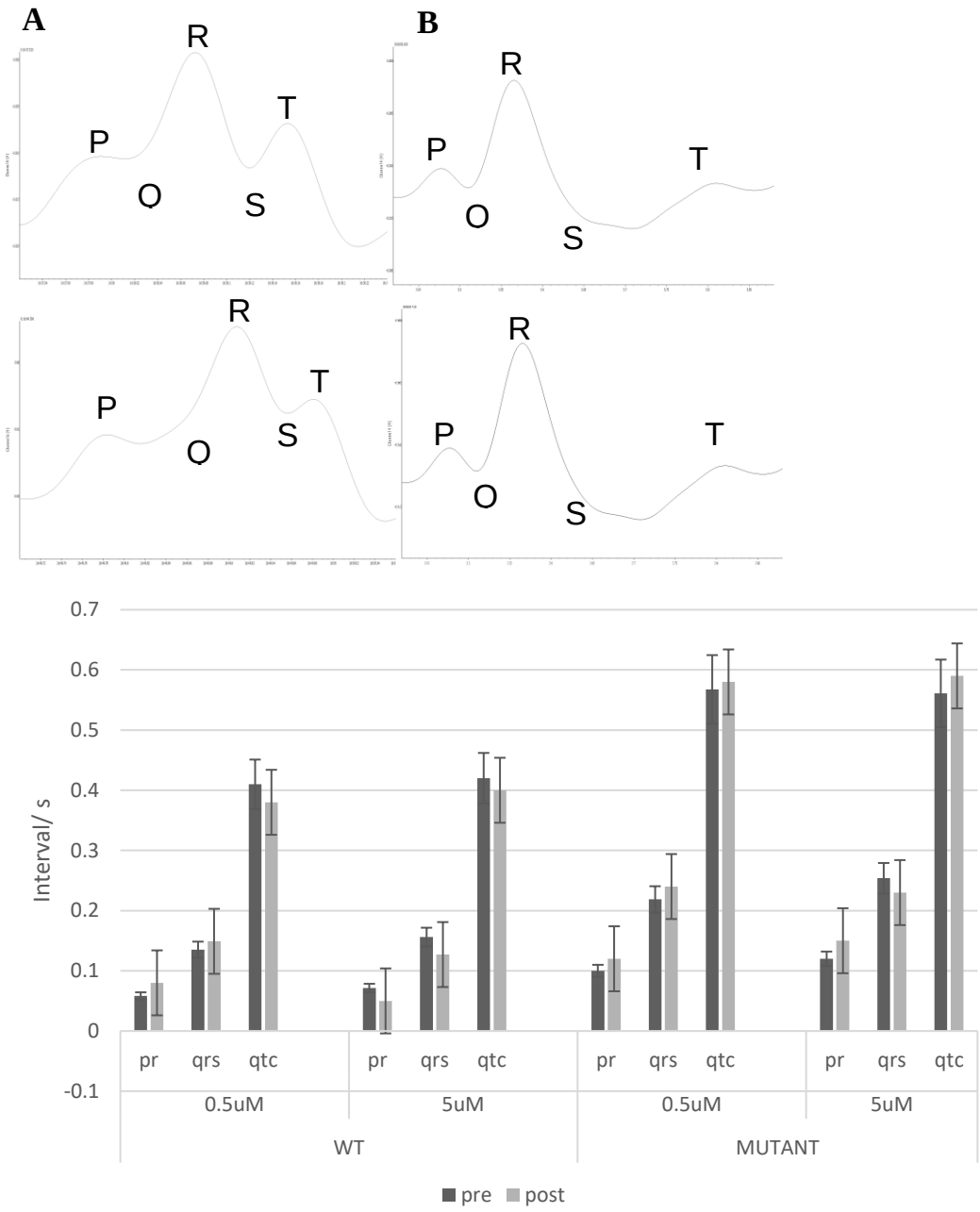

Figure 4.13 Analysis of control drug Penicillin on the cacna1c mutant at 0.5mM and 1mM.
A) wild type ECG signal before (Top) and after (bottom) 1mM penicillin treatment
B) cacna1c mutant ECG signal before (Top) and after (bottom) 1mM Penicillin treatment.
C) Intervals recorded with 0.5mM and 1mM Penicillin N=8 x3 for wild type and mutant. No drug effect observed for control drug penicillin.

The waveforms and ECG intervals for both wild type and *cacna1c* mutant showed no difference between pre and post treatment with penicillin as expected.

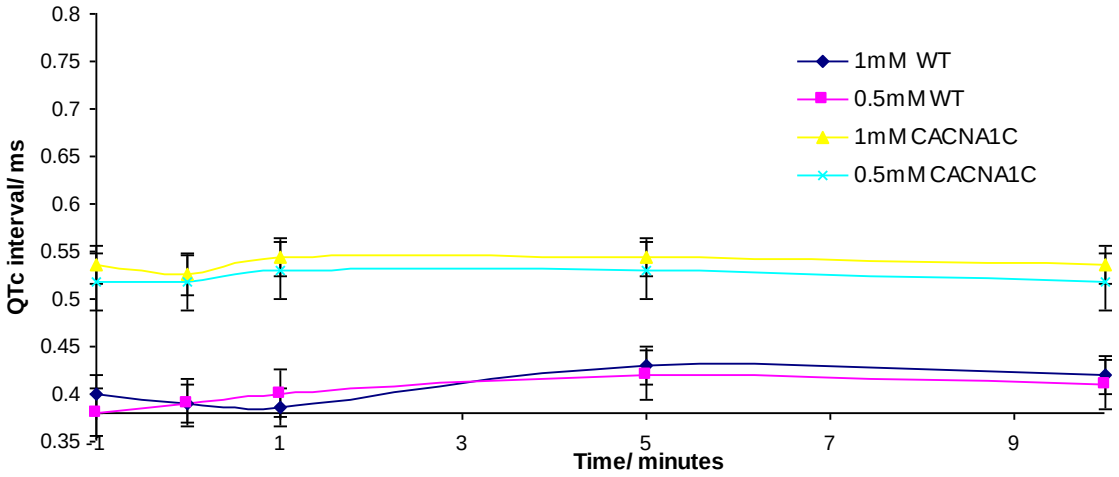

Figure 4.14 0.5mM and 1mM Penicillin treatment from 2 minutes pre treatment and up to 10minutes post treatment.

There was also no significant change in QTc across the 10 minute drug treatment for both wild type and *cacna1c* mutant as expected as Penicillin is not reported to cause cardiac problems in humans or zebrafish, **figure 4.14.**

4.3.7 Sodium channel blocker has additive effect on the *cacna1c* mutant phenotype.

Flecainide was selected to assess the effect of a sodium channel blocker on the *cacna1c* mutant phenotype. It is used as an anti-arrhythmic drug to treat a fast or irregular heart rhythm. It does this by regulating movement of sodium, prolonging the cardiac action potential. It is also occasionally used for Brugada patients (short QT) to exaggerate the

characteristic ECG phenotype of the disease to aide diagnosis (Yan and Antzelevitch, 1999). It is also used in LQT 3 which is caused by a mutation in the SCN5A gene encoding the sodium channel NaV1.5 causing prolonged sodium current causing delayed repolarisation, and hence a long QT (Moss and Kass, 2005). Sodium channel blocker cardiotoxicity has been extensively described. Tricyclic anti depressants act as sodium channel blockers and patients present with arrhythmic ECGs displaying wide QRS complexes (Amiri *et al,* 2016). Re-entrant rhythms are also seen from class 1c antiarrhythmics, such as flecainide, causing arrhythmias such as AV block. Flecainide also inhibits opening of potassium channels, in particular the Ikr channel (hERG) thereby prolonging the action potential (Andrikopoulos, Pastromas and Tzeis, 2015).

It was predicted that a sodium blocker such as flecainide will have an additive effect on the mutant phenotype, further reduce cardiac output and prolong the action potential. This was proven correct, flecainide had an additive effect on the mutant phenotype, with large increases in, PR, QRS and QTc intervals for both concentrations, **figure 4.15A.** The wild type was also affected, but only at the higher concentration.

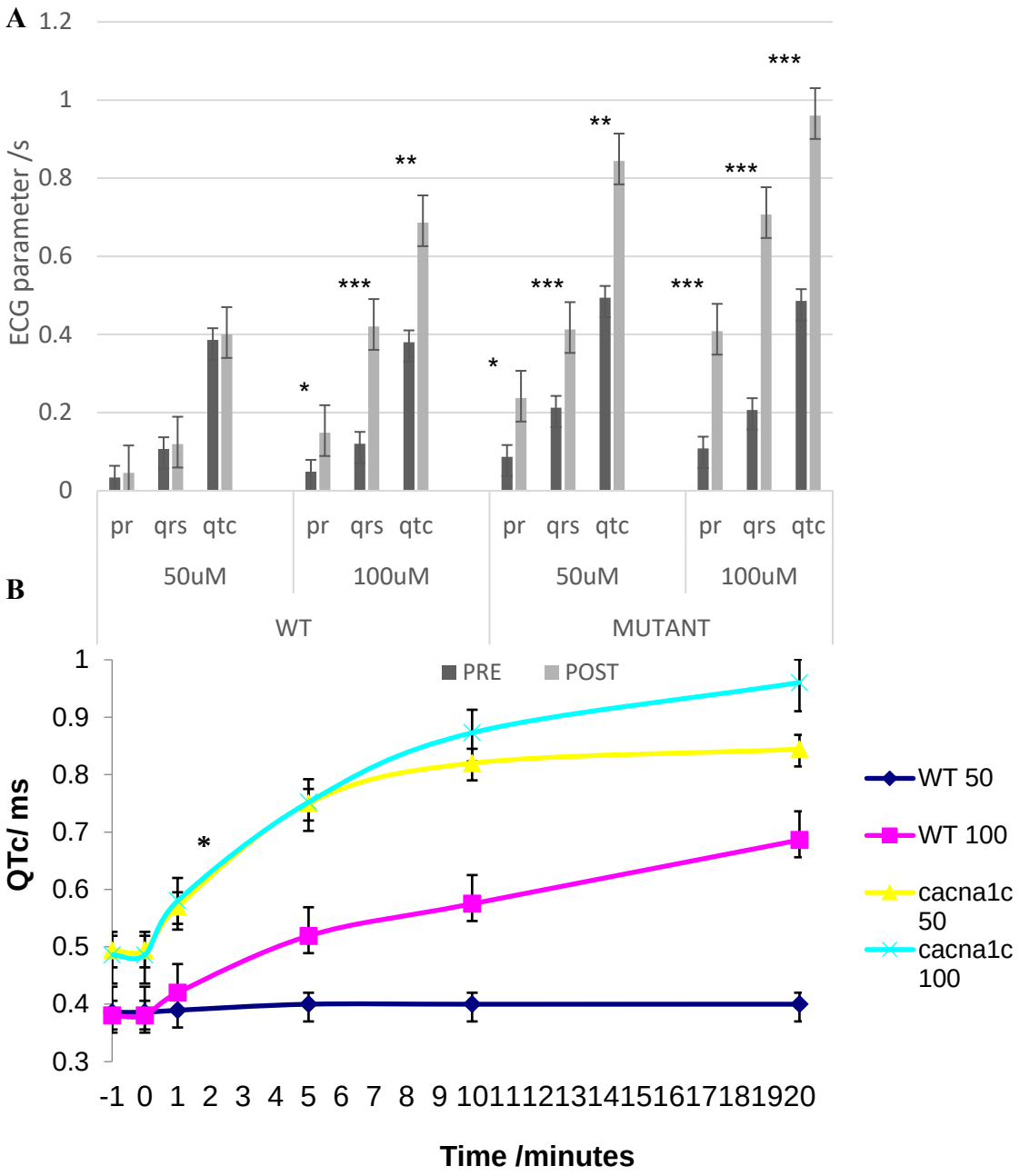

Figure 4.15 Effect of sodium channel flecainide blocker on wild type and cacna1c mutant 3dpf embryos at 50µM and 100µM.
A) There was a global increase in ECG intervals in both wild type (100µM) and mutant (both concentrations) with the more profound effect seen in the mutant. Sodium channel blocker caused QRS widening as well as prolongation of PR and QTc intervals.
B) Graph showing drug response of cacna1c mutant and wild type against time. -1 = baseline recording before drug was added. 0 = time at which drug was added. 1-20 minutes post drug treatment. The cacna1c mutant had a rapid response to the sodium blocker at both concentrations. Wild type did not respond at 50µM.

The effect over time was also assessed and the mutant had a more acute response to sodium channel blockade than the wild type, with a significantly bigger response 2 minutes post treatment than the wild type **figure 4.15B.**

4.3.8 Selective beta 1 beta-blocker increases prolongation of cardiac cycle.

The Beta-blocker selected was metoprolol which is a selective beta1 receptor blocker used to treat angina and hypertension. Conflicting literature information made it difficuly to predict whether metoprolol will increase or decrease the QTc and other parameters. Its use for treatment for tachycardia suggests it will lengthen the cardiac cycle and therefore ECG intervals, but it is also used for some long QT patients suggesting it would shorten the QT. However, Sun *et al,* 2014 investigated the toxicity of two beta blockers including metoprolol on zebrafish embryos and reported that metoprolol decreased the heart rate (Sun *et al,* 2014). It is therefore likely that if metoprolol lowers the heart rate, the cardiac cycle will be slower, therefore longer action potential phases and therefore longer ECG intervals recorded.

The results show that for both wild type and mutant, there was a global increase in ECG intervals. This was particularly observable for the 50μM dose, **figure, 4.16**A

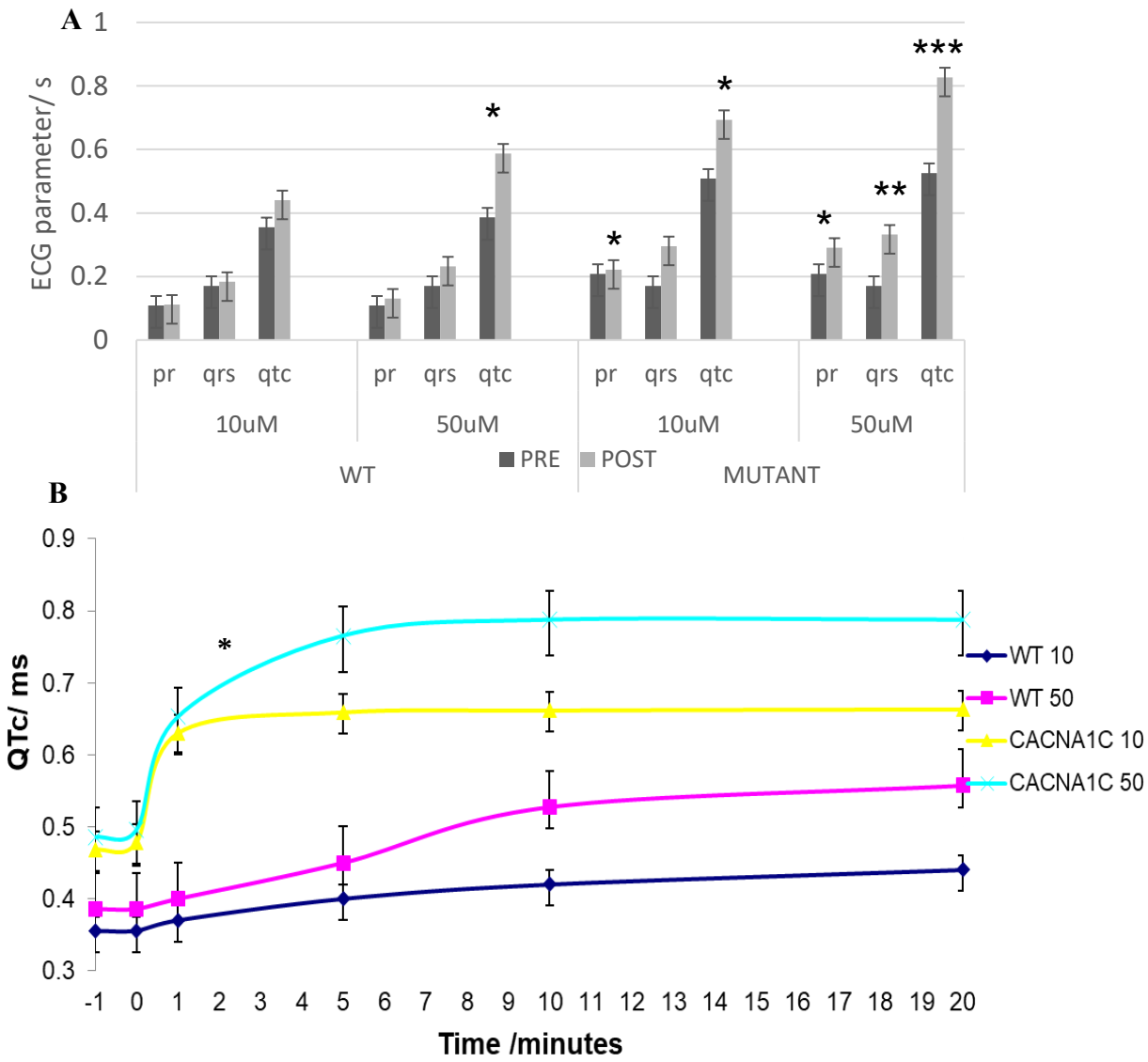

Figure 4.16. Effect of selective beta 1 beta-blocker metoprolol on wild type and cacna1c mutant 3dpf embryos at 10µM and 50µM.
A) There was a global increase in ECG intervals in both wild type and mutant with the more profound effect seen in the mutant.
B) Graph showing drug response of cacna1c mutant and wild type against time. -1 = baseline recording before drug was added. 0 = time at which drug was added. 1-20 minutes post drug treatment. The cacna1c mutant had a more acute response to the beta blocker than the wild type.

The response over time was also assessed and the mutant, once again had the more acute response to beta blocker treatment compared to wild type, with a significantly bigger response 2 minutes post treatment than wild type **Figure 4.16B.**

4.3. 9 Screening for asystolic events phenotype in *cacna1c* mutant.

A small subsection of positively screened *cacna1c* mutant embryos were observed to have periods where cardiac output halted completely for a short amount of time upon ECG recording. This was where the heart stopped beating for a short period of up to 20 seconds before resuming normal rhythm. This was observable under the microscope and on the ECG where the trace flat lined for short periods of time, usually for between 5 and 15 beats (PQRST). When these were subsequently observed under a light microscope, it was clear that during these periods the contractions in both atrium and ventricle stopped (asystolic event) and then restarted a few missed heart beats later. This phenotype, where electrical activity and cardiac output was paused for a period of several beats, was termed pauses.

4.3.9.1 Visual screening and population proportions

To investigate this phenotype further the clutch screening protocol embryo heartbeats were observed for this phenotype for 2-3 minutes from the screened group to determine the proportion of mutants displaying this phenotype. These numbers are reported in **table 4.3**

Total screened	2275
Total negative	1759
Total positive	516
Total A.S	62
A.S % positive	12.0155
A.S % total	2.72527

Table 4.3. Table shows proportion of screened cacna1c clutches screened as mutant, and out of those screened, which displayed the asystolic pauses phenotype. Whole clutches were screened into those positively identified as displaying a mutant cardiac phenotype, including those with the pauses phenotype and those that were negative for a cardiac phenotype (total positive and total negative) Of those screened as positive, those which had asystolic pauses (A.S) phenotype were also identified via observational screening (Total A.S). This is expressed as a % of total positively screened embryos (A.S % positive) and then as a % of total embryos screened (A.S % total).

This result shows that the proportion of embryos in the clutch with the pauses phenotype was very low and are present as a subpopulation of the screened homozygous mutants.

4.3.9.2 Inducing the asystolic events phenotype in the *cacna1c* mutant.

It was thought that this phenotype was the early signs of the more severe phenotype (large oedema) observable by 5 dpf developing. If this pauses phenotype could be induced in all homozygous mutants in the clutch then it may be useful as a screening tool at 2dpf to increase the accuracy of the visual screening. Environmental stresses were applied to the embryos to try and exacerbate the phenotype and induce pauses in the mutant, the clutches were exposed to high salinity and 30 rotations on an orbital shaker. These were selected as they were readily available. The embryos are normally

raised in an embryo medium E3. Following the initial screening, positively screened *cacna1c* mutants were exposed to increasing E3 concentrations at 12.5, 25, 35.5, 50, 75 and 100 times the usual 1x concentration (see 2.2.11 for standard protocol) for 30 minutes after an initial screening. This meant that numbers of embryos with the pauses phenotype before and after salinity or shaker stress could be compared. Embryos were exposed to 5 minutes on an orbital shaker at 100 rotations per minute. At high salinity (75 and 100x) an increase in embryos with asystolic pauses were observed, **figure 4.17 A**. Shaking induced pauses in both *cacna1c* mutants and wild type embryos at 3dpf, **figure 4.17 B.** This means that orbital shaking can not be used to induce pauses in the homozygous mutant as wild type embryos were also affected. In order to use stress to induce a more severe phenotype in the mutant to aide clutch screening, the negative siblings within the clutch need to not be affected.

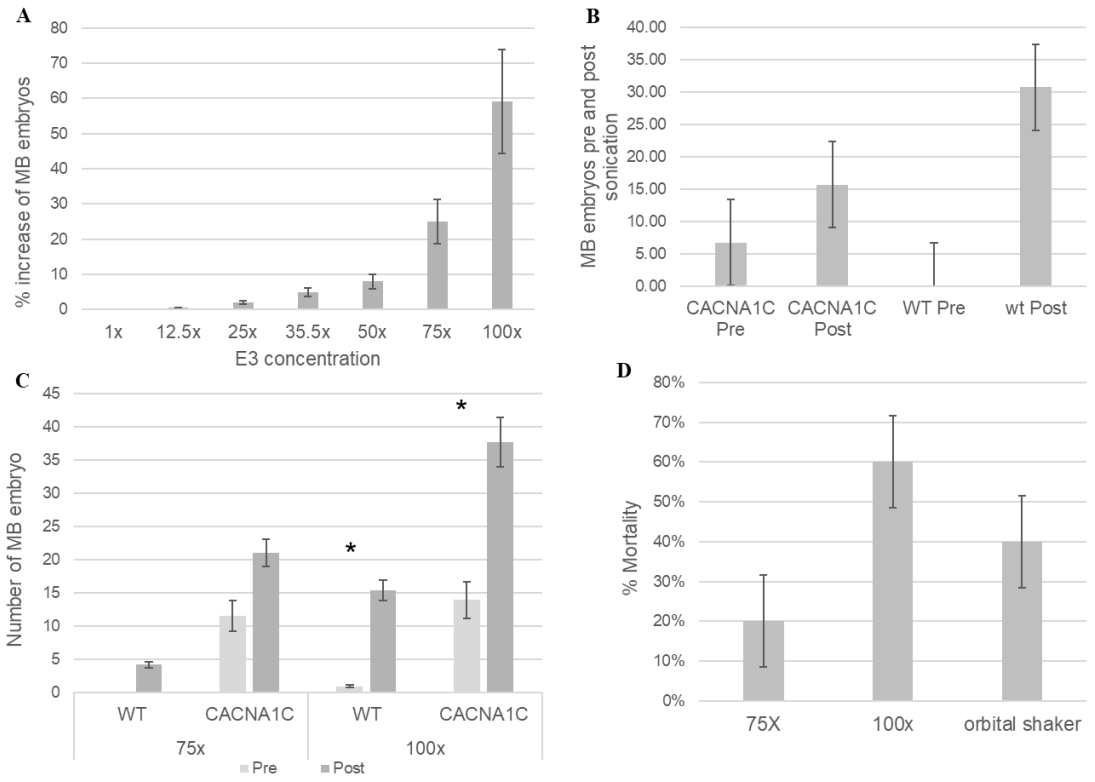

Figure 4.17 The effect of high salinity and orbital shaking on inducing the asystolic pauses phenotype in the cacna1c mutant and wild type controls.
A) % increase in number of embryos with asystolic pauses phenotype after exposure to different salt concentrations. N=20 per concentration of screened homozygous mutants.
B) Number of embryos with pauses phenotype before and after orbital shaking in cacna1c mutant and wild type.
C) Number of embryos with asystolic pauses phenotype before and after 75x and 100x E3 medium concentration in cacna1c and wild type. At 100x concentration increase in embryos with asystolic pauses is significant in both.
D) high % mortality in embryos (wild type and cacna1c) after high salt (75 and 100x E3 medium) and after orbital shaking. This high mortality % plus the induction of pauses in wild type is demonstrative of the unsuitability of asystolic pause induction to aide screening of cacna1c mutants.

Following the initial experiment using 6 increasing concentrations of E3 medium (n= 100 positively screened mutants per concentration) the top two salt concentrations, 75x and 100x were selected for further study as these showed the greatest increase in embryos with the pauses phenotype. The other concentrations did not have a significant difference and therefore were not useful for pause induction. Further *cacna1c* clutches and wild type control clutches were exposed for 30 minutes to 75 and 100x E3

concentration. Pre and post counts of number of embryos with asystolic pauses were collected. Results between wild type and *cacna1c* mutant compared, **figure 4.17 C**. Both *cacna1c* mutant and wild type showed an increase in embryos with the pauses phenotype after exposure to both concentrations. The results for wild type and *cacna1c* mutant were statistically significant for 100x concentration. This means that high salinity and orbital shaking both induce an increase in asystolic pauses in the mutant but also cause this phenotype in the wild type. As an effect was also seen in the wild type, this can not be used to help identify homozygous mutants as this approach would affect all genotypes. High mortality rates were observed for all these groups, **figure 4.17 D**. This suggests that significant injury occurs during this stress. Shorter exposure times (10 mins) were trialled for the salt exposures, but did not produce a change in the number of embryos with pauses phenotype and therefore not usable to induce the phenotype. A successful way of inducing the pauses phenotype in 3 dpf embryos without also inducing the same response in the wildtype controls. Therefore, salt or orbital shaking exposure could not be used to help screen the *cacna1c* clutches.

4.3.9.3 Video analysis of the asystolic events phenotype

Those embryos found to have asystolic pauses were separated out for further analysis by video recording. Video analysis allows a higher throughput of analysis compared to ECG and is therefore preferable, and was also used to find a different way to quantify the asystolic events. The *cacna1c* mutants screened positively for pauses were used for video analysis. SOHA (Semi-automated Optical Heartbeat Analysis) video analysis software (commercially available) was used to establish whether it was possible to detect the asystolic periods and if so, to characterise when these occur and how often. SOHA allowed input of raw video data, **figure 4.18A** which was then cropped down to

the heart and converted to a black and white .AVI file format. SOHA video analysing software allowed the user to mark the maximum diastole (relaxed heart) and systole (contracting heart) of the heart on the video, **figure 4.18B** and then plotted each diastole and systole (heart beat) in the video as a trace showing peaks (systole) and troughs (diastole), **figure 4.18 C**. As the embryo orientation used for video analysis (on its side) displayed both the atrium and ventricle, the ventricle was selected for analysis.

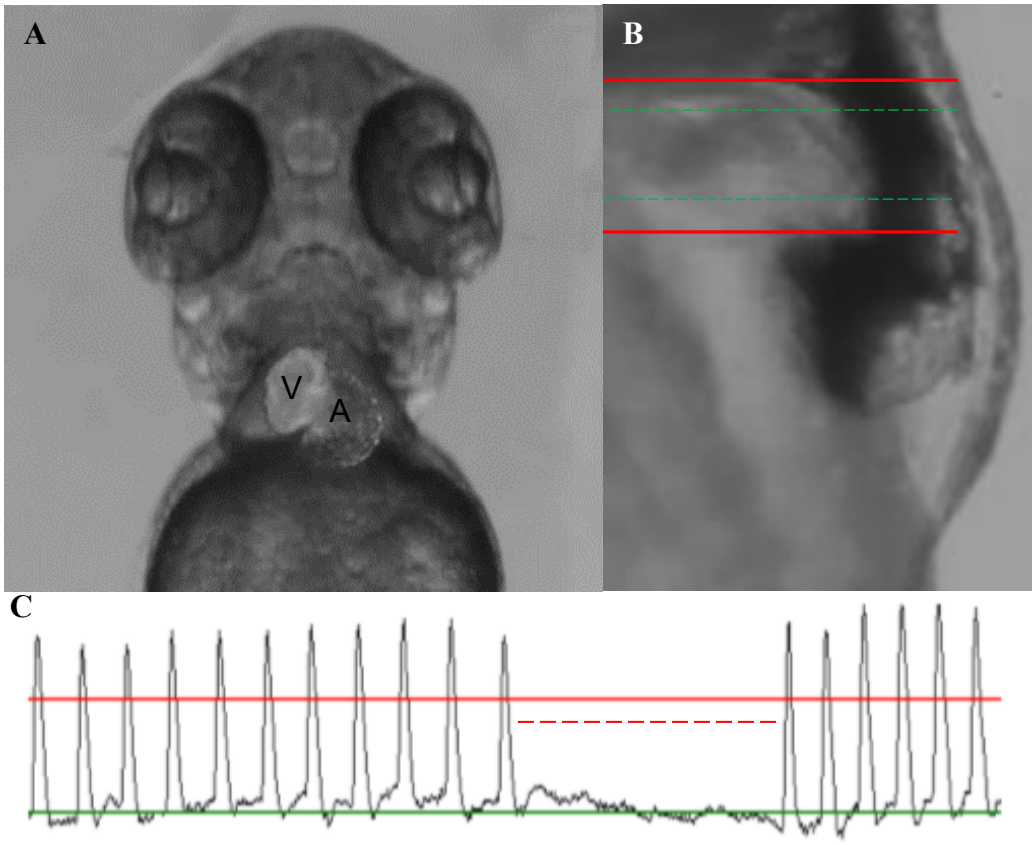

Figure 4.18 Video analysis of asystolic pauses phenotype using SOHA video analysing software.
A) image of a 3dpf zebrafish larvae with ventricle (V) and atrium (A) labelled. Heart fluorescence is an overlay from images taken from Tg(VMHC:red) and Tg(AMHC:mcherry) which have ventricle and atrium fluorescence respectively.
B) Embryo positioned on its side, with diastole position (red) and systole lines (green) overlaid.
C) Diastole and systole for each heart beat plotted. Period of asystole where diastole is maintained with no heart contraction (systole) for a period of 6 heart beats approx, indicated by the red dashed line.

From these traces, it was easily observable where the periods of heart inactivity (MB events) had occurred during that recording section. This indicated that the SOHA software was sensitive enough to detect these asystolic evernts. When all the diastole points from a recording were plotted together, it gave a clear picture of how many asystolic events there were and also how long their duration was. This further analysis was carried out in the SOHA software, the diastole points picked up in the recording to be plotted on a graph, with seconds representing the length of the video on the x axis and seconds representing the length of each diastole on the y axis **figure 4.19 A**. This easily visualised the number of pauses in the recording and also their duration. When this data for n=20 embryos with pauses phenotype was aggregated the average number of pauses observed in a 60 second segment and the average duration of the pauses were calculated **figure 4.19 B**.

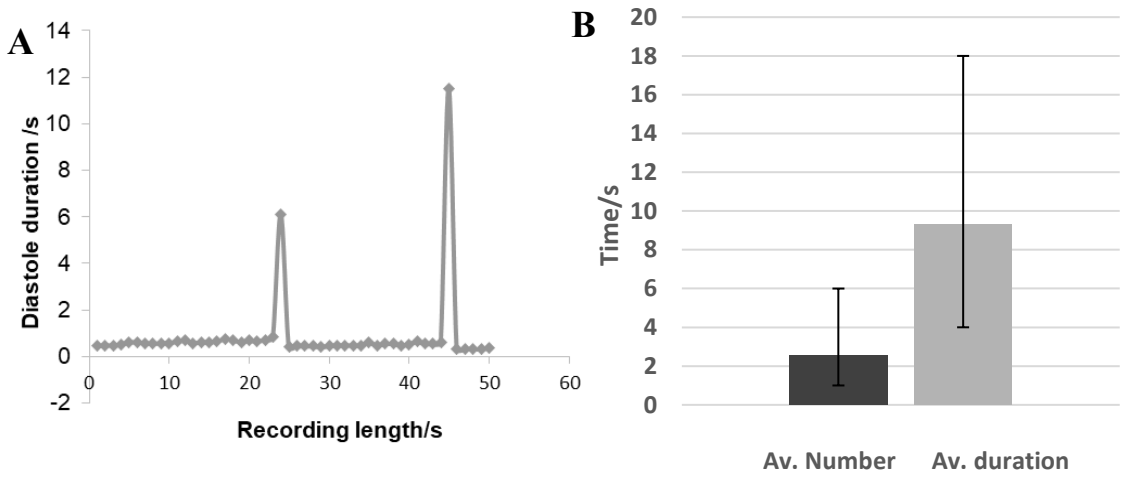

Figure 4.19 Output data (diastole plots) of video analysis and aggregated data from mutants pre-screened for asystolic pauses. 3dpf embryos n=20.
A) Example graph of plotted diastoles from a single recording. Peaks indicate asystolic pauses; y axis denotes length of the asystolic pause.
B) Aggregate data from the video analysis of the pauses phenotype. Average number of pauses in a 60 second section 2.57. Average duration of pauses section 9.33. error bars show standard deviation.

Results showed that on average in a 60 second section there were 2.57 asystolic pauses which lasted an average of 9.33 seconds. This showed that there was quite a variability

in the length of the asystolic pauses and that they occurred roughly every 10-30s in the embryos. This analysis allowed zebrafish embryos displaying the pauses phenotype to be analysed to gain information on how often and how long these asystolic pauses took place. This gives additional information about the phenotype of the *cacna1c* mutant. Given the low incidence in the population, it is likely that the variance in mutant phenotype is a result of the penetrance of the mutation.

4.3.10 Effect of chlorzoxazone treatment on the *cacna1c* mutant.

When the *cacna1c* mutant was treated with Isoprenaline, to assess the effect of a non-selective beta agonist on the heart, it was noted that the asystolic pauses were resolved, and that the heart rate, and ECG parameter measurements were all tending towards normal range. However, this was not a true rescue of the mutant phenotype as this did not address the underlying channelopathy and imbalance of charge. Isoprenaline works to increase cardiac output, but doesn't directly affect the cardiac action potential, it just stimulates the heart to beat faster. This prompted a search to find a potential rescue drug, which would truly rescue the phenotype.

4.3.10.1 Identification of chlorzoxazone as a candidate rescue drug.

A literature search was carried out to identify possible candidates that would truly reverse the phenotype to wild type, by reducing the QTc, increasing the heart rate and reducing both the frequency and duration of asystolic pauses by directly affecting the cardiac action potential and imbalance of charge in the myocytes caused by the calcium channelopathy. The literature search focused on novel therapeutic agents that had previously not been applied to the zebrafish model. chlorzoxazone was identified as it

had previously been shown to be effective in addressing calcium imbalance in neurons, it was hypothesised that it may produce a similar effect on the calcium imbalance in the cacnac1c mutant, and, consequently, Timothy syndrome patients (Liu, Lo and Wu, 2003, Seebohm, 2004 and Gao *et al*, 2012). This drug was also chosen as it is an existing drug on the market, and so there was the potential to repurpose it.

This drug is on the market as a smooth muscle relaxant, and its mode of action is to activate potassium channels to remove excess charge out of the cell as K^+ ions allowing the cell to return to a resting state ready for the next contraction.
It was suspected that it would work in a similar way in a cardiac setting, aiding repolarisation such that the heart returns to a resting state quicker, meaning that the QTc interval would reduce and the heart rate increase.

4.3.10.2 Chlorzoxazone LC50 assay and dosing range

An LD50 is the lethal dose (material) required for 50% mortality in a population. An LC50 is the concentration required for 50% mortality in a population and as such these two toxicological measurements are related. Several studies have reported on the strong correlation between murine LD50 drug assays and zebrafish LC50, therefore this was used as a starting point in calculating an initial dosing range (Ali, Mill and Richardson, 2011 & Ducharme *et al*, 2014). The lowest human/murine LD50 for chlorzoxazone is 50mg/kg and a concentration of 300μM for zebrafish calculated. Estimations of zebrafish weights for this were taken from Hu *et al*, 2000. A dosing range of 30μM, 100μM and 300μM was decided and n=18 *cacna1c* and n=20 wild type embryos were dosed per concentration plus 2% DMSO and E3 control groups. N=14 *cacna1c* and n=16 wild type were also assessed at 600 and 1000μM. Embryos were dosed for a 24

hour period and then counted for % mortality. Acute response was assessed 15 minutes after treatment. Control groups showed 0% mortality. Percentage mortality plotted against the log of the dose for wild type and *cacna1c* were used to calculate the dose which causes 50% mortality (LC50). LC50 was calculated as 197.9 µM for the wild type larvae and 180.2 µM for the mutant larvae, by using the equation of the trend line, inputting y=50 and solving for x, **figure 4.20**.

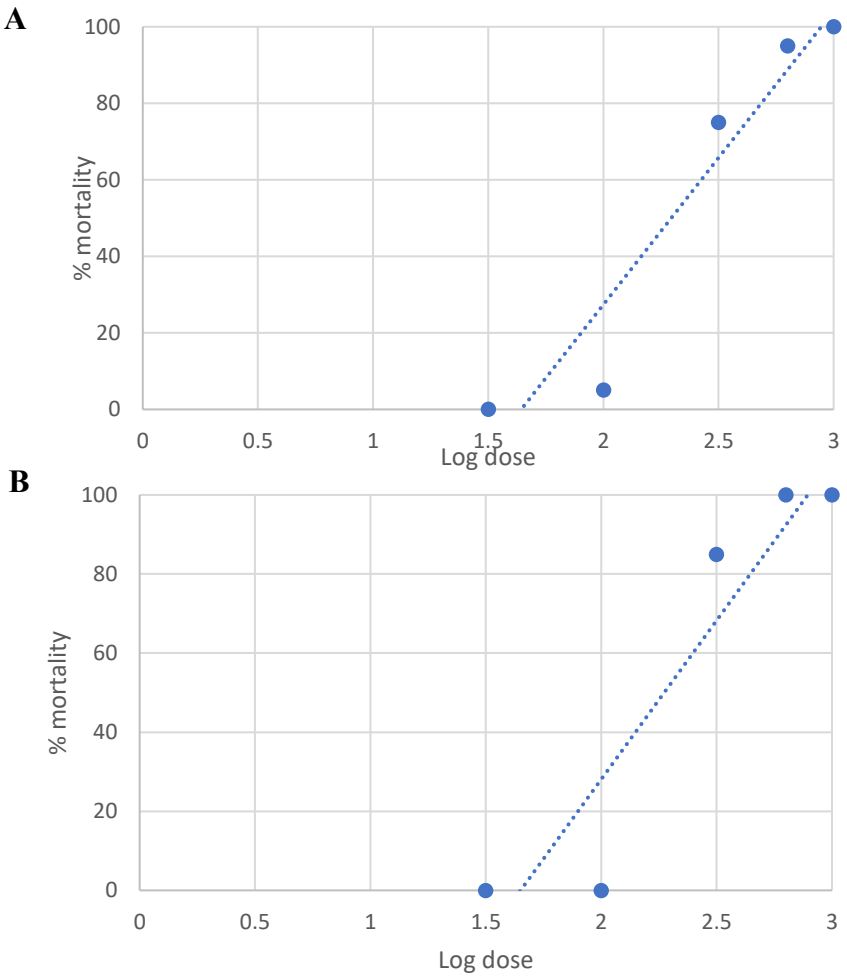

Figure 4.20 Log-Dose mortality charts for wild type and cacna1c mutant
A) wild type Log-Dose mortality chart when treated with chlorzoxazone.
B) cacna1c mutant Log-Dose mortality chart when treated with chlorzoxazone.
Percentage mortality against log-dose of chlorzoxazone plots. n=18 cacna1c 20 wild type x3. The trend used to calculate the concentration of 50% mortality- the LC50.

The assessment of the acute response after 15 minutes treatment identified several phenotypes. These were noted and the number of larvae displaying these phenotypes at the different concentrations were tabulated, **table 4.4**

A

Observed Phenotype wt	30µM	100µM	300µM	600µM	1000µM	E3	DMSO
Paralysis	0	0	20	16	16	0	0
Irregular heart beat	0	0	7	8	10	0	0
Bradycardia	0	0	0	2	1	0	0
Missing beats	0	0	0	0	0	0	0

B

Observed Phenotype cacna1c	30µM	100µM	300µM	600µM	1000µM	E3	DMSO
Paralysis	0	0	18	14	14	0	0
Irregular heart beat	0	0	1	3	5	0	0
Bradycardia	0	1	4	5	2	0	0
Missing beats	0	0	3	3	4	0	0

Table 4.4 Visual phenotypes observed 15 minutes post chlorzoxazone treatment for wild type and cacna1c mutant.
A) wild type acute response phenotypes.
B) cacna1c mutant acute response phenotypes.
Phenotypes observed after 15 minutes observation were paralysis and cardiac arrhythmias and show a dose-dependent increase. Asystolic pauses were only observed in mutant larvae. E3, DMSO, 30-300 µM n=18 cacna1c, n=20 wild type. 600-1000 µM dose n=14 cacna1c, n=16 wild type

Acute phenotypes observed appear to follow a dose-dependent increase, as expected. These phenotypes were paralysis and cardiac arrhythmias, this is consistent with the location of chlorzoxazones mode of action, the heart, muscles and neurons. Paralysis was noted in lack of fin movement and inability to self-right. Cardiac arrhythmias were observed by heart rate count and qualitative visualisation. These were bradycardia,

asystolic pauses (mutants only) and irregular heart beat. In the mutant, irregular heart rate and bradycardia occurred preceding periods of asystole. The phenotypes also correlate with the murine/human LD50 of 300µM.

These results of the LC50 and the therapeutic dose range used in adults of 250-750 mg (roughly 10 mg/kg or 60 µM dose) helped to decide a dose range of 10-100 µM for the chlorzoxazone rescue experiments.

4.3.10.3 Effect of chlorzoxazone as a rescue drug for the *cacna1c* mutant

As previously stated, the *cacna1c* mutant has a significantly slower heart rate and a significantly longer PR interval and QTc interval compared to wild type and sibling controls.

To investigate and analyse the chlorzoxazone response in the *cacna1c* mutant, heterozygous adults were crossed and raised in E3 medium and the resultant clutches were screened as described in 3.1.2. At 3dpf, ECG recordings were taken with chlorzoxazone (CHZ) drug treatment to assess the effect on heartrate, QTc and the pauses phenotype. ECGs were taken 5 minutes prior to drug treatment and up to 30mins post treatment using the single electrode recording system. This was because the primary phenotypes identified in the mutant were low heart rate, heart beat pauses and a long QT. These can easily be analysed using a single electrode system which is less time consuming to collect data. An initial experiment with 50µM CHZ treatment (n=5) showed on average, a significant reduction in asystolic pauses, and QTc interval and an increase heart rate after 10mins treatment, **figure 4.21A.**

The *cacna1c* mutants treated with CHZ, those with the asystolic pauses phenotype, displayed a complete absence of pauses post treatment **figure 4.21B**.

A	Average number of pauses/ minute	Heart rate	QTc	% reduction
Pre	3	85	0.703	12.8%
Post	0.4	104	0.613	

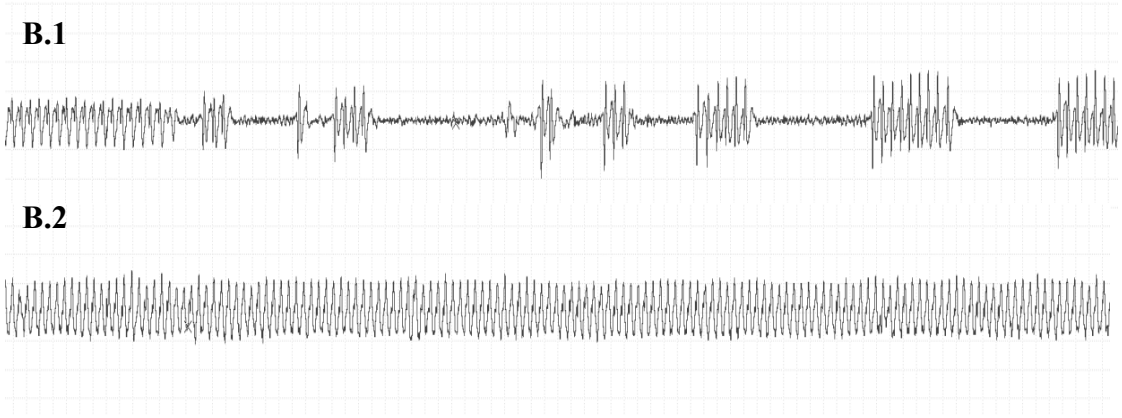

Figure 4.21 Preliminary experiment of the effect of candidate rescue drug chlorzoxazone on the cacna1c mutant phenotype by single electrode ECG recording system. N=5 3 dpf cacna1c homozygous mutants.
A) Table showing average number of asystolic pauses, heart rate and QTc interval pre and 10mins post 50μM CHZ treatment.
B) 1minute ECG trace sections, example of pauses phenotype pre and post CHZ (chlorzoxazone). treatment from one embryo. B.1) pre CHZ treatment and B.2) post treatment. No asystolic pauses after CHZ treatment and increased rhythmicity.

Following this initial experiment, which showed a positive effect on the mutant phenotype, a more in depth experiment was carried out to explore chlorzoxazone as a potential rescue drug for the *cacna1c* mutant. For this experiment, n=8 for wild type and *cacna1c* mutant for 10, 50 and 100μM CHZ concentrations and 2% DMSO controls were carried out. For both groups, DMSO showed no effect on heart rate or QTc.

For 10μM there was no significant difference on heart rate or QTc in the wild type group, however, there was significant reduction in QTc in the mutant. At 50μM, there

was a significant increase in heart rate and reduction in QTc for both the mutant and wild type. At 100μM there was no significant difference seen in the wild type but statistically significant difference in heart rate and QTc interval for the *cacna1c* mutant, these results are summarised in **figure 4.22**.

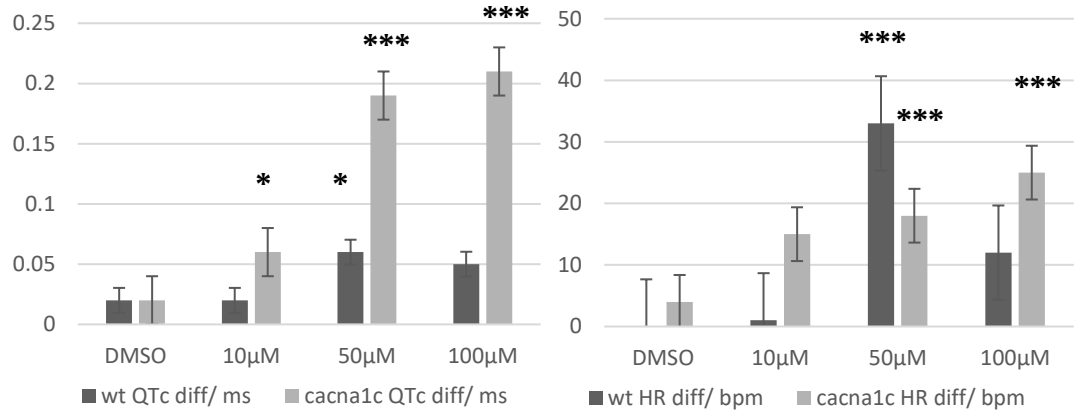

Figure 4.22. Analysis of rescue drug chlorzoxazone on the mutant phenotype across 3 concentrations. QTc and heart rate differences pre and 30 mins post treatment. All QTc changes were a reduction and all heart rate changes were an increase. The statistical significance of these were calculated using non-parametric Wilcoxon paired-signed test. DMSO control group does not have any effect on wild type or cacna1c. No response in the wild type at 10μM but a response seen in the mutant, with a significant reduction in QTc. There were significant changes in heart rate and QTc for both wild type and cacna1c at 50μM while at 100μM only significant changes were seen in the cacna1c mutant. Cacna1c mutant showed a positive dose-response correlation.

These results suggest that the use of CHZ at higher concentrations corrects both heart rate and QTc. The 100μM concentration is preferable as this produced a significant therapeutic effect in the *cacna1c* mutant without effecting the wild type. Dose response across total treatment time is shown in **figure 4.23**.

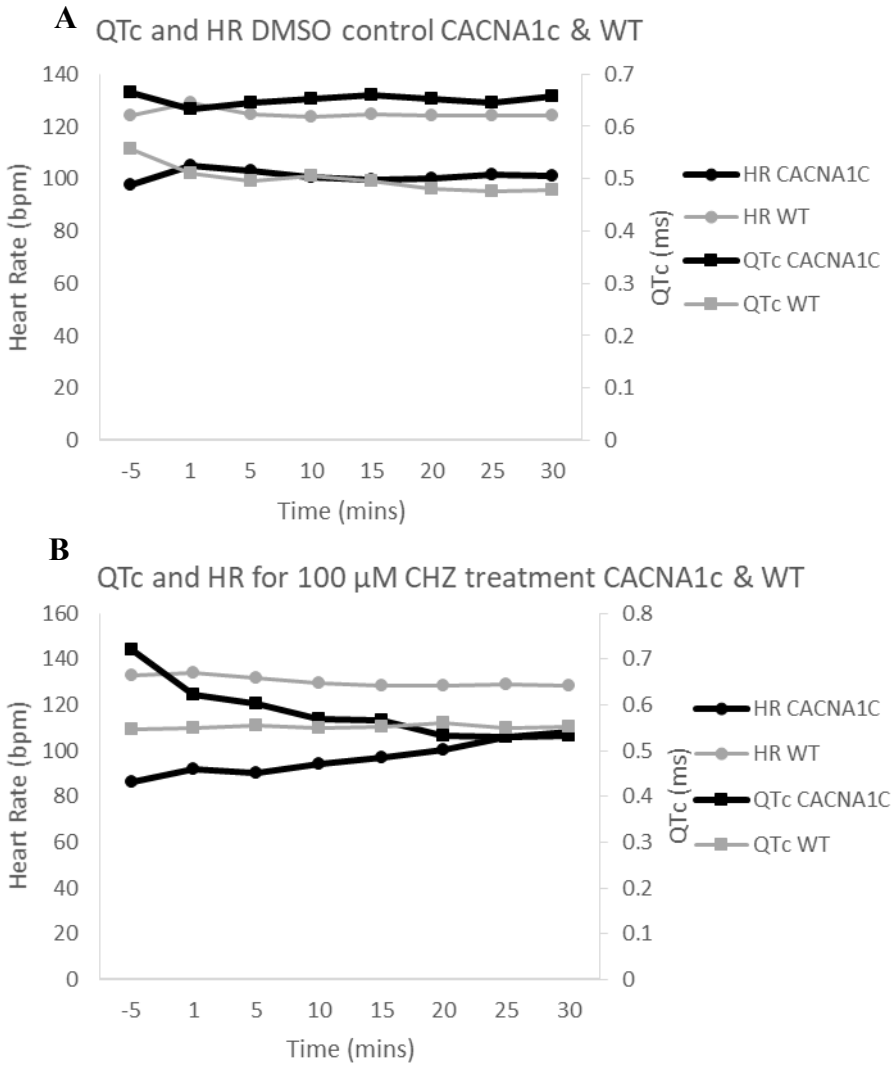

	Wild type		cacna1c	
	HR	QTc	HR	QTc
P value	0.2626	0.4838	0.0117	0.0117
significant	No	No	Yes	Yes

Figure 4.23 Comparison of DMSO control and 100µM chlorzoxazone treatment on the cacna1c mutant phenotype.
A) DMSO control treatment: QTc and heart rate against treatment time for wild type and cacna1c mutant. DMSO given at 0 minutes.
B) 100 µM CHZ treatment: QTc and heart rate recorded against treatment time for wild type and cacna1c mutant. Chlorzoxazone treatment given at 0 minutes. No significant change in QTc or heart rate in the wild type group, there is significant decrease in QTc and increase in heart rate in the cacna1c group.

The aim of this chapter was to demonstrate the utility of the ECG recording system to analyse a cardiac mutant. As well as amply demonstrating that clear, reliable differences between wild type and mutant lines can be detected, recorded and analysed using ECG recording and analysis techniques, a rescue of mutant phenotype has also been demonstrated. Use of chlorzoxazone for treatment of severe arrhythmias has not been reported previously and opens up a potential alternate use for CHZ in the treatment of calcium channel arrhythmias.

4.3.11 Comparison of Timothy syndrome and sa6050 zebrafish mutant.

The most well known human condition associated with calcium channel dysfunction with a long QT phenotype is Timothy syndrome. The 'classic' Timothy syndrome mutation is G406R located on exon 8 or alternate splice exon 8a. Analysis of the G406R mutation (exon 8/8a) associated with Timothy syndrome and the sa6050 *cacna1c* mutant were compared and the protein sequences were aligned to determine if it is possible to conclude that the zebrafish sa6050 line, coupled with phenotype data, is comparable to Timothy syndrome in humans. In Timothy syndrome, the mutation is a missense mutation within exon 8/8a producing a change in amino acid from glycine to arginine, causing a gain of function by the loss of voltage dependant activation (Splawski *et al*, 2004). In the zebrafish sa6050 mutation, the mutation is at an essential splice site, at the end of exon 6, chromosome 4. This causes the proceeding intron to not be cut out, and instead included in transcription, leading to an early stop codon and a greatly truncated protein, causing a loss of function, **figure 4.24.**

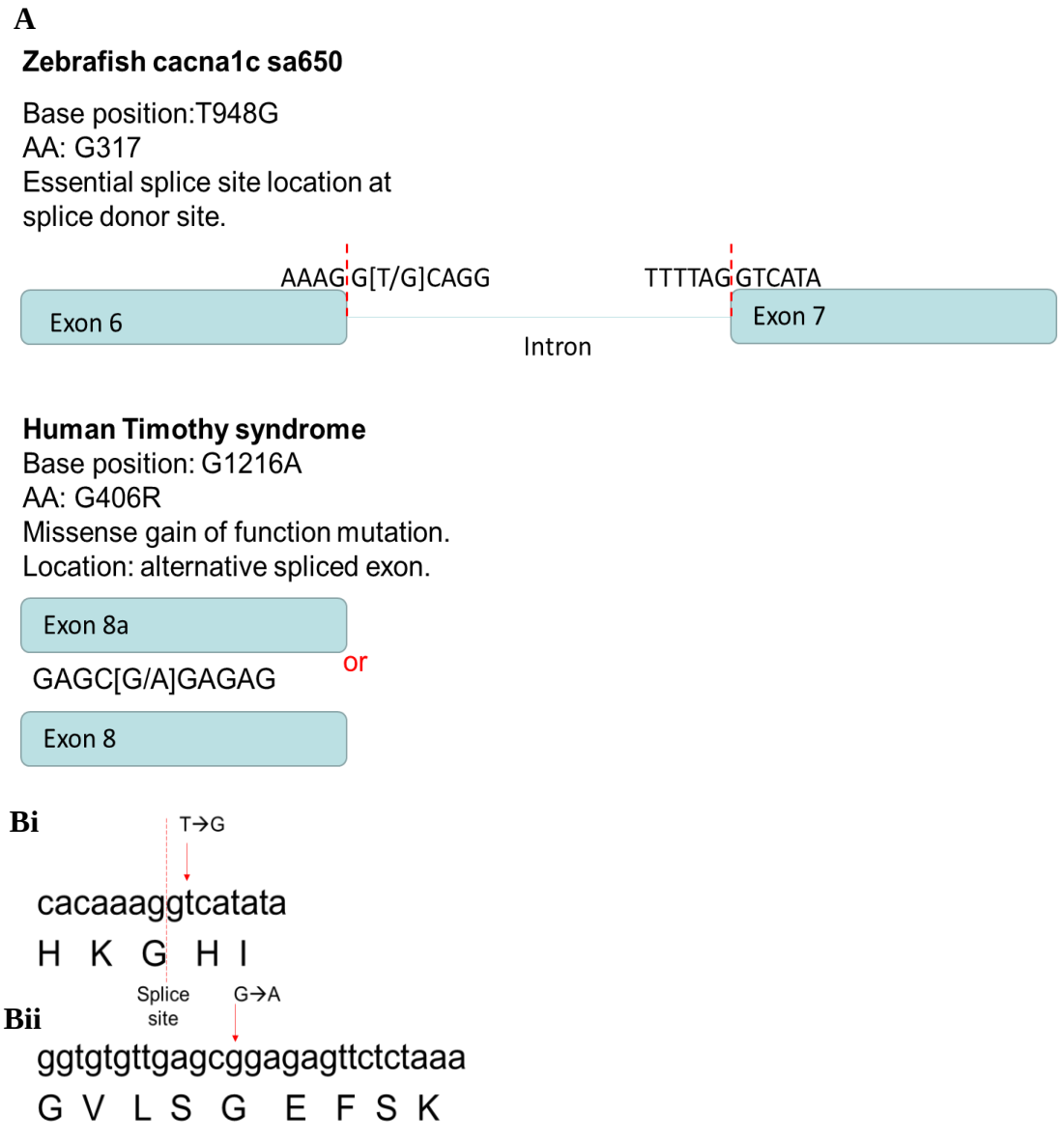

Figure 4.24. Summary of the mutation type and location of the Timothy syndrome mutation and the cacna1c sa6050 zebrafish mutation.
A) The sa6050 mutation is at an essential splice site resulting in the proceeding intron to be included, leading to an early stop codon and a truncated protein with a loss of function. Timothy syndrome has a point missense mutation leading to a gain of function mutation.
B) Alignment of nucleotide bases with amino acids for Bi) zebrafish sa6050 splice site mutation and Bii) Timothy G406R missense mutation.

Amino acid sequence alignment of human and zebrafish protein sequences was performed to look at the differences in location. The zebrafish sa6050 mutation is located at amino acid position 317, upstream of the human Timothy mutation at position 406. The other reported Timothy mutation is at position 402. Both the human and zebrafish proteins are over 2000 amino acids (zf 2196, hm 2221) so in the overall protein size are relatively close in sequence, **figure 4.25**.

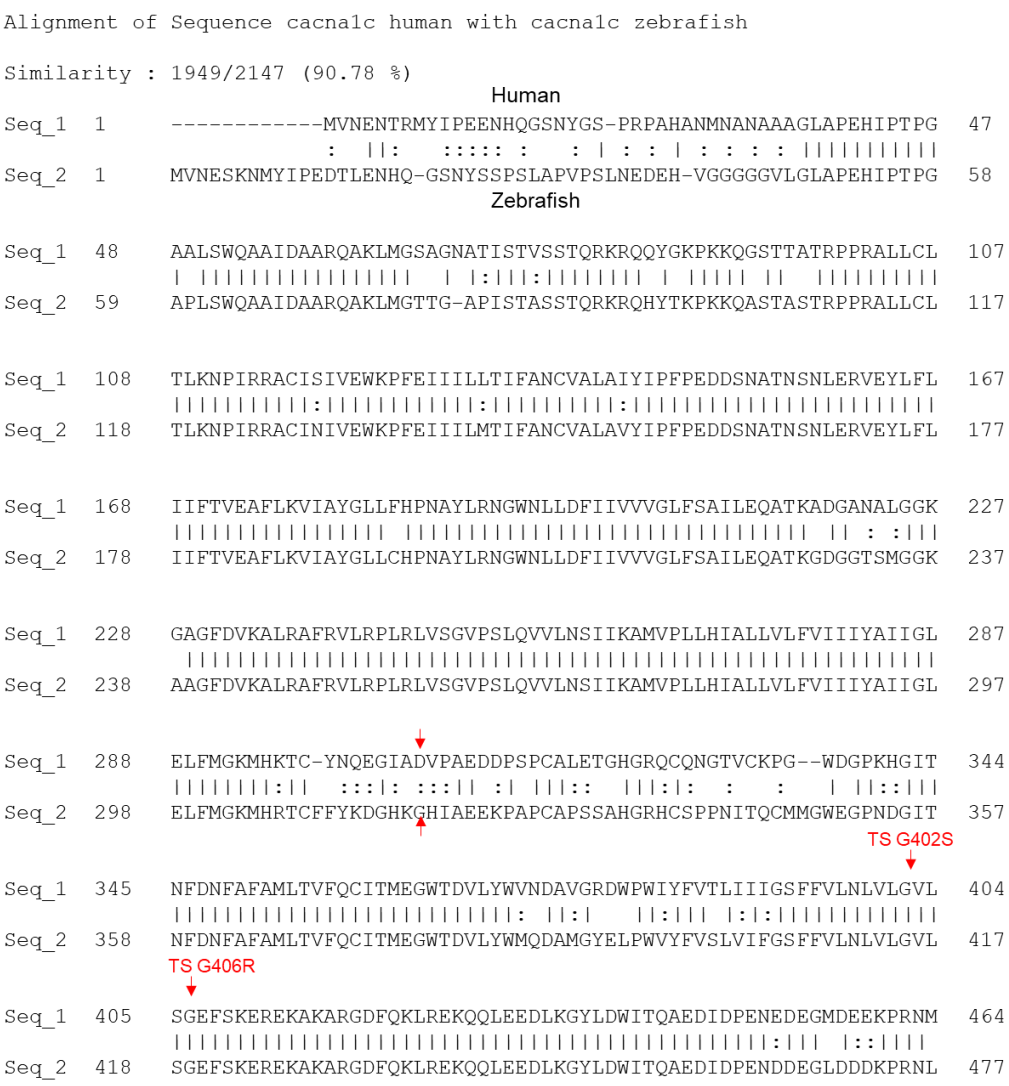

Figure 4.25 Sequence alignment of human cacna1c protein sequence against zebrafish cacna1c protein sequence. Double arrows show location of the sa6050 mutation is not a conserved residue in human. Arrows and labels also show the location of the 2 described Timothy syndrome (TS) mutations G402S and G406R. these are in highly conserved amino acid sequences, although the sa6050 and TS mutations are within 100 aa of each other.

Although there are differences in mutation type, location and contrasting gain and loss of function seen in these mutations, both produce a long QT phenotype.

4.4. Discussion

It has previously been established that ECG changes due to cardiac drug treatment can be measured and analysed by larval zebrafish ECG recording. Analysis of cardiac dysfunction by ECG measurement is advantageous as it is a robust, high resolution and comprehensive method allowing analysis of electrical activity as well as contractility. To further establish this method for cardiac analysis, it was important to establish its utility for detecting cardiac ECG differences as a result of genetic mutation. A mutant was chosen from the Sanger Institutes zebrafish mutation project *cacna1c* sa6050. This is an L-type calcium channel mutant with a suspected loss of function mutation from a point mutation at an essential splice site. This was a new *cacna1c* mutant and had not been characterised prior to this study.

4.4.1 Visual phenotype and genetic analysis of the *cacna1c* mutant.

Heterozygous *cacna1c* embryos were imported from the Sanger Institute and grown up to adulthood. These were then crossed and the resultant clutches screened for phenotypes associated with the *cacna1c* mutation. This was firstly to confirm the phenotype has manifested sufficiently to positively identify mutants within a mixed clutch, and secondly to check for Mendelian distribution to confirm positive identification of homozygous mutants. Thirdly, numerical distribution of phenotypes would confirm whether the heterozygous embryos had any phenotype.

Visual screening of *cacna1c* clutches from heterozygous adult crosses at 2 dpf revealed a proportion of embryos with a cardiac pheonotype. This was an observable cardiac oedema causing abnormal pericardial sac shape which were identifiable against negative siblings within the clutch and wild type controls. Counts from clutches showed

this proportion of heterozygous crosses to be an average of 28.82% presenting with this cardiac phenotype. Mendelian distribution supports this to be the homozygous mutants. There was no visual difference between negatively screened siblings and wild type controls, suggesting there is no visual cardiac phenotype in the heterozygous embryos as expected. The heart rate of wild type, negative siblings and screened mutants were also recorded. Negatively screened siblings had no significant difference in heart rate compared to wild type controls; however, the embryos screened for cardiac deformations had a significantly lower heart rate than both negative siblings and wild type controls. This confirms the visual screening as robust enough to identify homozygous mutants. The lower heart rate also is one of the first indications of the *cacna1c* phenotype, and suggests that the ECG will show further cardiac dysfunction.

Visually screened groups were genotyped, by the Sanger Institute, to check if the phenotype was strong enough at 2 dpf to accurately screen out the homozygous mutant. All those selected for having no cardiac phenotype were heterozygous or wild type, as expected. However, the result of those selected as homozygous mutant revealed that as well as homozygous mutants being selected, there were also heterozygous and wild type embryos selected indicating that the phenotype was not strong enough at 2dpf to accurately screen those out. There may also have been an environmental factor creating phenotype other than the mutant. To compensate for this, the positive group was rescreened at 3dpf before ECG recording, and at 5dpf, when the established phenotype of large cardiac oedema accompanied by a low heart rate by 5 dpf. Those used for ECG analysis on day 3, were kept in 96 well plates, labelled and those which did not develop the large oedema by 5 dpf, the result was discounted from the data set. While this ensured accuracy in the mutant result it also unfortunately introduced bias. This is a significant limitation of the work and further work would be required to address this

issue. Towards the end of the experiments when this was being addressed, the experiment that was planned was to cross the heterozygous adults, collect and grow up the clutch to 3 dpf and then blindly ECG as many as possible on that day. Those would then go into a 96 well plate and their ECGs labelled correspondingly and analysed. The embryos would then be genotyped and then compare the ECG and genotype results. This, if they all matched up, would substantially corroborate the mutant ECG result and link it to the genotype. Once this was established then screening and excluding results based on ECG result would be possible without bias. Unfortunately, this experiment could not be performed due to poor fecundity in the line, new generations grown up also failed to produce and time ran out. Going forward, the priority would be to stabilise the line so these vital experiments can be performed to strengthen the results detailed here.

Screening at 2 dpf and then rescreening at 5 dpf, while it introduced bias, it ensured that ECG analysis could be performed at 3 dpf, before the secondary systemic effects of the mutation developed, while ensuring the accuracy and robustness of the ECG result.

4.4.2. ECG analysis of the mutant phenotype

The purpose of this study was to analyse the direct consequence of the mutation before secondary and systemic effects of the compromised cardiac system start. The cardiac abnormalities observed at 2 dpf develop into the significant cardiac oedema and progressively slower heart rate observed at 5 dpf. The extent of the oedema was such that the heart was stretched out and clearly strained from the effect of the fluid. Although screening of mutants would be quicker at 5 dpf due to their more obvious and defined phenotype against their negative siblings, ECG analysis is extremely difficult with a profound oedema, this is due to the large increase in distance from the surface of

the pericardial sac and the heart, such that a signal is not possible. The heart rate is also so slow by this stage that dosing in the regular concentration of MS-222 (0.3 mg/ml) is enough to cause the heart to stop completely. At 5 dpf, the phenotype has developed sufficiently that the embryo has secondary and systemic effects beyond the arrhythmic phenotype which is a direct effect of the mutation. For this reason, heterozygous clutches were screened at 2 dpf and ECG signals recorded at 3 dpf. Previous work in Dhillon *et al*, 2013 had already confirmed 3 dpf as the earliest developmental stage from which to record detailed, reproducible ECG signal from zebrafish larvae. Having already used this stage as the standard for all wild type analysis it was sensible to record the mutant at this stage to allow for close comparison to this wild type data. Screening at 2 dpf facilitated this by allowing a full day of ECG recording to occur at 3 dpf. This was the optimal stage to analyse the *cacna1c* mutant ECG phenotype as it allows comparison to wild type data, while also early enough for analysis of the phenotype before secondary effects from the mutation.

ECG recordings of *cacna1c* mutant and wild type embryos were recorded and analysed using Labchart software to produce heart rate (RR interval), PR, QRS and QTc intervals. These were then tested for statistical significance and the results plotted. Results showed that all three of the ECG signal intervals were consistently prolonged than those recorded in sibling controls, with the PR and QTc intervals significantly prolonged in the homozygous mutant. This suggests that the mutation is affecting atrium and ventricle function, which is consistent with movement of calcium being affected. Movement of calcium from L-type calcium channels affects phases 0, 2, and 3 of the cardiac cycle. At phase 0 there is a rapid increase in voltage due to sodium channels opening and releasing sodium into the cell causing depolarisation. In the sinoatrial node cells in the atrium this membrane voltage increase is due to L-type

calcium channels which open in response to the pacemaker potential (phase 4). In phase 2 the membrane potential remains balanced due to movement of different ions in and out of the cell. L-type calcium channels are activated by movement of sodium in phase 0 open releasing calcium into the cell. This released calcium binds to and activates more calcium channels (Ryanodine receptors) releasing a large influx of calcium into the cell from intercellular calcium stores on the sarcoplasmic reticulum. This massive increase in calcium is what causes the myocyte to contract. This calcium mediated excitation-contraction coupling is how both the atrium and ventricle contract. In phase 3 of the action potential, the L-type calcium channels close, triggering the beginning of repolarisation. Potassium channels open and the sodium/calcium exchanger pumps calcium out of the cell giving a net loss of positive current, repolarising the cell back to resting potential. Loss of calcium in the cell causes the cell to relax, ending the contraction, (Golan *et al,* 2011, Verkerk and Remme, 2012 and Alday, *et al,* 2014). In a diseased state, where atrial depolarisation (PR) and ventricular repolarisation (QTc) are significantly lengthened this would suggest that movement of calcium into and out of the cardiac myocytes is inhibited. This would also explain the low heart rate, as contraction/relaxation would be slower giving a low heart rate.

All of this evidence together suggests that the ECG changes seen in the *cacna1c* mutant are result of decreased function in the L-type calcium channel as a result of the point mutation.

The ECG results shown here against sibling controls show clear, significant differences. Howver, through some of the proceeding drug treatment results, some variation in the baseline measurements was observed. This could possibly indicate a heterozygous response. However there was no bradycardia or ECG result specifically reported in the initial comparison when comparing those groups. Clearly further work on genetic

characterisation and further phenotypic analysis of this mutant is required to fully understand this mutant.

4.4.3 Potassium channel blocker has an additive effect on the mutant phenotype.

A potassium channel blocker was selected to assess its effect in the mutant ECG. Blocking potassium channels, in particular the hERG (I_{Kr}) channel, is well known to have an arrhythmic effect in both human and zebrafish. Blockage of potassium channels responsible for repolarisation leads to delayed repolarisation and as a result, a QT prolongation observed on the ECG (Langheinrich *et al*, 2003). The potassium blocker selected for this study was terfenadine. This is a well known hERG and zERG channel blocker with a well established QT prolongation effect, and is still frequently used to demonstrate a models utility to pattern arrhythmia (Pratt *et al*, 1996, Alzualde *et al*, 2016). It was predicted that the use of a potassium blocker on the *cacna1c* mutant would have an additive effect, and this was confirmed by ECG analysis. This was expected as aberrant calcium and potassium channel activity should have a drastic effect on the cardiac action potential.

4.4.4 Calcium channel blocker produces little effect in the mutant compared to wild type.

A calcium channel blocker was chosen to assess its effect on the mutant, as mutant response to a calcium channel blocker would be informative of the type of mutation this is. The calcium channel blocker selected was verapamil. This drug is used to treat hypertension and ventricular tachycardias, by reducing cardiac output by blocking

calcium channels (Salhanick and Shannon, 2003). With this mode of action, blocking calcium channels in a calcium channel mutant would have one of two effects. Firstly, if the mutation is causing a gain of function phenotype, blocking channels would partly correct the phenotype by reducing channel function. Secondly if this was a loss of function mutation then blocking the channels wouldn't have a big effect as function is already knocked down. The degree of this would depend on how much function is lost via the mutation. In this case, the wild type larvae had a much more pronounced response to verapamil than the mutant. Lack of response in the mutant to a calcium channel blocker would suggest a loss of function mutation as if function was already knocked down, and further knock down by drug treatment would be minimal compared to a wild type response. Further analysis of the splice site mutation location and effect on the transcription of the protein (see section 3.11) suggests a null mutation where a grossly truncated protein results in loss of function. This indicates that drug responses can be used to give information on the type of mutation without genetic analysis.

4.4.5 Non-selective beta-agonist increases the heart rate and reduces QTc

A non selective beta agonist was selected to assess the effect of increased cardiac output on the mutant phenotype. The non-selective beta agonist chosen was isoprenaline. Treatment of the beta agonist has a stimulating effect on the *cacna1c* mutant, and speeds up the heart rate such that it tends towards the wild type heart rate range, temporarily alleviating mutant phenotypes. Isoprenaline treatment was observed to increase heart rate, decrease PQRST intervals and decrease frequency of the pauses phenotype. However, this is only due to stimulating the heart to beat faster and does

not address the underlying charge imbalance from impaired calcium channel function. Because of this, the QTc remains unchanged after treatment. This means that treatment of isoprenaline is not a complete rescue of the mutant phenotype and this triggered the search for a drug which would completely reverse the phenotype to normal heart rate and QTc ranges (QTc 0.35-0.45ms and heart rate 110-130bpm at 28 degrees).

4.4.6 Non cardiac-acting control drug has no effect on either wild type or *cacna1c* embryos

A control drug, known to not have any cardiac phenotype in human and zebrafish was selected as a control. The control drug selected was penicillin. This drug was selected as it had been used in a previous zebrafish ECG study and was shown to not have a cardiac phenotype (Dhillon *et al*, 2013). As expected, penicillin did not have any effect on heart rate or QTc interval in either the wild type or *cacna1c* mutant embryos. This confirms that responses seen by other drugs are due to the drug treatment exclusively and not due to the experimental set up, anaesthesia, electrode position, embryo manipulation or experiment duration. The drawback of this drug is that it has poor uptake into zebrafish as it is a large molecule and perhaps a control drug such as metformin, which was also trialled for use would have been preferable.

4.4.7 Sodium channel blocker has an additive effect on *cacna1c* mutant.

Flecainide is a class 1c antiarrhythmic and is used to treat and prevent tachycardia and atrial fibrillation. As such, by blocking sodium channels, it causes the ventricular action potential duration to lengthen, thereby reducing the heart rate. In slowing the heart, and

lengthening the action potential, the ECG parameter intervals will also lengthen. In addition it has also been described that flecainide is a potassium channel blocker, including the hERG channel. It is well known and documented that hERG blockers cause a long QT phenotype (Andrikopoulos, Pastromas, and Tzeis, 2015). It was expected that this drug would exacerbate the mutant phenotype and cause an increase in QT as it reduced the heartrate. As predicted, flecainide treatment had an additive effect on the *cacna1c* mutant phenotype. In addition to inhibiting sodium channel function, and potassium channel function, it has also been reported that flecainide blocks the ryanodine receptor from opening, which reduces spontaneous release of calcium ions from the sarcoplasmic reticulum; hence its use as a therapeutic agent against ventricular tachycardia (Andrikopoulos, Pastromas, and Tzeis, 2015). This may be why there was such a pronounced effect on the mutant, with a global increase in all ECG parameters.

4.4.8 Selective beta 1 Beta-Blocker has an additive effect on the cacna1c mutant

A beta blocker was selected to assess the effect of decreasing cardiac output in the mutant. The beta blocker selected was metoprolol which is a selective beta 1 beta blocker used to treat hypertension and has been reported to cause bradycardia and arrhythmia in zebrafish (D'Amico *et al*, 2012). Beta blockers are used to control tachycardia, and as such were expected to exacerbate the phenotype by reducing heart rate, and in turn lengthen the ECG intervals. Metoprolol treatment reduced cardiac output as expected which caused a drop in heart rate and an increase in PR, QRS and QTc intervals at 50μM. The PR and QRS intervals lengthen in correlation with the

drop in heart rate, however, the QT interval is corrected for heart rate to produce the QTc, which had also lengthened, independent of the heart rate.

4.4.9 The use of a set of diversely acting cardiac acting drugs is informative on mutation target.

These 6 drugs were carefully selected as having diverse cardiac effects, known to effect human and zebrafish hearts. These were selected to firstly, block each main cardiac ion channel systematically and then secondly to increase and decrease the cardiac output. The collated data would then give an overall picture of the mutant phenotype, with respect to wild type larvae. Using a cross section of cardiac acting drugs can be used to help identify the phenotype instead of genetics. For example, treating the mutant with terfenadine had an additive effect to the mutant exacerbating the phenotype, whereas when a verapamil, a calcium channel blocker, was added there was almost no effect on the mutant QTc interval despite a significant response in the wild type. This further indicates a calcium channel abnormality in the mutant, which is confirmed via the genetic analysis. In addition, using drugs such as isoprenaline and metoprolol to increase and decrease cardiac output is also informative, stimulating the heart using isoprenaline in a disease state where there is already a tachycardic arrhythmia would greatly exacerbate and increase arrhythmicity, possibly to the point of cardiac arrest. However, in cases such as the sa6050, where there is a bradycardia, isoprenaline treatment can temporarily improve heart rate, decreasing arrhythmia. Similarly use of a beta blocker such as metoprolol to decrease output would improve rhythmicity in a tachycardic heart and be proarrhythmic with a bradycardia. A loss of function mutation in cardiac ion channels, such as in the case of the sa6050 mutation is aggravated upon

treatment with metoprolol, whereas it responded positively to isoprenaline treatment. Conversely, with gain of function mutations this may be reversed. Beta agonist and antagonist response can therefore also give information about the nature of the cardiac phenotype.

4.4.10 Screening for asystolic pauses phenotype and video analysis

A sub-phenotype observed throughout recordings can be described as sections of loss of rhythmicity, termed here as asystolic pauses. These are periods where the heart stops beating for a variable length of time before resuming rhythmicity. Embryos screened positively as a *cacna1c* mutant due to presence of cardiac deformations and low heart rate were observed for 2-3minutes to assess for the presence of the pauses phenotype. Those which were positively screened were analysed by video analysis using SOHA software (Semi-automated optical heartbeat anaylsis). This data was collated with ECG recording to give an overall picture of these periods of complete loss of cardiac output. Not all embryos screened for cardiac deformations (oedema) and low heart rate displayed this phenotype. It was initially thought that the pauses phenotype was part of the progression of the overall mutation effect as it developed towards the profound phenotype observed at 5dpf. It is clear from the original description of the mutant by Sanger and this study's observation that the embryos develop severe oedema along with other systemic effects by 5 dpf. However, there was no increase in the number of embryos displaying asystolic pauses at 5 dpf compared to 3 dpf so perhaps the low incidence is due to mutation penetrance.

Video analysis software detected each systole and diastole for each heart beat and produced an output clearly detecting asystolic pauses. Using systole/diastole outputs from the software can plot the diastoles, which clearly display 1) number of pauses

(number of peaks) and 2) quantifies the length of these asystolic pauses (y axis values). This helped to quantify and further characterise this phenotype.

4.4.11 Chlorzoxazone treatment on the *cacna1c* mutant reduces frequency of asystolic events, reduces QTc interval and increases heart rate.

Following the Isoprenaline result displaying an incomplete improvement in the mutant phenotype by stimulating the heart to increase heart rate, it became important to identify a drug which would truly rescue the mutant phenotype by addressing the calcium overload in the mutant cardiac myocytes. A literature search revealed candidates and chlorzoxazone was selected to be tested on the sa6050 mutant.

It is marketed as a centrally acting smooth muscle relaxant (Liu, Lo and Wu, 2003). Its mode of action as a muscle relaxant is to activate Ca^{2+} activated potassium channels ($I_{k(Ca)}$), which removes K+ from the cell, helping to remove excess charge build up in the cell caused by slow acting calcium channels, by increasing potassium movement out of the cell. This action partially corrects for the calcium overload allowing the cell to return to a resting state ready for the next contraction (Alvina and Khodakhah, 2010). Calcium channels are also highly expressed in the brain and this chlorzoxazone agonist activity has shown to have efficacy in reducing charge imbalance from calcium overload in the neurons of cacna1a^{S218L} mice, with equivalent affect predicted in human patients (Gao *et al*, 2012). This charge imbalance is similar to what is seen in Timothy patients (Dixon *et al*, 2011). It was suspected that chlorzoxazone treatment would have a similar effect on the calcium overload in the cardiac myocytes of the zebrafish sa6050 mutant, aiding the repolarisation phase, allowing the cell to return to a resting state

ready for the next heart beat. Also, as an already marketed drug, it appealed as it was readily available and had already undergone drug development, safety testing and clinical trials for suitability in patients (Waldon *et al*, 1994).

Mutants treated with 100uM chlorzoxazone were observed to have an increased heart rate, smaller QTc interval and improved rhythmicity and no effect was observed in the wild type controls.

As described earlier, a subsection of mutants display a loss of rhythmicity resulting in periods where heart beats are missed. Treatment of chlorzoxazone was shown to improve both the length and frequency of pauses in mutants displaying this phenotype. A drawback of this treatment is that while it removes excess charge from inside the cell, it does not address the calcium overload. Previous studies have shown that treatment with calcium activated potassium channel (SK channel) agonists may have a positive therapeutic effect in patients and mutant mice with calcium overload in neurons, removal of charge by activation of potassium channels (Gao *et al*, 2012 and Alvina and Khodakhah, 2010).

4.4.12 Comparison of sa6050 mutant to published *Island beat* mutant

Sequence analysis of the sa6050 mutant indicated loss of function due to a greatly truncated protein. Rottbauer, *et al*, 2001 published a total loss of function mutation in the *cacna1c* gene called the *island beat* mutant, with 2 splice variants. The two splice variants reported of the mutant *island beat (isl)* have a much more severe phenotype than the sa6050 mutant, despite the 2 splice variants described being truncated much further downstream, with more of the protein left intact compared to sa6050 mutant. The *Island beat* mutant fails to grow the ventricle properly and has a silent ventricle

with sporadically uncoordinated atrial contraction from individual myocytes. This, in humans would be a foetal fatal condition and as such is not a model of Timothy syndrome, but perhaps of the role of the L-type calcium channel in development, particularly cardiac development. It is interesting that the sa6050 mutant has more functionality and less severe phenotype than *isl:* the chambers are formed correctly, and both contract, albeit with a progressive arrhythmia and severe cardiac phenotype. It is suspected that the vastly truncated protein in sa6050 is compensated from the failed expression from the mutated gene on chromosome 4 by expression of gene copies located on chromosomes 8 and 11. There are also 2 splice variants of this gene which are not affected by the mutation. The *island beat* mutant is described as a total loss of function, and as the phenotype is so severe, it is likely that there is no compensation by alternate genes or splice variants, however, this would need to be confirmed by further analysis, for example RNAseq data.

The less severe phenotype seen in the sa6050 mutant compared to *island beat* suggests that the sa6050 mutant represents the human patient calcium channel arrhythmias more closely than *island beat* as in humans, calcium channel abnormalities are arrhythmic, characterised by QTc interval differences, and do not exhibit silent ventricle phenotype as this would be foetal fatal in humans.

4.4.13 Relevance of *cacna1c* mutant to human disease: Timothy syndrome.

In human disease, a gain of function mutation in the L-type calcium channel is characterised by a long QT phenotype. This is known as Timothy syndrome, a rare autosomal dominant disorder. The loss of function mutation in this calcium channel, in

human disease, is characterised by a short QT. This is known as Brugada syndrome. In the zebrafish *cacna1c* sa6050 mutant, a loss of function is assumed, due to the location of the mutation at an essential splice site and resultant truncated protein, but with a long QT.

Sequence analysis of the sa6050 mutant indicates a long QT phenotype with a loss of function mutation. This is interesting as in human a loss of function mutation in *cacna1c* leads to a short QT phenotype (Antzelevitch *et al,* 2007) and a gain of function mutation leads to a long QT, as described in Timothy syndrome (Wemhöner *et al,* 2015). Verapamil has also been reported to have efficacy in treating tachycardias associated with Timothy syndrome (Jacobs *et al,* 2016). But treatment with verapamil (Ca^{2+} blocker) on sa6050 had no effect, consistent with a loss of function mutation. Which would suggest that this sa6050 mutant can not be used specifically for Timothy syndrome, but may be useful for other calcium channel dysfunction induced arrhythmias.

Comparison of the location and nature of the mutations in Timothy syndrome with the sa6050 mutant showed that there are fundamental differences. Timothy syndrome arises from a missense, gain of function mutation, whereas the sa6050 mutant is assumed to be loss of function from severe truncation, and the point mutation is located at an essential splice site. Despite this, similar phenotypes are seen. Both have a characteristic long QT phenotype. Therefore, it may be possible to use this mutant to analyse long QT phenotype arising from a *cacna1c* mutation.

Incidence of the same phenotype from contrasting mutation fates in the same gene is interesting. Mechanistically, in Timothy syndrome, a long QT from a gain of function mutation arises due to a loss of voltage sensitivity, and therefore voltage gating, this

means that the channel is constitutively open. Therefore, constant calcium current flow, loss of pulse of on/off causing myocyte contraction/relaxation. If calcium always present, then the cell can not relax, removal of charge from the cell to return to resting potential for next heart beat takes longer and therefore QT interval, the repolarisation section on ECG, is prolonged (Wemhoner *et al,* 2015, Liao and Soong 2010 and Splawski *et al,* 2004).

In the sa6050 mutant, it is hypothesized that the highly truncated protein has very little/no function. This truncation includes most of the major pore forming regions of the protein, making it most likely that there would be almost total loss of function. This, therefore would explain the bradycardia seen in these mutants as movement of calcium in and out of the cell to facilitate cardiac contraction/relaxation would take much longer and would rely on the other calcium channels, which under normal circumstances have a more minor role compared to the L-type calcium channel cav1.2. This would also result in the prolonged ECG intervals also described in this chapter, including a long QT phenotype.

Overall, the sa6050 mutant is an L-type calcium channel mutant with a long QT phenotype which may be used to study and investigate calcium channelopathies resulting in LQT, and testing in this mutant could be used to highlight novel therapeutics. Chlorzoxazone, a smooth muscle relaxant, has been shown to reverse the mutant phenotype, increasing heart rate and reducing QTc interval towards normal range. It has already been indicated as a therapeutic in neuronal calcium overload, and here, it has been demonstrated that it may have a cardiac application also.

5. Overall conclusions

This study aimed to further validate the zebrafish as a model of human cardiac arrhythmia in terms of cardiotoxicity and in human cardiac disease. Zebrafish as a model of cardiac arrhythmia and toxicity has been widely demonstrated, but barriers still exist which prevent translation from small-scale research studies to use as a screen for pharmaceutical drug development. Use of zebrafish larvae in drug screening is advantageous as they have conserved drug responses to human and represent an *in vivo* vertebrate model with high-throughput potential.

The requirements and possibilities of introducing an *in vivo* zebrafish screen was discussed as part of the introduction to this project. Further validation of the zebrafish model to demonstrate how translatable zebrafish results are to human responses is required to convince many pharma companies to use zebrafish assays (Redfern *et al* 2008). Also, one of the biggest concerns surrounding the use of zebrafish as a screen is dosing and ADME (absorption, distribution, metabolism and excretion). Zebrafish are exposed to a drug concentration in their surrounding medium and then, with larval forms, drug uptake is dependent on transdermal absorption. The efficiency of drug uptake depends on the individual compounds pharmacology and even if taken up successfully, there is still a question mark over metabolism while the larva is still developing (Redfern *et al*, 2008). There are also standardisation requirements surrounding husbandry and strains across labs to limit the impact of these on results (Planchart, *et al*, 2016). Even though some zebrafish assays with toxicological end points have been established in some CROs (contact research organisations), for large-scale implementation of a zebrafish screen to happen, a big collaborative effort is

required between laboratories, pharmaceutical companies and regulatory authorities to overcome these hurdles (Redfern *et al,* 2008).

This project proposes that an *in vivo* larval zebrafish ECG screen would be an effective tool for cardiac safety testing and (through the use of arrhythmic mutants) drug discovery. Despite demonstrating the potential for a high throughput system, there are still other considerations to answer before such a system is implemented as part of the drug development pathway. The current gold standard for detecting hERG interaction is a high throughput *in vitro* whole-cell voltage clamp assay capable of producing accurate data on hundreds of compounds a week. While the zebrafish would function better as a multi-end point assay, manual handling and orientation of embryos needs to be removed to compete with this. (Redfern, *et al,* 2008).

A principal aim of this project was to make steps towards a high throughput larval zebrafish recording system, and this was achieved through the development of reliable, reusable, resilient metal microfabricated electrodes. Utilising a microfabricated approach to ECG recording replaces the fragile glass capillaries with a recording device more suitable to a high throughput setting. Development of microfabricated electrode arrays successfully recording from zebrafish larvae, represents a significant advancement to the development of a high throughput ECG system. Further work is required to automate the recording process, however, a recent publication by Fuad, Kaslin and Wlodkowic, 2018, demonstrated an automated process for cardiac analysis, using a millifluidic system for automated embryo handling and positioning for imaging, producing high resolution images and heart rate analysis. This system was also compatible with drug treatments. Integrating the microfabricated electrode arrays developed as part of this study, with technologies such as the millifluidic lab-on-a-chip approach described in Fuad, Kaslin and Wlodkowic, 2018; would automate embryo

handling, positioning and recording, allowing high-throughput recording of ECGs. This would mark a significant step forward to using the zebrafish as a cardiotoxicity model for pharmaceutical development. Teaming this technology with automated ECG parameter measurement software also developed as part of this project, but not presented here, would complement and enable full automation of ECG recording procedure and analysis, (Barrett *et al*, 2015 – as yet unpublished).

Throughout this project various advancements and developments to the larval ECG recording procedure have been made. At the start of the project, the single electrode recording system as described in Dhillon *et al*, 2013 was in use. Demonstration of the use of metal electrodes, both twisted pair and microfabricated for larval zebrafish recording, are significant novel aspects of this work. Similarly, demonstration of a standardised dual electrode system recording distinct signals from two recording positions on the heart has not been shown previously. Various novel method developments of different recording platforms and embryo handling and orientation have been described during this work such as the stage allowing microfabricated recordings and the plate for on going temperature control and monitoring throughout experiments. In total, many different recording approaches have been demonstrated here showcasing the zebrafish as an arrhythmia model through ECG recording techniques. This work to develop ECG recording techniques for zebrafish larvae was done as an alternative to other cardiotoxicity tools such as video and imaging analysis. This visual approach is possible in zebrafish embryos due to their optical transparency, however to utilise an ECG recording tool is closer to diagnostics performed in human. The data obtained from an ECG recording is also more detailed and gives a better overall picture of cardiac function. For example; visual screening for QT prolongation, is done by looking for induction of AV block, which is a separate phenotype itself and

as demonstrated by ECG recording, zebrafish can exhibit a long QT phenotype without having AV block. This makes ECG recording a more sensitive tool for analysing changes in cardiac function through drug treatment. In addition, multiple end points can be picked up by ECG analysis of the trace. For example, PR interval, QRS width, QT interval and heart rate (RR interval) can all be analysed from one recording. Each of these gives different information and gives an overall picture of cardiac function.

Another principal aim of this study was to demonstrate the capability of the larval recording system for recording aberrant ECG signals due to genetic mutation and not from drug treatment. This was successfully performed using the *cacna1c* sa6050 mutant which is part of a family of genes encoding the L-type calcium channel. This mutant, created as part of the Wellcome trust Sanger Institutes zebrafish mutation project, was chosen due to its significant cardiac phenotype observed at 5 dpf. It was also demonstrated that in-depth analysis of a mutant phenotype can be performed using ECG recording analysis and using a set of cardiac drugs can be informative of the nature of the mutation without genotyping. For example, looking at blocking different ion channels in turn and increasing and decreasing cardiac output revealed that blocking cardiac calcium channels had little effect on the mutant leading to a prediction of a loss of function mutation. If ion channel function is knocked down due to a mutation, knocking it down with a drug on top of that will not have much effect. In addition, increasing the heart rate had a positive effect on the mutant which lead to the search for a rescue drug that addressed the underlying charge build up caused by excess calcium. This platform also allowed identification of a novel use for a current drug, Chlorzoxazone, which rescued the mutant phenotype. Although the *cacna1c* mutant used in this study did not relate directly to a human disease mutation, the cacnac1c sa6050, may prove useful for further study of calcium channel abnormalities. With the

rise in CRISPR/cas9 technology for the creation of zebrafish mutant lines, a zebrafish mutant with the Timothy mutation, G496R could be created and assessed by ECG. Chlorzoxazone treatment could then be tested in this model to see if there is a positive effect on the mutant phenotype. However, a significant limitation to this mutant characterisation is that the genotype was not identified in those screened as homozygous mutant. There were problems visually screening the mutant at 2 dpf. Screening was performed at 2dpf to allow ECG recording at 3 dpf. However, identification of mutants was not accurate enough at this stage which lead to larvae being kept after ECG to check back at 5 dpf when the more pronounced cardiac phenotype had developed. The results were those screened as mutant developed the severe phenotype at 5 dpf were kept and the small proportion of those that didn't were excluded. Sorting retrospectively in this way, while ensuring accuracy in the ECG results, introduced bias to the experiment. While the mutant ECG phenotype was confidently identified and reported here, it wasn't without introducing bias into the experiment, which, going forward needs to be addressed for future experiments. For example, performing ECGs on the entire clutch and then genotyping and correlating the genotype to the ECG would go a long way to demonstrating the ECG phenotype observed here is directly linked to the genotype. Unfortunately, this experiment was not performed due to problems with embryo fecundity towards the end of the project.

The aims of this study were to develop ECG recording techniques for zebrafish larvae, to develop recording technologies capable of high throughput and to demonstrate the utility of such a system to analyse cardiac mutants and this has been achieved. Further work to expand on what is presented here, can be done to implement the microfabricated electrodes as part of an automated high throughput system and create a proper genetic model of Timothy syndrome using CRISPR/cas9 techniques.

In conclusion, this study has taken steps to further validate the zebrafish larvae as a model of human cardiac arrhythmia. Use of electrographic techniques gives high resolution data for comparative analysis to human cardiac conditions and assessment of drug responses.

6. References

[online] https://www.sads.org/library/long-qt-syndrome#.Wp59nOjFLIV [Accessed March, 2018].

ABRAMS, D.J. and MACRAE, C.A., 2014. Long QT syndrome. *Circulation,* **129**(14), pp. 1524-1529.

AHUMADA, G.G., 1987. Cardiovascular pathophysiology*. Oxford University Press, USA*.

ALDAY, A., ALONSO, H., GALLEGO, M., URRUTIA, J., LETAMENDIA, A., CALLOL, C. and CASIS, O., 2014. Ionic channels underlying the ventricular action potential in zebrafish embryo. *Pharmacological research,* **84**, pp. 26-31.

ALI, S., VAN MIL, H.G. and RICHARDSON, M.K., 2011. Large-scale assessment of the zebrafish embryo as a possible predictive model in toxicity testing. *PloS one,* **6**(6): e21076.

ALVINA, K. and KHODAKHAH, K., 2010. KCa channels as therapeutic targets in episodic ataxia type-2. *The Journal of neuroscience : the official journal of the Society for Neuroscience,* **30**(21), pp. 7249-7257.

ALZUALDE, A., HOLGADO, O., BERTRAN, E., GEITER-WILKE, A., MURIANA, A. and ROBERTS, S., 2016. Assessing cardiotoxicity in the zebrafish embryo, *Journal of Pharmacological and Toxicological Methods*, **81**, pp. 371-371.

AMIRI, H., ZAMANI, N., HASSANIAN-MOGHADDAM, H. and SHADNIA, S., 2016. Cardiotoxicity of tricyclic antidepressant treated by 2650 mEq sodium bicarbonate: A case report. *JRSM cardiovascular disease,* **5**, pp. 1-3.

ANDRIKOPOULOS, G.K., PASTROMAS, S. and TZEIS, S., 2015. Flecainide: Current status and perspectives in arrhythmia management. *World journal of cardiology,* **7**(2), pp. 76-85.

ANTZELEVITCH, C., 2001. The Brugada syndrome: ionic basis and arrhythmia mechanisms. *Journal of cardiovascular electrophysiology,* **12**(2), pp. 268-272.

ANTZELEVITCH, C., POLLEVICK, G.D., CORDEIRO, J.M., CASIS, O., SANGUINETTI, M.C., AIZAWA, Y., GUERCHICOFF, A., PFEIFFER, R., OLIVA, A., WOLLNIK, B., GELBER, P., BONAROS, E.P., JR, BURASHNIKOV, E., WU, Y., SARGENT, J.D., SCHICKEL, S., OBERHEIDEN, R., BHATIA, A., HSU, L.F., HAISSAGUERRE, M., SCHIMPF, R., BORGGREFE, M. and WOLPERT, C., 2007. Loss-of-function mutations in the cardiac calcium channel underlie a new clinical entity characterized by ST-segment elevation, short QT intervals, and sudden cardiac death. *Circulation,* **115**(4), pp. 442-449.

ANYUKHOVSKY, E.P., 2011. Early prediction of proarrhythmic cardiotoxicity in the drug development process*, Oxford University Press*.

ARNAOUT, R., FERRER, T., HUISKEN, J., SPITZER, K., STAINIER, D.Y., TRISTANI-FIROUZI, M. and CHI, N.C., 2007. Zebrafish model for human long QT syndrome. *Proceedings of the National Academy of Sciences of the United States of America,* **104**(27), pp. 11316-11321.

ARONOV, A.M., 2005. Predictive in silico modeling for hERG channel blockers. *Drug discovery today,* **10**(2), pp. 149-155.

ARTMAN, M., BENSON, D.W., SRIVASTAVA, D. and NAKAZAWA, M., 2005. Cardiovascular Development and Congenital Malformations. *Blackwell Publishing* IBSN-13:978-1-4051-3128-5.

ASNANI, A. and PETERSON, R.T., 2014. The zebrafish as a tool to identify novel therapies for human cardiovascular disease. *Disease models & mechanisms,* **7**(7), pp. 763-767.

BAKKERS, J., 2011. Zebrafish as a model to study cardiac development and human cardiac disease. *Cardiovascular research,* **91**(2), pp. 279-288.

BERGHMANS, S., BUTLER, P., GOLDSMITH, P., WALDRON, G., GARDNER, I., GOLDER, Z., RICHARDS, F.M., KIMBER, G., ROACH, A. and ALDERTON, W., 2008. Zebrafish based assays for the assessment of cardiac, visual and gut function—potential safety screens for early drug discovery. *Journal of pharmacological and toxicological methods,* **58**(1), pp. 59-68.

BINDER, V. and ZON, L.I., 2013. High throughput in vivo phenotyping: The zebrafish as tool for drug discovery for hematopoietic stem cells and cancer. *Drug Discovery Today: Disease Models,* **10**(1), pp. e17-e22.

BOCZEK, N.J., BEST, J.M., TESTER, D.J., GIUDICESSI, J.R., MIDDHA, S., EVANS, J.M., KAMP, T.J. and ACKERMAN, M.J., 2013. Exome sequencing and systems biology converge to identify novel mutations in the L-type calcium channel, CACNA1C, linked to autosomal dominant long QT syndrome. *Circulation.Cardiovascular genetics,* **6**(3), pp. 279-289.

BRAÑA, I., ZAMORA, E. and TABERNERO, J., 2013. Cardiotoxicity. In *Side Effects of Medical Cancer Therapy.* Springer, pp. 483-530.

BROWN, D.R., SAMSA, L.A., QIAN, L. and LIU, J., 2016. Advances in the study of heart development and disease using zebrafish. *Journal of cardiovascular development and disease,* **3**(2), pp. 13.

BURGGREN, W.W., DUBANSKY, B. and BAUTISTA, N.M., 2017. Cardiovascular development in embryonic and larval fishes. In *Fish Physiology.* Elsevier, pp. 107-184.

BURNS, C.G., MILAN, D.J., GRANDE, E.J., ROTTBAUER, W., MACRAE, C.A. and FISHMAN, M.C., 2005. High-throughput assay for small molecules that modulate zebrafish embryonic heart rate. *Nature chemical biology,* **1**(5), pp. 263-264.

BUSCH-NENTWICH, E., KETTLEBOROUGH, R., DOOLEY, C., SCAHILL, C., SEALY, I., WHITE, R., HERD, C., MEHROKE, S., WALI, N. and CARRUTHERS, S., HALL, A., COLLINS, J., GIBBONS, R., PUSZTAI, Z., CLARK, R., STEMPLE, D.L., 2013. Sanger institute zebrafish mutation project mutant data submission. *ZFIN Direct Data Submission*.

CHAUDHARI, G.H., CHENNUBHOTLA, K.S., CHATTI, K. and KULKARNI, P., 2013. Optimization of the adult zebrafish ECG method for assessment of drug-induced QTc prolongation. *Journal of Pharmacological and toxicological methods,* **67**(2), pp. 115-120.

CHEN, J.N., HAFFTER, P., ODENTHAL, J., VOGELSANG, E., BRAND, M., VAN EEDEN, F.J., FURUTANI-SEIKI, M., GRANATO, M., HAMMERSCHMIDT, M., HEISENBERG, C.P., JIANG, Y.J., KANE, D.A., KELSH, R.N., MULLINS, M.C. and NUSSLEIN-VOLHARD, C., 1996. Mutations affecting the cardiovascular system and other internal organs in zebrafish. *Development,* **123**, pp. 293-302.

CHI, N.C., SHAW, R.M., JUNGBLUT, B., HUISKEN, J., FERRER, T., ARNAOUT, R., SCOTT, I., BEIS, D., XIAO, T. and BAIER, H., 2008. Genetic and physiologic dissection of the vertebrate cardiac conduction system. *PLoS Biology,* **6**(5), pp. e109.

CHICO, T.J., INGHAM, P.W. and CROSSMAN, D.C., 2008. Modeling cardiovascular disease in the zebrafish. *Trends in Cardiovascular Medicine,* **18**(4), pp. 150-155.

CROWCOMBE, J., DHILLON, S.S., HURST, R.M., EGGINTON, S., MÜLLER, F., SÍK, A. and TARTE, E., 2016. 3D Finite Element Electrical Model of Larval Zebrafish ECG Signals. *PLoS one,* **11**(11), pp. e0165655.

D'AMICO, L., SENG, W.L., YANG, Y., SUTER, W. and MCGRATH, P., 2012. Assessment of drug-induced cardiotoxicity in zebrafish. In: *Zebrafish: Methods for Assessing Drug Safety and Toxicity:* John Wiley & Sons, Inc*,* pp. 45-54.

DE LEEUW, D., KRAAKMAN, P., BONGAERTS, P., MUTSAERS, C. and KLAASSEN, D., 1994. Electroplating of conductive polymers for the metallization of insulators. *Synthetic Metals,* **66**(3), pp. 263-273.

DENAYER, T., STÖHR, T. and VAN ROY, M., 2014. Animal models in translational medicine: Validation and prediction. *New Horizons in Translational Medicine,* **2**(1), pp. 5-11.

DEPIL, K., BEYL, S., STARY-WEINZINGER, A., HOHAUS, A., TIMIN, E. and HERING, S., 2011. Timothy mutation disrupts the link between activation and inactivation in Ca(V)1.2 protein. *The Journal of biological chemistry,* **286**(36), pp. 31557-31564.

DEUTSCHMAN, C.S., HARRIS, A.P. and FLEISHER, L.A., 1994. Changes in heart rate variability under propofol anesthesia: a possible explanation for propofol-induced bradycardia. *Anesthesia & Analgesia,* **79**(2), pp. 373-377.

DHILLON, S.S., DÓRÓ, É., MAGYARY, I., EGGINTON, S., SÍK, A. and MÜLLER, F., 2013. Optimisation of embryonic and larval ECG measurement in zebrafish for quantifying the effect of QT prolonging drugs. *PLoS one,* **8**(4), pp. e60552.

DING, Y., LONG, P.A., BOS, J.M., SHIH, Y.H., MA, X., SUNDSBAK, R.S., CHEN, J., JIANG, Y., ZHAO, L., HU, X., WANG, J., SHI, Y., ACKERMAN, M.J., LIN, X., EKKER, S.C., REDFIELD, M.M., OLSON, T.M. and XU, X., 2016. A modifier screen identifies DNAJB6 as a cardiomyopathy susceptibility gene. *JCI insight,* **1**(14),

DIXON, R.E., YUAN, C., CHENG, E.P., NAVEDO, M.F. and SANTANA, L.F., 2012. Ca2+ signaling amplification by oligomerization of L-type Cav1.2 channels. *Proceedings of the National Academy of Sciences of the United States of America,* **109**(5), pp. 1749-1754.

DRIESSEN, M., VITINS, A.P., PENNINGS, J.L., KIENHUIS, A.S., VAN DE WATER, B. and VAN DER VEN, LEO TM, 2015. A transcriptomics-based hepatotoxicity comparison between the zebrafish embryo and established human and rodent in vitro and in vivo models using cyclosporine A, amiodarone and acetaminophen. *Toxicology letters,* **232**(2), pp. 403-412.

DUCHARME, N.A., REIF, D.M., GUSTAFSSON, J. and BONDESSON, M., 2015. Comparison of toxicity values across zebrafish early life stages and mammalian studies: implications for chemical testing. *Reproductive Toxicology,* **55**, pp. 3-10.

DUFENDACH, K.A., GIUDICESSI, J.R., BOCZEK, N.J. and ACKERMAN, M.J., 2013. Maternal mosaicism confounds the neonatal diagnosis of type 1 Timothy syndrome. *Pediatrics,* **131**(6), pp. e1991-5.

DUNLOP, J., BOWLBY, M., PERI, R., VASILYEV, D. and ARIAS, R., 2008. High-throughput electrophysiology: an emerging paradigm for ion-channel screening and physiology. *Nature reviews Drug discovery,* **7**(4), pp. 358.

EBNER, T.J. and CHEN, G., 1995. Use of voltage-sensitive dyes and optical recordings in the central nervous system. *Progress in neurobiology,* **46**(5), pp. 463-506.

ETO, K., MAZILU-BROWN, J.K., HENDERSON-MACLENNAN, N., DIPPLE, K.M. and MCCABE, E.R., 2014. Development of catecholamine and cortisol stress responses in zebrafish. *Molecular genetics and metabolism reports,* **1**, pp. 373-377.

ETHERIDGE, S.P., BOWLES, N.E., ARRINGTON, C.B., PILCHER, T., ROPE, A., WILDE, A.A., ALDERS, M., SAAREL, E.V., TAVERNIER, R. and TIMOTHY, K.W., 2011. Somatic mosaicism

contributes to phenotypic variation in Timothy syndrome. *American journal of medical genetics Part A,* **155**(10), pp. 2578-2583.

FABER, G.M., SILVA, J., LIVSHITZ, L. and RUDY, Y., 2007. Kinetic properties of the cardiac L-type Ca2 channel and its role in myocyte electrophysiology: a theoretical investigation. *Biophysical journal,* **92**(5), pp. 1522-1543.

FINK, M., CALLOL-MASSOT, C., CHU, A., RUIZ-LOZANO, P., IZPISUA BELMONTE, J.C., GILES, W., BODMER, R. and OCORR, K., 2009. A new method for detection and quantification of heartbeat parameters in Drosophila, zebrafish, and embryonic mouse hearts. *BioTechniques,* **46**(2), pp. 101-113.

FLUCHER, B.E. and FRANZINI-ARMSTRONG, C., 1996. Formation of junctions involved in excitation-contraction coupling in skeletal and cardiac muscle. *Proceedings of the National Academy of Sciences of the United States of America,* **93**(15), pp. 8101-8106.

FOROUHAR, A., HOVE, J., CALVERT, C., FLORES, J., JADVAR, H. and GHARIB, M., 2004. Electrocardiographic characterization of embryonic zebrafish, *Engineering in Medicine and Biology Society, 2004. IEMBS'04. 26th Annual International Conference of the IEEE* 2004, IEEE, pp. 3615-3617.

FRANZ, M.R., SWERDLOW, C.D., LIEM, L.B. and SCHAEFER, J., 1988. Cycle length dependence of human action potential duration in vivo. Effects of single extra stimuli, sudden sustained rate acceleration and deceleration, and different steady-state frequencies. *The Journal of clinical investigation,* **82**(3), pp. 972-979.

FROST, C.M., WEI, B., BAGHMANLI, Z., CEDERNA, P.S. and URBANCHEK, M.G., 2012. PEDOT electrochemical polymerization improves electrode fidelity and sensitivity. *Plastic and Reconstructive Surgery,* **129**(4), pp. 933-942.

FUAD, N.M., KASLIN, J. and WLODKOWIC, D., 2018. Lab-on-a-Chip imaging micro-echocardiography (iμEC) for rapid assessment of cardiovascular activity in zebrafish larvae. *Sensors and Actuators B: Chemical,* **256**, pp. 1131-1141.

FUKUYAMA, M., WANG, Q., KATO, K., OHNO, S., DING, W., TOYODA, F., ITOH, H., KIMURA, H., MAKIYAMA, T. and ITO, M., 2014. Long QT syndrome type 8: novel CACNA1C mutations causing QT prolongation and variant phenotypes. *Europace,* **16**(12), pp. 1828-1837.

GAO, Z., TODOROV, B., BARRETT, C.F., VAN DORP, S., FERRARI, M.D., VAN DEN MAAGDENBERG, A.M., DE ZEEUW, C.I. and HOEBEEK, F.E., 2012. Cerebellar ataxia by enhanced Ca(V)2.1 currents is alleviated by Ca2+-dependent K+-channel activators in Cacna1a(S218L) mutant mice. *The Journal of neuroscience : the official journal of the Society for Neuroscience,* **32**(44), pp. 15533-15546.

GEHRIG, J., REISCHL, M., KALMÁR, É., FERG, M., HADZHIEV, Y., ZAUCKER, A., SONG, C., SCHINDLER, S., LIEBEL, U. and MÜLLER, F., 2009. Automated high-throughput mapping of promoter-enhancer interactions in zebrafish embryos. *Nature Methods,* **6**(12), pp. 911-916.

GOLAN, D.E., TASHJIAN, A.H. and ARMSTRONG, E.J., 2011. *Principles of pharmacology: the pathophysiologic basis of drug therapy.* Lippincott Williams & Wilkins.

GOLDENBERG, I., MOSS, A.J. and ZAREBA, W., 2006. QT interval: how to measure it and what is" normal". *Journal of cardiovascular electrophysiology,* **17**(3), pp. 333-336.

GOLDENBERG, I., ZAREBA, W. and MOSS, A.J., 2008. Long QT syndrome. *Current problems in cardiology,* **33**(11), pp. 629-694.

GOLDMAN, M.J., MOWRY, J.B. and KIRK, M.A., 1997. Sodium bicarbonate to correct widened QRS in a case of flecainide overdose. *The Journal of emergency medicine,* **15**(2), pp. 183-186.

GOLDSMITH, P., 2004. Zebrafish as a pharmacological tool: the how, why and when. *Current opinion in pharmacology,* **4**(5), pp. 504-512.

GONZÁLEZ-ROSA, J.M., BURNS, C.E. and BURNS, C.G., 2017. Zebrafish heart regeneration: 15 years of discoveries. *Regeneration,* **4**, 105–123 (2017).

GREEN, E.M., WAKIMOTO, H., ANDERSON, R.L., EVANCHIK, M.J., GORHAM, J.M., HARRISON, B.C., HENZE, M., KAWAS, R., OSLOB, J.D., RODRIGUEZ, H.M., SONG, Y., WAN, W., LEINWAND, L.A., SPUDICH, J.A., MCDOWELL, R.S., SEIDMAN, J.G. and SEIDMAN, C.E., 2016. A small-molecule inhibitor of sarcomere contractility suppresses hypertrophic cardiomyopathy in mice. *Science,* **351**(6273), pp. 617-621.

GUT, P., REISCHAUER, S., STAINIER, D.Y. and ARNAOUT, R., 2017. Little Fish, Big Data: Zebrafish as a Model for Cardiovascular and Metabolic Disease. *Physiological Reviews,* **97**(3), pp. 889-938.

HALLARE, A., NAGEL, K., KÖHLER, H. and TRIEBSKORN, R., 2006. Comparative embryotoxicity and proteotoxicity of three carrier solvents to zebrafish (Danio rerio) embryos. *Ecotoxicology and environmental safety,* **63**(3), pp. 378-388.

HARMER, A., VALENTIN, J. and POLLARD, C., 2011. On the relationship between block of the cardiac Na channel and drug-induced prolongation of the QRS complex. *British journal of pharmacology,* **164**(2), pp. 260-273.

HASSEL, D., SCHOLZ, E.P., TRANO, N., FRIEDRICH, O., JUST, S., MEDER, B., WEISS, D.L., ZITRON, E., MARQUART, S., VOGEL, B., KARLE, C.A., SEEMANN, G., FISHMAN, M.C., KATUS, H.A. and ROTTBAUER, W., 2008. Deficient zebrafish ether-a-go-go-related gene channel gating causes short-QT syndrome in zebrafish reggae mutants. *Circulation,* **117**(7), pp. 866-875.

HEDLEY, P.L., JØRGENSEN, P., SCHLAMOWITZ, S., WANGARI, R., MOOLMAN-SMOOK, J., BRINK, P.A., KANTERS, J.K., CORFIELD, V.A. and CHRISTIANSEN, M., 2009. The genetic basis of long QT and short QT syndromes: a mutation update. *Human mutation,* **30**(11), pp. 1486-1511.

HEDRICK, M.S. and WINMILL, R.E., 2003. Excitatory and inhibitory effects of tricaine (MS-222) on fictive breathing in isolated bullfrog brain stem. *American Journal of Physiology-Regulatory, Integrative and Comparative Physiology,* **284**(2), pp. R405-R412.

HENNESSEY, J.A., BOCZEK, N.J., JIANG, Y., MILLER, J.D., PATRICK, W., PFEIFFER, R., SUTPHIN, B.S., TESTER, D.J., BARAJAS-MARTINEZ, H. and ACKERMAN, M.J., 2014. A CACNA1C variant associated with reduced voltage-dependent inactivation, increased CaV1. 2 channel window current, and arrhythmogenesis. *PLoS One,* **9**(9), pp. e106982.

HILL, A.J., TERAOKA, H., HEIDEMAN, W. and PETERSON, R.E., 2005. Zebrafish as a model vertebrate for investigating chemical toxicity. *Toxicological sciences,* **86**(1), pp. 6-19.

HOAGE, T., DING, Y. and XU, X., 2012. Quantifying cardiac functions in embryonic and adult zebrafish. *Cardiovascular development.* Springer, pp. 11-20.

HOEFEN, R., REUMANN, M., GOLDENBERG, I., MOSS, A.J., JIN, O., GU, Y., MCNITT, S., ZAREBA, W., JONS, C. and KANTERS, J.K., 2012. In silico cardiac risk assessment in patients with long QT syndrome: type 1: clinical predictability of cardiac models. *Journal of the American College of Cardiology,* **60**(21), pp. 2182-2191.

HOWE, D.G., BRADFORD, Y.M., EAGLE, A., FASHENA, D., FRAZER, K., KALITA, P., MANI, P., MARTIN, R., MOXON, S.T. and PADDOCK, H., 2016. The Zebrafish Model Organism Database: new support for human disease models, mutation details, gene expression phenotypes and searching. *Nucleic acids research,* **45**(D1), pp. D758-D768.

HOWE, K., CLARK, M.D., TORROJA, C.F., TORRANCE, J., BERTHELOT, C., MUFFATO, M., COLLINS, J.E., HUMPHRAY, S., MCLAREN, K. and MATTHEWS, L., 2013. The zebrafish reference genome sequence and its relationship to the human genome. *Nature,* **496**(7446), pp. 498.

HU, N., SEDMERA, D., YOST, H.J. and CLARK, E.B., 2000. Structure and function of the developing zebrafish heart. *The Anatomical Record,* **260**(2), pp. 148-157.

HU, N., YOST, H.J. and CLARK, E.B., 2001. Cardiac morphology and blood pressure in the adult zebrafish. *The Anatomical Record: An Official Publication of the American Association of Anatomists,* **264**(1), pp. 1-12.

HUGHES, N.P., TARASSENKO, L. and ROBERTS, S.J., 2004. Markov models for automated ECG interval analysis, *Advances in Neural Information Processing Systems*, pp. 611-618.

IAIZZO, P.A., 2009. Handbook of cardiac anatomy, physiology, and devices. *Springer Science & Business Media.*

J BETZENHAUSER, M., S PITT, G. and ANTZELEVITCH, C., 2015. Calcium channel mutations in cardiac arrhythmia syndromes. *Current molecular pharmacology,* **8**(2), pp. 133-142.

JACOBS, A., KNIGHT, B.P., MCDONALD, K.T. and BURKE, M.C., 2006. Verapamil decreases ventricular tachyarrhythmias in a patient with Timothy syndrome (LQT8). *Heart Rhythm,* **3**(8), pp. 967-970.

JOHNSTON, H.J., VERDON, R., GILLIES, S., BROWN, D.M., FERNANDES, T.F., HENRY, T.B., ROSSI, A.G., TRAN, L., TUCKER, C. and TYLER, C.R., 2017. Adoption of in vitro systems and zebrafish embryos as alternative models for reducing rodent use in assessments of immunological and oxidative stress responses to nanomaterials. *Critical reviews in toxicology*, pp. 1-20.

KARI, G., RODECK, U. and DICKER, A., 2007. Zebrafish: an emerging model system for human disease and drug discovery. *Clinical Pharmacology & Therapeutics,* **82**(1), pp. 70-80.

KARLSSON, J., VON HOFSTEN, J. and OLSSON, P., 2001. Generating transparent zebrafish: a refined method to improve detection of gene expression during embryonic development. *Marine Biotechnology,* **3**(6), pp. 522-527.

KEßLER, M., ROTTBAUER, W. and JUST, S., 2015. Recent progress in the use of zebrafish for novel cardiac drug discovery. *Expert opinion on drug discovery,* **10**(11), pp. 1231-1241.

KETTLEBOROUGH, R.N., BUSCH-NENTWICH, E.M., HARVEY, S.A., DOOLEY, C.M., DE BRUIJN, E., VAN EEDEN, F., SEALY, I., WHITE, R.J., HERD, C. and NIJMAN, I.J., 2013. A systematic genome-wide analysis of zebrafish protein-coding gene function. *Nature,* **496**(7446), pp. 494.

KRAMER, J., OBEJERO-PAZ, C.A., MYATT, G., KURYSHEV, Y.A., BRUENING-WRIGHT, A., VERDUCCI, J.S. and BROWN, A.M., 2013. MICE models: superior to the HERG model in predicting Torsade de Pointes. *Scientific reports,* **3**, pp. 2100.

LANGHEINRICH, U., 2003. Zebrafish: a new model on the pharmaceutical catwalk. *Bioessays,* **25**(9), pp. 904-912.

LANGHEINRICH, U., VACUN, G. and WAGNER, T., 2003. Zebrafish embryos express an orthologue of HERG and are sensitive toward a range of QT-prolonging drugs inducing severe arrhythmia☆. *Toxicology and applied pharmacology,* **193**(3), pp. 370-382.

LEONG, I., SKINNER, J., SHELLING, A. and LOVE, D., 2010. Zebrafish as a model for long QT syndrome: the evidence and the means of manipulating zebrafish gene expression. *Acta physiologica,* **199**(3), pp. 257-276.

LETAMENDIA, A., QUEVEDO, C., IBARBIA, I., VIRTO, J.M., HOLGADO, O., DIEZ, M., BELMONTE, J.C.I. and CALLOL-MASSOT, C., 2012. Development and validation of an automated high-throughput system for zebrafish in vivo screenings. *PLoS one,* **7**(5), pp. e36690.

LIANG, P., LAN, F., LEE, A.S., GONG, T., SANCHEZ-FREIRE, V., WANG, Y., DIECKE, S., SALLAM, K., KNOWLES, J.W., WANG, P.J., NGUYEN, P.K., BERS, D.M., ROBBINS, R.C. and WU, J.C., 2013. Drug screening using a library of human induced pluripotent stem cell-derived cardiomyocytes reveals disease-specific patterns of cardiotoxicity. *Circulation,* **127**(16), pp. 1677-1691.

LIAO, P. and SOONG, T.W., 2010. CaV1. 2 channelopathies: from arrhythmias to autism, bipolar disorder, and immunodeficiency. *Pflügers Archiv-European Journal of Physiology,* **460**(2), pp. 353-359.

LIESCHKE, G.J. and CURRIE, P.D., 2007. Animal models of human disease: zebrafish swim into view. *Nature Reviews Genetics,* **8**(5), pp. 353-367.

LIN, C., 2008. Frequency-domain features for ECG beat discrimination using grey relational analysis-based classifier. *Computers & Mathematics with Applications,* **55**(4), pp. 680-690.

LIN, E., RIBEIRO, A., DING, W., HOVE-MADSEN, L., SARUNIC, M.V., BEG, M.F. and TIBBITS, G.F., 2014. Optical mapping of the electrical activity of isolated adult zebrafish hearts: acute effects of temperature. *American Journal of Physiology-Regulatory, Integrative and Comparative Physiology,* **306**(11), pp. R823-R836.

LIU, C.C., LI, L., LAM, Y.W., SIU, C.W. and CHENG, S.H., 2016. Improvement of surface ECG recording in adult zebrafish reveals that the value of this model exceeds our expectation. *Scientific reports,* **6**, pp. 25073.

LIU, Y., LO, Y. and WU, S., 2003. Stimulatory effects of chlorzoxazone, a centrally acting muscle relaxant, on large conductance calcium-activated potassium channels in pituitary GH 3 cells. *Brain research,* **959**(1), pp. 86-97.

LU, F., LANGENBACHER, A.D. and CHEN, J., 2016. Transcriptional Regulation of Heart Development in Zebrafish. *Journal of cardiovascular development and disease,* **3**(2), pp. 14.

MACRAE, C.A., 2013. Recent advances in in vivo screening for antiarrhythmic drugs. *Expert opinion on drug discovery,* **8**(2), pp. 131-141.

MACRAE, C.A., 2010. Cardiac Arrhythmia: In vivo screening in the zebrafish to overcome complexity in drug discovery. *Expert opinion on drug discovery,* **5**(7), pp. 619-632.

MACRAE, C.A. and PETERSON, R.T., 2003. Zebrafish-based small molecule discovery. *Chemistry & biology,* **10**(10), pp. 901-908.

MCGRATH, P. and LI, C., 2008. Zebrafish: a predictive model for assessing drug-induced toxicity. *Drug discovery today,* **13**(9), pp. 394-401.

MENKE, A.L., SPITSBERGEN, J.M., WOLTERBEEK, A.P. and WOUTERSEN, R.A., 2011. Normal anatomy and histology of the adult zebrafish. *Toxicologic pathology,* **39**(5), pp. 759-775.

MILAN, D.J., JONES, I.L., ELLINOR, P.T. and MACRAE, C.A., 2006. In vivo recording of adult zebrafish electrocardiogram and assessment of drug-induced QT prolongation. *American Journal of Physiology-Heart and Circulatory Physiology,* **291**(1), pp. H269-H273.

MILAN, D.J. and MACRAE, C.A., 2008. Zebrafish genetic models for arrhythmia. *Progress in biophysics and molecular biology,* **98**(2), pp. 301-308.

MILAN, D.J., JONES, I.L., ELLINOR, P.T. and MACRAE, C.A., 2006. In vivo recording of adult zebrafish electrocardiogram and assessment of drug-induced QT prolongation. *American journal of physiology.Heart and circulatory physiology,* **291**(1), pp. H269-73.

MILAN, D.J., KIM, A.M., WINTERFIELD, J.R., JONES, I.L., PFEUFER, A., SANNA, S., ARKING, D.E., AMSTERDAM, A.H., SABEH, K.M., MABLY, J.D., ROSENBAUM, D.S., PETERSON, R.T., CHAKRAVARTI, A., KAAB, S., RODEN, D.M. and MACRAE, C.A., 2009. Drug-sensitized zebrafish screen identifies multiple genes, including GINS3, as regulators of myocardial repolarization. *Circulation,* **120**(7), pp. 553-559.

MILAN, D.J., PETERSON, T.A., RUSKIN, J.N., PETERSON, R.T. and MACRAE, C.A., 2003. Drugs that induce repolarization abnormalities cause bradycardia in zebrafish. *Circulation,* **107**(10), pp. 1355-1358.

MITTELSTADT, S., HEMENWAY, C., CRAIG, M. and HOVE, J., 2008. Evaluation of zebrafish embryos as a model for assessing inhibition of hERG. *Journal of pharmacological and toxicological methods,* **57**(2), pp. 100-105.

MOSS, A.J. and KASS, R.S., 2005. Long QT syndrome: from channels to cardiac arrhythmias. *The Journal of clinical investigation,* **115**(8), pp. 2018-2024.

MURPHEY, R.D., STERN, H.M., STRAUB, C.T. and ZON, L.I., 2006. A chemical genetic screen for cell cycle inhibitors in zebrafish embryos. *Chemical biology & drug design,* **68**(4), pp. 213-219.

NACHIMUTHU, S., ASSAR, M.D. and SCHUSSLER, J.M., 2012. Drug-induced QT interval prolongation: mechanisms and clinical management. *Therapeutic advances in drug safety,* **3**(5), pp. 241-253.

NAVARRETE, E.G., LIANG, P., LAN, F., SANCHEZ-FREIRE, V., SIMMONS, C., GONG, T., SHARMA, A., BURRIDGE, P.W., PATLOLLA, B., LEE, A.S., WU, H., BEYGUI, R.E., WU, S.M., ROBBINS, R.C., BERS, D.M. and WU, J.C., 2013. Screening drug-induced arrhythmia using human induced pluripotent stem cell-derived cardiomyocytes and low-impedance microelectrode arrays. *Circulation,* **128**(11 Suppl 1), pp. S3-13.

NEMTSAS, P., WETTWER, E., CHRIST, T., WEIDINGER, G. and RAVENS, U., 2010. Adult zebrafish heart as a model for human heart? An electrophysiological study. *Journal of Molecular and Cellular Cardiology,* **48**(1), pp. 161-171.

NERBONNE, J.M. and KASS, R.S., 2005. Molecular physiology of cardiac repolarization. *Physiological Reviews,* **85**(4), pp. 1205-1253.

NGUYEN, C.T., LU, Q., WANG, Y. and CHEN, J., 2008. Zebrafish as a model for cardiovascular development and disease. *Drug Discovery Today: Disease Models,* **5**(3), pp. 135-140.

NÜRNBERG, A. and PIERRE, H., 2017. An introduction to little-known aspects of nonclinical regulatory writing. *Medical Writing,* **26**, pp. 9-19.

ÖSTMAN-SMITH, I., WISTEN, A., NYLANDER, E., BRATT, E., GRANELLI, A.D., OULHAJ, A. and LJUNGSTRÖM, E., 2009. Electrocardiographic amplitudes: a new risk factor for sudden death in hypertrophic cardiomyopathy. *European heart journal,* **31**(4), pp. 439-449.

PARDO-MARTIN, C., CHANG, T., KOO, B.K., GILLELAND, C.L., WASSERMAN, S.C. and YANIK, M.F., 2010. High-throughput in vivo vertebrate screening. *Nature methods,* **7**(8), pp. 634-636.

PEAL, D.S., MILLS, R.W., LYNCH, S.N., MOSLEY, J.M., LIM, E., ELLINOR, P.T., JANUARY, C.T., PETERSON, R.T. and MILAN, D.J., 2011. Novel chemical suppressors of long QT syndrome identified by an in vivo functional screen. *Circulation,* **123**(1), pp. 23-30.

PETTIT, S., DES ETAGES, S.A., MYLECRAINE, L., SNYDER, R., FOSTEL, J., DUNN, R.T.,2ND, HAYMES, K., DUVAL, M., STEVENS, J., AFSHARI, C. and VICKERS, A., 2010. Current and future applications of toxicogenomics: Results summary of a survey from the HESI Genomics State of Science Subcommittee. *Environmental health perspectives,* **118**(7), pp. 992-997.

PLANCHART, A., MATTINGLY, C.J., ALLEN, D., CEGER, P., CASEY, W., HINTON, D., KANUNGO, J., KULLMAN, S.W., TAL, T., BONDESSON, M., BURGESS, S.M., SULLIVAN, C., KIM, C., BEHL, M., PADILLA, S., REIF, D.M., TANGUAY, R.L. and HAMM, J., 2016. Advancing toxicology research using in vivo high throughput toxicology with small fish models. *Altex,* **33**(4), pp. 435-452.

POON, K.L. and BRAND, T., 2013. The zebrafish model system in cardiovascular research: A tiny fish with mighty prospects. *Global Cardiology Science and Practice,* (1), pp. 4.

POON, K., LIEBLING, M., KONDRYCHYN, I., GARCIA-LECEA, M. and KORZH, V., 2010. Zebrafish cardiac enhancer trap lines: new tools for in vivo studies of cardiovascular development and disease. *Developmental Dynamics,* **239**(3), pp. 914-926.

PRATT, C.M., RUBERG, S., MORGANROTH, J., MCNUTT, B., WOODWARD, J., HARRIS, S., RUSKIN, J. and MOYÉ, L., 1996. Dose-response relation between terfenadine (Seldane) and the QTc interval on the scalar electrocardiogram: distinguishing a drug effect from spontaneous variability. *American Heart Journal,* **131**(3), pp. 472-480.

RANGER, S., SHELDON, R., FERMINI, B. and NATTEL, S., 1993. Modulation of flecainide's cardiac sodium channel blocking actions by extracellular sodium: a possible cellular mechanism for the action of sodium salts in flecainide cardiotoxicity. *The Journal of pharmacology and experimental therapeutics,* **264**(3), pp. 1160-1167.

RASCHI, E., VASINA, V., POLUZZI, E. and DE PONTI, F., 2008. The hERG K channel: target and antitarget strategies in drug development. *Pharmacological research,* **57**(3), pp. 181-195.

REDFERN, W.S., WALDRON, G., WINTER, M.J., BUTLER, P., HOLBROOK, M., WALLIS, R. and VALENTIN, J., 2008. Zebrafish assays as early safety pharmacology screens: paradigm shift or red herring? *Journal of pharmacological and toxicological methods,* **58**(2), pp. 110-117.

REISCHAUER, S., ARNAOUT, R., RAMADASS, R. and STAINIER, D.Y., 2014. Actin binding GFP allows 4D in vivo imaging of myofilament dynamics in the zebrafish heart and the identification of Erbb2 signaling as a remodeling factor of myofibril architecture. *Circulation research,* **115**(10), pp. 845-856.

REUTER, H., 1984. Ion channels in cardiac cell membranes. *Annual Review of Physiology,* **46**(1), pp. 473-484.

ROBERTS, J.A., MIGUEL-ESCALADA, I., SLOVIK, K.J., WALSH, K.T., HADZHIEV, Y., SANGES, R., STUPKA, E., MARSH, E.K., BALCIUNIENE, J., BALCIUNAS, D. and MULLER, F., 2014. Targeted transgene integration overcomes variability of position effects in zebrafish. *Development (Cambridge, England),* **141**(3), pp. 715-724.

ROPER, C., SIMONICH, S.L.M. and TANGUAY, R.L., 2018. Development of a high-throughput in vivo screening platform for particulate matter exposures. *Environmental Pollution,* **235**, pp. 993-1005.

ROTTBAUER, W., BAKER, K., WO, Z.G., MOHIDEEN, M.P., CANTIELLO, H.F. and FISHMAN, M.C., 2001. Growth and function of the embryonic heart depend upon the cardiac-specific L-type calcium channel α1 subunit. *Developmental cell,* **1**(2), pp. 265-275.

ROYER, A., VAN VEEN, T.A., LE BOUTER, S., MARIONNEAU, C., GRIOL-CHARHBILI, V., LEONI, A.L., STEENMAN, M., VAN RIJEN, H.V., DEMOLOMBE, S., GODDARD, C.A., RICHER, C., ESCOUBET, B., JARRY-GUICHARD, T., COLLEDGE, W.H., GROS, D., DE BAKKER, J.M., GRACE, A.A., ESCANDE, D. and CHARPENTIER, F., 2005. Mouse model of SCN5A-linked hereditary Lenegre's disease: age-related conduction slowing and myocardial fibrosis. *Circulation,* **111**(14), pp. 1738-1746.

RUBINSTEIN, A.L., 2003. Zebrafish: from disease modeling to drug discovery. *Current Opinion in Drug Discovery and Development,* **6**(2), pp. 218-223.

SALHANICK, S.D. and SHANNON, M.W., 2003. Management of calcium channel antagonist overdose. *Drug Safety,* **26**(2), pp. 65-79.

SANGUINETTI, M.C. and MITCHESON, J.S., 2005. Predicting drug–hERG channel interactions that cause acquired long QT syndrome. *Trends in pharmacological sciences,* **26**(3), pp. 119-124.

SANTORIELLO, C. and ZON, L.I., 2012. Hooked! Modeling human disease in zebrafish. *The Journal of clinical investigation,* **122**(7), pp. 2337-2343.

SARITHA, C., SUKANYA, V. and MURTHY, Y.N., 2008. ECG signal analysis using wavelet transforms. *Bulg.J.Phys,* **35**(1), pp. 68-77.

SCHWARTZ, P.J., CROTTI, L. and INSOLIA, R., 2012. Long-QT syndrome: from genetics to management. *Circulation. Arrhythmia and electrophysiology,* **5**(4), pp. 868-877.

SCHWERTE, T., PREM, C., MAIROSL, A. and PELSTER, B., 2006. Development of the sympatho-vagal balance in the cardiovascular system in zebrafish (Danio rerio) characterized by power spectrum and classical signal analysis. *The Journal of experimental biology,* **209**(Pt 6), pp. 1093-1100.

SEDMERA, D., RECKOVA, M., DEALMEIDA, A., SEDMEROVA, M., BIERMANN, M., VOLEJNIK, J., SARRE, A., RADDATZ, E., MCCARTHY, R.A. and GOURDIE, R.G., 2003. Functional and morphological evidence for a ventricular conduction system in zebrafish and Xenopus hearts. *American Journal of Physiology-Heart and Circulatory Physiology,* **284**(4), pp. H1152-H1160.

SEEBOHM, G., 2005. Activators of cation channels: potential in treatment of channelopathies. *Molecular pharmacology,* **67**(3), pp. 585-588.

SHIEH, C. and GOPALAKRISHNAN, M., 2008. Potassium Channels. *Encyclopedia of Molecular Pharmacology.* Springer, pp. 990-998.

SPLAWSKI, I., TIMOTHY, K.W., SHARPE, L.M., DECHER, N., KUMAR, P., BLOISE, R., NAPOLITANO, C., SCHWARTZ, P.J., JOSEPH, R.M. and CONDOURIS, K., 2004. Ca v 1.2 calcium channel dysfunction causes a multisystem disorder including arrhythmia and autism. *Cell,* **119**(1), pp. 19-31.

SPLAWSKI, I., SHEN, J., TIMOTHY, K.W., LEHMANN, M.H., PRIORI, S., ROBINSON, J.L., MOSS, A.J., SCHWARTZ, P.J., TOWBIN, J.A., VINCENT, G.M. and KEATING, M.T., 2000. Spectrum of mutations in long-QT syndrome genes. KVLQT1, HERG, SCN5A, KCNE1, and KCNE2. *Circulation,* **102**(10), pp. 1178-1185.

SPLAWSKI, I., TIMOTHY, K.W., DECHER, N., KUMAR, P., SACHSE, F.B., BEGGS, A.H., SANGUINETTI, M.C. and KEATING, M.T., 2005. Severe arrhythmia disorder caused by

cardiac L-type calcium channel mutations. *Proceedings of the National Academy of Sciences of the United States of America,* **102**(23), pp. 8089-96; discussion 8086-8.

SPOMER, W., PFRIEM, A., ALSHUT, R., JUST, S. and PYLATIUK, C., 2012. High-throughput screening of zebrafish embryos using automated heart detection and imaging. *Journal of laboratory automation,* **17**(6), pp. 435-442.

STAINIER, D.Y., 2001. Zebrafish genetics and vertebrate heart formation. *Nature Reviews Genetics,* **2**(1), pp. 39.

STAINIER, D.Y., FOUQUET, B., CHEN, J.N., WARREN, K.S., WEINSTEIN, B.M., MEILER, S.E., MOHIDEEN, M.A., NEUHAUSS, S.C., SOLNICA-KREZEL, L., SCHIER, A.F., ZWARTKRUIS, F., STEMPLE, D.L., MALICKI, J., DRIEVER, W. and FISHMAN, M.C., 1996. Mutations affecting the formation and function of the cardiovascular system in the zebrafish embryo. *Development,* **123**, pp. 285-292.

STOYEK, M.R., QUINN, T.A., CROLL, R.P. and SMITH, F.M., 2016. Zebrafish heart as a model to study the integrative autonomic control of pacemaker function. *American journal of physiology.Heart and circulatory physiology,* **311**(3), pp. H676-88.

STOYEK, M.R., SCHMIDT, M.K., WILFART, F.M., CROLL, R.P. and SMITH, F.M., 2017. The in vitro zebrafish heart as a model to investigate the chronotropic effects of vapor anesthetics. *American journal of physiology.Regulatory, integrative and comparative physiology,* **313**(6), pp. R669-R679.

SUKARDI, H., CHNG, H.T., CHAN, E.C.Y., GONG, Z. and LAM, S.H., 2011. Zebrafish for drug toxicity screening: bridging the in vitro cell-based models and in vivo mammalian models. *Expert opinion on drug metabolism & toxicology,* **7**(5), pp. 579-589.

SUN, L., XIN, L., PENG, Z., JIN, R., JIN, Y., QIAN, H. and FU, Z., 2014. Toxicity and enantiospecific differences of two β-blockers, propranolol and metoprolol, in the embryos and larvae of zebrafish (Danio rerio). *Environmental toxicology,* **29**(12), pp. 1367-1378.

SUN, P., ZHANG, Y., YU, F., PARKS, E., LYMAN, A., WU, Q., AI, L., HU, C., ZHOU, Q. and SHUNG, K., 2009. Micro-electrocardiograms to study post-ventricular amputation of zebrafish heart. *Annals of Biomedical Engineering,* **37**(5), pp. 890-901.

TESSADORI, F., VAN WEERD, J.H., BURKHARD, S.B., VERKERK, A.O., DE PATER, E., BOUKENS, B.J., VINK, A., CHRISTOFFELS, V.M. and BAKKERS, J., 2012. Identification and functional characterization of cardiac pacemaker cells in zebrafish. *PLoS one,* **7**(10), pp. e47644.

THOMAS, D., KARLE, C. and KIEHN, J., 2006. The cardiac hERG/IKr potassium channel as pharmacological target: structure, function, regulation, and clinical applications. *Current pharmaceutical design,* **12**(18), pp. 2271-2283.

TSAI, C., WU, C., CHIANG, F., TSENG, C., LEE, J., YU, C., WANG, Y., LAI, L., LIN, J. and HWANG, J., 2011. In-vitro recording of adult zebrafish heart electrocardiogram—a platform for pharmacological testing. *Clinica chimica acta,* **412**(21-22), pp. 1963-1967.

TSUTSUI, H., HIGASHIJIMA, S., MIYAWAKI, A. and OKAMURA, Y., 2010. Visualizing voltage dynamics in zebrafish heart. *The Journal of physiology,* **588**(12), pp. 2017-2021.

VERKERK, A.O. and REMME, C.A., 2012. Zebrafish: a novel research tool for cardiac (patho) electrophysiology and ion channel disorders. *Frontiers in physiology,* **3**, pp. 255.

VOGNSEN, M., FABIAN-JESSING, B.K., SECHER, N., LOFGREN, B., DEZFULIAN, C., ANDERSEN, L.W. and GRANFELDT, A., 2017. Contemporary animal models of cardiac arrest: A systematic review. *Resuscitation,* **113**, pp. 115-123.

VORNANEN, M. and HASSINEN, M., 2016. Zebrafish heart as a model for human cardiac electrophysiology. *Channels,* **10**(2), pp. 101-110.

WAGNER, G. and STRAUSS, D., 2013. Marriott's practical electrocardiography*.* 12 edn. *Lippincott, Williams &Wilkins (LLW)*.

WALDMAN, H.J., 1994. Centrally acting skeletal muscle relaxants and associated drugs. *Journal of pain and symptom management,* **9**(7), pp. 434-441.

WARREN, K.S., WU, J.C., PINET, F. and FISHMAN, M.C., 2000. The genetic basis of cardiac function: dissection by zebrafish (Danio rerio) screens. *Philosophical Transactions of the Royal Society B: Biological Sciences,* **355**(1399), pp. 939-944.

WEMHONER, K., FRIEDRICH, C., STALLMEYER, B., COFFEY, A.J., GRACE, A., ZUMHAGEN, S., SEEBOHM, G., ORTIZ-BONNIN, B., RINNE, S., SACHSE, F.B., SCHULZE-BAHR, E. and DECHER, N., 2015. Gain-of-function mutations in the calcium channel CACNA1C (Cav1.2) cause non-syndromic long-QT but not Timothy syndrome. *Journal of Molecular and Cellular Cardiology,* **80**, pp. 186-195.

WULFF, H., CASTLE, N.A. and PARDO, L.A., 2009. Voltage-gated potassium channels as therapeutic targets. *Nature reviews Drug discovery,* **8**(12), pp. 982.

YAN, G.X. and ANTZELEVITCH, C., 1999. Cellular basis for the Brugada syndrome and other mechanisms of arrhythmogenesis associated with ST-segment elevation. *Circulation,* **100**(15), pp. 1660-1666.

YANIK, M.F., WASSERMAN, S.C., CHANG, T., GILLELAND, C.L. and PARDO, C., 2016. High-throughput platform for in-vivo sub-cellular screens on vertebrate larvae*, Massachusetts Institute of Technology,* US8865630B2.

YAZAWA, M., HSUEH, B., JIA, X., PASCA, A.M., BERNSTEIN, J.A., HALLMAYER, J. and DOLMETSCH, R.E., 2011. Using induced pluripotent stem cells to investigate cardiac phenotypes in Timothy syndrome. *Nature,* **471**(7337), pp. 230.

YU, F., ZHAO, Y., GU, J., QUIGLEY, K.L., CHI, N.C., TAI, Y. and HSIAI, T.K., 2012. Flexible microelectrode arrays to interface epicardial electrical signals with intracardial calcium transients in zebrafish hearts. *Biomedical Microdevices,* **14**(2), pp. 357-366.

ZHANG, X., BEEBE, T., JEN, N., LEE, C., TAI, Y. and HSIAI, T.K., 2015. Flexible and waterproof micro-sensors to uncover zebrafish circadian rhythms: The next generation of cardiac monitoring for drug screening. *Biosensors and Bioelectronics,* **71**, pp. 150-157.

ZHANG, X., TAI, J., PARK, J. and TAI, Y., 2014. Flexible MEA for adult zebrafish ECG recording covering both ventricle and atrium, *Micro Electro Mechanical Systems (MEMS), 2014 IEEE 27th International Conference on* 2014, IEEE, pp. 841-844.

ZON, L.I. and PETERSON, R.T., 2005. In vivo drug discovery in the zebrafish. *Nature reviews Drug discovery,* **4**(1), pp. 35-44.